

A COMPARISON OF SEPARATION TECHNIQUES APPLIED TO NATURAL  
WATER SAMPLES PRIOR TO ANALYSIS

By

Dennis Romero

Submitted in Partial Fulfillment  
Of the Requirements for the

Master of Science in Geochemistry

New Mexico Institute of Mining and Technology  
Department of Earth and Environmental Sciences

Socorro, New Mexico

August 2002

# A COMPARISON OF SEPARATION TECHNIQUES APPLIED TO NATURAL WATER SAMPLES PRIOR TO ANALYSIS

## ABSTRACT

After observing that studies involving filtration effects on natural water samples yielded results similar to those of geological membrane experiments, we conducted a series of laboratory and field experiments to examine this similarity. During the lab phase, we synthesized dilute sodium chloride and multi-component aqueous solutions mixed with varying amounts of sodium-saturated bentonite to simulate natural water samples with low concentrations of total dissolved solids (TDS) and high levels of total suspended sediment (TSS). We subjected these synthetic solutions to filtration, centrifugation, and dialysis prior to chemical analysis. We observed a decrease of up to 24% in major ion concentrations after filtration. We also noted that TDS concentrations for samples subjected to dialysis and centrifugation were within 2 to 8% of their actual concentrations. During the field phase, we obtained water samples from the Rio Puerco and Rio Grande following large runoff events to examine the effects of different solid-liquid separation methods on the concentration of dissolved species in the samples. We filtered the field samples collected and analyzed major ion concentrations in the filtrate. We observed that the concentrations of chemical species in the filtrate as a function of volume filtered varied by up to 8%. We concluded that, under certain circumstances, hyperfiltration might be occurring during the filtration of natural water samples. We believe this phenomena may be caused by the rapid accretion of sediment onto a 0.45  $\mu\text{m}$  filter, and, while much more prevalent for trace metals, can occur for some major cations and anions. We also concluded that the solid-liquid separation techniques of centrifugation and dialysis show promise for the treatment of aqueous sample prior to chemical analysis.

In addition to examining chemical variations of aqueous solutions as a function of filtered volume and as a function of solid-liquid separation method, we measured and analyzed filtration rates for each experiment using the filter cake model developed by chemical engineers during the early 1900s. We noted that plotting inverse flow rates versus cumulative volume filtered for each experiment yielded a linear relationship, just as described by the filter cake model. We were also able to calculate values for the resistance of the filter medium used ( $R_m$ ), as well as the resistance due to the accretion of sediment onto the filter ( $\alpha$ ). Although we noted some problems associated with using the filter cake model to predict the behavior of natural water samples subject to filtration, we concluded that it may be possible to extend the filter cake model to adequately describe and predict clogging rates associated with filtering natural water samples.

## TABLE OF CONTENTS

List of Figures .....	iii
List of Tables .....	xii
Introduction.....	1
Theory .....	19
Filter Effects on Concentrations of Dissolved Species .....	19
Clays as Semi-Permeable Membranes .....	22
Classical Filtration Theory .....	38
Modern Filtration Theory .....	47
Dialysis as a Solid-Liquid Separation Technique .....	56
Centrifugation as a solid-liquid separation technique .....	58
Methods .....	62
Lab Phase .....	62
Preparation of Synthetic Solutions .....	63
Filtration of Synthetic Solutions .....	65
Dialysis of Synthetic Solutions.....	66
Centrifugation of Synthetic Solutions.....	70
Chemical Analysis of Sample Filtrate .....	71
Field Phase .....	72
Sample Locations and Methods .....	72
Filtration.....	74
Dialysis .....	75
Centrifugation .....	75
Chemical Analysis of Sample Filtrate and Sediments.....	75
Results and Interpretations.....	76
Lab Phase .....	76
Measurement of filter cake resistance .....	76
Chemical Analysis of Filtrate Aliquots .....	93
Chemical Analysis of Dialysis and Centrifugation Samples .....	141
Implications and Future Work .....	161
Conclusions.....	165
References Cited .....	168

## LIST OF FIGURES

Figure 1 -	Effect of accretion of sediments on filtrate iron concentration for water from Lake Alenåshålan, Sweden (redrawn from Danielson, 1982).....	3
Figure 2 -	Effect of accretion of sediments on filtrate iron concentration for water from Lake Alenåshålan, Sweden, using a glass fiber filter (redrawn from Danielson, 1982).....	4
Figure 3 -	Effect of accretion of sediments on filtrate iron concentration for Black Beck, Scotland (redrawn from Laxen and Chandler, 1982) .....	5
Figure 4 -	Variation of iron concentration with increasing filtrate volumes for three rivers. Filtration performed with a Microfiltration System 0.45 µm pore size/47 mm diameter filter paper (redrawn from Horowitz et al., 1992).....	6
Figure 5-	Variation of Al, Fe, Cu, and Zn concentrations with increasing filtrate volumes for the Tangipahoa River at Robert, LA. Filtration performed with a Gelman Capsule filter (redrawn from Horowitz et al., 1996).....	7
Figure 6 -	Ion reduction factors for an early reverse osmosis field test using a 0.45 µm cellulose acetate membrane (from Loeb, 1964). Crossflow configuration used in this study.....	9
Figure 7 -	Typical retention curve for a reverse osmosis system using a cellulose acetate membrane (from Matsuura, 1994). Crossflow configuration used in this study. ....	10
Figure 8 -	Vertical cross-section of field filter cell used by Briggs (1906).....	11
Figure 9 -	Results of Briggs' filtration study for a 1.0 mN K <sub>2</sub> SO <sub>4</sub> solution (redrawn from Briggs, 1906).....	14
Figure 10 -	Results of Briggs' filtration study for a 1.0 mN solution of NaHCO <sub>3</sub> (redrawn from Briggs, 1906). ....	15
Figure 11 -	Results of Briggs' filtration study for a 1.0 mN KNO <sub>3</sub> solution (redrawn from Briggs, 1906).....	16
Figure 12 -	Results of one experiment used to demonstrate the osmotic properties of a compacted clay plug - line added for purposes of comparison (redrawn from McKelvey and Milne, 1962).....	17

Figure 13 - Range of diameters for some colloidal particles and pore sizes of typical filter media (modified from Stumm and Morgan, 1981) .....	21
Figure 14 - Principles of osmosis, osmotic pressure, and reverse osmosis. Note that the activity of the solvent in solution I is much less than that in solution II ( $a_I \ll a_{II}$ ) (modified from Matsuura, 1994).....	24
Figure 15 - Schematic diagram of the formation of the concentration polarization layer (CPL) in a static cell system. System has been rotated to the left $90^\circ$ for ease of viewing (redrawn after Fritz, 1986).....	26
Figure 16 - Electrical double layer overlap in a clay pore (redrawn from Marine and Fritz, 1981).....	29
Figure 17 - A conceptual diagram of hyperfiltration through a clay membrane located between two highly permeable units in a static cell system (redrawn from Fritz and Marine, 1983). Note: There is also a flux of salt through the membrane.....	32
Figure 18 - The four stages of filtration (modified from Sperry, 1916) .....	48
Figure 19 - Dialysis set-up used for the separation of $KNO_3$ from $AgI$ sol (Shaw, 1989) .....	60
Figure 20 - Filter cell used in study .....	67
Figure 21 - Schematic diagram of dialysis cell used in study.....	68
Figure 22 - Map Showing Sample Locations.....	73
Figure 23 - Plots of Filtration Time / Volume Filtered against Volume Filtered for suspended clay loads of 5 mg/L. The slope of the linear portion of the curve is used to determine the resistance of the filter cake, $\alpha$ .....	78
Figure 24 - Plots of Filtration Time / Volume Filtered against Volume Filtered for suspended clay loads of 10 mg/L. The slope of the linear portion of the curve is used to determine the resistance of the filter cake, $\alpha$ .....	79
Figure 25 - Plots of Filtration Time / Volume Filtered against Volume Filtered for suspended clay loads of 15 mg/L. The slope of the linear portion of the curve is used to determine the resistance of the filter cake, $\alpha$ .....	80
Figure 26 - Plots of Filtration Time / Volume Filtered against Volume Filtered for suspended clay loads of 25 mg/L. The slope of the linear portion of the curve is used to determine the resistance of the filter cake, $\alpha$ .....	81

- Figure 27 - Plots of Filtration Time / Volume Filtered against Volume Filtered for suspended clay loads of 50 mg/L. The slope of the linear portion of the curve is used to determine the resistance of the filter cake,  $\alpha$ .....82
- Figure 28 - Plots of Filtration Time / Volume Filtered against Volume Filtered for suspended clay loads of 75 mg/L. The slope of the linear portion of the curve is used to determine the resistance of the filter cake,  $\alpha$ .....83
- Figure 29 - Plots of Filtration Time / Volume Filtered against Volume Filtered for suspended clay loads of 100 mg/L. The slope of the linear portion of the curve is used to determine the resistance of the filter cake,  $\alpha$ .....84
- Figure 30 - Plots of Filtration Time / Volume Filtered against Volume Filtered for suspended clay loads of 102 mg/L. The slope of the linear portion of the curve is used to determine the resistance of the filter cake,  $\alpha$ .....85
- Figure 31 - Plots of Filtration Time / Volume Filtered against Volume Filtered for suspended clay loads of 281.5 mg/L. The slope of the linear portion of the curve is used to determine the resistance of the filter cake,  $\alpha$ .....86
- Figure 32 - Plots of Filtration Time / Volume Filtered against Volume Filtered for suspended clay loads of 484 mg/L. The slope of the linear portion of the curve is used to determine the resistance of the filter cake,  $\alpha$ .....87
- Figure 33 - Plots of Filtration Time / Volume Filtered against Volume Filtered for suspended clay loads of 4,100 mg/L. The slope of the linear portion of the curve is used to determine the resistance of the filter cake,  $\alpha$ .....88
- Figure 34 - Plots of Filtration Time / Volume Filtered against Volume Filtered for suspended clay loads of 32,100 mg/L. The slope of the linear portion of the curve is used to determine the resistance of the filter cake,  $\alpha$ .....89
- Figure 35 - Plot of concentration of  $\text{Na}^+$  and  $\text{Cl}^-$  in filtrate as a function of volume filtered. Suspended clay concentration of 5 mg/L. Error bars represent an analytical uncertainty of two standard deviations. True dissolved concentrations are denoted by the data point for “zero volume filtered.”...94
- Figure 36 - Plot of concentration of  $\text{Na}^+$  and  $\text{Cl}^-$  in filtrate as a function of volume filtered. Suspended clay concentration of 10 mg/L. Error bars represent an analytical uncertainty of two standard deviations. True dissolved concentrations are denoted by the data point for “zero volume filtered.”...95
- Figure 37 - Plot of concentration of  $\text{Na}^+$  and  $\text{Cl}^-$  in filtrate as a function of volume filtered. Suspended clay concentration of 15 mg/L. Error bars represent an

analytical uncertainty of two standard deviations. True dissolved concentrations are denoted by the data point for “zero volume filtered.” ...96

Figure 38 - Plot of concentration of  $\text{Na}^+$  and  $\text{Cl}^-$  in filtrate as a function of volume filtered. Suspended clay concentration of 25 mg/L. Error bars represent an analytical uncertainty of two standard deviations. True dissolved concentrations are denoted by the data point for “zero volume filtered.” ...97

Figure 39 - Plot of concentration of  $\text{Na}^+$  and  $\text{Cl}^-$  in filtrate as a function of volume filtered. Suspended clay concentration of 50 mg/L. Error bars represent an analytical uncertainty of two standard deviations. True dissolved concentrations are denoted by the data point for “zero volume filtered.” ...98

Figure 40 - Plot of concentration of  $\text{Na}^+$  and  $\text{Cl}^-$  in filtrate as a function of volume filtered. Suspended clay concentration of 75 mg/L. Error bars represent an analytical uncertainty of two standard deviations. True dissolved concentrations are denoted by the data point for “zero volume filtered.” ...99

Figure 41 - Plot of concentration of  $\text{Na}^+$  and  $\text{Cl}^-$  in filtrate as a function of volume filtered. Suspended clay concentration of 100 mg/L. Error bars represent an analytical uncertainty of two standard deviations. True dissolved concentrations are denoted by the data point for “zero volume filtered.” .100

Figure 42 - Results of tap water experiment with 282 mg/L of suspended clay. This figure suggests that solute sieving effects were not important during this filtration. Symbols are larger than error bars of two standard deviations. True dissolved concentrations are denoted by the data point for “zero volume filtered.” ..... 104

Figure 43 - Results of tap water experiment with 425 mg/L of suspended clay. Error bars represent an analytical uncertainty of two standard deviations. True dissolved concentrations are denoted by the data point for “zero volume filtered.” ..... 105

Figure 44 - Results of tap water experiment with 425 mg/L of suspended clay. Error bars represent an analytical uncertainty of two standard deviations. True dissolved concentrations are denoted by the data point for “zero volume filtered.” ..... 106

Figure 45 - Results of tap water experiment with 425 mg/L of suspended clay. Error bars represent an analytical uncertainty of two standard deviations. True dissolved concentrations are denoted by the data point for “zero volume filtered.” ..... 107

Figure 46 - Results of tap water experiment with 425 mg/L of suspended clay. Error bars represent an analytical uncertainty of two standard deviations. True dissolved concentrations are denoted by the data point for “zero volume filtered.” .....	108
Figure 47 - Results of tap water experiment with 425 mg/L of suspended clay. Error bars represent an analytical uncertainty of two standard deviations. True dissolved concentrations are denoted by the data point for “zero volume filtered.” .....	109
Figure 48 - Results of tap water experiment with 425 mg/L of suspended clay. Error bars represent an analytical uncertainty of two standard deviations. True dissolved concentrations are denoted by the data point for “zero volume filtered.” .....	111
Figure 49 - Results of tap water experiment with 425 mg/L of suspended clay. Error bars represent an analytical uncertainty of two standard deviations. True dissolved concentrations are denoted by the data point for “zero volume filtered.” .....	112
Figure 50 - Results of tap water experiment with 425 mg/L of suspended clay. Error bars represent an analytical uncertainty of two standard deviations. True dissolved concentrations are denoted by the data point for “zero volume filtered.” .....	113
Figure 51 - Results of tap water experiment with 425 mg/L of suspended clay. Error bars represent an analytical uncertainty of two standard deviations. True dissolved concentrations are denoted by the data point for “zero volume filtered.” .....	114
Figure 52 - Results of tap water experiment with 102 mg/L of suspended clay. Error bars represent an analytical uncertainty of two standard deviations. True dissolved concentration is denoted by the data point for “zero volume filtered.” .....	117
Figure 53 - Results of tap water experiment with 282 mg/L of suspended clay. Error bars represent an analytical uncertainty of two standard deviations. True dissolved concentration is denoted by the data point for “zero volume filtered.” .....	118
Figure 54 - Results of tap water experiment with 425 mg/L of suspended clay. Error bars represent an analytical uncertainty of two standard deviations. True dissolved concentration is denoted by the data point for “zero volume filtered.” .....	119



- Figure 55 - Plot of filtrate concentration as function of sample filtered for Rio Grande water sample with a suspended solids concentration of 4,100 mg/L. Error bars represent an analytical uncertainty of two standard deviations. ....121
- Figure 56 - Plot of filtrate concentration as function of sample filtered for Rio Grande water sample with a suspended solids concentration of 4,100 mg/L. Error bars represent an analytical uncertainty of two standard deviations. ....122
- Figure 57 - Plot of filtrate concentration as function of sample filtered for Rio Grande water sample with a suspended solids concentration of 4,100 mg/L. Error bars represent an analytical uncertainty of two standard deviations. ....123
- Figure 58 - Plot of filtrate concentration as function of sample filtered for Rio Grande water sample with a suspended solids concentration of 4,100 mg/L. Error bars represent an analytical uncertainty of two standard deviations. ....124
- Figure 59 - Plot of filtrate concentration as function of sample filtered for Rio Grande water sample with a suspended solids concentration of 4,100 mg/L. Error bars represent an analytical uncertainty of two standard deviations. ....125
- Figure 60 - Plot of filtrate concentration as function of sample filtered for Rio Grande water sample with a suspended solids concentration of 4,100 mg/L. Error bars represent an analytical uncertainty of two standard deviations. ....126
- Figure 61 - Plot of filtrate concentration as function of sample filtered for Rio Grande water sample with a suspended solids concentration of 4,100 mg/L. Error bars represent an analytical uncertainty of two standard deviations. ....127
- Figure 62 - Plot of filtrate concentration as function of sample filtered for Rio Puerco water sample with a suspended solids concentration of 32,100 mg/L. Error bars represent an analytical uncertainty of two standard deviations. ....128
- Figure 63 - Plot of filtrate concentration as function of sample filtered for Rio Puerco water sample with a suspended solids concentration of 32,100 mg/L. Error bars represent an analytical uncertainty of two standard deviations. ....129
- Figure 64 - Plot of filtrate concentration as function of sample filtered for Rio Puerco water sample with a suspended solids concentration of 32,100 mg/L. Error bars represent an analytical uncertainty of two standard deviations. ....130
- Figure 65 - Plot of filtrate concentration as function of sample filtered for Rio Puerco water sample with a suspended solids concentration of 32,100 mg/L. Error bars represent an analytical uncertainty of two standard deviations. ....131

- Figure 66 - Plot of filtrate concentration as function of sample filtered for Rio Puerco water sample with a suspended solids concentration of 32,100 mg/L. Error bars represent an analytical uncertainty of two standard deviations. .... 132
- Figure 67 - Plot of filtrate concentration as function of sample filtered for Rio Puerco water sample with a suspended solids concentration of 32,100 mg/L. Error bars represent an analytical uncertainty of two standard deviations. .... 133
- Figure 68 - Plot of filtrate concentration as function of sample filtered for Rio Puerco water sample with a suspended solids concentration of 32,100 mg/L. Error bars represent an analytical uncertainty of two standard deviations. .... 134
- Figure 69 - Scanning Electron Microscope (SEM) photograph of an unused 0.45  $\mu\text{m}$  MFS filter 2500 times magnification..... 137
- Figure 70 - Scanning Electron Microscope (SEM) photograph of a 0.45  $\mu\text{m}$  MFS filter at 500 times magnification after approximately 500 mL of Rio Grande water has been filtered. .... 138
- Figure 71 - A Conceptual Image of the Processes that may be occurring during Filtration (modified from Corapcioglu and Jiang, 1991)..... 140
- Figure 72 - Plot comparing solution concentration as a function of separation method for a NaCl solution with a suspended clay concentration of 5 mg/L. Solid line indicates actual solution concentration before addition of clay. Error bars represent an analytical uncertainty of two standard deviations. .... 142
- Figure 73 - Plot comparing solution concentration as a function of separation method for a NaCl solution with a suspended clay concentration of 10 mg/L. Solid line indicates actual solution concentration before addition of clay. Error bars represent an analytical uncertainty of two standard deviations. .... 143
- Figure 74 - Plot comparing solution concentration as a function of separation method for a NaCl solution with a suspended clay concentration of 15 mg/L. Solid line indicates actual solution concentration before addition of clay. Error bars represent an analytical uncertainty of two standard deviations. .... 144
- Figure 75 - Plot comparing solution concentration as a function of separation method for a NaCl solution with a suspended clay concentration of 25 mg/L. Solid line indicates actual solution concentration before addition of clay. Error bars represent an analytical uncertainty of two standard deviations. .... 145

Figure 76 - Plot comparing solution concentration as a function of separation method for a NaCl solution with a suspended clay concentration of 50 mg/L. Solid line indicates actual solution concentration before addition of clay. Error bars represent an analytical uncertainty of two standard deviations. .... 146

Figure 77 - Plot comparing solution concentration as a function of separation method for a NaCl solution with a suspended clay concentration of 75 mg/L. Solid line indicates actual solution concentration before addition of clay. Error bars represent an analytical uncertainty of two standard deviations. .... 147

Figure 78 - Plot comparing solution concentration as a function of separation method for a NaCl solution with a suspended clay concentration of 100 mg/L. Solid line indicates actual solution concentration before addition of clay. Error bars represent an analytical uncertainty of two standard deviations. .... 148

Figure 79 - Plot comparing solution concentration as a function of separation method for a water sample from the Rio Grande with a suspended solids concentration of 4,100 mg/L. Error bars represent an analytical uncertainty of two standard deviations. .... 151

Figure 80 - Plot comparing solution concentration as a function of separation method for a water sample from the Rio Grande with a suspended solids concentration of 4,100 mg/L. Error bars represent an analytical uncertainty of two standard deviations. .... 152

Figure 81 - Plot comparing solution concentration as a function of separation method for a water sample from the Rio Grande with a suspended solids concentration of 4,100 mg/L. Error bars represent an analytical uncertainty of two standard deviations. .... 153

Figure 82 - Plot comparing solution concentration as a function of separation method for a water sample from the Rio Grande with a suspended solids concentration of 4,100 mg/L. Error bars represent an analytical uncertainty of two standard deviations. .... 154

Figure 83 - Plot comparing solution concentration as a function of separation method for a water sample from the Rio Grande with a suspended solids concentration of 4,100 mg/L. Error bars represent an analytical uncertainty of two standard deviations. .... 155

Figure 84 - Plot comparing solution concentration as a function of separation method for a water sample from the Rio Puerco with a suspended solids concentration of 32,100 mg/L. Error bars represent an analytical uncertainty of two standard deviations. .... 156

Figure 85 - Plot comparing solution concentration as a function of separation method for a water sample from the Rio Puerco with a suspended solids concentration of 32,100 mg/L. Error bars represent an analytical uncertainty of two standard deviations. .... 157

Figure 86 - Plot comparing solution concentration as a function of separation method for a water sample from the Rio Puerco with a suspended solids concentration of 32,100 mg/L. Error bars represent an analytical uncertainty of two standard deviations. .... 158

Figure 87 - Plot comparing solution concentration as a function of separation method for a water sample from the Rio Puerco with a suspended solids concentration of 32,100 mg/L. Error bars represent an analytical uncertainty of two standard deviations. .... 159

Figure 88 - Plot comparing solution concentration as a function of separation method for a water sample from the Rio Puerco with a suspended solids concentration of 32,100 mg/L. Error bars represent an analytical uncertainty of two standard deviations. .... 160

## LIST OF TABLES

Table 1 -	Sedimentation rates under gravity for uncharged spheres with a density of $2.0 \text{ g/cm}^3$ in water at $20^\circ\text{C}$ (Shaw, 1980) .....	59
Table 2 -	Suspended Solids Concentrations of Binary Solutions Used in Study .....	63
Table 3 -	Suspended Solids Concentrations of Multicomponent Solutions Used in Study .....	65
Table 4 -	Recommended conditions for Spectra/Por 1 RC dialysis tubing (Spectra-Por, 1994) .....	69
Table 5 -	Trace elements found in representative samples of Spectra/Por 1 RC dialysis tubing (Spectra-Por, 1994).....	69
Table 6 -	Values of filter cake resistance ( $\alpha$ ) and filter medium resistance ( $R_m$ ) determined in this study .....	90
Table 7 -	Typical $R_m$ values for filter media used in industrial processes (Grace, 1956) .....	90
Table 8 -	Maximum effluent solute reduction in binary salt experiments .....	102
Table 9 -	Maximum effluent solute reduction in tap water experiments .....	102
Table 10 -	Maximum effluent solute reduction in river water filtration experiments	135
Table 11 -	Maximum effluent solute reduction as a function of separation method.	161
Table 12 -	Comparison of Analyte Concentrations as a Function of Separation Method for Rio Grande and Rio Puerco Samples .....	161

## INTRODUCTION

Filtration of water samples with a 0.45  $\mu\text{m}$  filter prior to analysis has long been standard practice. There are a number of filtration protocols available for various samples and analytical methods (APHA, 1992; ASTM, 1993). Although it is necessary to remove suspended particulate from water samples to prevent damage to sensitive analytical equipment, in some cases sample filtration prior to analysis may be skewing the results of analytical techniques.

Kennedy et al. (1974) showed that fine-grained, suspended solids can pass through a 0.45  $\mu\text{m}$  filter, causing up to an order of magnitude error in the analysis of aluminum (Al), titanium (Ti), manganese (Mn), and iron (Fe) in natural surface waters. Mora and Harrison (1983) found that reported concentrations of metal ions in natural waters might be inaccurate due to adsorption of these ions onto the filter and filtration unit. Meadows et al. (1978) stated that the presence of trace elements in the form of insoluble particulate after sample filtration might lead to erroneous analytical results. Numerous scientists have discussed the possibilities of sample contamination and adsorptive losses that may adversely affect the determination of chemical species (Batley and Gardner, 1977; Horowitz et al. 1996; Spencer and Manheim, 1969; Robertson, 1968; Laxen and Harrison, 1981; Benoit, 1994).

While these findings are interesting, perhaps the most intriguing examinations of sample filtration involve the study of changing species concentrations as a function of sample volume filtered (Danielson, 1981; Laxen and Chandler, 1982; Horowitz et al., 1992). Danielson (1981) provided the first comprehensive study of the chemical changes

in sample filtrate because of the amount of sample filtered and found that filter loading has a profoundly adverse impact on the determination of the concentration of Fe in solution. By measuring the concentration of dissolved iron as a function of filter load (filter load is defined as the volume of sample filtered divided by the filter's cross-sectional area), Danielson (1981) showed that iron concentrations measured in solution decreased by up to 95% of initial values as filter loading increased (Figures 1 and 2). Laxen and Chandler (1982) also found that the concentrations of chemical species in sample filtrates could decrease by as much as 20 to 40% as the filtered volume increases (Figure 3). Horowitz et al. (1992 and 1996) also studied the effects of filter loading on dissolved concentrations of Fe and Al and found that the concentrations of these chemical species in sediment-laden waters can decrease from 40 to 85% as the amount of water filtered increases (Figure 4). In addition, Horowitz et al. (1996) later found that the trace metals of chromium (Cr), copper (Cu), zinc (Zn), nickel (Ni), and lead (Pb) also exhibited a similar trend (Figure 5).

The samples used by Danielson (1981) were collected from Lake Alenåshålan in southwestern Sweden. Lake Alenåshålan is surrounded by peat bogs and has very high levels of iron and humic substances in its water, in both dissolved and colloidal forms. Laxen and Chandler studied water from Esthwaite and Black Beck, a freshwater lake and slow moving stream, respectively. Horowitz et al. (1992) examined Keg Creek, a stream containing finely divided kaolin from nearby mines; the Ohoopce River, an organic rich stream; and the Chattahoochee River, a large controlled river

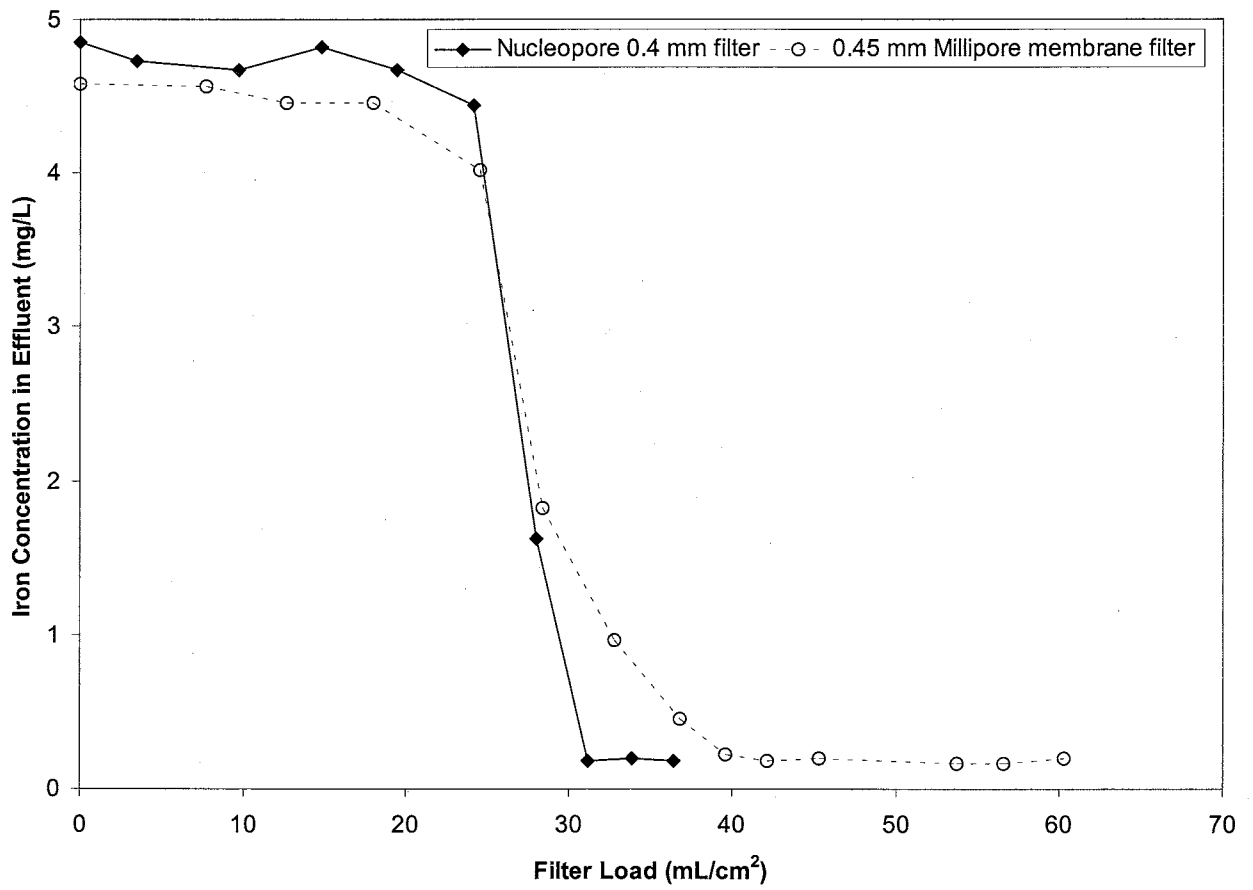


**Figure 1 -** Effect of accretion of sediments on filtrate iron concentration for water from Lake Alenåshålan, Sweden (redrawn from Danielson, 1982)



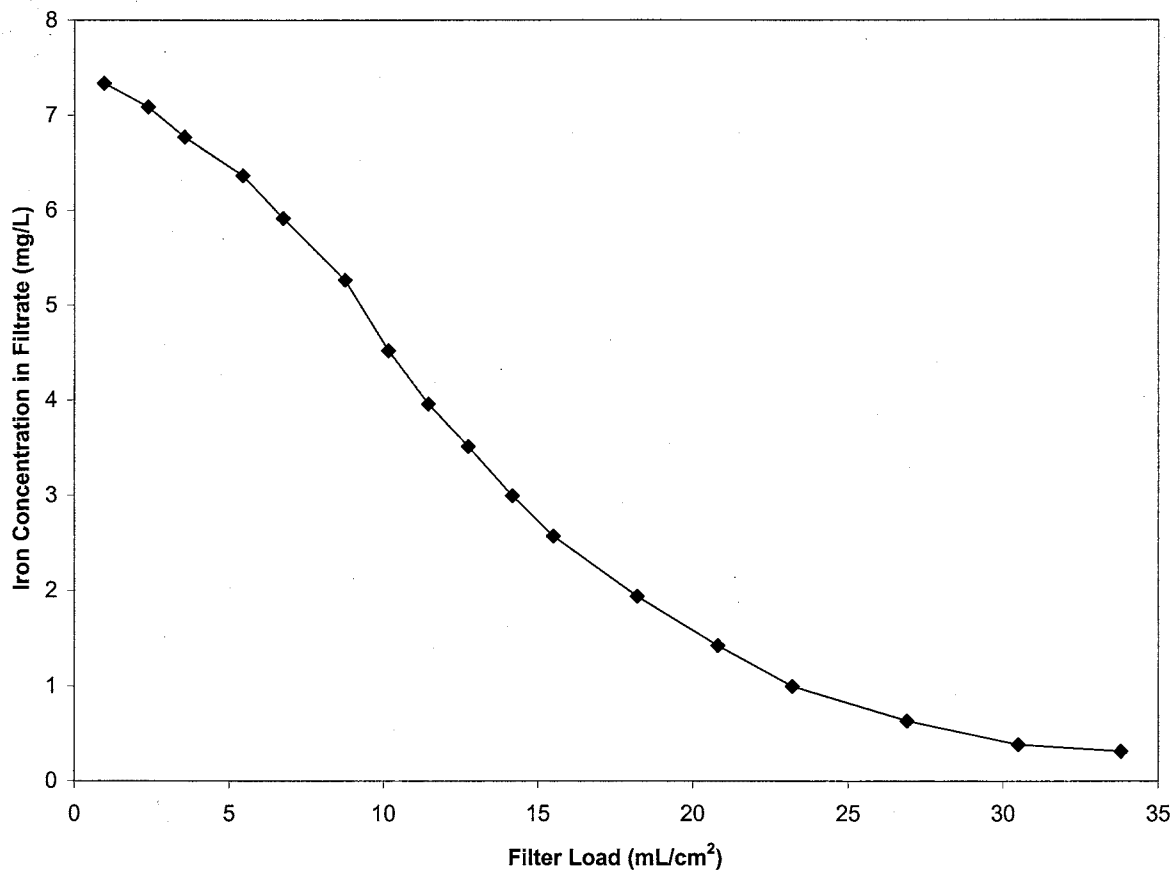


**Figure 2 -** Effect of accretion of sediments on filtrate iron concentration for water from Lake Alenåshålan, Sweden, using a glass fiber filter (redrawn from Danielson, 1982)

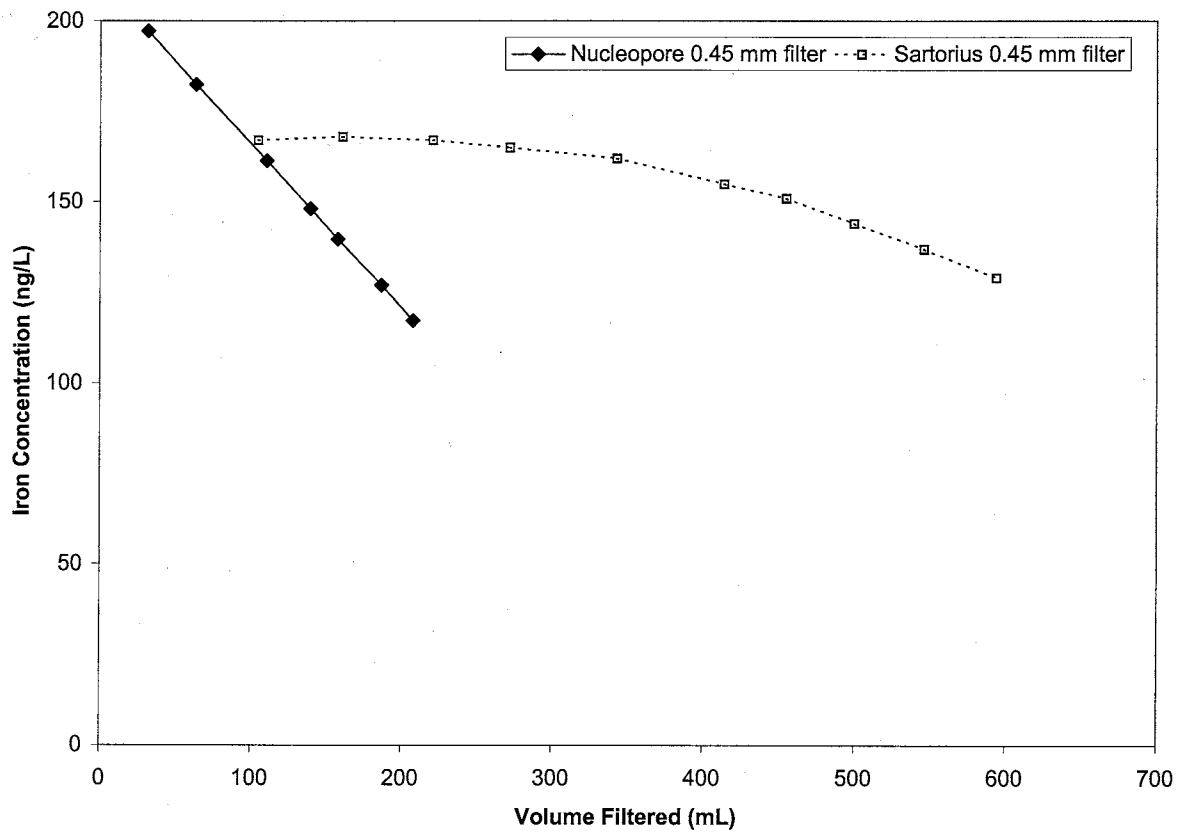


**Figure 3 -** Effect of accretion of sediments on filtrate iron concentration for Black Beck, Scotland (redrawn from Laxen and Chandler, 1982)

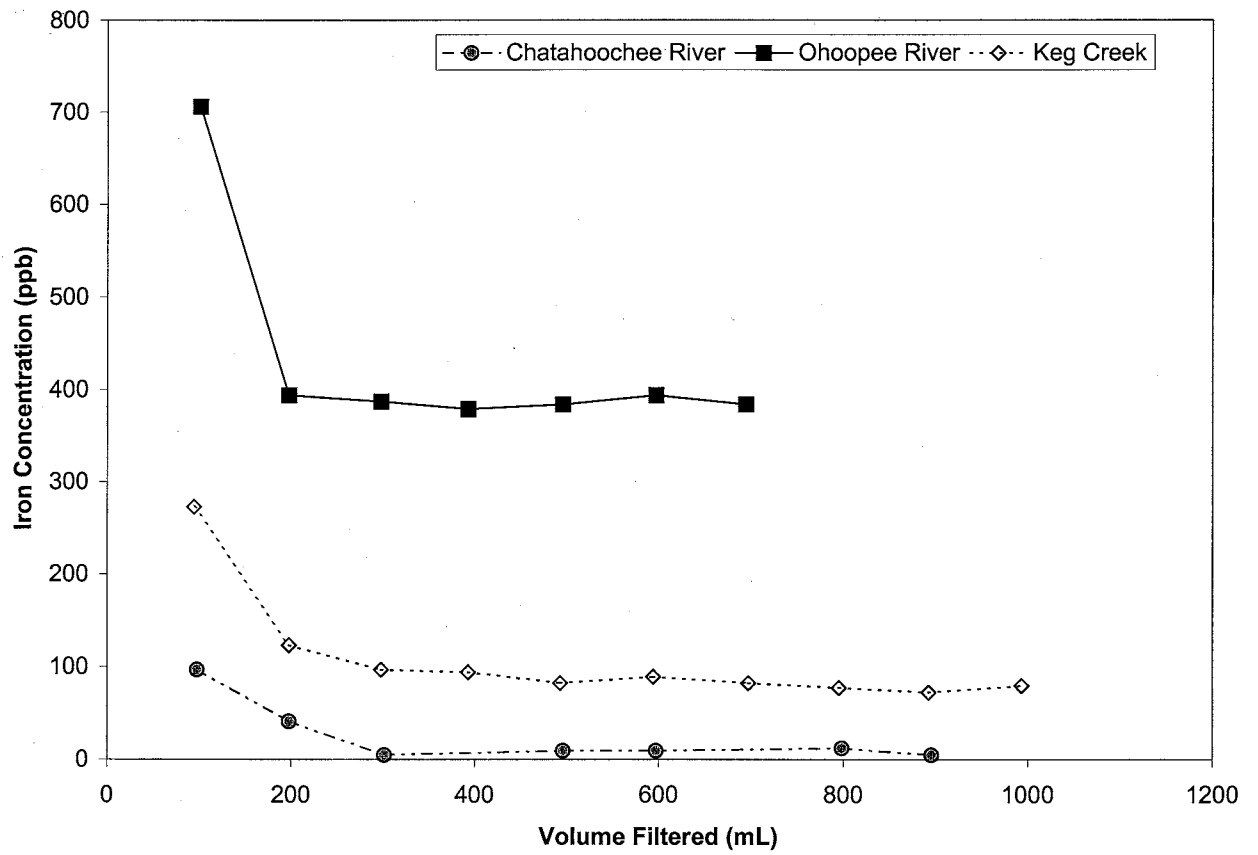


**Figure 4 -** Variation of iron concentration with increasing filtrate volumes for three rivers. Filtration performed with a Microfiltration System 0.45  $\mu\text{m}$  pore size/47 mm diameter filter paper (redrawn from Horowitz et al., 1992)

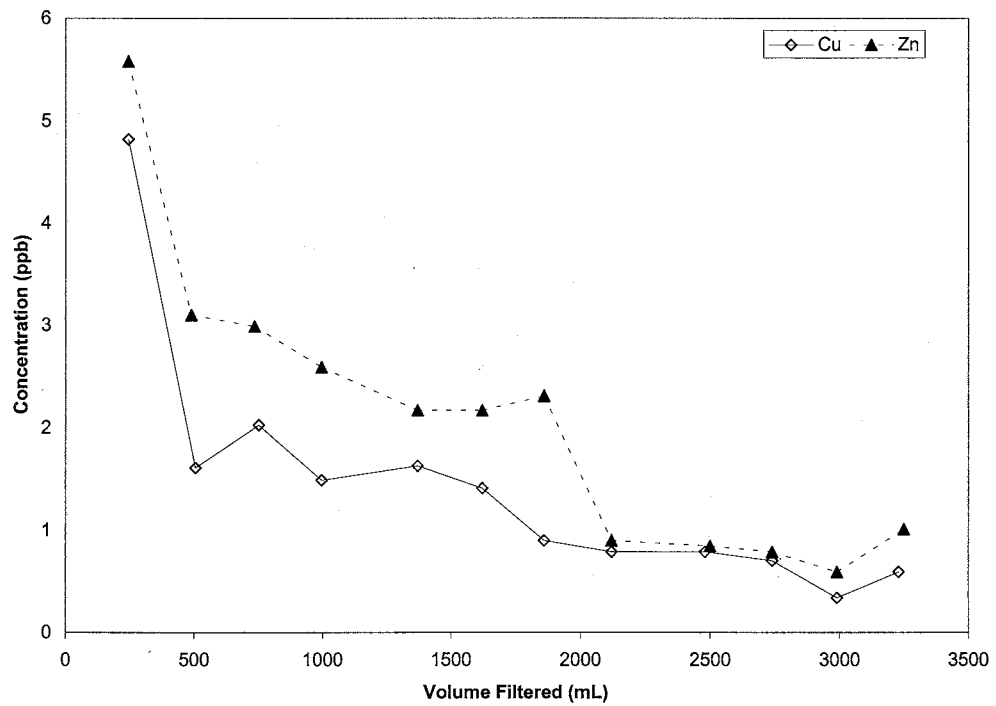
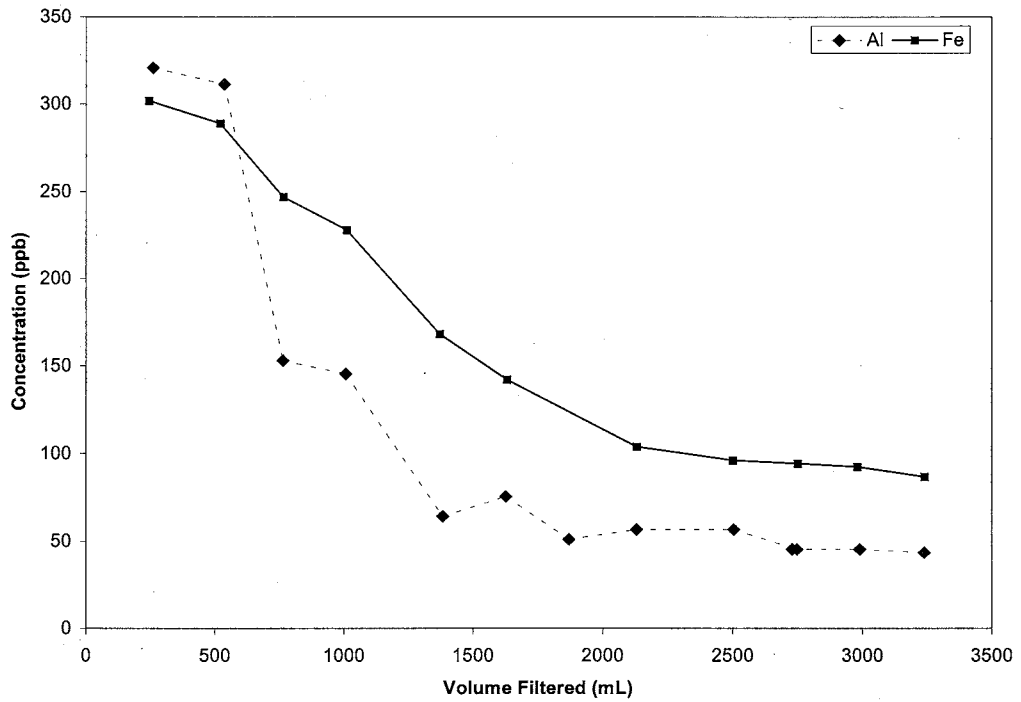


**Figure 5-** Variation of Al, Fe, Cu, and Zn concentrations with increasing filtrate volumes for the Tangipahoa River at Robert, LA. Filtration performed with a Gelman Capsule filter (redrawn from Horowitz et al., 1996)

receiving urban runoff and treated sewage effluent. The values of the suspended sediment loads for these studies were not reported. However, Horowitz et al.'s (1996) study of the Mississippi River at St. Francisville, LA, and the Tangipahoa River at Robert, LA, reported suspended sediment loads of 157 mg/L and 39 mg/L respectively.

All the aforementioned studies clearly show a tendency for the concentrations of numerous trace elements in filtrate to decrease significantly as the filtered volume increases. When the results from these four studies (Danielson, 1982; Laxen and Chandler, 1982; Horowitz et al., 1992; Horowitz et al., 1996) (Figures 1 – 5) are compared with data from reverse osmosis experiments (Loeb, 1964; Matsuura, 1994) (Figures 6 and 7), there is a definite similarity. The solute concentrations in Figures 1 - 7 all decrease significantly as the amount of solution being filtered/hyperfiltered increases.

In an early filtration study, Briggs (1906) attempted to answer the same major questions that are still being asked today - how should water samples with high colloidal loads be prepared for chemical analysis? Briggs (1906) attempted to devise an easy and expeditious field method for removing suspended clay particles from water samples. After considering the processes of sedimentation, centrifugation, and flocculation, Briggs decided that filtration would be the easiest and quickest field method for removing suspended clay from water samples.

Briggs' (1906) attempts to design a field filtration unit capable of operating under a partial vacuum failed, so he abandoned this approach and pursued the idea of using a compressive pressure for field filtration. This ultimately led to the design of the first apparatus designed to filter water samples in the field (Figure 8). Briggs' filter cell

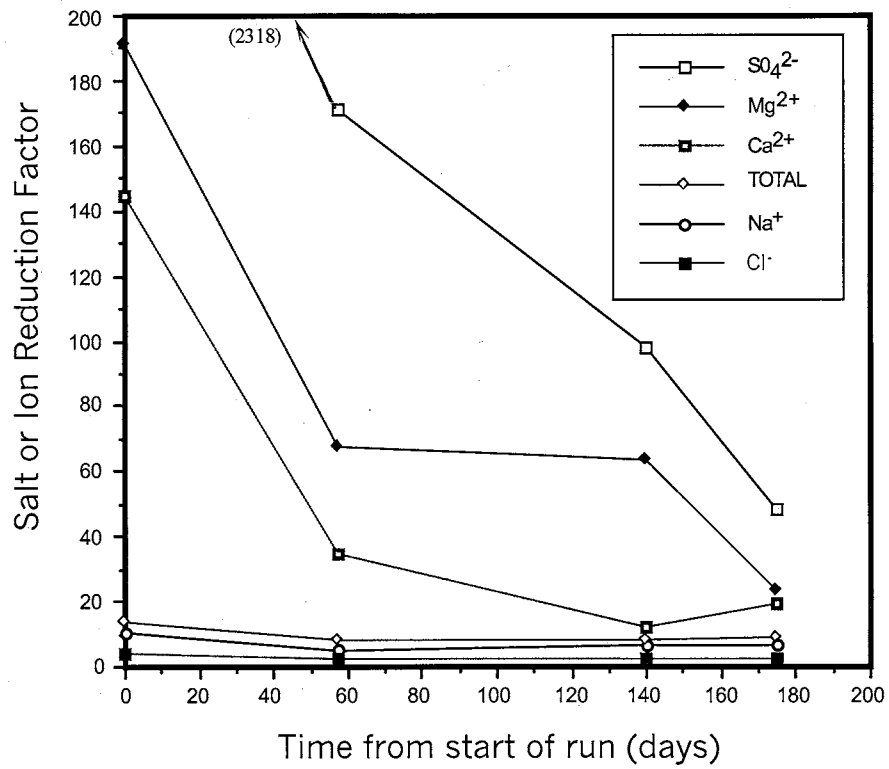


**Figure 6 -** Ion reduction factors for an early reverse osmosis field test using a 0.45  $\mu\text{m}$  cellulose acetate membrane (from Loeb, 1964). Crossflow configuration used in this study.

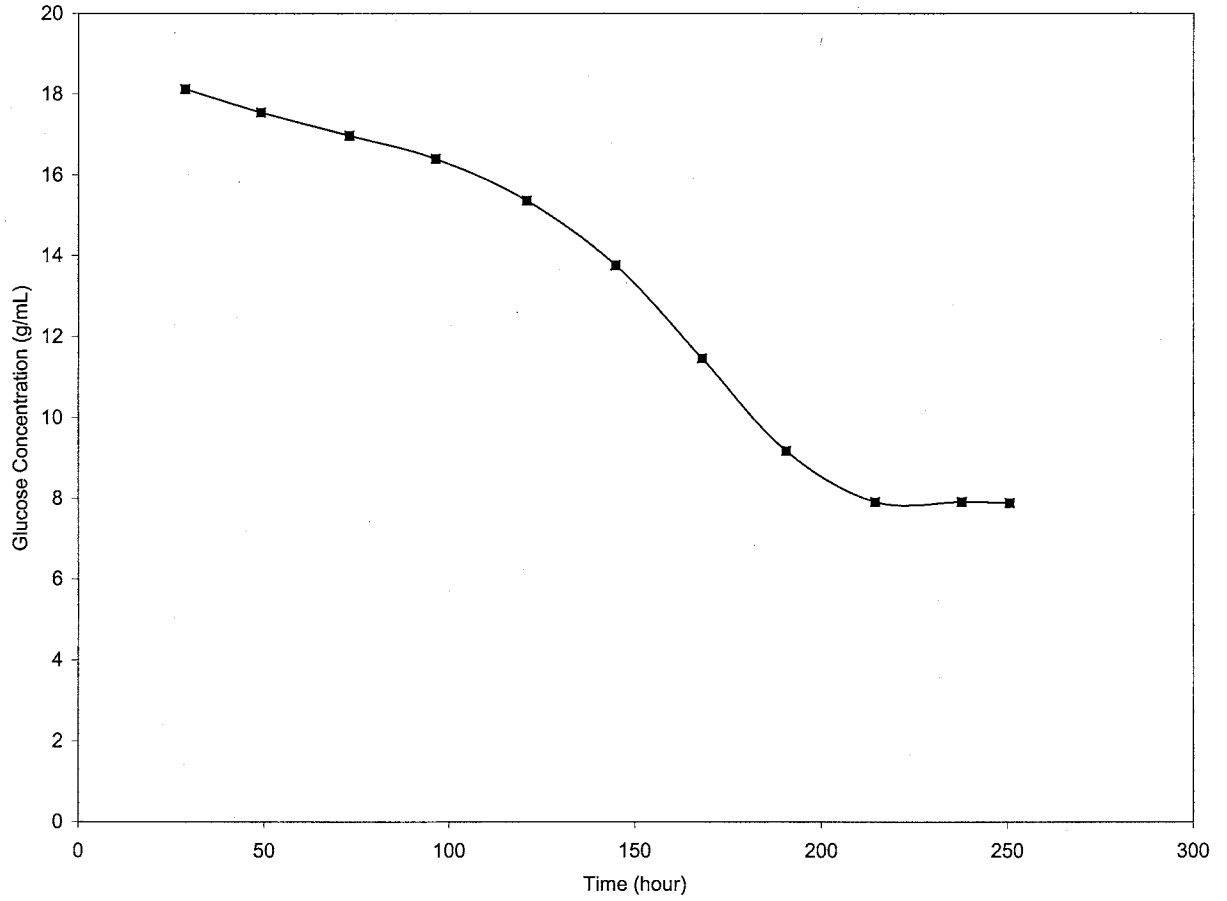


**Figure 7 -** Typical retention curve for a reverse osmosis system using a cellulose acetate membrane (from Matsuura, 1994). Crossflow configuration used in this study.

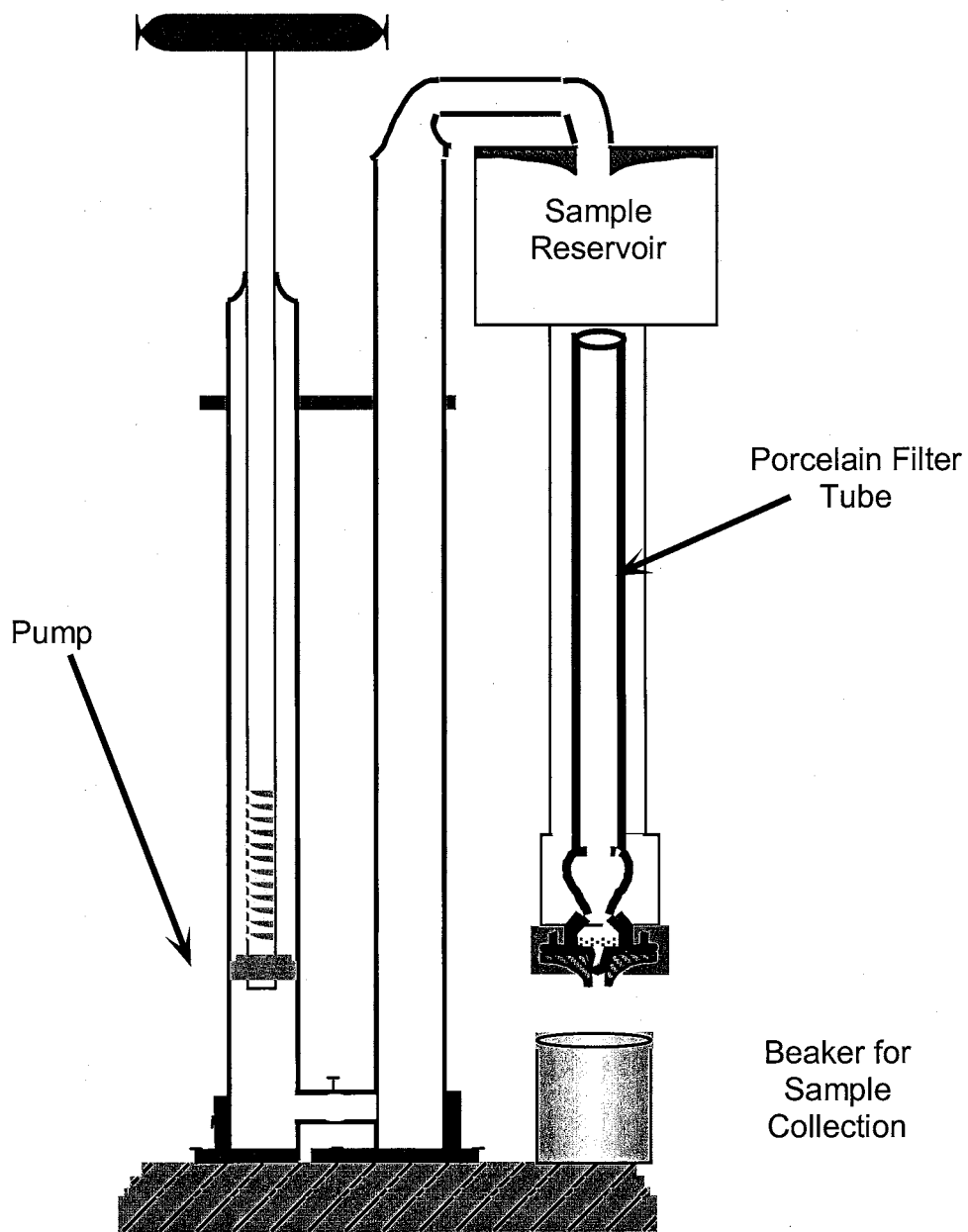


Figure 8 - Vertical cross-section of field filter cell used by Briggs (1906)



consisted of an unglazed porcelain tube closed at one end and cemented to a glazed porcelain cap at the other. The glazed porcelain cap fit into a rubber gasket. The sample was poured into Briggs' cell by disconnecting the reservoir from the air chamber and filling both the metal cylinder surrounding the filter tube and the reservoir with water. After filling the reservoir, the air chamber was reconnected and pressure applied using the hand pump.

After building the filter, Briggs (1906) examined the performance of his cell using simple binary salt solutions containing large amounts of suspended kaolinite. Briggs' cell efficiently removed the clay from the salt solutions. However, using a crude conductivity meter and titrations, Briggs (1906) found that the concentrations of the salts in solutions initially decreased and eventually returned to their actual concentrations (Figures 9 - 11). Briggs found that this effect was greatest for solutions composed of complex ions ( $\text{SO}_4^{2-}$ ,  $\text{HCO}_3^-$ ,  $\text{NO}_3^-$ ). As seen in Figures 9 - 11, the conductivity for these solutions decreased by up to 40% as the filtered volume increased.

Briggs' results show a remarkable similarity to the findings of McKelvey and Milne (1962) that examined the membrane properties of compacted clays. McKelvey and Milne (1962) forced a dilute sodium chloride (NaCl) solution through a compacted clay plug and measured the NaCl concentration of the filtrate. The trend shown in Figure 12 is typical of results from clay membrane studies. A thin layer of sediments, which, in some cases, contains a significant portion of clay minerals, often builds up during filtration of natural water samples. Numerous theoretical and experimental studies have shown that clays can act as membranes (McKelvey and Milne, 1962; Coplen and Henshaw, 1973;

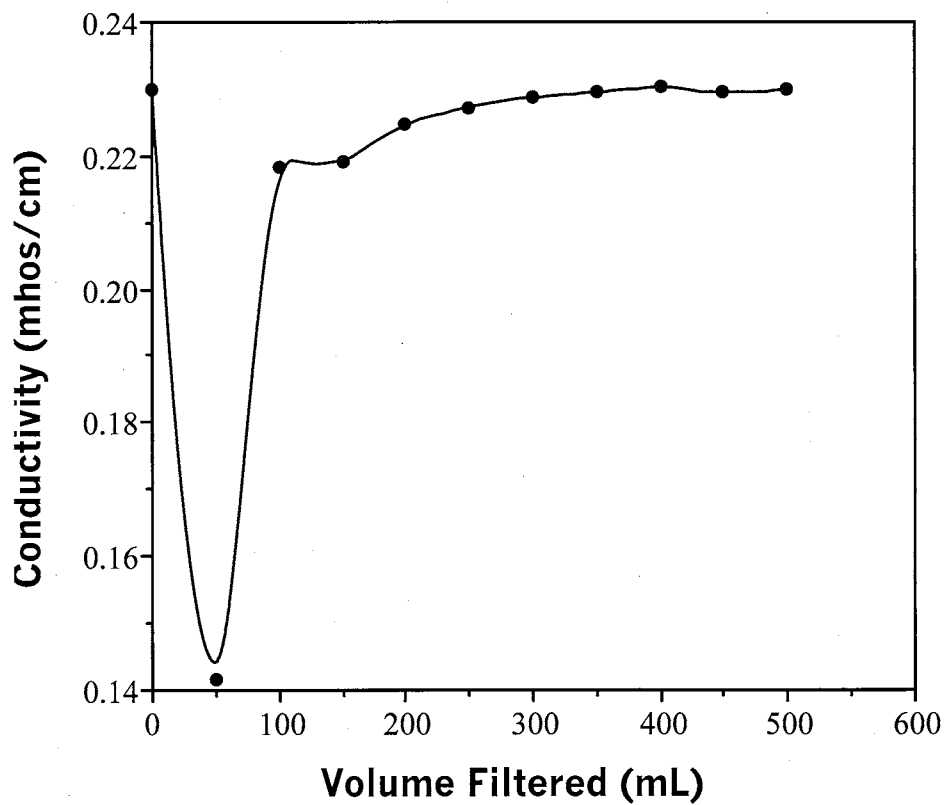


**Figure 9 -** Results of Briggs' filtration study for a 1.0 mN  $K_2SO_4$  solution (redrawn from Briggs, 1906)

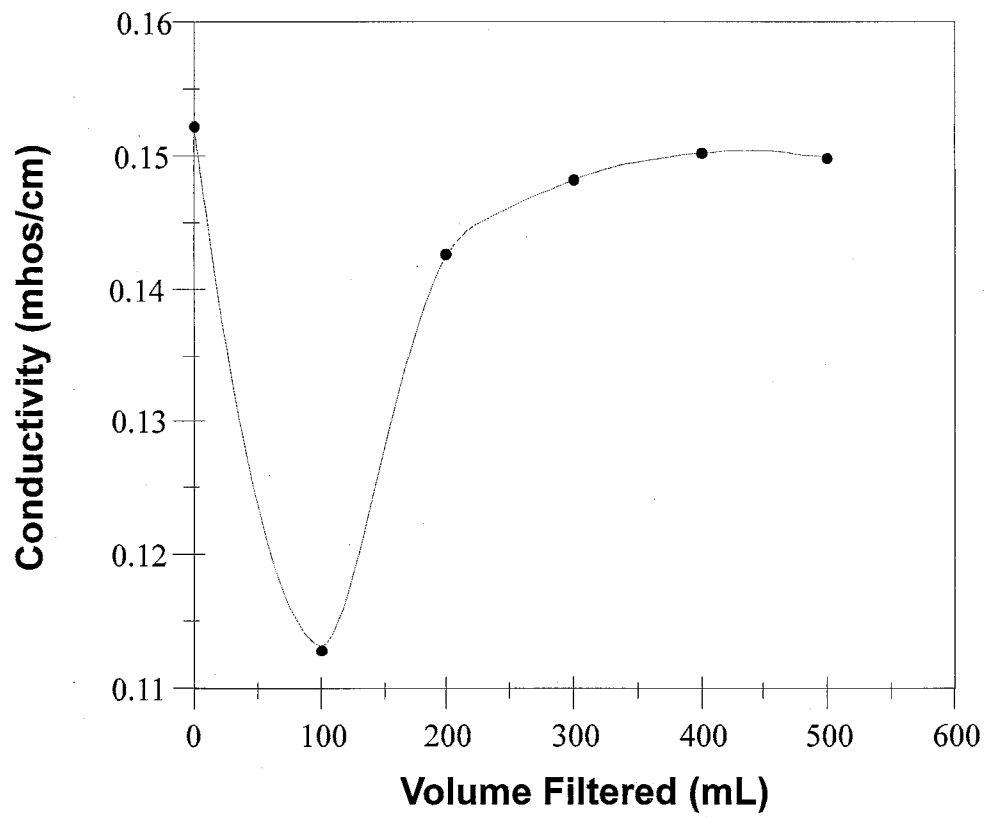


**Figure 10 -** Results of Briggs' filtration study for a 1.0 mN solution of  $\text{NaHCO}_3$  (redrawn from Briggs, 1906).

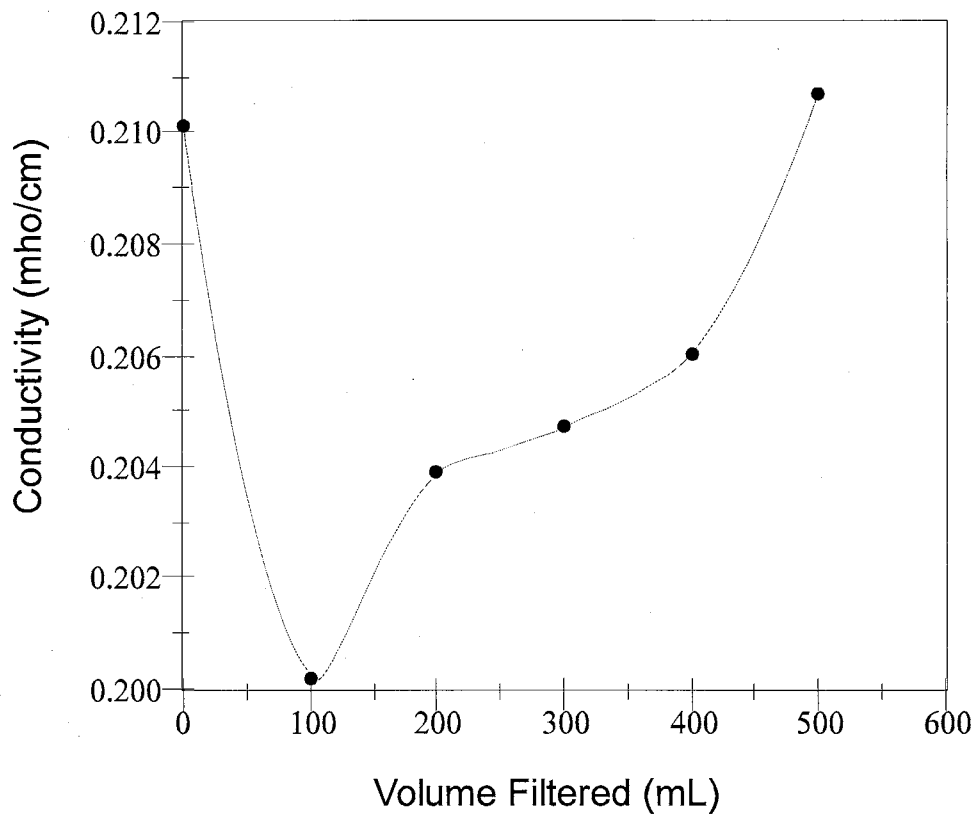


**Figure 11 -** Results of Briggs' filtration study for a 1.0 mN  $\text{KNO}_3$  solution (redrawn from Briggs, 1906).

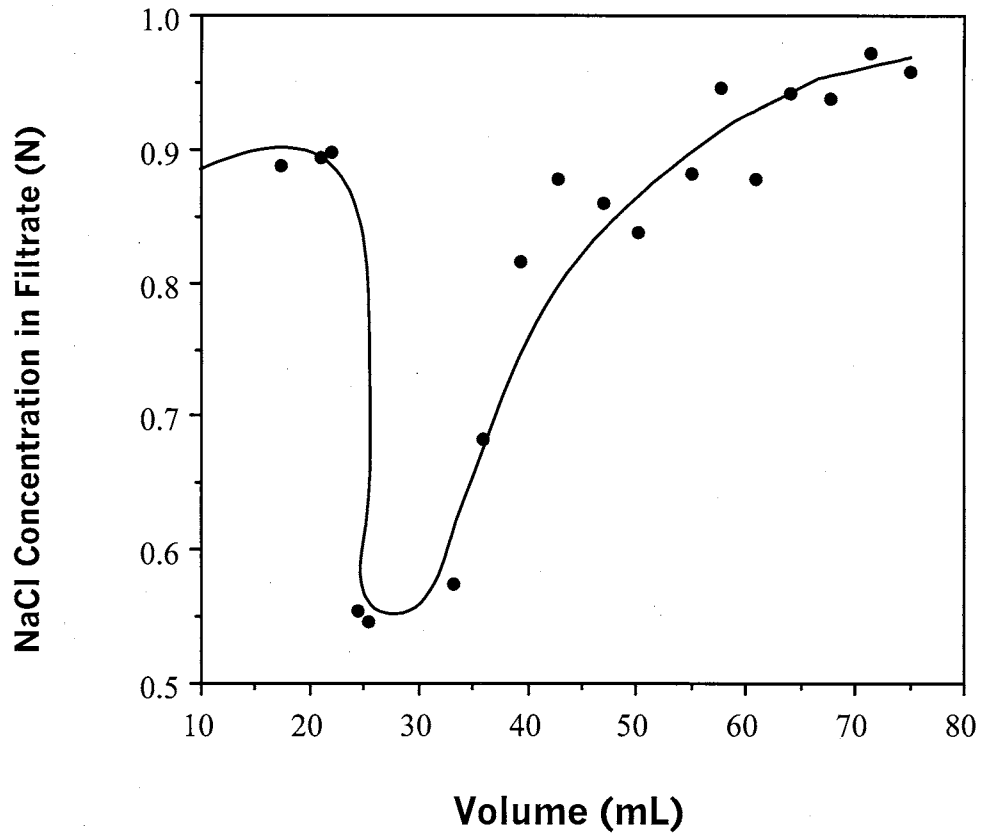


**Figure 12 -** Results of one experiment used to demonstrate the osmotic properties of a compacted clay plug - line added for purposes of comparison (redrawn from McKelvey and Milne, 1962)

Kharaka and Berry, 1973; Kharaka and Smalley, 1976; Marine and Fritz, 1981; Graf, 1982; Fritz and Marine, 1983; Fritz and Eady, 1985; and Whitworth and Fritz, 1994). Is it possible that this thin layer of sediment may be acting as a solute sieve during the filtration of natural water samples?

Horowitz et al. (1992) noted that concentrations of certain species in filtrate are significantly reduced as levels of suspended sediments in a water increase. Horowitz et al. (1992) concluded that filter clogging was the main reason for this trend. Horowitz et al. also stated that the suspended sediments created a highly effective "pre-filter" during sample filtration. This "pre-filter" may, in fact, be the accretion of a clay membrane.

The goals of this thesis are to (1) determine if the use of filtration to prepare natural water samples for chemical analysis is altering solute concentrations by the mechanism of solute-sieving and (2) to develop a sampling protocol that will lead to a more reliable way of sample preparation for the chemical analyses of natural waters.

## THEORY

### *Filter Effects on Concentrations of Dissolved Species*

Horowitz et al. (1992) stated, "existing filtration studies tend to examine one of two categories: chemical effects or physical effects." The studies involving the physical effects of filtration focus on the role of colloidal material which may pass through the pores of filter paper (Sheldon, 1972; Stumm and Billinski, 1973; Kennedy et al., 1974; Laxen and Harrison, 1981; Horowitz et al., 1989); these colloidal particles are often referred to as filtration artifacts and may cause up to an order of magnitude error in the reported concentrations of Al, Mn, Ti, and Fe (Kennedy et al., 1974). The basic approach of these studies has been to vary the effective pore sizes of the membrane filters used in sample preparation and examine the accompanying changes in the concentrations of trace metals.

All material in a water sample, which passes through a 0.45  $\mu\text{m}$  filter, is assumed to be dissolved (ASTM, 1992; APHA, 1992, USGS, 1994). This operational definition of "dissolved" material is not entirely true because there are a variety of fine organic and inorganic particles in natural waters that are capable of passing through a 0.45  $\mu\text{m}$  filter (Figure 13; Sheldon and Sutcliffe, 1969; Kennedy et al., 1972; Wagemann and Brunskill, 1975; Laxen and Chandler, 1982; Horowitz et al., 1992). This material is termed colloidal and can consist of particles ranging from 1 to 1000 nanometers (nm) in diameter (Shaw, 1989 and Hunter, 1993). Since the nominal pore size of filters typically used to filter natural water samples is 0.45  $\mu\text{m}$  (450 nm), it is easy to see that some colloidal material may pass through the filter while preparing a water sample for analysis.

Mineralogical (clay and hydroxide particles) and biological (bacterium) particulate are the two most common sources of filtration artifacts (Kennedy et al., 1972; Sheldon and Sutcliffe, 1972). Marine chemists have long known that the separation of suspended matter from seawater by filtration may affect the analytical determination of dissolved, inorganic species (Armstrong, 1958; Goldberg et al., 1952; Sheldon and Sutcliffe, 1969; Sheldon, 1972) and have used this arbitrary definition with some reserve (Grasshoff, 1976). Figure 13 compares the range of diameters for some colloidal particles with the pore sizes of typical filter media.

According to conventional wisdom, colloidal material passes through 0.45  $\mu\text{m}$  filters, biasing reported concentrations of Al, Mn, Fe, and Ti towards high levels (Kennedy et al., 1974; Laxen and Chandler, 1982; Horowitz et al., 1995). The inclusion of colloidal material in filtered samples has been called "the most significant factor affecting the concentrations of a number of trace elements in filtrate" (Horowitz et al., 1992). However, numerous studies examining the industrial process of filtration have shown that solids accumulating on the filter base significantly decrease the nominal pore size of a filter, and, in fact, the void space of these solids will eventually represent the true pore size of the filter. In addition, if certain sediments that accumulate on the surface of the filter during filtration do act as a membrane, reported concentrations of certain species might be biased towards lower levels. This possibility has not been previously investigated, even though the data of Briggs (1906) strongly suggests this may be the case.



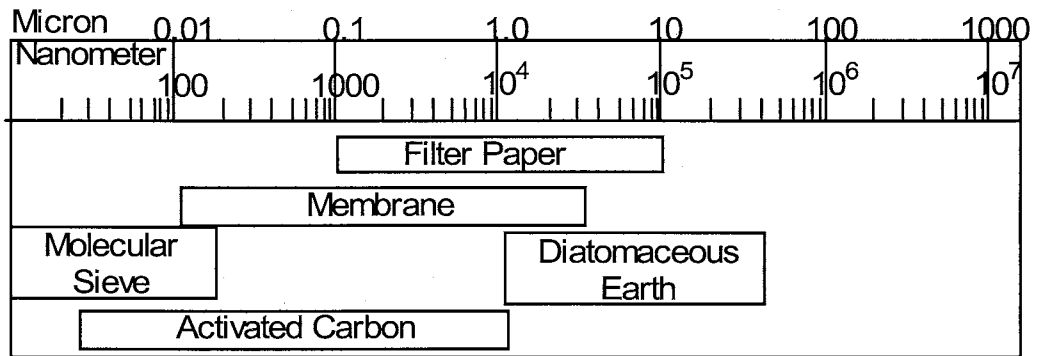
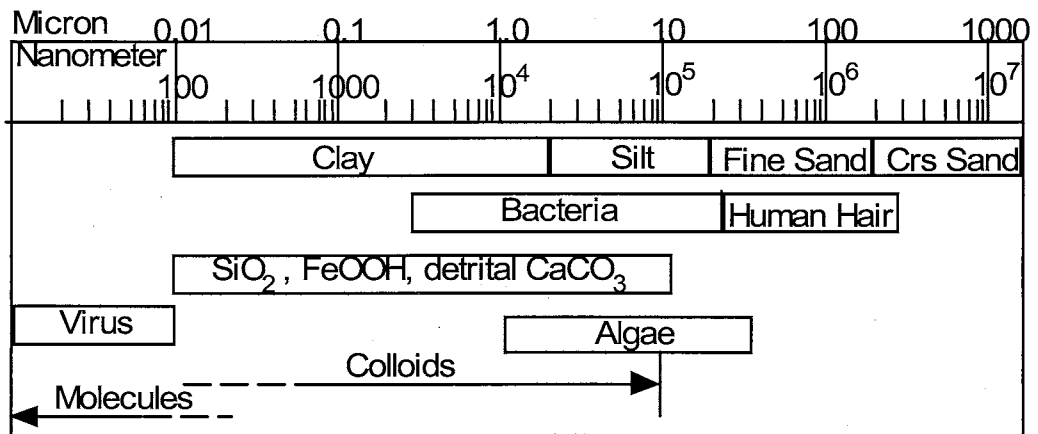


**Figure 13 -** Range of diameters for some colloidal particles and pore sizes of typical filter media (modified from Stumm and Morgan, 1981)

Filtration studies examining the chemical effects of filtration tend to emphasize possible sources of contamination associated with filtration, as well as methods used to minimize and eliminate these contamination sources (Wagemann and Graham, 1974; Mart, 1979; Cooney, 1980; Robertson, 1968; Laxen and Harrison, 1981; Nriagu et al., 1993; Spencer and Manheim, 1969; Benoit, 1994), and the adsorption of trace elements and species onto filters and filtration equipment (Meadows et al., 1978; Batley and Gardner, 1977; Jardine et al., 1986; Robertson, 1972; Liu et al., 1977; Walsh et al., 1988). These studies demonstrate that contamination of water samples can be negligible if a reasonable amount of care is taken. On the other hand, the adsorption of species onto filters and filtration equipment is somewhat difficult to quantify or eliminate and presents a considerable problem with regard to the analysis of trace metals in solution.

### ***Clays as Semi-Permeable Membranes***

Many of the studies examining filtration artifacts noted that the amount of water passing through the filter significantly decreased over time. All attributed this observation to the clogging of filter pores. Horowitz et al. (1992) stated that the accretion of sediments onto the filter seemed to act as a prefilter to the water. The waters examined by Horowitz et al. (1992) and Horowitz et al. (1996) all contained a significant amount of suspended clay particles. It may be possible that these clay particles settle onto the filter and act as a semi-permeable membrane.

Osmosis is defined as the passage of a pure solvent into a solution separated from it by a semipermeable membrane; a membrane permeable to the solvent but not the solute (Atkins, 1994). Using this definition the membrane would be perfect. This is seldom the

case (Fritz, 1986). Therefore, for the purposes of the current study, osmosis will be defined as the separation of two electrolyte solutions of different activities which results in a flow of the solvent from the electrolyte solution with the lower solvent activity to that of the higher (Figure 14 a). As the solvent flows into the chamber of Solution II, the level of Solution II increases until the flow of the solvent stops at some equilibrium point (Figure 14 b). The difference between the solution levels at this equilibrium point is often converted to hydrostatic pressure and called the osmotic pressure ( $\pi$ ) of the system. If an external pressure greater than  $\pi$  is applied to the chamber containing Solution II (Figure 14 c), the flow of the pure solvent is reversed; this implies that a less concentrated, or purer, solution will be produced in the chamber containing Solution I, while the chamber containing Solution II will be left with a much more concentrated solution. The process illustrated in Figure 14 c is termed reverse osmosis, or hyperfiltration and is the process by which potable water is produced from seawater in regions such as the Middle East.

Both clays and shales can act as semi-permeable membranes. Experimental studies have shown that clays can cause fractionation of both solutes and stable isotopes during hyperfiltration of solutions (McKelvey and Milne, 1962; Kharaka and Berry, 1973; Coplen and Hanshaw, 1973; Whitworth and Fritz, 1994) as well as other osmotic effects (Young and Low, 1965; Kemper and Rollins, 1966; Olsen, 1969). Although the vast majority of studies that examine the membrane properties of clays deal with compacted clay discs, loosely compacted clays can also act as membranes. Fritz and Eady (1985)

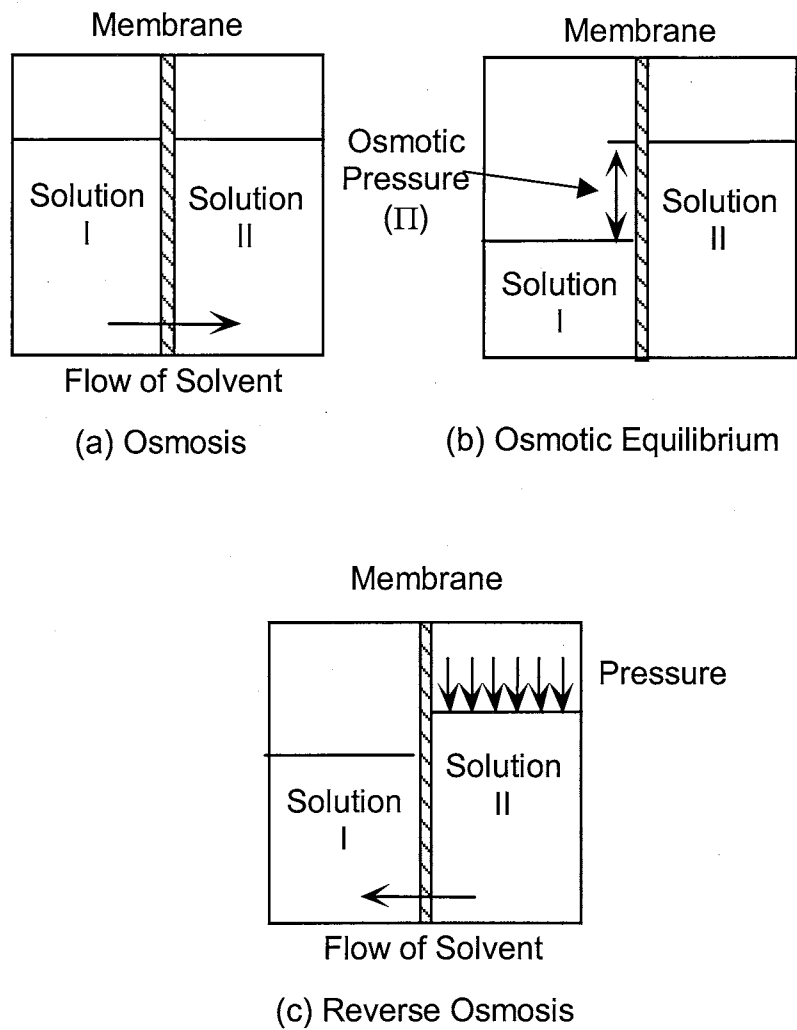


**Figure 14 -** Principles of osmosis, osmotic pressure, and reverse osmosis. Note that the activity of the solvent in solution I is much less than that in solution II ( $a_I \ll a_{II}$ ) (modified from Matsuura, 1994).

showed that a 12  $\mu\text{m}$  thick clay wafer aspirated onto filter paper can act as an effective membrane.

Hyperfiltration may also occur during filtration of waters with high colloidal loads as the colloidal particles clog the filter and form a layer of sediments over the filter base. This layer of sediments may cause solute-sieving to occur and might be responsible for the decrease in solute concentration with increasing filter loading.

Fritz and Marine (1983) described a one-dimensional hyperfiltration system in which all of the solution flux must pass through the membrane. This system is initially formed when an aqueous solution with a solute concentration of  $c_i$  is forced toward a membrane by some driving pressure (Figure 15 a). Since water will pass through the membrane more easily than the solute, the solute will begin to accumulate at the high pressure membrane interface (Fig 15 b), thereby forming a concentration polarization layer (CPL). As the CPL forms, the concentration at the membrane increases thereby allowing a greater amount of the solute at the high pressure interface to enter the membrane (Fig 15 c). As more solute enters the membrane, its efficiency decreases, causing the effluent concentration ( $c_e$ ) to increase (Fig 15 c). An equilibrium, or steady state, condition is eventually achieved in which both the influent and effluent concentrations ( $c_i$  and  $c_e$  respectively) are identical (Fig 15 d). At equilibrium, the membrane efficiency is zero. Although the membrane efficiency is zero at steady state, a CPL still exists at the high pressure membrane interface (Figure 15 d). Under steady state conditions, the CPL profile is constant (Fritz and Marine, 1983).

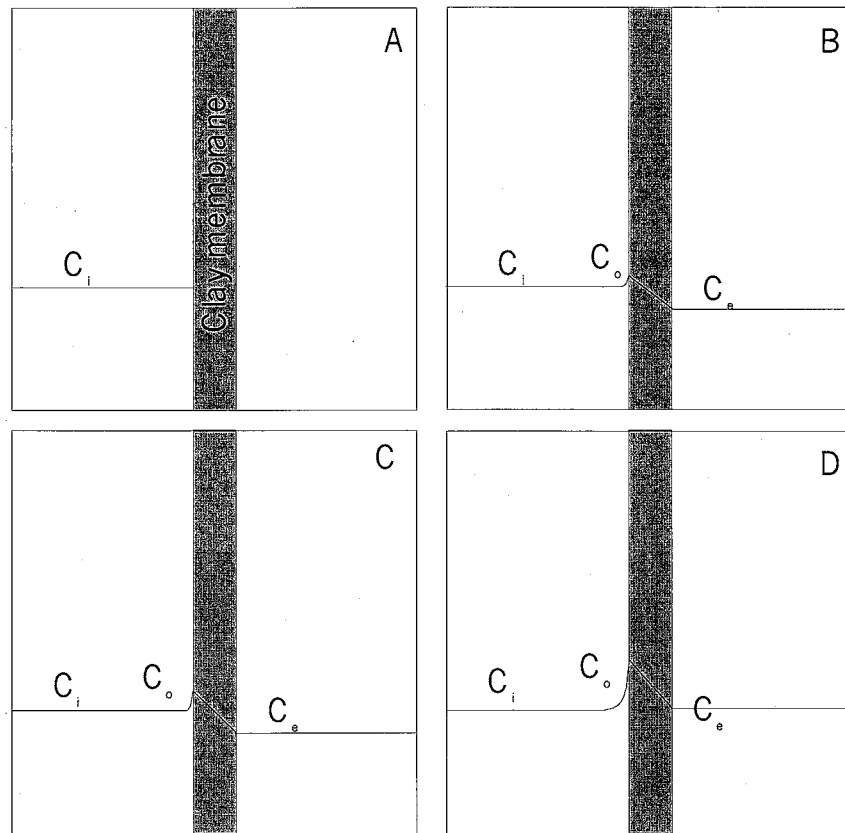


**Figure 15 -** Schematic diagram of the formation of the concentration polarization layer (CPL) in a static cell system. System has been rotated to the left  $90^\circ$  for ease of viewing (redrawn after Fritz, 1986).

showed that a 12  $\mu\text{m}$  thick clay wafer aspirated onto filter paper can act as an effective membrane.

The one-dimensional model of CPL development presented by Fritz and Marine (1983) gives us a first analogy to solute-sieving effects during filtration of natural waters due to sediment build up on the filter paper. The point of departure between Fritz and Marine's (1983) conceptual model and what may occur during filtration of natural waters is that in Fritz and Marine's model, the membrane is of constant thickness, while during filtration, the membrane thickness is constantly increasing.

Although numerous studies have examined the membrane properties of clays and shales, the two that did the best job of relating membrane theory to geological materials were probably Marine and Fritz (1981) and Fritz and Marine (1983). Marine and Fritz (1981) contains a description of a conceptual model of clays and shales acting as membranes which is used to explain anomalous hydraulic heads in a buried Triassic basin at the Savannah River plant near Aiken, South Carolina. Marine and Fritz focused on the concept of geological membranes, whereas Fritz and Marine (1983) presented many of the governing equations that explain and predict membrane properties. Fritz and Marine (1983) applied these governing equations, originally developed by Katalsky and Curran (1962), to both clays and shales.

Marine and Fritz (1981) attribute the membrane properties of clays and clay-rich sediments to the net negative surface charge of clay particles. This negative surface charge attracts cations onto the surface of the clay particles. Three major mechanisms have been established which lead to this net negative surface charge (Grim, 1968):

1. Broken bonds at the edges of the aluminosilicate units give rise to non-neutral charges.
2. Substitutions within the lattice by an ion of lower valence, such as  $Al^{3+}$  for  $Si^{4+}$  in the tetrahedral sheet or  $Mg^{2+}$  for  $Al^{3+}$  in the octahedral sheet result in a charge imbalance.
3. Dissociation of the hydrogen atoms of exposed hydroxyl groups. Replacement of these hydrogen atoms with a cation may also occur, but dissociation is the most probable mechanism for a net negative charge imbalance.

Bentonite and kaolinite are the clay minerals used in most membrane studies (McKelvey and Milne, 1962; Young and Low, 1965; Kemper and Rollins, 1966; Olsen, 1969; Kharaka and Berry, 1973; Coplen and Hanshaw, 1973; Whitworth and Fritz, 1994). Because there is little evidence of isomorphous substitution in kaolinite, broken bonds at the edges of the aluminosilicate units are the primary cause of a negative surface charge in this clay (Counts, 1975). The surface charge on kaolinite is highly pH dependent. At certain pHs, kaolinite essentially has a neutral charge. This pH is termed the zero point of charge (ZPC) for kaolinite and typically occurs below a pH of 5.5 (Marshall and Krinbull, 1942), which means that kaolinite particles suspended in most natural waters will typically have a slight negative surface charge. Grim (1968) stated that isomorphous substitution in smectite clays, such as bentonite, is responsible for over 80% of the net negative surface charge on the clay particles, with broken bonds and dissociation of hydrogen atoms from exposed hydroxyl groups contributing to the remainder of the negative surface charge.

The negative surface charge on the clay particles attracts cations that ultimately form a layer of positive charges on the clay particles (Figure 16). The formation of these adjacent layers constitutes an electrical double layer, which has been described in depth



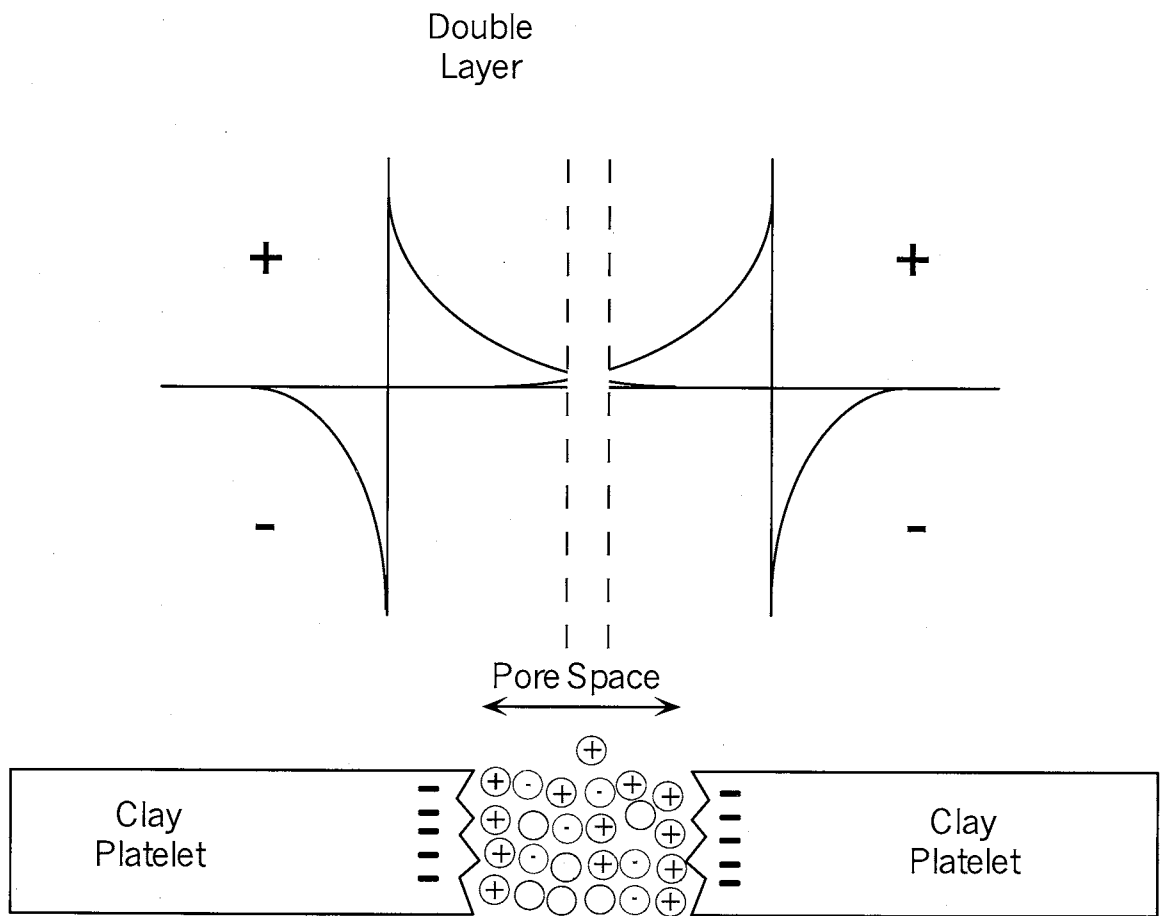


**Figure 16 -** Electrical double layer overlap in a clay pore (redrawn from Marine and Fritz, 1981)

by Guoy-Chapman Theory and the Stern Model of the Double Layer (Shaw, 1980). The concentration of cations decreases away from the mineral surface until the concentrations

of cations and anions, and thus the charge density, are identical to that of the bulk solution. This ambient condition usually exists in the middle of the clay pore (Figure 16).

Compacted clay platelets often have overlapping double layers, affecting all charged species in solution (Marine and Fritz, 1981). When this overlap occurs, the cations become the dominant species in the pore space and repel other cations that attempt to enter the pore. Anions are similarly repelled by the negative surface charge on the clay platelets. Water, being neutral in charge, does pass through the clay pores. This is the mechanism that causes the clay to act as a membrane - it allows the passage of solvent, while retarding the passage of the solute.

There are three mathematical models used to describe membrane processes: a solution-diffusion model, an irreversible thermodynamic model, and a fine pore model (Matsuura, 1994). Although there are inherent advantages and disadvantages to each of these approaches, the vast majority of studies concerning the membrane properties of clays have used the solution-diffusion approach. Fritz and Marine (1983) presented perhaps the most thorough explanation of the solution-diffusion model and its pertinence to geological applications.

The following derivation of the governing equations for the steady state, solution-diffusion model of membrane transport were first developed by Katchalsky and Curran (1965) and later applied to geological media by Fritz and Marine (1983). The governing equations describe a system with a unidirectional flux perpendicular to the membrane face, with fluxes measured in a positive manner from right to left.

The flux of dissolved ions through the clay membrane shown in Figure 17 is described by the following relationship:

$$\frac{\partial C}{\partial t} = -\nabla J_m = -\frac{\partial J_m}{\partial x} \quad (1)$$

where  $C$  = concentration of solute (moles/cm<sup>3</sup>)  
 $J_m$  = salt flux through membrane (moles/cm<sup>2</sup> sec)

The ions exiting the membrane at the low pressure interface,  $x_e$ , is the difference between salt ions advected toward the membrane by hydraulic forces ( $J_s$ ) and the salt ions diffusing away from the high pressure interface ( $J_d$ ) which is expressed as

$$J_m = J_s - J_d \quad (2)$$

Both fluxes ( $J_s$  and  $J_d$ ) are measured in units of moles/cm<sup>2</sup> sec. The flux of salt ions advected towards the high pressure interface ( $J_s$ ) is equal to the solution flux,  $J_v$  (cm/sec), multiplied by the concentration of the solution,  $C$  (moles/cm<sup>3</sup>), as seen in the following relationship

$$J_s = J_v C \quad (3)$$

By assuming that the diffusion of salt ions away from the high-pressure interface is only in the x-direction, the diffusive flux ( $J_d$ ) is described by Fick's Law

$$J_d = -D \frac{\partial C}{\partial x} \quad (4)$$

where  $D$  = diffusion coefficient of the solute in the x direction (cm<sup>2</sup>/sec)

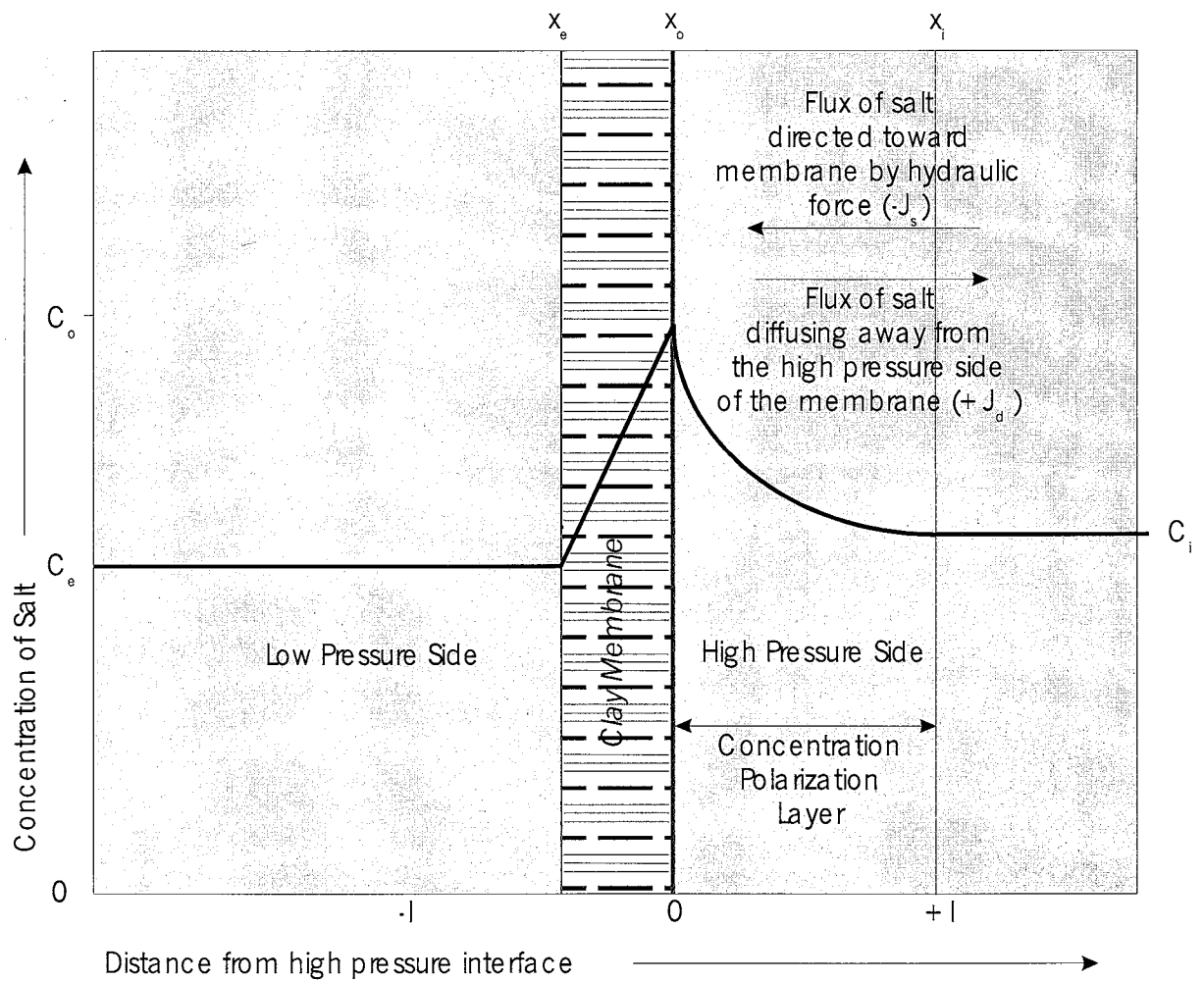


**Figure 17 -** A conceptual diagram of hyperfiltration through a clay membrane located between two highly permeable units in a static cell system (redrawn from Fritz and Marine, 1983). Note: There is also a flux of salt through the membrane.

By combining Equations (2) and (4) and substituting them back into Equation (1), we obtain the following relationship

$$\frac{\partial C}{\partial t} = -J_v \frac{\partial C}{\partial x} - D \frac{\partial^2 C}{\partial x^2} \quad (5)$$

Under steady state conditions  $\frac{\partial C}{\partial t} = 0$ , Equation (5) can be simplified to

$$\frac{d^2 C}{dx^2} = -\frac{J_v}{D} \frac{dC}{dx} \quad (6)$$

Integrating Equation (6) and combining all integration constants yields

$$\frac{dC}{dx} = A \cdot \exp\left(\frac{-J_v x}{D}\right) \quad (7)$$

where A = integration constant

As stated earlier, the concentration of the solute exiting the membrane at the low pressure interface ( $C_e$ ) and the concentration of the solute entering the membrane at the high pressure interface ( $C_o$ ) are both constant at steady state. Fritz and Marine (1983) used this fact to define the steady state filtration coefficient, K as

$$K = \frac{C_e}{C_o} \quad (8)$$

The filtration coefficient for each membrane is a dimensionless constant, which ranges from 1.0 for porous media with no membrane properties to zero for ideal membranes.

Under steady state conditions, the solute flux leaving the membrane at the point  $x_e$  equals the solute concentration at the low pressure interface multiplied by the advective solution flux at steady state,  $J_v$ , expressed by

$$J_m = C_e J_v \quad (9)$$

Solving Equation (8) for  $C_o$  and substituting it into Equation (9) yields

$$J_m = (C_o K) J_v \quad (10)$$

By substituting Equations (3) and (4) into Equation (2), the steady state solute flux ( $J_m$ ) at the high pressure interface,  $x_o$ , can be expressed as

$$J_m = J_s - J_d = C_o J_v + D \frac{dC}{dx} \quad (11)$$

Further substitution of Equation (10) into Equation (11) yields

$$C_o K J_v = C_o J_v + D \frac{dC}{dx} \quad (12)$$

Solving Equation (12) for  $\frac{dC}{dx}$  and evaluating the expression at  $x = 0$  yields the relationship

$$\left( \frac{dC}{dx} \right)_{x=0} = - \frac{C_o (1 - K) J_v}{D} \quad (13)$$

Equations (7) and (13) are equivalent expressions for  $\frac{dC}{dx}$ . By setting both expressions equal and evaluating them at  $x = 0$ , the integration constant,  $A$ , in Equation (7) is found to be

$$A = - \frac{C_o (1 - K) J_v}{D} \quad (14)$$

By substituting this expression for  $A$  back into Equation (7), we obtain

$$\frac{dC}{dx} = - \frac{C_o (1 - K) J_v}{D} \exp\left(\frac{-J_v x}{D}\right) \quad (15)$$

By definition,  $\frac{dC}{dx}$  is the slope of the CPL at any distance,  $x$ , from the high-pressure interface. Equation (15) can be evaluated at any point  $x$  away from the high

pressure membrane interface for the slope of the CPL at that point. In addition, Equation (15) can be integrated in order to determine the solute concentration at any point along the CPL as a function of the variable  $x$ . Integrating Equation (15) yields

$$C(x) = C_o(1 - K)\exp\left(-\frac{J_v x}{D}\right) + B \quad (16)$$

where  $C(x)$  = solute concentration at any point along the CPL

$B$  = second constant of integration

Marine and Fritz (1983) evaluated the second integration constant,  $B$ , by realizing that at the point  $x_i$  the solution concentration is not affected by the CPL and is equal to the bulk solution concentration  $C_i$ . Using this idea, Fritz and Marine (1986) developed a boundary condition for Equation (16) which stated that at  $x = x_i$ ,  $C(x_i) = C_i$  which, when applied to Equation (16), led to

$$C(x_i) = C_i = C_o(1 - K)\exp\left(-\frac{J_v x_i}{D}\right) + B \quad (17)$$

Solving Equation (17) for  $B$  yields

$$B = C_i - C_o(1 - K)\exp\left(-\frac{J_v x_i}{D}\right) \quad (18)$$

Substituting this value of  $B$  back into Equation (16) gives an expression for the solution concentration at any distance away from the high pressure interface

$$C(x) = C_o(1 - K)\left[\exp\left(\frac{-J_v x}{D}\right) - \exp\left(\frac{-J_v x_i}{D}\right)\right] + C_i \quad (19)$$

Equation (19) can be used to evaluate the solute concentration at the high pressure interface,  $C_o$ , by using the boundary condition  $C(0) = C_o$  at  $x = 0$ , which yields

$$C_o = \frac{C_i}{K + (1 - K)\exp\left(\frac{-J_v x_i}{D}\right)} \quad (20)$$

The importance of Equation (20) lies in the fact that it relates the solute concentration at the high pressure membrane interface to the initial bulk solution concentration in the reservoir, the steady state solution flux, and the diffusion coefficient of the salt ions. In other words, all major variables used to describe one-dimensional reverse osmosis behavior are included in this relationship. However, since K is a function of  $C_o$ , Equation (20) cannot be used alone to solve for  $C_o$  as an unknown.

In addition to the above derivation, Fritz and Marine (1983) discuss four relationships, originally developed for biological applications by Kedem and Katchalsky (1963) and Staverman (1952), which are useful for describing membrane properties of porous media. Using non-equilibrium thermodynamics, Kedem and Katchalsky (1963) developed the following two relationships for  $J_s$  and  $J_v$  in an isothermal, isoelectric system

$$J_v = L_p \Delta P - \sigma L_p \Delta \Pi \quad (21)$$

and

$$J_s = C_s (1 - \sigma) J_v + \omega \Delta \Pi \quad (22)$$

- where  $\Delta P$  = hydraulic pressure difference across membrane (dyne/cm<sup>2</sup>)  
 $\Delta \Pi$  = theoretical osmotic pressure capable of being generated across membrane due only to solution properties (dyne/cm<sup>2</sup>)  
 $C_s$  = mean solute concentration across membrane (mole/cm<sup>3</sup>)  
 $L_p$  = permeability coefficient of membrane (cm<sup>3</sup>/dyne sec)  
 $\omega$  = diffusion coefficient of solute across membrane, also called the solute permeability coefficient (moles/dyne sec)  
 $\sigma$  = reflection coefficient (dimensionless)



The reflection coefficient,  $\sigma$ , is defined as the ratio of the observed osmotically induced hydraulic pressure,  $\Delta P$ , to that calculated solely from solution properties,  $\Delta \Pi$  (Staverman, 1952). According to Fritz and Marine (1983), the variable  $\sigma$  is measured when the solution flux toward the high pressure membrane interface,  $J_v$ , is zero. The reflection coefficient is expressed as

$$\sigma = \left( \frac{\Delta P}{\Delta \Pi} \right)_{J_v=0} \quad (23)$$

Fritz and Marine (1983) define osmotic efficiency as the reflection coefficient,  $\sigma$ , expressed in terms of a percentage value. Ideal membranes have a reflection coefficient of one and an efficiency of 100 percent. Porous media with no membrane properties have a reflection coefficient of zero, or an efficiency of zero percent.

Fritz and Marine (1983) developed an alternate approximate expression for the reflection coefficient in terms of the solute concentration entering and exiting the membrane

$$\sigma = \frac{C_o - C_e}{C_o + C_e} \quad (24)$$

When using the above relationship, the reflection coefficient for an ideal membrane is also one - the solute concentration exiting the membrane is zero ( $C_e = 0$ ), thereby making  $\sigma$  in Equation (24) equal to one. For media with no membrane properties, the solute concentration exiting the membrane is equal to that entering the membrane ( $C_e = C_o$ ), thereby making  $\sigma$  in Equation (24) equal to zero.

Although the Fritz and Marine (1983) model is the most complete analysis of geological membranes to date, there are problems associated with it because many of the

variables must be measured in-situ. Although the literature is full of examples of geological membrane systems (Bredehoeft et al., 1963; Hanshaw and Hill, 1969; Hanshaw, 1972; Marine and Fritz, 1981), there has yet to be a comprehensive study that relates the governing equations of membrane transport to actual field conditions. Despite this shortcoming, the concept of geological membranes does show the potential to explain many different subsurface phenomena, and as this study will demonstrate, may be present during filtration of many natural waters.

### ***Classical Filtration Theory***

In the literature regarding the filtration of natural waters, few studies mention any aspect of the physical laws that govern filtration (Horowitz et al. 1996; Spencer and Manheim, 1969; Robertson, 1968; Laxen and Harrison, 1981; Danielson, 1982; Laxen and Chandler, 1982). Before examining the effects of filtration on the chemistry of natural water, it is helpful to have a firm understanding of the basics of filtration theory.

Filtration is defined as the separation of suspended solids from a liquid by passage through a pervious medium (Dickey, 1960). In order for filtration to occur, the following items must either be present or produced by this process: a filter, a filter base, driving pressure, filtrate, and filter resistance. A filter is the pervious medium upon which the suspended solids accumulate and through which the filtrate must pass. The filter base supports the filter and often consists of a porous frit or some other type of support. The filter resistance is a result of the frictional drag of the filtrate as it passes through the filter cake and filter. The driving pressure forces the filtrate through the filter and is a function of the resistance caused by both the filter and the cake of suspended

solids that accumulate on the filter. This driving pressure is a sum of the external pressure applied and the hydrostatic head of the solution being filtered. The maximum pressure during filtration occurs at the interface between the filter cake and solution.

Chemical engineers have long described solid-liquid filtration in terms of four mechanisms: filter medium filtration, depth filtration, cake filtration, and permeability filtration (Dickey, 1960). However, in all actual filtration processes, a combination of two or more of these mechanisms may be present. A combination of these mechanisms can be accounted for by adjusting the mathematical analysis of the process to consider all mechanisms involved, or by assuming that the dominant mechanism is the only one contributing to the filtration process (Akers and Ward, 1977).

Filter medium filtration is defined as filtration dependent only upon the pore size of the filter. The only particles retained in this case are those particles larger than the pore size of the filter; all smaller particles are allowed to pass through the filter and are considered part of the filtrate. This mechanism is relatively uncommon and describes the filter as nothing more than a sieve. Examples of this process are the retention of fine particles on woven filter cloths or the screening of large particles by a screen.

Depth filtration is similar to filter medium filtration in that filtration is due only to the filtering medium. However, a depth filter will retain particles smaller than the filter pores. A depth filter may be considered a wound filter cartridge or a packed sand bed supported on a screen or mesh. During the initial periods of operation, depth filters retain larger particles on the upstream side of the filter and retain finer particles as the filtrate travels toward the downstream portion of the filter. As the depth filter is loaded with more and more solids, the filtration resistance increases until the cartridge must be

replaced or the sand bed cleaned out. This build up of filter resistance is due to the deposition of finer particles onto the larger particles retained on the upstream side of the filter. When the deposition of these finer particles begins to occur, the upstream portion of the filter will begin to exhibit greater amounts of particle retention until complete blockage occurs.

Depth filters are usually constructed with a graded porosity, with the finest pores located on the downstream side of the bed and the coarsest located on the upstream side. Both depth and media filtration are used when only a small amount of solids are present in solution to avoid the blockage of pores and subsequent reduction in filtrate flux.

Cake filtration is the most commonly used industrial filtration process and is very similar to what occurs during filtration of natural water through a 0.45  $\mu\text{m}$  filter. The term cake filtration describes the continuous accumulation of solids to such a great degree that a "cake," or layer, of solids is deposited onto the filter media. The accumulation of these solids continues until the filter chamber is completely filled or the resistance caused by the filter cake causes the flow rate of the filtrate to drop below an acceptable level. Due to its similarity with the filtration of natural waters, this approach for describing the filtration of natural waters will be used here to help quantify the filtration of natural waters with a 0.45  $\mu\text{m}$  filter.

Permeability filtration is a simplified version of cake filtration. Unlike cake filtration, permeability filtration describes the separation of a solid-liquid mixture by filtration through a bed of permeable material with fixed dimensions. The dimensions of the bed are constant throughout filtration and are not significantly altered by the

accumulation of solid particles. In the mid-1800s, Poiseuille used the analogy of flow through a capillary tube to describe filtration theory and developed the relationship

$$V = \frac{P\pi r^4}{8\mu l} \quad (25)$$

where

- V = volume of filtrate
- P = pressure drop across capillary
- r = radius of capillary
- $\mu$  = coefficient of viscosity
- l = length of capillary

By assuming that capillary length and bed thickness were equal, Poiseuille attempted to model filtration data using Equation (25). Poiseuille eventually failed to adequately describe filtration data using Equation (25), but his work did illustrate the dramatic effect that a decrease in pore size would have on filtration resistance, as measured by the volume of filtrate passing through the filter.

D'Arcy using the empirical relationship he used to describe the flow of water through porous media led to Equation (26) subsequently modeled filtration.

$$u = \frac{KP}{L} \quad (26)$$

where

- u = velocity of water
- K = permeability of porous bed to water
- L = thickness of filter bed

D'Arcy later modified this empirical relationship to describe the flow of any fluid through a bed of porous material yielding

$$q = \frac{dV}{d\theta} = \frac{kAP}{\mu L} \quad (27)$$

where

- q = flow rate,  $\frac{dV}{d\theta}$
- $\theta$  = time of filtration

$A$  = cross-sectional area of filter cake  
 $k$  = intrinsic permeability of filter cake  
 $\mu$  = dynamic viscosity of fluid  
 $L$  = bed thickness

This form of D'Arcy's Law can be further modified to include a filtration resistance term. Filtration resistance can be thought of as the difficulty with which a liquid passes through a filter and filter cake. In this sense, filtration resistance is the inverse of the property of permeability, which is often defined as the ease with which a fluid passes through porous media. Thus, filtration resistance ( $\alpha$ ) is often defined as the inverse of permeability (i.e.  $\alpha = \frac{1}{k}$ ). By using the idea of filtration resistance in D'Arcy's Law, we can rewrite Equation (27) as

$$\frac{dV}{d\theta} = \left(\frac{1}{\alpha}\right)\left(\frac{AP}{\mu L}\right) \quad (28)$$

where  $\alpha$  = average specific cake resistance

Equation (28) is an idealized description of filtration through a porous bed of fixed thickness,  $L$ ; however, the mechanism of cake filtration describes a bed of porous material with a constantly changing thickness. It is possible to describe cake filtration by modifying Equation (28) to eliminate the thickness term,  $L$ . In order to eliminate the thickness term from Equation (28), one must assume that each layer of cake that is deposited onto the filter is identical to the previous layer. After making this assumption, one can describe the total volume,  $V$ , of filter cake deposited as either

$$V = LA \quad (29)$$

where  $L$  = final thickness of filter cake  
 $A$  = cross-sectional area of filter cake

or

$$V = vV' \quad (30)$$

where  $v$  = volume of cake deposited per unit volume of filtrate  
 $V'$  = total volume of filtrate collected

By equating Equation (29) and (30), we can solve for the thickness term,  $L$ , as

$$L = \frac{vV}{A} \quad (31)$$

By substituting Equation (31) back into Equation (28), we are left with

$$\frac{dV}{d\theta} = \left(\frac{1}{\alpha}\right) \left(\frac{A^2 P}{\mu v V}\right) \quad (32)$$

For a constant pressure filtration, the variables in Equation (32) can be separated and integrated to yield

$$\theta = \left(\frac{\alpha \mu v}{2A^2 P}\right) V^2 \quad (33)$$

Although Equation (33) does correctly imply a parabolic relationship between filtration time and filtrate volume, it did not adequately describe time-discharge data for early filtration experiments. Sperry (1916) pointed out that this form of the filtration equation failed to account for the filtration resistance produced by the filter itself. Sperry (1916) felt that the total filtration resistance was the sum of the resistance provided by the filter and the filter cake acting in series. In order to account for the resistance due to the filter, Sperry (1917) developed the following empirical relationship

$$\frac{dV}{d\theta} = \frac{PA^2}{\mu(\alpha vV + R_m A)} \quad (34)$$

where  $R_m$  = the resistance due to the filter with dimensions of  $L^{-1}$   
 $\alpha$  = average specific cake resistance with dimensions of  $L$

2

Separating variables in Equation (34) and integrating over a constant pressure filtration yields

$$\theta = \frac{\alpha v \mu}{2PA^2} V^2 + \frac{\mu R_m}{PA} V \quad (35)$$

which can be rewritten as

$$\frac{\theta}{V} = \left( \frac{\alpha v \mu}{2PA^2} \right) V + \frac{\mu R_m}{PA} \quad (36)$$

Equation (36) is written in the form of a straight line, with a slope of  $\frac{\alpha v \mu}{2PA^2}$  and a y-intercept of  $\frac{\mu R_m}{PA}$ . By plotting  $\frac{\theta}{V}$  vs.  $V$  for experimental filtration data, one can evaluate both  $\alpha$  and  $R_m$  by computing the slope and y-intercept and using equation (36) to solve for the remaining two unknowns,  $\alpha$  and  $R_m$  (Sperry, 1917). Equation (36) is known as the Sperry Rate Equation and was the first relationship to adequately relate all of the principle variables used in cake filtration (Dickey, 1960). The Sperry equation can also be rewritten to include both the concentration of solids in the solution being filtered and the moisture content of the resulting filter cake (Perry, 1965), but Equation (36) is



the simplest form to deal with. Although the Sperry Rate Equation is purely empirical in nature and is technically valid only for filter cakes composed of incompressible particles, it is still the basic equation used by chemical engineers to analyze filtration processes and evaluate pilot scale tests.

Classical filtration theory was advanced further during later years by attempting to incorporate the factors of filter cake compressibility (Rietema, 1953; Ruth, 1935; Grace, 1953; Kottwitz and Boylan, 1958), cake porosity (Tiller, 1953; Tiller, 1955; Tiller, 1958; Tiller and Cooper, 1960), sedimentation of the suspended solids (Tiller et al, 1995), and the physical properties of the suspended particles (Carman, 1937; Ruth, 1946). Of these studies, the most practical advance came from Carman (1937) who related Kozeny's work on groundwater flow to filtration and developed the following relationship

$$\alpha = \frac{(1 - \varepsilon)^2 k S_o^2}{g \varepsilon^3} \quad (37)$$

where

- $\varepsilon$  = the porosity of the suspended solids
- $S_o$  = the specific surface of the particles
- $k$  = Kozeny constant, taken as 5.0 for constant pressure filtration
- $g$  = gravitational constant

Equation (37) is known as the Kozeny-Carman equation and is important because it allows the filtration resistance to be predicted solely from the properties of the suspended particles. Vajda (1990) who developed a set of dynamic equations to model the process of filtration presented a much more mathematically sophisticated interpretation of classical filtration theory. Vajda's (1990) treatment of filtration as a four step process resulted in a fairly complete mathematical expression for filtration; yet, the relationships

he developed cannot be solved analytically and rely heavily on the speed and accuracy of computer processors to provide meaningful results.

How does the preceding discussion of filtration theory relate to the filtration of natural waters through a 0.45  $\mu\text{m}$  filter? Simply put, every study examining the effects of filtration on water quality data has assumed that the 0.45  $\mu\text{m}$  membrane filter is the only medium of filtration at work. This is not necessarily the case - the accumulation of colloidal material onto the filter also acts as a filter. Sperry (1916) described this concept best in his classic paper entitled The Principles of Filtration:

*“At point A (Figure 18), a mixture is shown in a confined space and in contact with a filter base. Directly below is shown a receptacle to catch the filtrate. At the instant shown, filtration is at the very point of starting. Here can be observed the importance of the filter base, for at this step it comprises the entire filtering medium. At no other point in the process of filtration is this true. It initiates filtration, supplying for the first time being the porous mass which will later be composed mostly of solids from the mixture.*

*At point B (Figure 18), flow of the liquid through the porous mass has proceeded for a certain length of time. The liquid or filtrate has been collected in the receptacle below, while the solids, unable to pass through the porous mass with the liquid, are necessarily left as a deposit upon the filter base. The filtering medium now no longer consists of the filter base only, but of two parts, the filter base plus the deposited solids or cake.”*

- D. R. Sperry (1916)

The studies mentioned in this section were all on the cutting edge of research when they were first presented, and, in fact, are very applicable to the present day separation technology of filtration. However, filtration is presently viewed from a somewhat different perspective. Many of the studies published in recent years have focused on the accretion and interaction of colloidal material onto the upstream side of the filter.

### ***Modern Filtration Theory***

Modern filtration theory focuses on cake filtration. Most recent approaches to filtration theory have attempted to model the deposition of the solid particles at the high pressure filter interface (Blatt et al., 1970; Houi and Lenormand, 1986; Whitehouse et al., 1986; Pines et al., 1989; Schmitz et al., 1990; Vajda and Toros, 1990; Tassopoulos et al.,

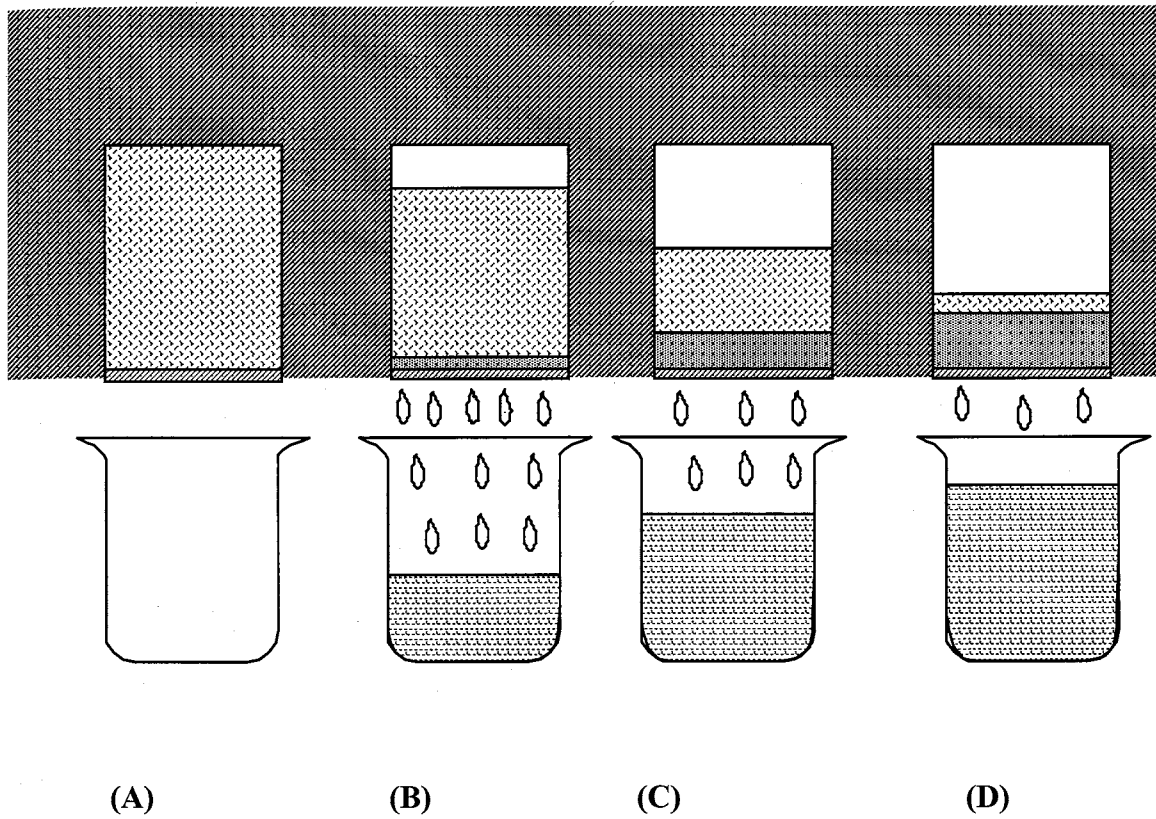


**Figure 18 -** The four stages of filtration (modified from Sperry, 1916)

1990; Sharma and Lei, 1991; Ding et al., 1993; Lu and Hwang, 1993; Denisov, 1994; Kozicki and Kuang, 1994; Bowen and Jenner, 1995; Lu and Hwang, 1995; Bowen and Jenner, 1996). The term filtration is presently used to refer to any pressure-driven

separation process for solid-liquid mixtures. These processes are classified as hyperfiltration, ultrafiltration, and microfiltration, depending on the membrane pore size and operating conditions (Song and Elimelech, 1995).

Microfiltration has long been considered a process which separates particles ranging in size from 0.02 to 10  $\mu\text{m}$  from a liquid suspension. The range of particle sizes covered by microfiltration is considered to be the upper end of membrane ultrafiltration theory and the lower end of classical particle filtration theory (Xu-Jiang, 1995). With this in mind, one can see that the filtration of natural waters with a 0.45  $\mu\text{m}$  membrane filter is in this gray zone between microfiltration and ultrafiltration (Figure 13). If the filter pore size is significantly reduced by the accumulation of solid particles onto the 0.45  $\mu\text{m}$  filter, then this standard separation process definitely falls into the regime of ultrafiltration. By extending this line of reasoning, if the sediments which accumulate onto the filter do indeed have membrane properties, then the filtration of these water samples may best be characterized by the process of hyperfiltration.

Membrane ultrafiltration is defined as a pressure-driven process which separates macrosolutes and colloidal particles which range from  $10^{-3}$   $\mu\text{m}$  to 10  $\mu\text{m}$  from a solvent or solution (Bowen and Williams, 1996). The colloidal particles involved in this process are quite diverse, ranging from metal oxides to whey to blood plasma. This process is often used to concentrate proteins in blood plasma and dairy products. The limiting factor in membrane ultrafiltration is the density of particles forming what is also termed a concentration polarization layer. An increased zone of concentration of solutes and particles forms at the membrane interface, thereby occasionally clogging the membrane. As with the process of reverse osmosis, this phenomenon is also termed the concentration

polarization layer (CPL). However, the CPL formed during filtration is typically composed of particles with a sharp distribution gradient, while the CPL formed during the reverse osmosis process is composed of dissolved species also with a sharply varied concentration distribution.

There are various models used to describe modern filtration theory: the inertial migration model (Altena and Belfort, 1984), the shear induced hydrodynamic convection and diffusion (Romero and Davis, 1988, 1990) models, the erosion models (Fane et al., 1982), the particle adhesion models (Mackley and Sherman, 1992), and the pore blocking model (Le and Howell, 1984). By far, the most popular models for describing the accumulation of solids at the high-pressure filter interface have been those which utilize the concept of a concentration polarization layer (CPL); these being the gel-polarization, or gel-layer, model (Blatt et al., 1970) and the osmotic pressure model (Vilker et al., 1981). The CPL was traditionally thought to occur only in the process of hyperfiltration; however, this phenomenon has been extended to the realm of ultrafiltration. According to Blatt et al. (1970), the concept and mathematical analysis of concentration polarization falls into three areas:

1. Diffusive ultrafiltration (reverse osmosis), usually involving microsolute in solution, and usually conducted at high pressures.
2. Ultrafiltration of macromolecules in solution (concentration, purification and fractionation of proteins, and dissolved polymers).
3. Ultrafiltration of colloids.

The concept of concentration polarization is important to modern filtration theory because it may hold the key to predicting both permeate rates and flux decline in crossflow and static filtration systems.

Blatt et al.'s (1970) gel-layer model was developed to examine and interpret experimental hyperfiltration and ultrafiltration data and attempt to expand upon existing microfiltration theory. The gel-layer model uses the inertial lift and rheology of colloidal particles and the concept of shear induced diffusion caused by the walls of the filtration cell to explain experimental data. The gel-layer theory begins with one mass balance equation. This equation has two unknowns, permeate velocity and the particle concentration distribution over the membrane, which makes solving the equation impossible without some assumptions. Blatt et al. (1970) developed their model largely from experimental results they observed during batch ultrafiltrations of proteins. As such, the gel-layer model is empirical in nature. The assumptions made in the gel-layer model are (1) there is a fixed surface concentration of solid particles on the surface of the membrane and (2) the mass transfer coefficients for impermeable surfaces are similar to heat transfer coefficients used in heat transfer theory. Neither assumption has been proven valid for either dead end or crossflow filtration, which is one of the largest shortcomings for this particular model. The gel-layer model is also unable to predict specific conditions resulting in a limiting flux for a filtration system. In addition, the gel-layer model does not apply to filtration systems with a pressure dependent permeate flux.

The osmotic pressure model of filtration (Vilker, 1981) also has fundamental problems similar to those of the gel-layer model, which may be why some regard both

models as fundamentally identical (Wijmans et al., 1985). The major shortcoming in this model also regards particle concentrations on the membrane filter -- the particle concentration in the CPL and the membrane must be estimated from empirical relationships.

One other recent approach to filtration theory which has gained some notoriety is the resistance in series model (Reihanian et al., 1983). This model was developed in order to explain the effects of increasing filter resistance with time and to predict the permeate flux at any point during a filtration run. Basically, this model assumes that the filter cake deposited onto the filter base consists of discrete layers of solid particles which are identical to each other. This particular model is ideal for constant pressure filtration of solid-liquid mixtures in which the particle size is fairly uniform. The model uses numerical methods in order to predict filtration resistance and permeate flux at any point during a constant pressure filtration. Results of numerical simulations using this approach match experimental results very well (Reihanian et al., 1983). However, this approach may not work for solid-liquid mixtures with non-uniform particle sizes.

Blatt et al. (1972) were the first to use the ideas of John Happel (Happel and Brenner, 1965) to describe the interactions of particles during filtration. In chapters six through eight of Happel and Brenner's 1965 text, Low Reynolds Number Hydrodynamics, John Happel developed a series of mathematical models used to explain the interaction of spherical particles suspended in a viscous fluid, the wall effects on the motion of a single particle suspended in a fluid, and the flow of a fluid relative to assemblages of spherical particles. Others (Song and Elimelech, 1995; Bowen and Jenner, 1995; Bowen and Williams, 1996) later extended these concepts and models to



describe filtration theory. In fact, many engineers presently refer to a dead end, or static, filtration cell as a Happel cell.

Filtration cells can also be constructed to perform crossflow filtration. Crossflow filtration describes filtration operations where the feed, or permeate, flow is parallel to that of the filtrate. Song and Elimelech (1995) presented a new approach for describing the concentration polarization of non-interacting spherical particles during crossflow filtration. Song and Elimelech (1995) used Happel's conceptual framework to develop a dimensionless parameter which describes the extent of concentration polarization as well as the behavior of the permeate flux during crossflow filtration. This dimensionless number, known as the filtration number ( $N_F$ ), is considered to be the ratio of the energy needed to bring a particle from the membrane filter surface to the bulk suspension over the thermal energy of the particle. The  $N_F$  is important in crossflow filtration because, for a given slurry and operational conditions, there will be a critical value of  $N_F$  which will determine whether or not a CPL exists above the membrane filter surface. When  $N_F$  is less than this critical value, a CPL is formed directly above the filter. However, when  $N_F$  is greater than the critical value a cake of solids will form between the CPL and the filter surface. Using Song and Elimelech's (1995) model, it is now possible to predict the extent of both the CPL and formation of a filter cake for any crossflow system without any simplifying assumptions.

Bowen and Jenner (1995) developed a dynamic model to describe the process of dead end filtration and the formation of a filter cake onto a membrane surface. Bowen and Jenner (1995) felt that the resistance of any filter cake is dependent upon the interparticle spacing between the deposited particles. They contend that this spacing is

largely due to the interactions between the particles. Bowen and Jenner used this basic idea to develop a dynamic model for the filtration of colloidal particles which uses electroviscous effects, entropic pressures, and extended Derjaguin-Landau-Verwey-Overbeek (DLVO) theory of colloidal stability to account for these important particle interactions. Bowen and Jenner (1995) combined the works of Kozeny (1927), Carman (1938), Happel (1958), and modern colloidal theory to derive a set of simultaneous equations that can be solved for the permeate flux as a function of time without any simplifying assumptions.

Bowen and Williams (1996) later compared this dynamic model with classical filtration theory and experimental data for the filtration of bovine serum albumin (BSA) with an average diameter of 3.20 nm. Bowen and Williams found that the dynamic model was significantly more accurate in predicting experimental results than classical filtration theory. Both the pH and ionic strength of the BSA solutions were varied in order to test the limits of the model. The only significant deviation between the model's predicted results and the actual experimental data occurred at high ( $\sim -40$  mV) zeta potential values. The Bowen and Williams study was a milestone in filtration - this was the first time that filtration rates of protein solutions were predicted prior to filtration solely from physicochemical data and operating conditions.

Since the physical properties of the colloidal load in natural waters can be quite similar to proteins (colloidal size, net surface charge, tendency to flocculate, etc.), the dynamic model developed by Bowen and Jenner (1995) may be helpful in modeling the process of the filtration of natural waters through a 0.45  $\mu\text{m}$  filter. Although the approach taken by Bowen and Jenner does show a great amount of promise in this regard,

it may be some time before the research regarding filtration of natural waters catches up with modern filtration theory.

The last major item of modern filtration theory concerns the structure of the filter cake. Whereas classical filtration theory doesn't discuss the structure of the solid particles onto the filter base, modern filtration theory regards this structure as a subject of great interest. Numerous studies have attempted to examine the structure and patterns of the particles composing the filter cake from both a theoretical and experimental point of view (Houi and Lenormand, 1986; Tassopoulos et al., 1989; Lu and Hwang, 1993).

Houi and Lenormand (1986) set the standard for these studies. Using a static cell filter apparatus designed by Lenormand et al. (1985), Houi and Lenormand (1986) were able to videotape the deposition of glass, risan, and polystyrene particles ranging from 2 to 100  $\mu\text{m}$  in size onto a filter base during the process of microfiltration. After closely examining these videotapes, Houi and Lenormand found that the colloidal particles consistently developed a filter cake with a dendritic morphology (Figure 18). Combining these observations and the concepts of interparticle forces, Brownian diffusion, gravitational forces, and chemical interactions, Houi and Lenormand (1986) were able to develop a statistical model which could predict the two-dimensional morphology of a filter cake by using solution properties and operating parameters.

Working independently of Houi and Lenormand (1986), Tassopoulos et al. (1989) developed a discrete stochastic model which also predicted a dendritic morphology for filter cakes formed in static filter cells. The importance of Tassopoulos et al.'s work (1989) lies in the fact that they were the first to determine the pore size distribution for filter cakes in both two and three-dimensions. In addition, they also found that the

porosities of filter cakes are independent of the solid particle size and may be directly dependent upon the Peclet Number ( $P_e$ ) for the system.

Lu and Hwang (1993) built upon the work of Houi and Lenormand (1986) to describe a mechanism which may cause dendritic morphologies in filter cakes. Lu and Hwang (1993) used the concept of critical friction angles of particles to describe cake formation during constant pressure filtration. The size of the friction angle was used to develop a numerical program which was able to predict the positions and locations of deposited particles. This program was able to accurately simulate the structure of filter cakes and the variations of both permeate flux and filter resistance throughout numerous constant pressure filtration experiments.

The colloidal nature of suspended sediments in natural waters may be analogous to the colloidal material used in filtration studies. If this proves to be true, it may be possible to extend much of the work regarding filtration theory to the topic of filtering water samples with a 0.45  $\mu\text{m}$  filter. If, in fact, the colloidal material forms a cake on the 0.45  $\mu\text{m}$  filter, then this cake may be the prefilter noted by Horowitz et al. (1992). The natural water sample (the solute) must pass through this filter cake, which could make the interaction between the sediments and solute of paramount importance in explaining the adverse filtration effects noted by others (Danielson, 1982; Laxen and Chandler, 1983; Horowitz et al., 1992; Horowitz et al., 1996).

### ***Dialysis as a Solid-Liquid Separation Technique***

In the 1860s, Thomas Graham proposed that dialysis be used as the basic distinction between colloidal and "true" solutions. In Graham's experiments, suspended

colloidal material was retained on one side of a membrane formed into a bag while this bag was immersed in a wash solution. The colloids were retained inside the bag, while the solute present in the colloidal solution passed through the membrane and into the wash solution.

The process of dialysis is characterized by simplicity, gentle conditions, and adaptability to a range of scales from a few hundred microliters to several liters of solution (Saltonstall, 1992). Despite newer methods that can provide solid - liquid separation in orders of magnitude into the thousands, the simplicity and ease of dialysis have helped dialysis retain its popularity over the course of time.

The pores of a membrane used for dialysis must be large enough to allow the free passage of the solvent and solute molecules, while restricting the movement of colloidal material. The majority of dialysis membranes are made from cellophane, cuprophane, visking, or colloidun (a partially evaporated solution of cellulose nitrate in alcohol and ether). Pores are formed in these materials by a network of fibrils. The pore sizes of these membranes are described in terms of a molecular weight cut-off (MWCO) and can range from 500 to tens of thousands of daltons ( $1 \text{ Da} = 1 \text{ g/mol}$ ). The MWCO of a membrane is the size, or weight, of the largest molecule which is capable of freely passing through the membrane. Dialysis membranes are commercially available in the form of sheets or tubing. Dialysis tubing is very convenient to use, as it can be filled with a solution, tied off at both ends, and used as a bag. Prior to use, it is often necessary to rinse the dialysis tubing with deionized water several times to remove any soluble impurities associated with its manufacture.

Dialysis is, by definition, a diffusive process. Small molecules and ions migrate through the membrane due to the concentration difference between the solutions on either side of the membrane. The force which drives chemical species across the membrane is caused by a difference in chemical potential between the inside and outside of the dialysis tube. This chemical potential is expressed in terms of a concentration difference between solutions on either side of the membrane. If the solutions on both sides of the dialysis tubing are well mixed, the rate of dialysis for a chemical species is directly proportional to the concentration difference across the membrane and the membrane area, while inversely proportional to the membrane thickness, as seen in the following relationship (Hunter, 1994)

$$\frac{dC_i}{dt} = -\left(\frac{KA}{d}\right)(C_i - C_o) \quad (38)$$

where

- K = permeability of membrane
- A = membrane area
- d = thickness of membrane
- t = time since beginning of dialysis
- C<sub>i</sub> = concentration of chemical species inside dialysis bag
- C<sub>o</sub> = concentration of chemical species outside dialysis bag

A typical industrial application for dialysis involves the removal of an extraneous electrolyte from a sol. One of the most common examples of this is the removal of KNO<sub>3</sub> from AgI sol (Figure 19). Stirring accelerates this separation process. This stirring maintains a high concentration gradient across the membrane, thereby increasing the rate of electrolyte diffusion across the membrane.

### ***Centrifugation as a solid-liquid separation technique***

As seen in Table 1, the practical lower limit for sedimentation under gravity of particles suspended in an aqueous solution is approximately 1  $\mu\text{m}$ . Colloidal particles sediment so slowly under the forces of gravity that the effect is completely offset by the mixing tendencies of diffusion and convection (Shaw, 1980).

**Table 1 -** Sedimentation rates under gravity for uncharged spheres with a density of  $2.0 \text{ g/cm}^3$  in water at  $20^\circ\text{C}$  (Shaw, 1980)

Particle Radius	Sedimentation Rate
$10^{-9} \text{ m}$ (1 nm)	$2.2 \times 10^{-12} \text{ m/s}$ (8.0 nm/hr)
$10^{-8} \text{ m}$ (10 nm)	$2.2 \times 10^{-10} \text{ m/s}$ (0.8 $\mu\text{m/hr}$ )
$10^{-7} \text{ m}$ (100 nm)	$2.2 \times 10^{-8} \text{ m/s}$ (80 $\mu\text{m/hr}$ )
$10^{-6} \text{ m}$ (1 $\mu\text{m}$ )	$2.2 \times 10^{-6} \text{ m/s}$ (8.0 mm/hr)
$10^{-5} \text{ m}$ (10 $\mu\text{m}$ )	$2.2 \times 10^{-4} \text{ m/s}$ (0.8 m/hr)

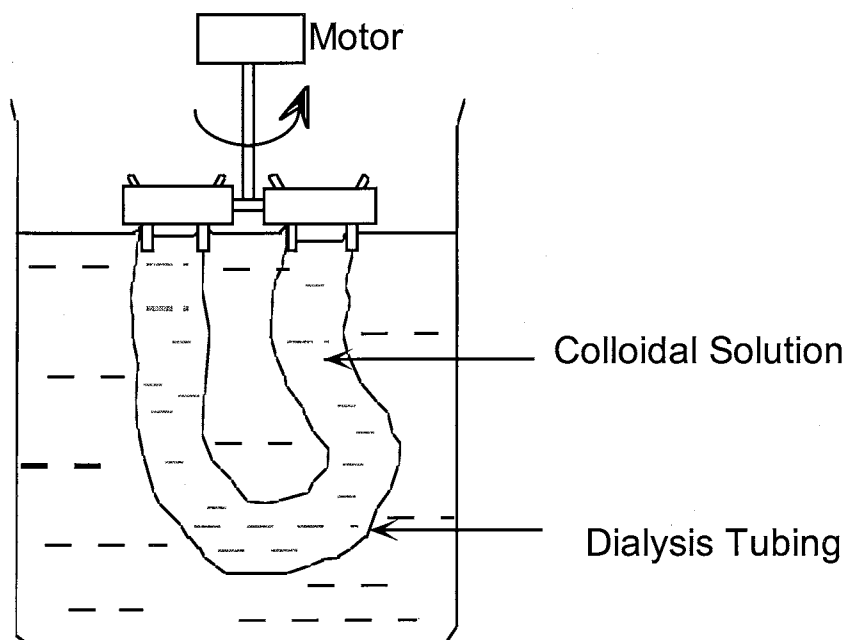


**Figure 19 -** Dialysis set-up used for the separation of  $\text{KNO}_3$  from AgI sol (Shaw, 1989)

By employing centrifugal forces instead of gravity, sedimentation can also be used as a solid-liquid separation method. A centrifuge increases gravitational forces on the particles in a colloidal suspension by spinning the entire sample at high angular velocities. This increase in gravitational force is termed the relative centrifugal force (RCF) and is expressed by the following relationship (Sorvall, 1968)

$$RCF = \frac{4\pi^2 r \omega^2}{32.6} \quad (39)$$

where RCF = relative centrifugal force, expressed in g  
r = radius of centrifugal chamber (ft)  
 $\omega$  = angular velocity of centrifuge (revolutions per second)

The above relationship can be quite useful. For example, a solution centrifuged at 10,000 rpm would be exposed to an RCF of 16,800 g. This RCF would be in excess of



the force necessary to settle particles larger than 0.1  $\mu\text{m}$  in diameter with a specific gravity of 2.5 (Jackson, 1956).

Using a centrifuge as a solid-liquid separation method is simple and expeditious in a lab setting. However, the major disadvantage to using centrifugation as a solid-liquid separation method for natural waters is the fact that each sample would have to be stored in a container and taken back to a laboratory for centrifugation. Such sample transportation practices have been shown to cause changes in the trace-metal chemistry of natural waters (Robertson, 1968).

## METHODS

This study was divided into lab and field phases. The lab phase examined the response of dilute clay/salt solutions to the solid-liquid separation methods of filtration, dialysis, and centrifugation. The field phase involved the filtration, centrifugation, and dialysis of water samples taken from local rivers.

### ***Lab Phase***

Both binary (single salt) and multicomponent solutions were mixed with varying amounts of sodium-saturated bentonite to simulate natural waters with different suspended sediment loads. These “synthetic natural waters” were then subjected to the processes of filtration, dialysis, and centrifugation in an effort to determine the effects of these separation techniques on the dissolved concentrations of the major cation and anion species present in solution.

Sodium-saturated bentonite was chosen to replicate the suspended sediment load of a natural water for three reasons: (1) clays are a common suspended sediment in natural waters; (2) bentonite is considered to have average membrane properties; and (3) cation exchange would be minimized in a sodium chloride solution with a sodium-saturated clay. A dilute sodium chloride solution was chosen to model a natural water with a low level of dissolved solids for two major reasons: (1) a sodium chloride would minimize the process of cation exchange with a sodium-saturated clay and (2) sodium chloride solutions have been shown to be minimally retarded by clay membranes. This minimal retardation allowed any membrane effects produced in the study to be attributed to the formation of a membrane.

## Preparation of Synthetic Solutions

A series of binary salt/clay solutions were prepared using NaCl, Type I deionized water, and sodium saturated Wyoming bentonite. Prior to preparing these solutions, roughly 100 g of NaCl was oven dried at 105°C for 24 hours and subsequently stored in a lab dessicator until used. The solutions all contained a similar amount of NaCl and deionized water, but the amount of clay added to each solution varied from 5 mg/L to 100 mg/L. A total of seven binary solutions were prepared with various clay loads (Table 2). Each of the binary solutions were prepared in the following manner:

1. Approximately 3000 g of deionized water and the appropriate amount of NaCl were placed in a clean 4.0 L stoppered glass container and mixed for a minimum of two hours with a magnetic stirrer.
2. Following this initial mixing period, approximately 50 to 100 g of the solution was pipetted into a preweighed Nalgene bottle and stored for later analysis. The concentrations of dissolved species in this sample are considered to be an accurate measure of the “true” dissolved concentrations of Na and Cl for the solution.
3. After correcting for any evaporation in the volume of the initial sample, a small amount of bentonite was weighed and added to the dilute solution. After adding the clay to the salt solution, the entire solution was mixed for a period of twelve to twenty four hours to allow the clay to fully mix with the solvent.

**Table 2 -** Suspended Solids Concentrations of Binary Solutions Used in Study

Solution No.	Deionized water (g)	NaCl (mg)	Clay (mg)	Suspended Solids Concentration (mg/L)	NaCl Concentration (mg/L)
1	2944.21	45.30	283.90	98.61	15.37
2	3187.40	52.40	232.10	74.34	16.44
3	2962.12	46.50	143.22	50.06	15.70
4	3292.55	50.10	79.50	24.91	15.22
5	3262.57	50.20	47.10	14.98	15.39
6	3337.72	58.20	32.20	10.00	17.44
7	3317.39	49.60	16.90	5.29	14.95

A series of multicomponent solutions with varying clay loads were also synthesized in order to examine the effects of filtration on various dissolved species in water. The multicomponent solutions were prepared with sodium-saturated bentonite and tap water from Socorro, NM. The amount of suspended clay in the multicomponent solutions ranged from 100 mg/L to 495 mg/L (Table 3). Each of the multicomponent solutions were prepared in the following manner:

1. Approximately 1000 g of tap was poured into each of two clean 4.0 L stoppered glass containers.
2. A small amount of sodium saturated bentonite was added to one of the containers and mixed with a magnetic stirrer for a period of 12 hours.
3. The second container of tap water was also mixed with a sterilized magnetic stirbar for a twelve-hour period.
4. Prior to filtering the clay-tap water solution, three 20-mL samples were taken from the control solution and analyzed for alkalinity via titration with 3.0 mN H<sub>2</sub>SO<sub>4</sub>. A 50 mL sample of the control solution was also saved for later analysis.

**Table 3 - Suspended Solids Concentrations of Multicomponent Solutions Used in Study**

Solution No.	Tap water (g)	Clay (mg)	Suspended Solids Concentration (mg/L)
1	1001.45	102.59	102.45
2	1002.67	282.25	281.50
3	999.57	424.72	424.90

### Filtration of Synthetic Solutions

After preparing each of the synthetic solutions, approximately 1 L of each solution was filtered through a 47 mm diameter, 0.45  $\mu\text{m}$  pore size, Micro Filtration System (MFS) cellulose acetate filter using the cell shown in Figure 20. All filters used were soaked in a 10% nitric acid ( $\text{HNO}_3$ ) solution for twelve hours followed by two consecutive twelve hour rinses with Type I deionized water in order to eliminate possible contamination leaching out of the filter, as recommended by Benes and Steinnes (1974).

Each filtration was conducted under constant pressure using a compressed air source. The pressures for each filter run varied from 35 psi to 85 psi. Aliquots of filtrate were collected in preweighed Nalgene bottles. The volume of each aliquot was determined by weighing the bottle with the collected sample and subtracting the mass of the bottle from this measurement. Since the densities of the solutions were extremely close to 1.00 g/mL, the mass of each sample served as a very close approximation to the sample volume. Each aliquot was saved for later chemical analysis. In addition, the time required for the filtration of each aliquot was recorded in order to determine the resistance of the filter cake formed.

Approximately 10 to 15 mL of each aliquot filtered from the multicomponent solutions was separated into a separate 60 mL HDPE sample bottle and acidified with 1

mL of concentrated  $\text{HNO}_3$ . These samples were split and acidified in order to determine aluminum concentrations.

### Dialysis of Synthetic Solutions

The possibility of using dialysis to separate suspended solids from water samples has been explored as an alternative to filtration. Past studies (Benes and Stiennes, 1973; Benes and Stiennes, 1974) have shown that dialysis does show some promise as a method for solid-liquid separation in natural waters.

The dialysis cell used in this study (Figure 21) consisted of a bag made of a 10 to 25 cm long piece of Spectra/Por 1 Regenerated Cellulose (RC) dialysis tubing which was filled with Type I deionized water and tied in knots at both ends. The manufacturer of the tubing, Spectrum Microgon, lists the mean diameter of the pores in the tubing as 6 to 8 nm. The pore size for the tubing actually represents the molecular weight cutoff (MWCO), which is defined as the largest molecular weight of solute that will be retained by the tubing.

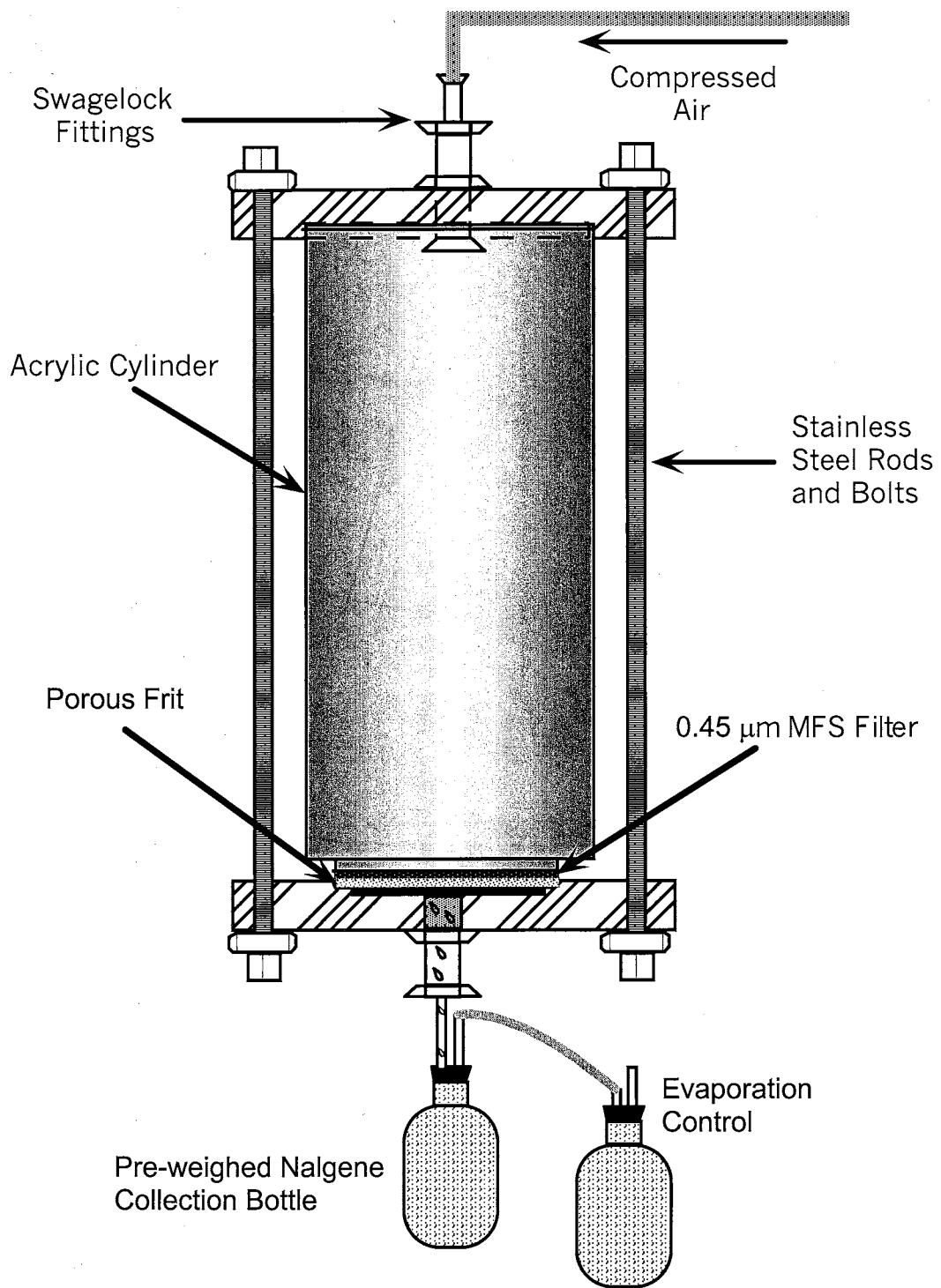


**Figure 20 -** Filter cell used in study

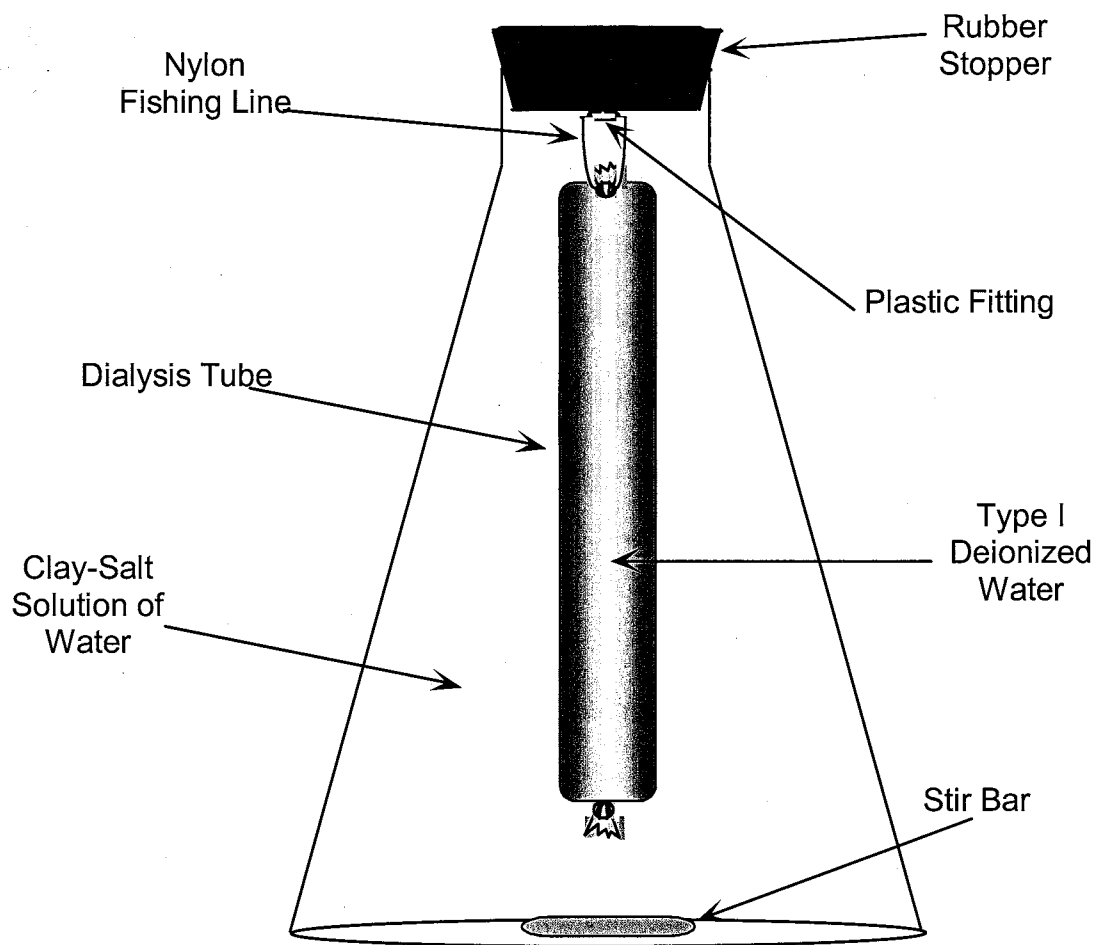


**Figure 21 -** Schematic diagram of dialysis cell used in study



Prior to constructing the dialysis cell, the tubing was soaked in 0.4 N sulfuric acid (H<sub>2</sub>SO<sub>4</sub>) for 24 hours followed by two consecutive 12-hour soakings in deionized water. The dialysis tubing is quite versatile and can be used in most pH and temperature ranges of natural waters (Table 4). Technical support personnel at Spectrum Microgon suggested this treatment in order to eliminate contamination from trace elements in the tubing (Table 5). In addition, the manufacturer recommends that the tubing soak in deionized water for a minimum of 24 hours to remove glycerin which coats the tubing. Unless otherwise stated, the dialysis tubing was handled with clean latex gloves to eliminate possible contamination.

**Table 4 -** Recommended conditions for Spectra/Por 1 RC dialysis tubing (Spectra-Por, 1994)

Variable	Range of Values
pH	2 - 12
Temperature	2 °C - 60 °C

**Table 5 -** Trace elements found in representative samples of Spectra/Por 1 RC dialysis tubing (Spectra-Por, 1994)

Trace Element Contained in Spectra Por 1 RC Dialysis Tubing	Concentration (ppm)
Cd	< 0.02
Cr	0.1 - 2.0
Cu	0.8 - 1.2
Fe	10 - 60
S	0.1% by mass
Mn	0.1 - 0.3
Ni	1.3 - 1.7
Zn	1.5 - 5.0
Pb	2.0 - 6.0

After filling the dialysis tubing with deionized water and tying off both ends, the tubing was tied to a plastic fitting which had been screwed into a rubber stopper and placed into a large mouthed 1000 mL Erlenmeyer flask (Figure 21). Fishing line was chosen as the most suitable material for tying the dialysis tubing to the rubber stopper. Other materials tested for this purpose proved unreliable and tended to contaminate the dialysis cell by falling apart in the cell solution.

Once the dialysis tubing was in place, approximately 900 to 950 mL of the clay-salt solutions were poured into the beaker and mixed with a magnetic stirrer in order to facilitate the dialysis process. The conductivity of the solution surrounding the cell was checked periodically and plotted against time in order to determine when the solutions in the cell had reached an equilibrium state. All experiments with the dialysis cells were conducted with room temperature, with the outer solution in the cell continuously stirred.

After the solution in the cell reached an equilibrium condition, the dialysis tube was removed from the cell and its outer surface rinsed with a small amount of deionized water. The tubing was then placed in a clean polyethylene beaker to allow the upper end of the bag to be cut open and the solution in the bag pipetted into a Nalgene sample bottle for later analysis.

### Centrifugation of Synthetic Solutions

Centrifugation was another solid-liquid separation method examined in this study. As with dialysis, earlier studies (Meadows et al., 1982; Horowitz, 1992) have shown that centrifugation prior to, or as a substitute for, filtration is a very effective method for removing suspended solids from water samples. Approximately 500 mL of each binary

clay-salt solution was centrifuged at 10,000 rpm (16,800 g) for 10 minutes in order to separate clay particles from the bulk solution.

The centrifuge used in this study was a DuPont Sorvall RC-58 Refrigerated Ultracentrifuge. The Sorvall RC-58 is ideal for separating suspended solids from water samples due to its wide range of speeds and its ability to keep centrifuged samples at a constant temperature between 10 and 50 °C. The centrifuge bottles used in this study were 250 mL, thick walled, HDPE Nalgene centrifuge bottles. All bottles were washed with a 10% HNO<sub>3</sub> solution and subsequently rinsed with deionized water prior to their use.

After centrifuging the samples, approximately 50 mL of each sample was pipetted from the upper third of the centrifuge bottle and stored in a Nalgene sample bottle for later analysis.

#### Chemical Analysis of Sample Filtrate

All major anions and cations were analyzed using a Dionex 2000i/SP Ion Chromatograph. Aluminum concentrations were determined with a Varian Spectra AA-600 graphite furnace atomic absorption spectrophotometer. Bicarbonate concentrations were determined via alkalinity titrations using 3 mN H<sub>2</sub>SO<sub>4</sub> as the titrant. Each of the aliquots of filtrate from the binary solutions were analyzed for Na<sup>+</sup> and Cl<sup>-</sup>. The multicomponent solutions were analyzed for Ca<sup>2+</sup>, Mg<sup>2+</sup>, Na<sup>+</sup>, K<sup>+</sup>, HCO<sub>3</sub><sup>-</sup>, CO<sub>3</sub><sup>2-</sup>, Cl<sup>-</sup>, SO<sub>4</sub><sup>2-</sup>, F<sup>-</sup>, and Al.

## ***Field Phase***

### **Sample Locations and Methods**

The natural water samples used in this study were collected from the Rio Grande and Rio Puerco at locations 20 and 25 miles north of Socorro, NM (Figure 22). Both rivers were sampled following heavy rainfall events. The Rio Puerco was chosen as a sampling site due to the fact that it drains a watershed with a large area of exposed shale and clay formations, which would ensure that a large amount of clay would be present as suspended sediment in any water sample collected. The Rio Grande near Bernardo was chosen as a sampling point because it was directly upstream of the confluence of the Rio Grande with the Rio Puerco. This reach of the Rio Grande drains a watershed with a large amount of sands and farmland. There would be a minimal amount of clay present in the sample taken from the Rio Grande near Bernardo, which would provide a contrast with the sample taken from the Rio Puerco.

Samples were collected using a five-gallon polyethylene bucket tied to a rope and placed in two 10 liter polyethylene storage containers. Both storage containers had been washed with a 5% HNO<sub>3</sub> solution and rinsed twice with deionized water. Prior to filling the storage containers, they were rinsed with the river water they were to store. At the time of sampling, the flow at the Rio Grande Floodway at Bernardo was reported by the USGS to be 1150 cfs, while the flow at the Rio Puerco near Bernardo was estimated by the USGS to be approximately 200 cfs.

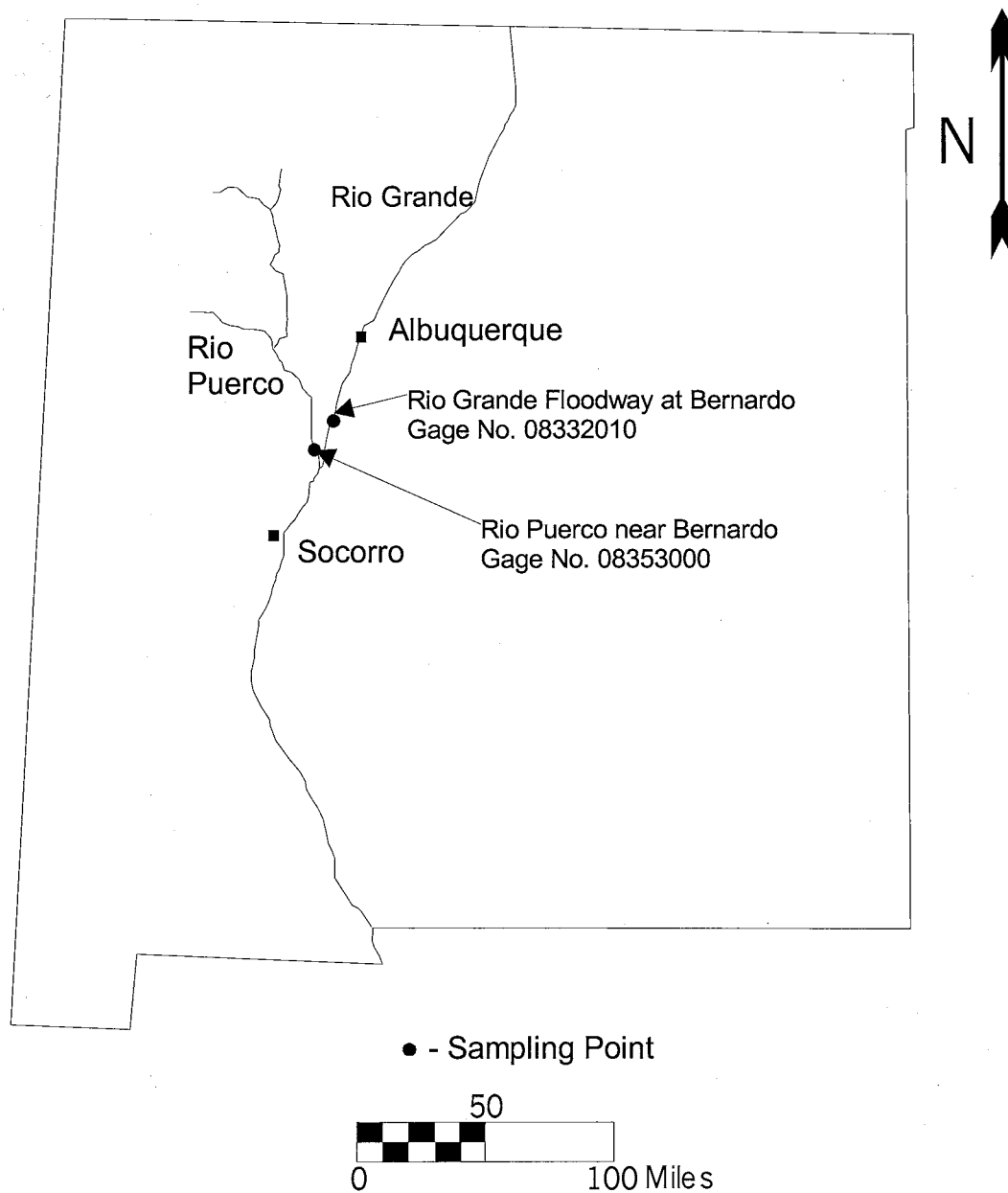


**Figure 22 -** Map Showing Sample Locations

The high levels of suspended solids made field filtration impossible. Both samples were taken back to the lab for filtration, dialysis and centrifugation. Each sample container was placed in a shaker bath and continuously agitated to ensure that the colloidal material would remain suspended in the samples.

### Filtration

Approximately 1 L of each sample was filtered through a 47 mm, 0.45  $\mu\text{m}$  MFS cellulose acetate filter using the filter cell shown in Fig 20. As with the lab phase of the study, the filters used were soaked in a 10%  $\text{HNO}_3$  solution for 24 hours followed by two consecutive 12 hour soakings in distilled water.

As with the lab phase, each filtration was conducted under constant pressure using a compressed air source. The pressures for each filter run were increased to 100 psi due to clogging of the filter caused by the high levels of suspended sediment. The filtrate was collected in preweighed 60-mL HDPE Nalgene bottles, in aliquots of approximately 20 to 35 mL. The volume of each aliquot was determined by weighing the bottle with the collected sample and subtracting the mass of the bottle from this measurement. Although each sample contained higher TDS concentrations than the synthetic solutions, the densities of each filtered sample did not vary significantly from a value of 1.00 g/mL, making calculations of volumes filtered sufficiently accurate. Again, each aliquot was saved for later chemical analysis, and the time required for the filtration of each aliquot was recorded in order to determine the resistance of the filter cake which formed on the MFS filter.

## Dialysis

The dialysis of both the Rio Grande and Rio Puerco samples was identical to the process used for the synthetic solutions. However, the synthetic solutions reached an equilibrium in five days, while it took the Rio Grande and Rio Puerco cells seven and ten days, respectively, for the conductivity measurements to reach an equilibrium point.

## Centrifugation

The centrifugation of the Rio Grande and Rio Puerco samples was very similar to that of the synthetic solutions. However, due to the high levels of suspended solids in both field samples, the time required for the centrifuge to force the solids from solution increased to fifteen minutes at 10,000 rpm (16,800 g).

## Chemical Analysis of Sample Filtrate and Sediments

The concentrations of the major anions and cations in each of the filtrate aliquots were analyzed with a Dionex 2000i/SP Ion Chromatograph. Each aliquot was analyzed for  $\text{Ca}^{2+}$ ,  $\text{Mg}^{2+}$ ,  $\text{Na}^+$ ,  $\text{K}^+$ ,  $\text{Cl}^-$ ,  $\text{SO}_4^{2-}$ , and  $\text{F}^-$ . Due to the small volume of each aliquot, the samples were not split and acidified for trace metal analysis. The small aliquot volume also made alkalinity titrations unrealistic.

Sediments from the Rio Grande and Rio Puerco collected onto the filter were analyzed via X-ray diffraction to determine the mineralogy and relative amount of clays and minerals present in the rivers' suspended loads.

## RESULTS AND INTERPRETATIONS

### Lab Phase

#### Measurement of filter cake resistance

The times required to filter each aliquot of each synthetic solution ( $\theta$ ) and the volume ( $V$ ) of each aliquot were tabulated in order to determine the resistance of the filter cake and the filter itself. By plotting  $\theta/V$  against  $V$ , the resistance to flow due to the filter cake ( $\alpha$ ) and the filter ( $R_m$ ) can be determined using the relationships:

$$\alpha = \left( \frac{2PA^2}{\mu v} \right) m \quad (40)$$

and

$$R_m = \left( \frac{PA}{\mu} \right) b \quad (41)$$

where  $m$  = the slope of the linear portion of the  $\theta/V$  vs.  $V$  curve  
 $b$  = the y-intercept of the linear portion of the  $\theta/V$  vs.  $V$  curve

All terms in the above two relationships can be directly measured or controlled during a filter run, with the exception of the variable  $v$  in Equation (40). The term  $v$  is defined as the volume of cake produced per unit volume of slurry filtered. The easiest and most accurate way to determine  $v$  is by using the solid weight fraction of the slurry in conjunction with the density of the solid particles in the slurry, as seen in the following relationship

$$v = \frac{\omega_c}{\rho_s V} \quad (42)$$

where  $\omega_c$  = weight of solids in slurry (g)  
 $\rho_s$  = density of solids in slurry ( $\text{g/cm}^3$ )



$V$  = volume of filtrate ( $\text{cm}^3$ )

As seen in Figures 23 through 34, data from each of the filter runs show a linear relationship when  $\theta/V$  is plotted against  $V$ . The filter run for the Rio Grande sample is shown in Figure 33. Figure 33 does not show a definite linear relationship, which is likely due to the heterogeneous nature of the suspended solids noted in this sample. The Rio Grande sample had quite a bit of debris such as plant matter present. This debris may have interrupted the formation of a filter cake during this particular filter run. In addition, the filter cake that was formed during the filtration of the Rio Grande Sample may have undergone some compaction that could also explain the trend seen in Figure 33.

The slopes and intercepts for each of the data sets were determined by entering only the data, which fell onto the linear portion of these Sperry plots into a statistics package on a handheld calculator which fitted a linear equation to the data. After converting all data into similar units, the resistance of the filter cake and the filter medium were calculated using Equations (40) and (41). The experimental values for  $\alpha$  and  $R_m$  are presented in Table 6. The values of  $\alpha$  for the slurries were within one order of magnitude of those calculated by Tiller (1956) and Grace (1956) for dilute kaolin slurries.

With the exception of the synthetic surface water with a TSS of 102.45 mg/L,  $R_m$  could not be determined due to the fact that each of the data sets yielded a negative value for the y-intercept, making any physical interpretation meaningless.

The value for  $R_m$  calculated from data obtained in the eighth filter run is  $6.62 \times 10^9 \text{ m}^{-1}$ . This value indicates the resistance to flow provided by the  $0.45 \text{ }\mu\text{m}$  cellulose

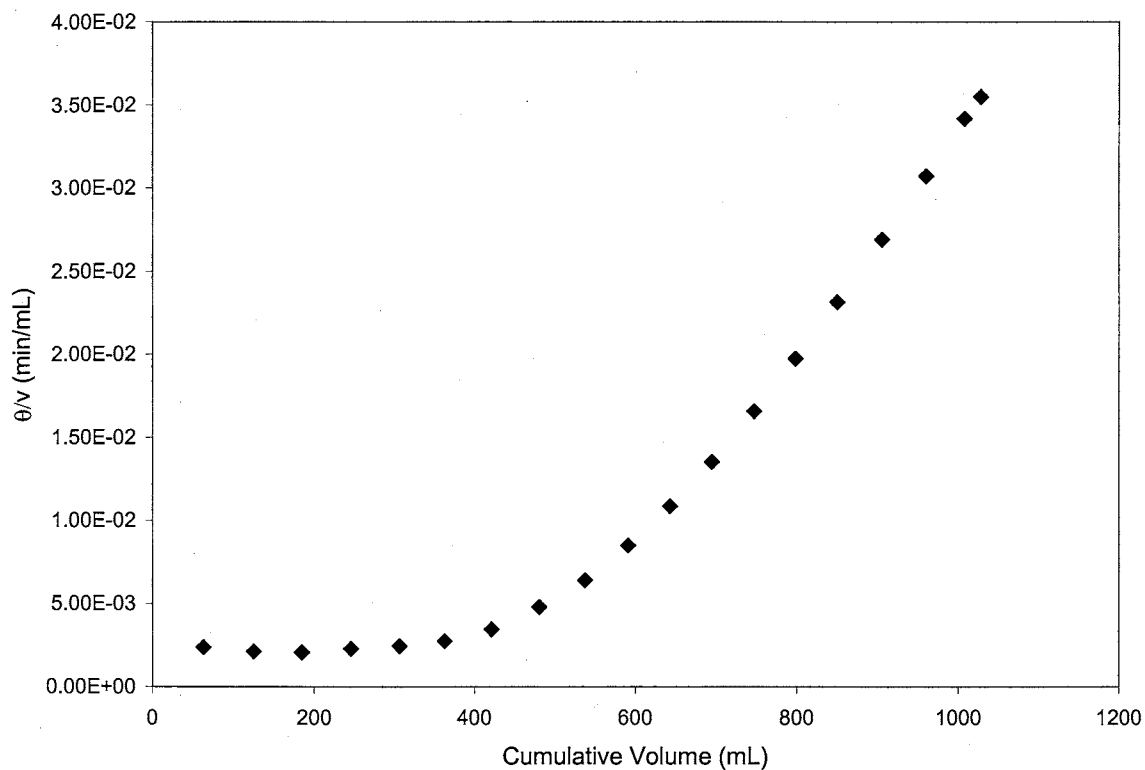


**Figure 23 -** Plots of Filtration Time / Volume Filtered against Volume Filtered for suspended clay loads of 5 mg/L. The slope of the linear portion of the curve is used to determine the resistance of the filter cake,  $\alpha$ .

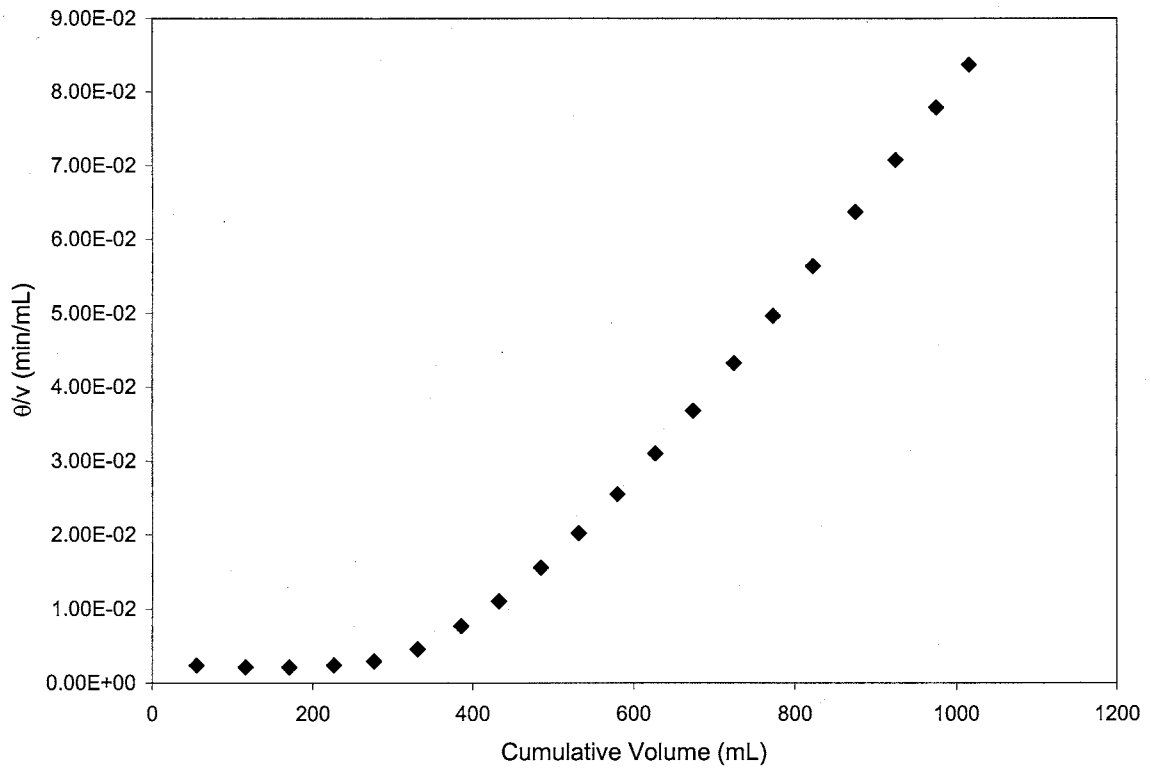


**Figure 24 -** Plots of Filtration Time / Volume Filtered against Volume Filtered for suspended clay loads of 10 mg/L. The slope of the linear portion of the curve is used to determine the resistance of the filter cake,  $\alpha$ .

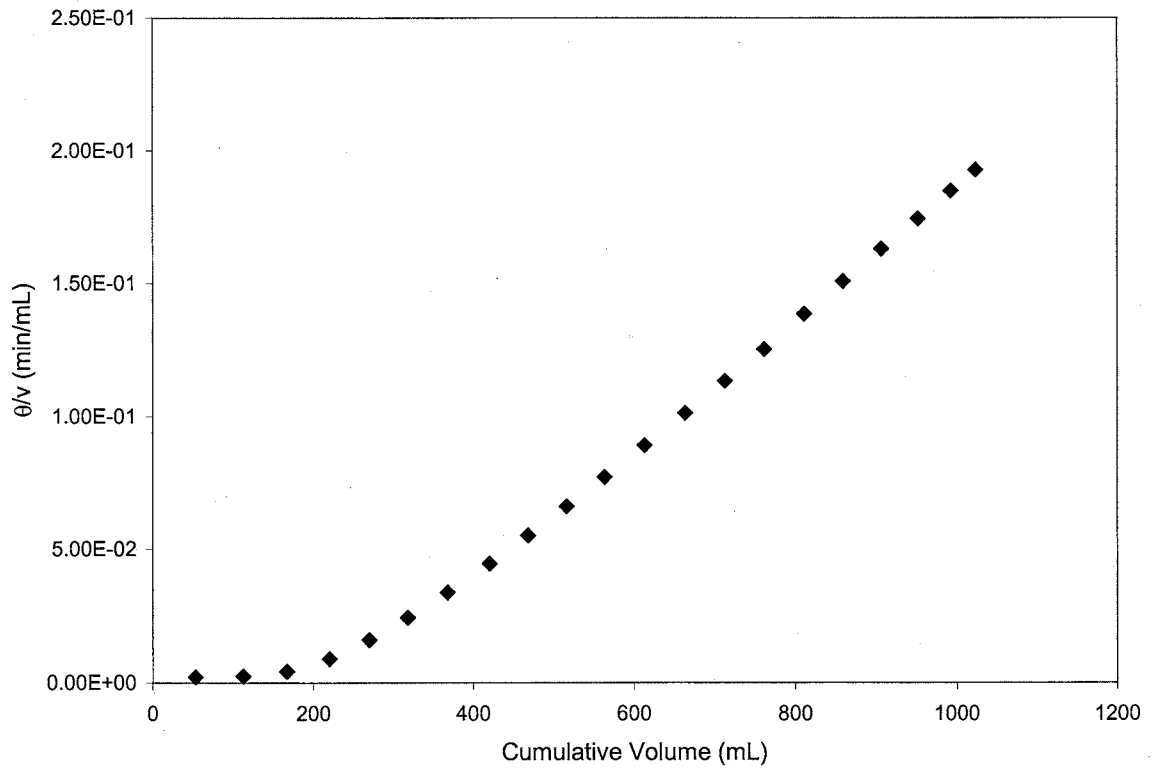


**Figure 25 -** Plots of Filtration Time / Volume Filtered against Volume Filtered for suspended clay loads of 15 mg/L. The slope of the linear portion of the curve is used to determine the resistance of the filter cake,  $\alpha$ .

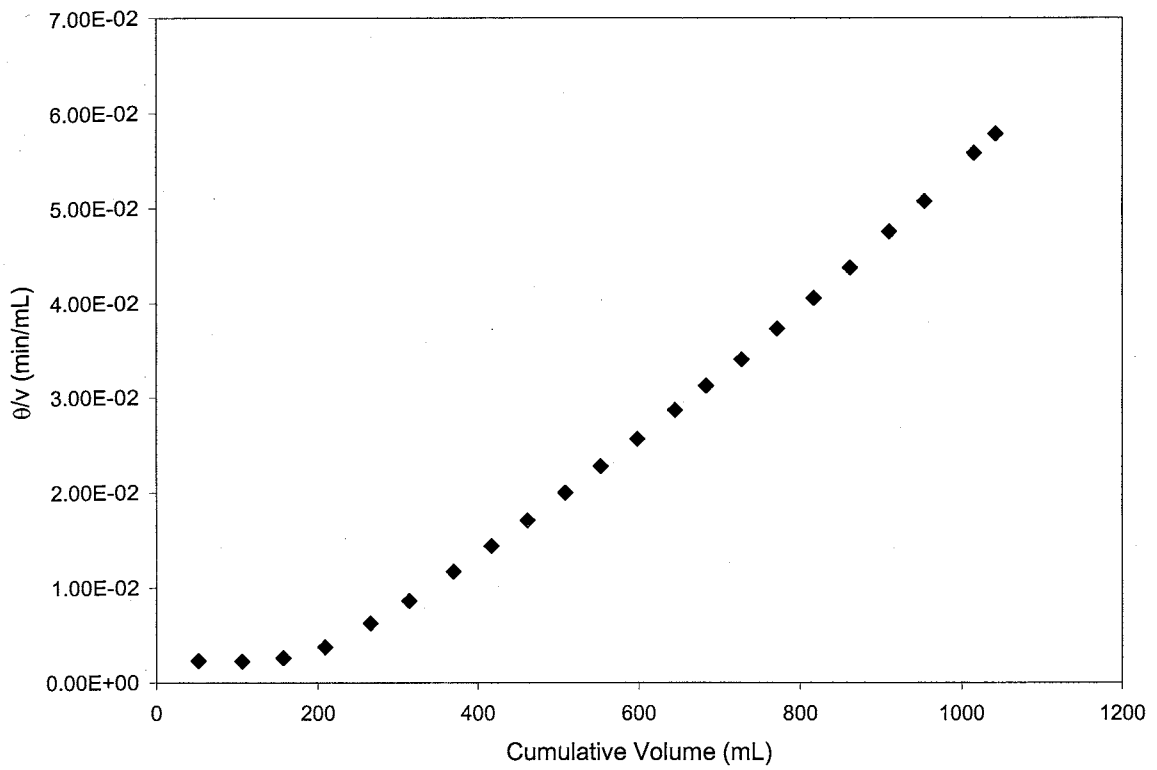


**Figure 26 -** Plots of Filtration Time / Volume Filtered against Volume Filtered for suspended clay loads of 25 mg/L. The slope of the linear portion of the curve is used to determine the resistance of the filter cake,  $\alpha$ .

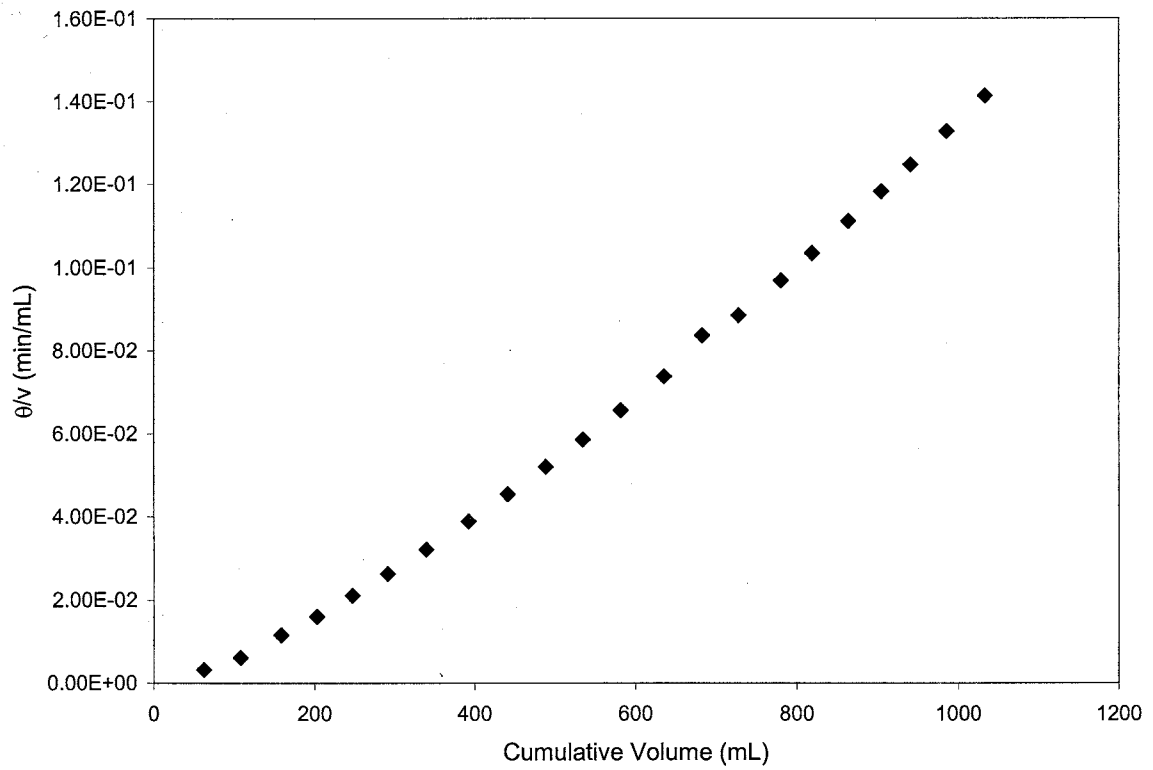


**Figure 27 -** Plots of Filtration Time / Volume Filtered against Volume Filtered for suspended clay loads of 50 mg/L. The slope of the linear portion of the curve is used to determine the resistance of the filter cake,  $\alpha$ .

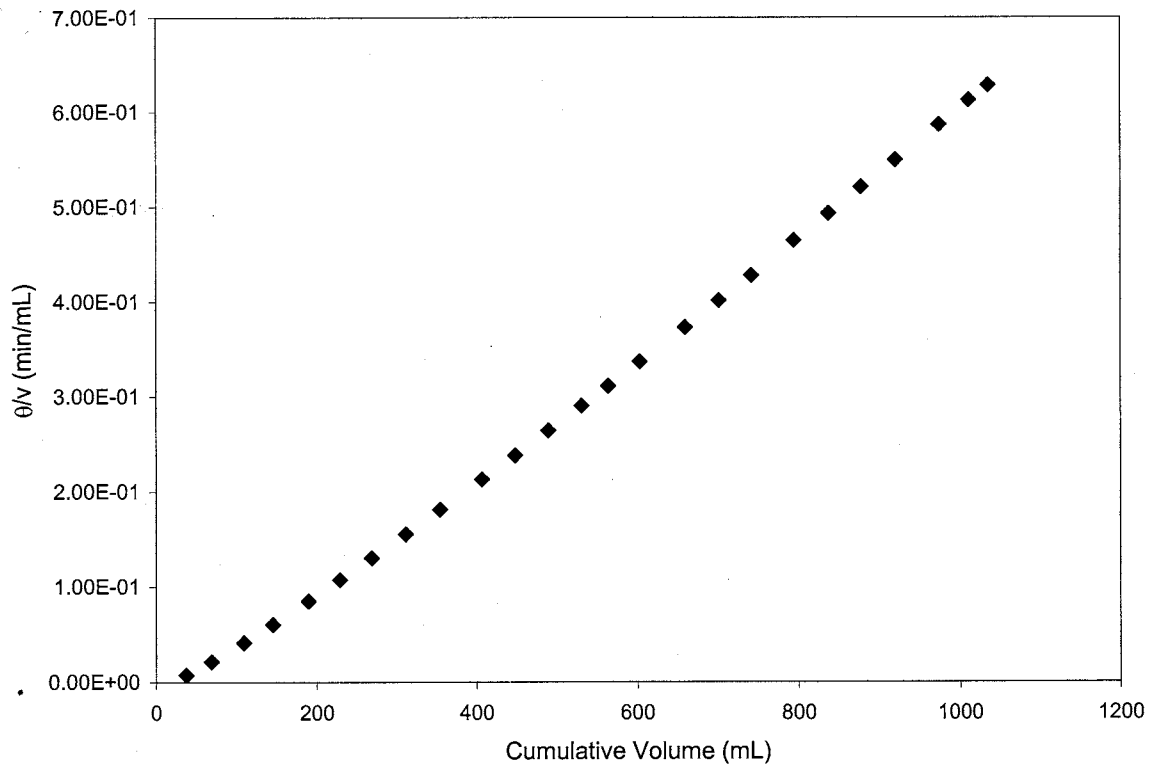


**Figure 28 -** Plots of Filtration Time / Volume Filtered against Volume Filtered for suspended clay loads of 75 mg/L. The slope of the linear portion of the curve is used to determine the resistance of the filter cake,  $\alpha$ .

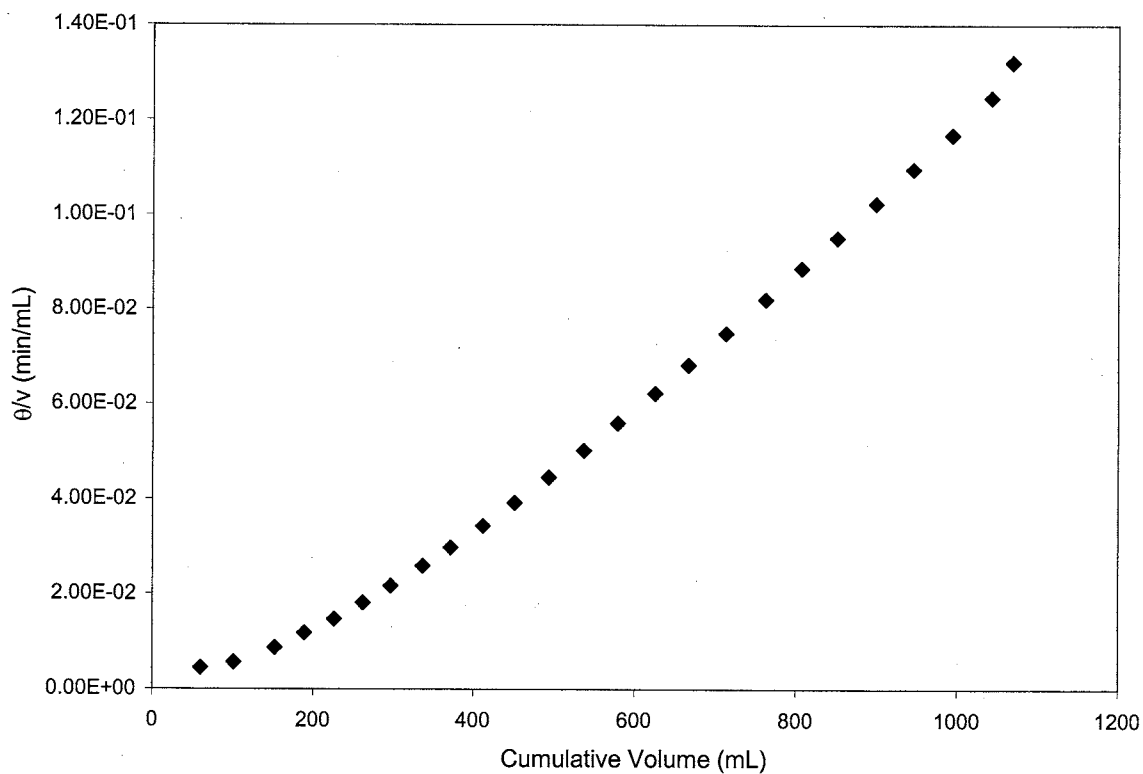


**Figure 29 -** Plots of Filtration Time / Volume Filtered against Volume Filtered for suspended clay loads of 100 mg/L. The slope of the linear portion of the curve is used to determine the resistance of the filter cake,  $\alpha$ .



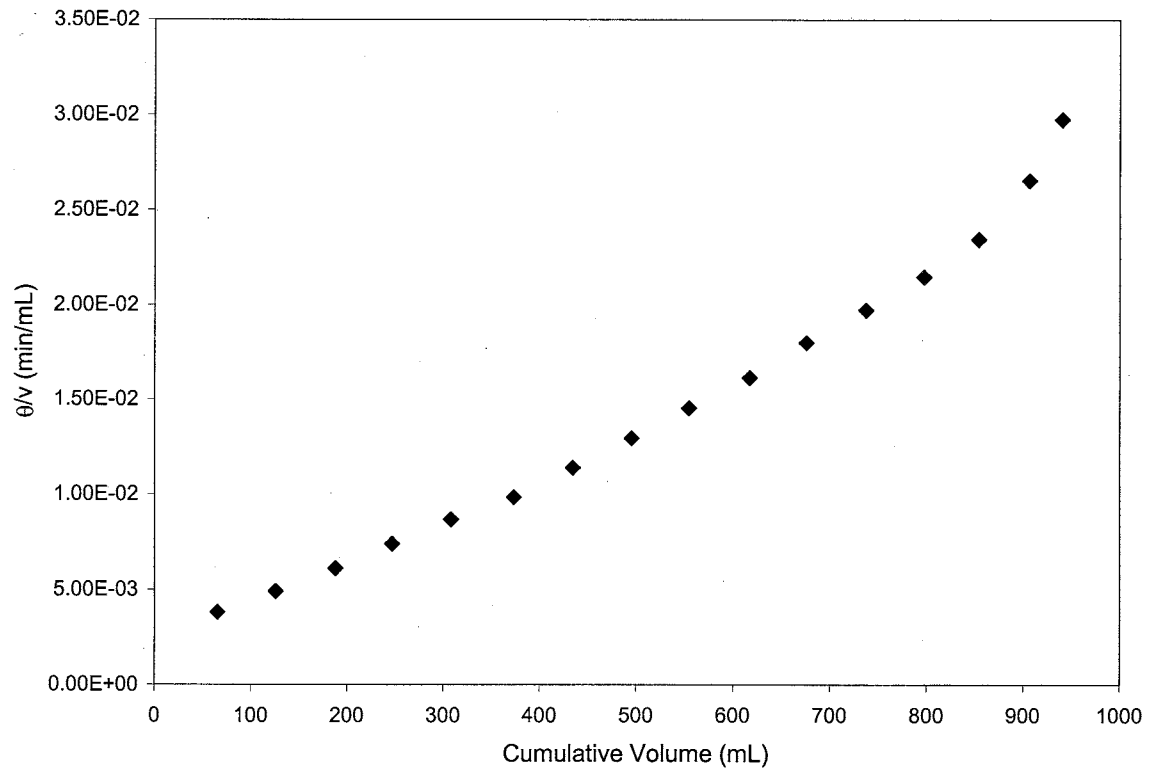


**Figure 30 -** Plots of Filtration Time / Volume Filtered against Volume Filtered for suspended clay loads of 102 mg/L. The slope of the linear portion of the curve is used to determine the resistance of the filter cake,  $\alpha$ .

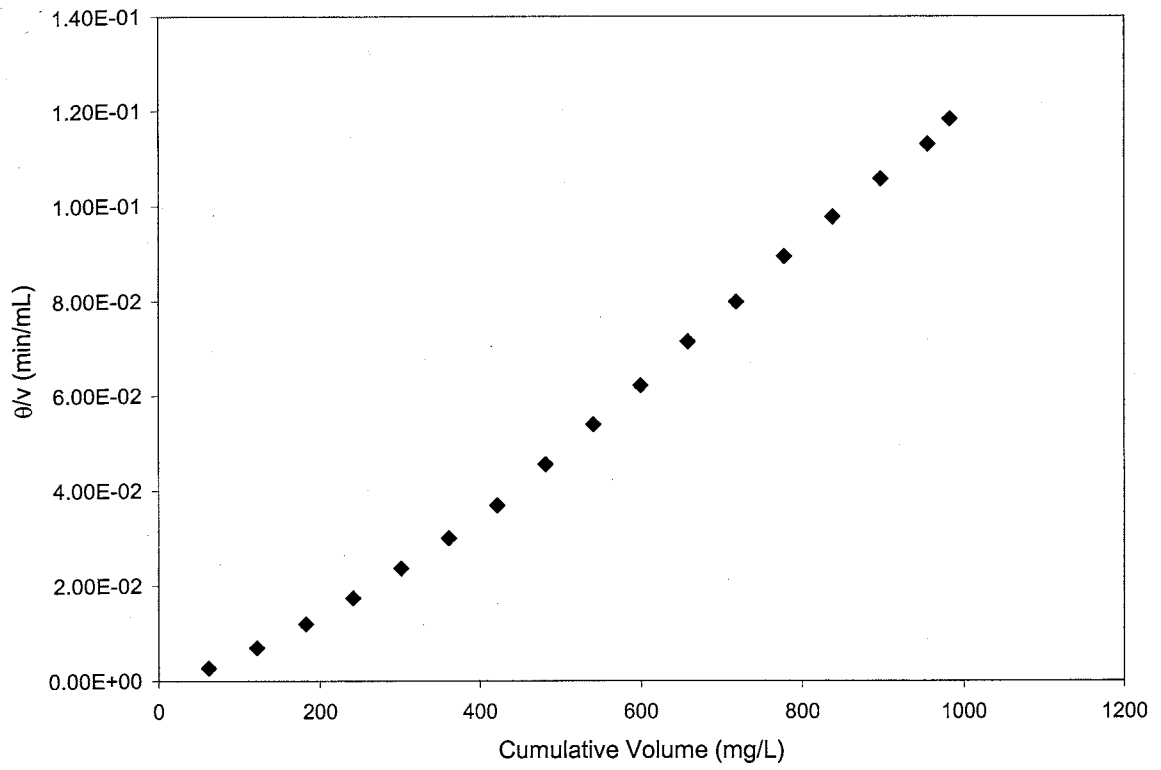


**Figure 31 -** Plots of Filtration Time / Volume Filtered against Volume Filtered for suspended clay loads of 281.5 mg/L. The slope of the linear portion of the curve is used to determine the resistance of the filter cake,  $\alpha$ .

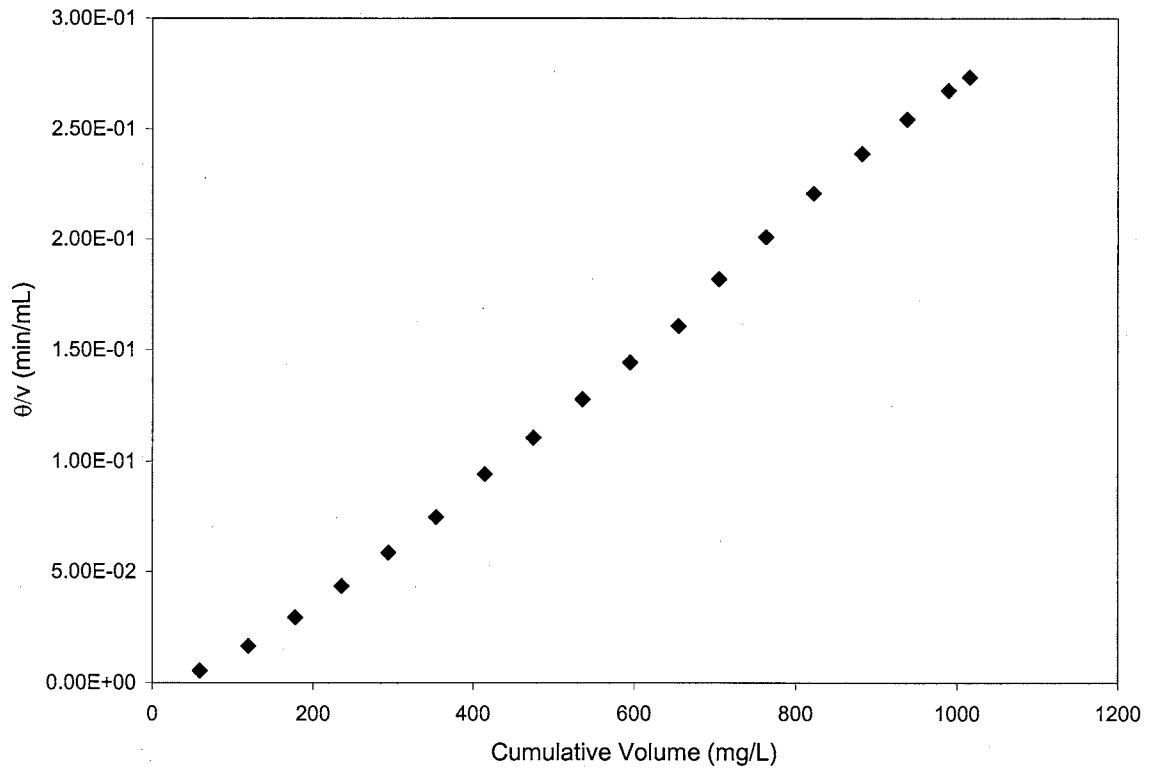


**Figure 32 -** Plots of Filtration Time / Volume Filtered against Volume Filtered for suspended clay loads of 484 mg/L. The slope of the linear portion of the curve is used to determine the resistance of the filter cake,  $\alpha$ .

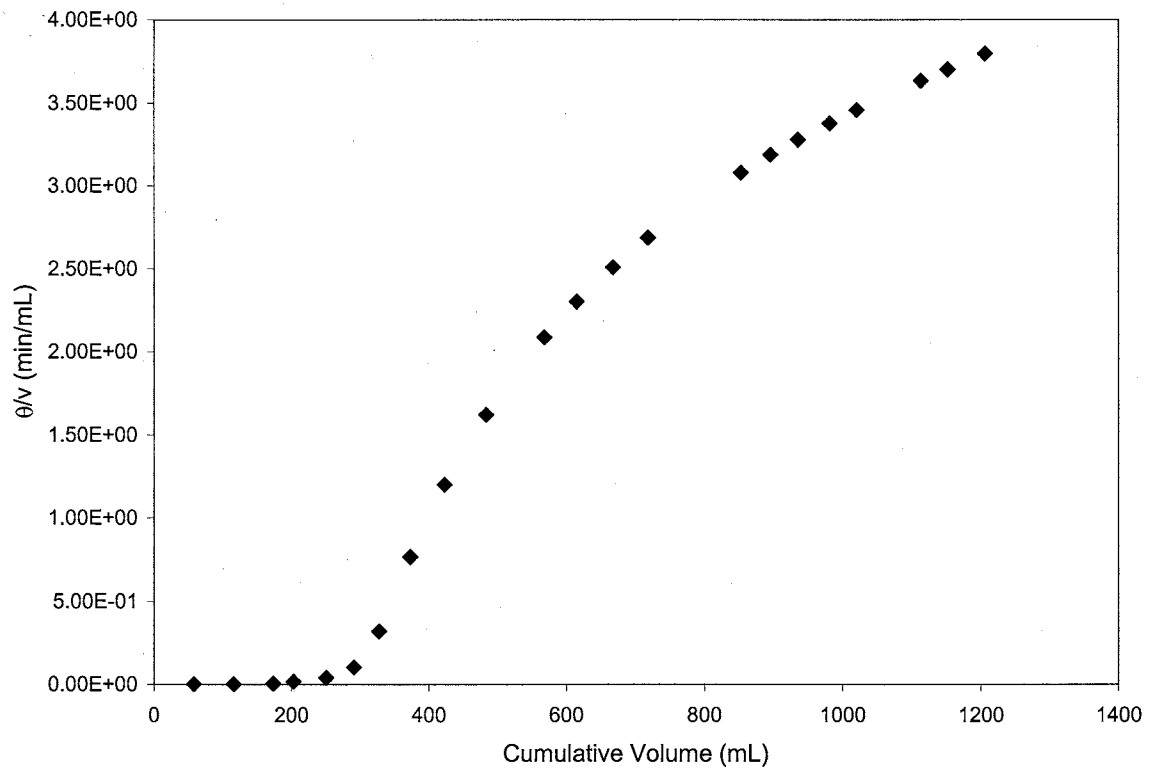


**Figure 33 -** Plots of Filtration Time / Volume Filtered against Volume Filtered for suspended clay loads of 4,100 mg/L. The slope of the linear portion of the curve is used to determine the resistance of the filter cake,  $\alpha$ .

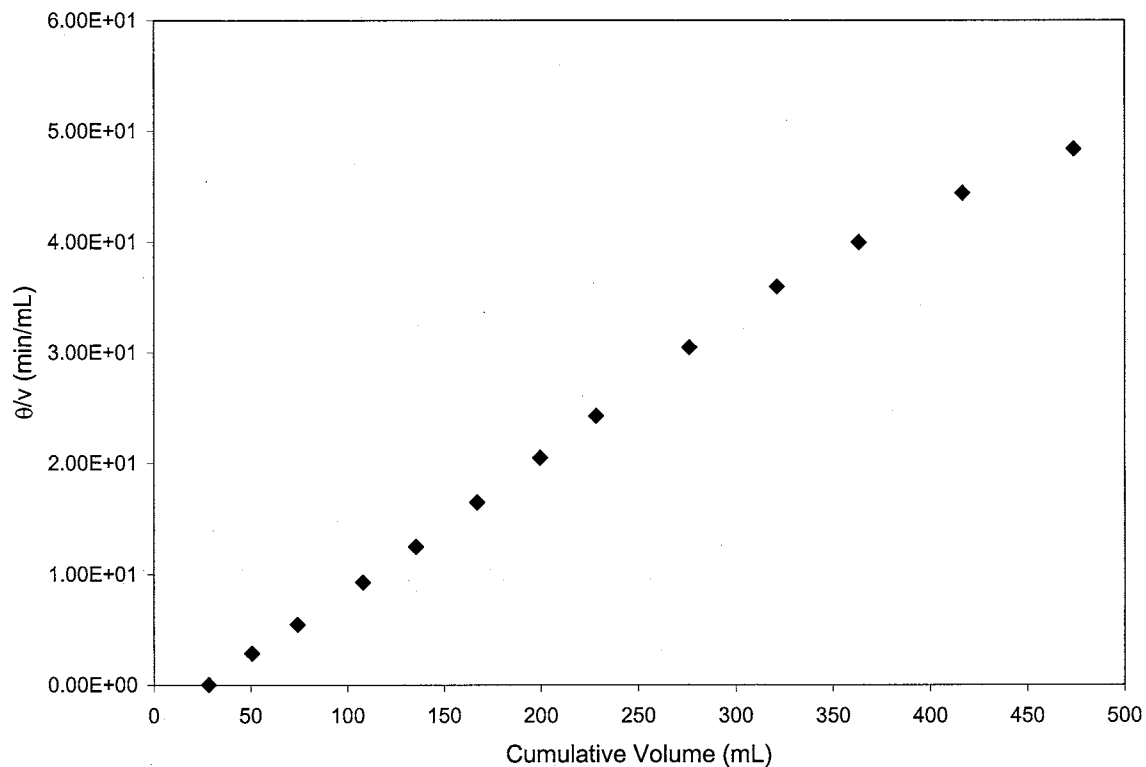


**Figure 34 -** Plots of Filtration Time / Volume Filtered against Volume Filtered for suspended clay loads of 32,100 mg/L. The slope of the linear portion of the curve is used to determine the resistance of the filter cake,  $\alpha$ .

acetate filters used in this study. This value is relatively high when compared to values for other filter media, which have been determined from past studies (Table 7).

**Table 6-** Values of filter cake resistance ( $\alpha$ ) and filter medium resistance ( $R_m$ ) determined in this study

Suspended Sediments (mg/L)	Pressure (Pa)	L (m)	Slope (s/m <sup>6</sup> )	Intercept (s/m <sup>3</sup> )	$R_m$ (m <sup>-1</sup> )	$\alpha$ (m <sup>-2</sup> )
5.29	448159.22	$1.91 \times 10^{-5}$	$3.79 \times 10^9$	Neg. Value	N/A	$1.60 \times 10^{15}$
10.00	448159.22	$5.08 \times 10^{-5}$	$7.79 \times 10^9$	Neg. Value	N/A	$1.57 \times 10^{15}$
14.98	448159.22	$5.84 \times 10^{-5}$	$1.46 \times 10^{10}$	Neg. Value	N/A	$1.96 \times 10^{15}$
24.91	448159.22	$7.62 \times 10^{-5}$	$3.96 \times 10^9$	Neg. Value	N/A	$3.19 \times 10^{14}$
50.06	448159.22	$1.27 \times 10^{-4}$	$9.15 \times 10^9$	Neg. Value	N/A	$3.68 \times 10^{14}$
74.34	448159.22	$1.65 \times 10^{-4}$	$3.61 \times 10^{10}$	Neg. Value	N/A	$9.69 \times 10^{14}$
98.61	689475.73	$1.78 \times 10^{-4}$	$8.38 \times 10^9$	Neg. Value	N/A	$2.60 \times 10^{14}$
102.45	586054.37	$2.03 \times 10^{-4}$	$1.59 \times 10^9$	$1.05 \times 10^{-4}$	$6.62 \times 10^9$	$4.09 \times 10^{13}$
281.50	551580.58	$3.05 \times 10^{-4}$	$8.46 \times 10^9$	Neg. Value	N/A	$7.45 \times 10^{13}$
424.90	586054.37	$5.33 \times 10^{-4}$	$1.67 \times 10^{10}$	Neg. Value	N/A	$1.04 \times 10^{14}$
4,100	448159.22	$3.16 \times 10^{-3}$	$2.72 \times 10^{11}$	Neg. Value	N/A	$1.54 \times 10^{14}$
32,100	689475.73	$6.35 \times 10^{-2}$	$7.55 \times 10^{12}$	Neg. Value	N/A	$7.56 \times 10^{14}$

**Table 7 -** Typical  $R_m$  values for filter media used in industrial processes (Grace, 1956)

Filter Medium	$R_m$ (m <sup>-1</sup> )
175-TW Cotton Twill	$4.59 \times 10^5$
No. 8 Cotton Duck	$2.81 \times 10^6$
SN-7 Filament Nylon, Duck	$1.12 \times 10^6$
AF-220 Woven Wool Felt	$9.58 \times 10^5$
FE-420 Orlon, Satin	$6.30 \times 10^5$

Although one would tend to think that the  $R_m$  value for a 0.45  $\mu\text{m}$  cellulose acetate filter calculated from the data in this study shows that this type of filter is many orders of magnitude more resistant to flow than filter media used in industrial processes, this is simply not the case. The classical approach of determining  $R_m$  and  $\alpha$  through Sperry resistance plots fails to take particle sedimentation into account. Sperry (1917) was the first to realize that by failing to account for sedimentation forces,  $\alpha$  and  $R_m$  values determined experimentally could be erroneously high. However, the effects of sedimentation could not be quantified during the process of filtration until recently (Tiller et al., 1995). Tiller et al. (1995) showed that sedimentation plays a major role in batch filtration processes on horizontal surfaces and can cause unacceptable errors in the determination of both  $R_m$  and  $\alpha$  in filtration processes using gravity as the driving force and in constant pressure filtration runs with a low driving pressure.

In order to avoid this problem, Tiller (1997) recommends replacing  $\alpha$  with a term known as the average specific resistance ( $\alpha_{av}$ ). According to Tiller (1997), the resistance of the filter medium,  $R_m$ , is only important during the first few minutes of filtration. During the first few minutes of filtration, all of the driving pressure drop takes place across the filter medium, with the filter medium providing the only appreciable resistance. As a layer of solids begin to build on the filter medium, the majority of the pressure drop occurs across the filter cake, thereby making the resistance of the filter medium insignificant when compared to the specific cake resistance. The specific filter cake resistance,  $\alpha$ , changes as the layer of solids accumulates onto the filter medium. The variable  $\alpha$  can be thought of as the local resistance of the filter cake at a certain point

in time during the filtration, whereas  $\alpha_{av}$  is considered an average resistance value over the entire filtration.

Tiller (1990a and 1990b) presents an alternative to the classic Sperry approach of calculating  $\alpha$  and  $R_m$ . As with every other derivation of the filtration equation, Tiller (1990b) begins by describing the filtrate flow rate ( $q$ ) in terms of pressure ( $p$ ), viscosity ( $\mu$ ), cake resistance, ( $R_c$ ), medium resistance ( $R_m$ ), and total resistance ( $R$ ).

$$q = \frac{P}{\mu(R_c + R_m)} = \frac{P}{\mu R} \quad (43)$$

By introducing the concept of an average specific resistance ( $\alpha_{av}$ ) and a ratio of mass of suspended solids/unit area of filter base ( $w_c$ ), Tiller (1990b) expressed the flow rate as

$$q = \frac{P}{\mu(\alpha_{av}w_c + R_m)} \quad (44)$$

Note that in this case, the units for  $\alpha_{av}$  are  $M L^{-1}$  vice  $L^{-2}$ . Existing filtration literature uses both units to describe cake resistance. Rearranging Equation (44) into resistance form leads to

$$\frac{P}{\mu q} = \alpha_{av}w_c + R_m \quad (45)$$

Thus, both the cake and medium resistance can be determined by plotting  $\frac{P}{\mu q}$  against  $w_c$ .

By using this procedure, constant pressure filtration data plot as a straight line with a positive y-intercept.



The difficulty in using Equation (45) for modeling filtration of dilute slurries and natural waters lies in determining the variable  $w_c$ . The ratio  $w_c$  is determined using the relationship

$$w_c = \frac{\rho_s L}{1 - \frac{s}{s_c}} \quad (46)$$

where  $\rho_s$  = density of suspended solids  
L = measured thickness of filter cake  
s = mass fraction of inert solids in the slurry  
 $s_c$  = average fraction of inert cake solids measured after filtration

All of the terms in Equation (46) are constant with the exception of the thickness of the filter cake, L. As solid particles accumulate onto the filter media, the value of L increases. When dealing with very dilute slurries such as natural waters, this quantity is very difficult to measure. The most accurate instruments which could measure this variable during filtration would be an endoscope or CATSCAN equipment, which was not available for this study.

### Chemical Analysis of Filtrate Aliquots

One of the major objectives of this study was to examine the effects of filtration on the concentrations of the major chemical species in natural waters. The variation of  $\text{Na}^+$  and  $\text{Cl}^-$  concentrations in the filtrate as a function of the volume filtered for the binary salt - clay solutions can be seen in Figures 35 through 41.

The filtrate with suspended clay concentrations of 5 to 15 mg/L showed no appreciable change in  $\text{Na}^+$  or  $\text{Cl}^-$  concentrations. However, once the clay load was

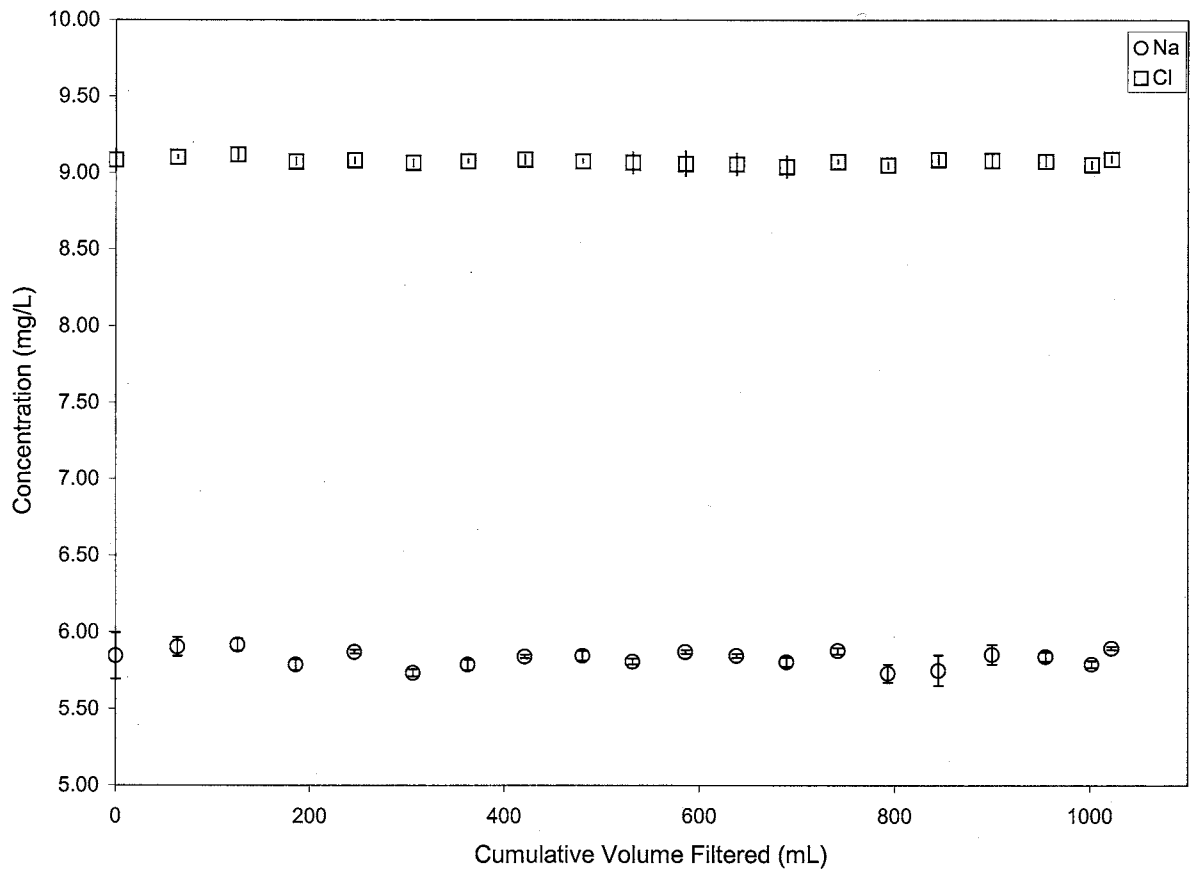


**Figure 35 -** Plot of concentration of Na<sup>+</sup> and Cl<sup>-</sup> in filtrate as a function of volume filtered. Suspended clay concentration of 5 mg/L. Error bars represent an analytical uncertainty of two standard deviations. True dissolved concentrations are denoted by the data point for “zero volume filtered.”

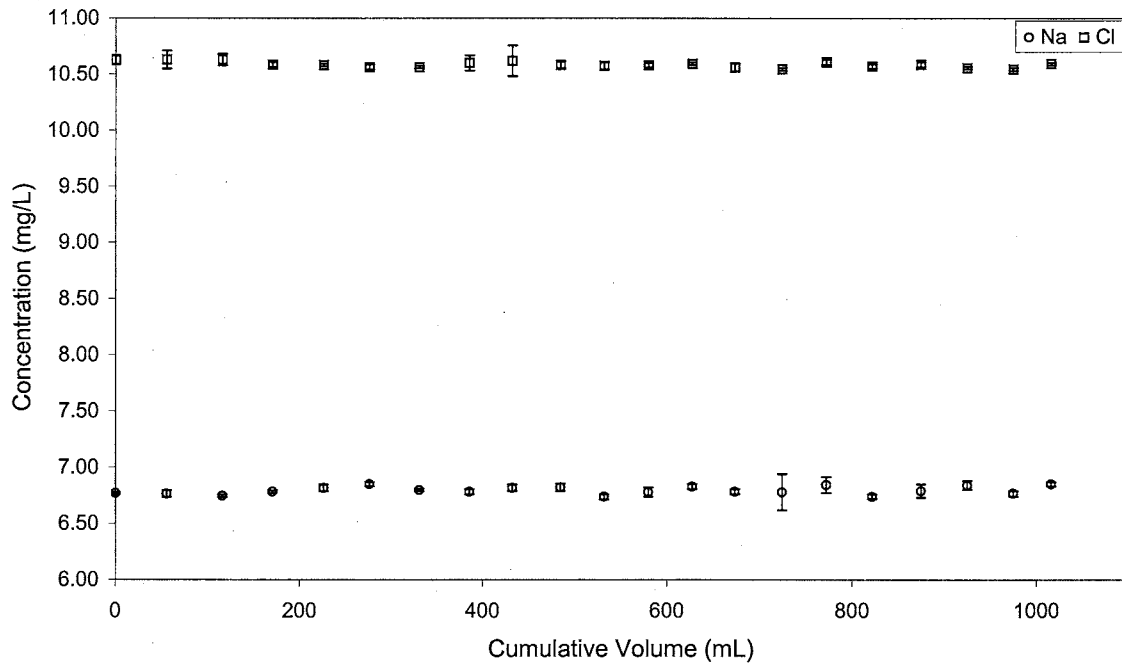


**Figure 36 -** Plot of concentration of Na<sup>+</sup> and Cl<sup>-</sup> in filtrate as a function of volume filtered. Suspended clay concentration of 10 mg/L. Error bars represent an analytical uncertainty of two standard deviations. True dissolved concentrations are denoted by the data point for “zero volume filtered.”

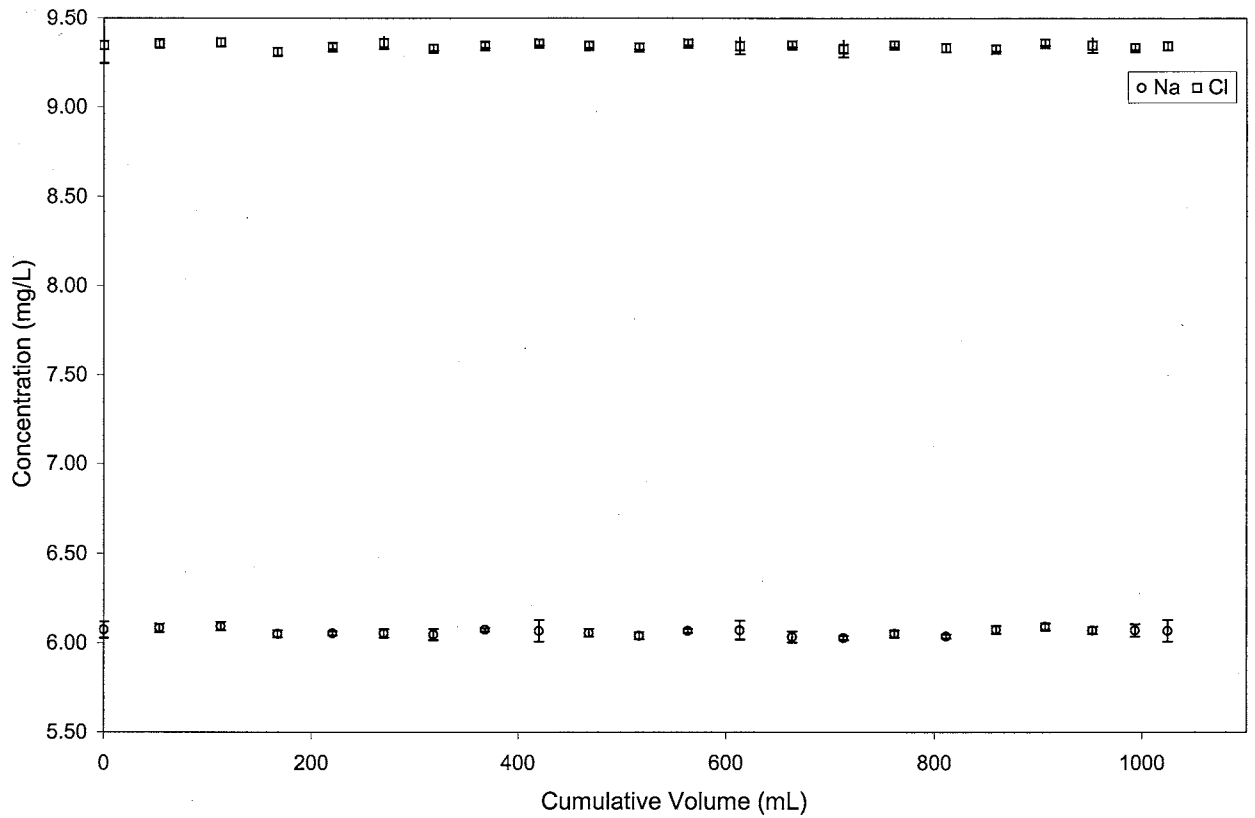


**Figure 37 -** Plot of concentration of Na<sup>+</sup> and Cl<sup>-</sup> in filtrate as a function of volume filtered. Suspended clay concentration of 15 mg/L. Error bars represent an analytical uncertainty of two standard deviations. True dissolved concentrations are denoted by the data point for “zero volume filtered.”

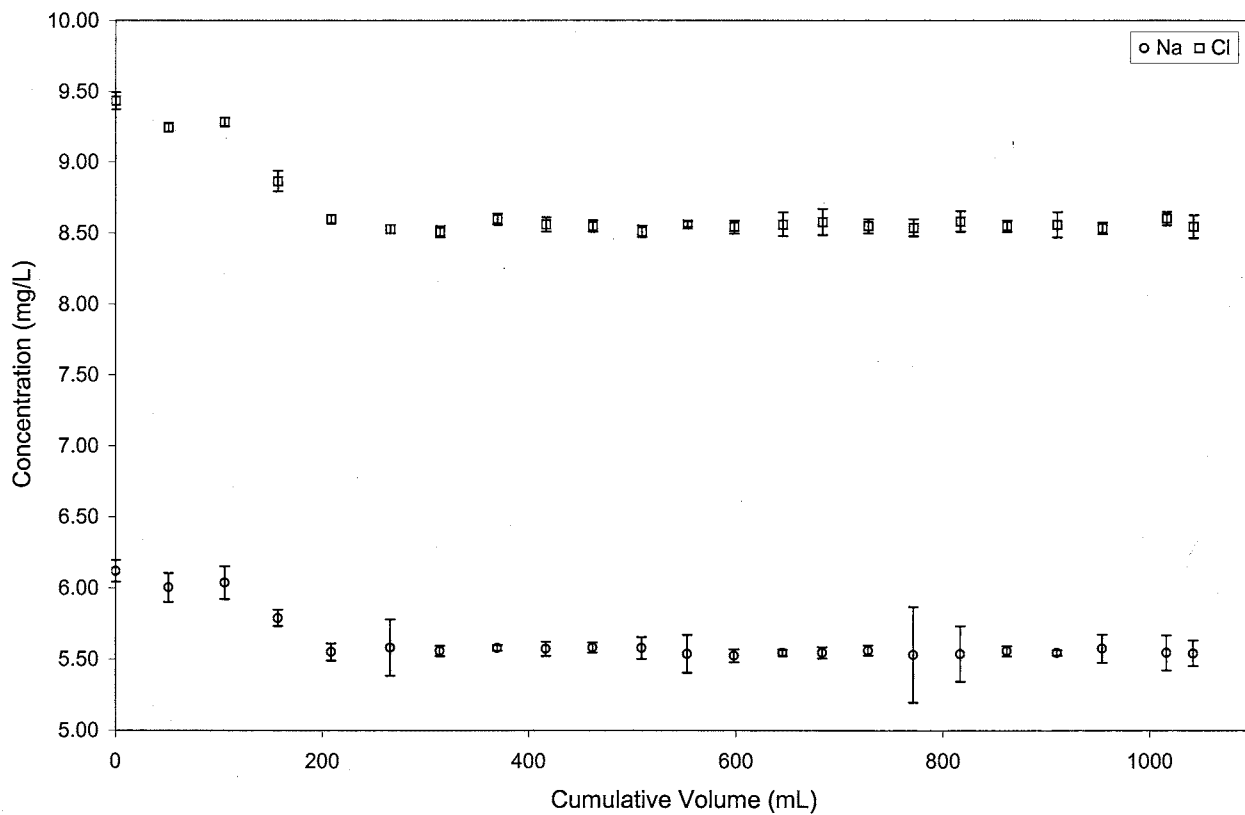


**Figure 38 -** Plot of concentration of Na<sup>+</sup> and Cl<sup>-</sup> in filtrate as a function of volume filtered. Suspended clay concentration of 25 mg/L. Error bars represent an analytical uncertainty of two standard deviations. True dissolved concentrations are denoted by the data point for “zero volume filtered.”

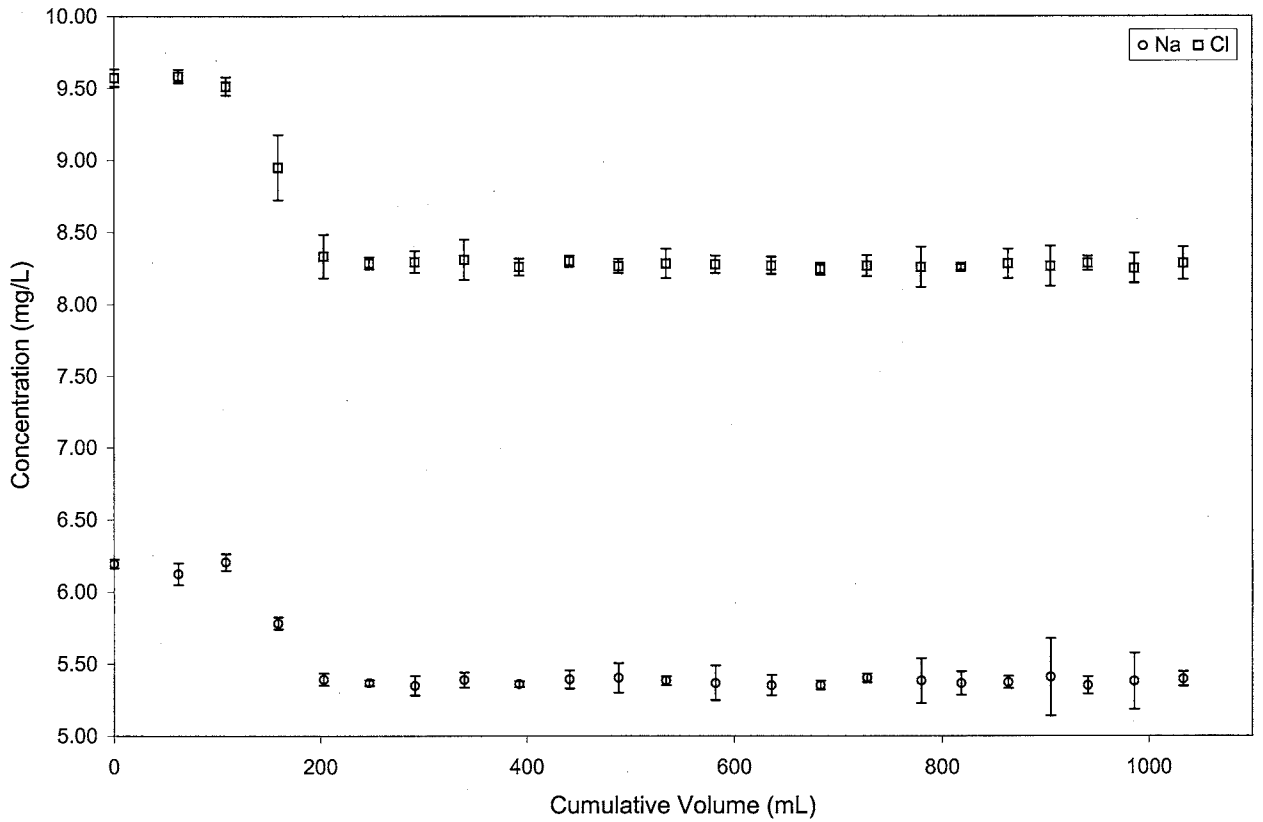


**Figure 39 -** Plot of concentration of Na<sup>+</sup> and Cl<sup>-</sup> in filtrate as a function of volume filtered. Suspended clay concentration of 50 mg/L. Error bars represent an analytical uncertainty of two standard deviations. True dissolved concentrations are denoted by the data point for “zero volume filtered.”

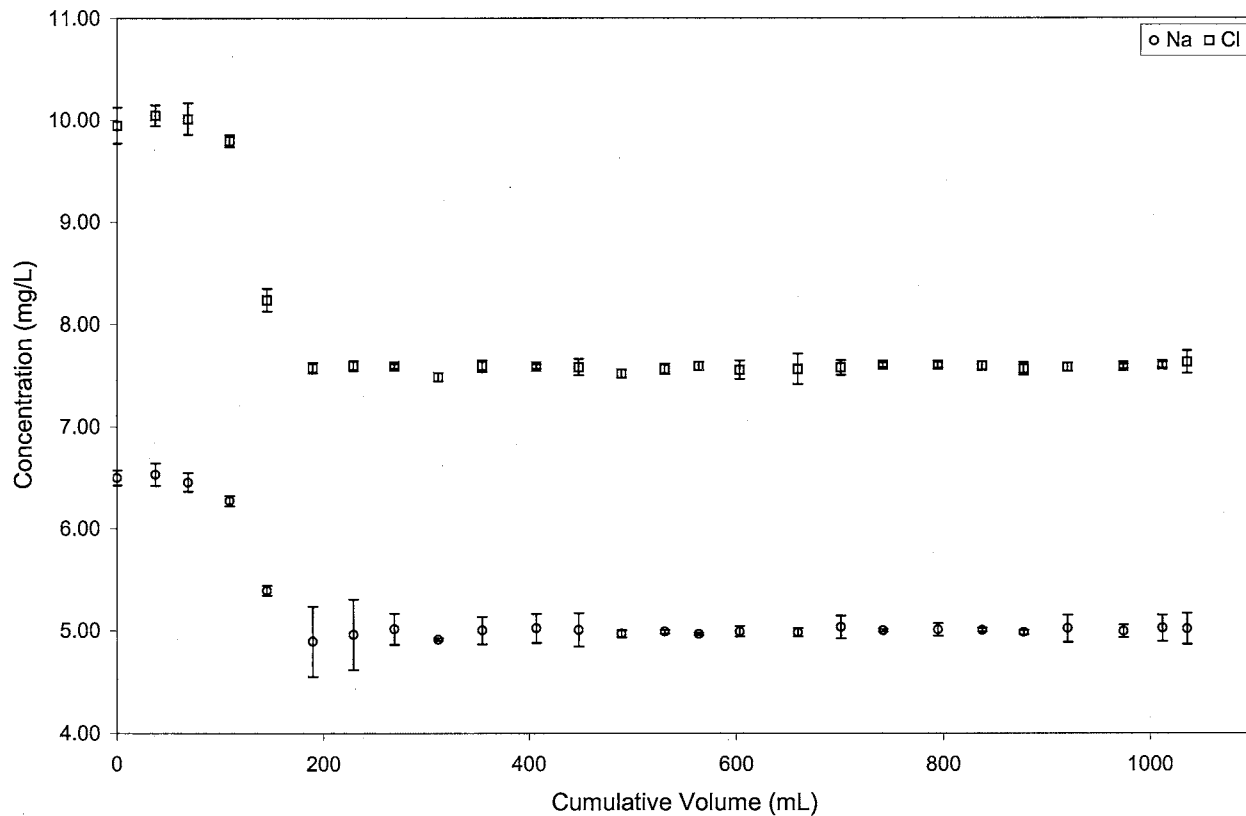


**Figure 40 -** Plot of concentration of Na<sup>+</sup> and Cl<sup>-</sup> in filtrate as a function of volume filtered. Suspended clay concentration of 75 mg/L. Error bars represent an analytical uncertainty of two standard deviations. True dissolved concentrations are denoted by the data point for “zero volume filtered.”

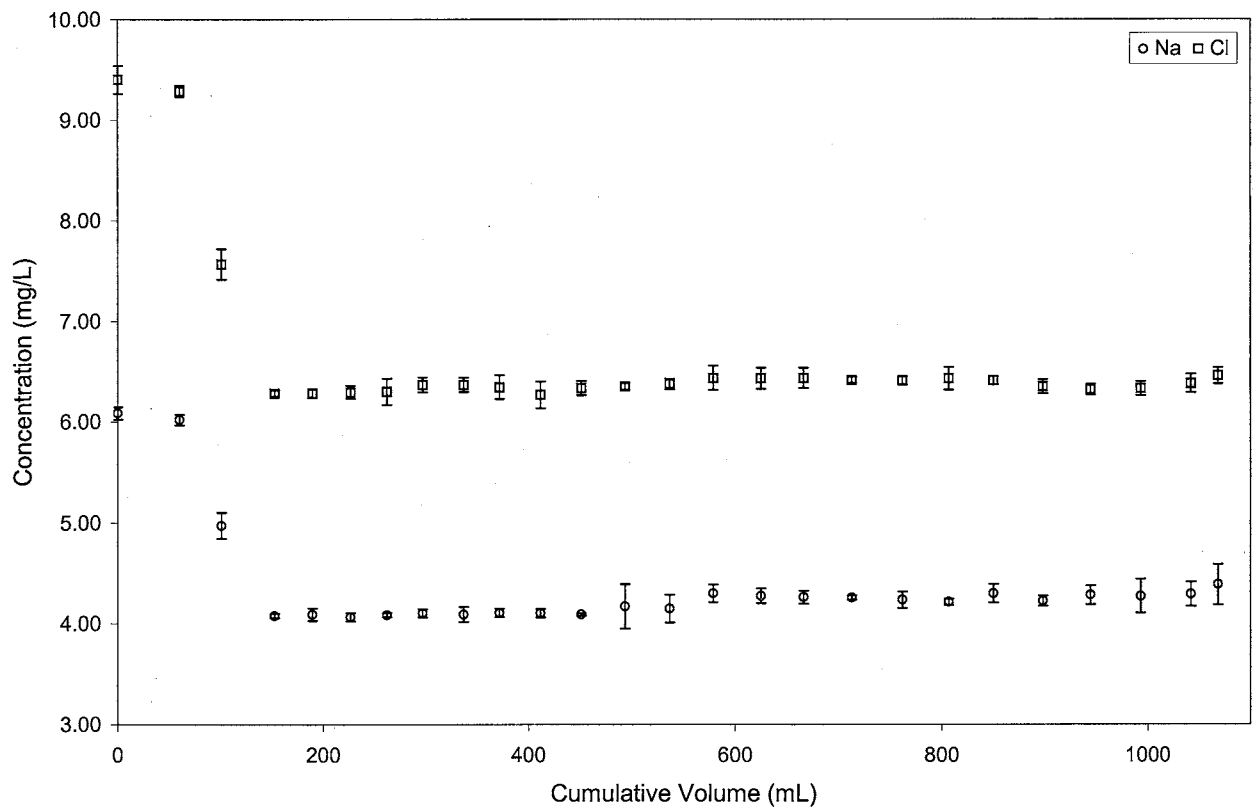


**Figure 41 -** Plot of concentration of Na<sup>+</sup> and Cl<sup>-</sup> in filtrate as a function of volume filtered. Suspended clay concentration of 100 mg/L. Error bars represent an analytical uncertainty of two standard deviations. True dissolved concentrations are denoted by the data point for “zero volume filtered.”



increased to 25 mg/L, a definite reduction in the concentrations of Na<sup>+</sup> and Cl<sup>-</sup> was observed in the filtrate. This drop in Na<sup>+</sup> and Cl<sup>-</sup> concentrations was noted after the first 100 mL of the clay/salt solution was filtered. Although there was only a 7.5% drop in the concentrations of Na<sup>+</sup> and Cl<sup>-</sup>, the drop was significant in that it was greater than a two standard deviation analytical uncertainty. The cation and anion analyses of all filtrate aliquots have a charge balance within 1.5%, where charge balance is defined as

$$\%CB = \frac{|\Sigma cations - \Sigma anions|}{|\Sigma cations + \Sigma anions|} \times 100\%$$

where %CB = percent charge balance  
Σcations = sum of cations present (meq)  
Σanions = sum of anions present (meq)

This drop in the solute concentration of the filtrate suggests that very little clay is needed to affect the speciation of a very dilute aqueous solution. Interestingly, the solute concentration of the filtrate never reached its original value in this filter run, which was predetermined during the synthesis of the sample.

The filter runs conducted with clay loads of 50, 75, and 100 mg/L yielded similar results (Figures 37 - 39). Each of these resulted in decreases of solute concentrations of 13.4%, 17.4%, and 32.5% respectively. The solute concentrations in each of these filter runs dropped dramatically after the first 100 to 150 mL of the clay/salt solutions was filtered. All of the aliquots analyzed have a charge balance equal to or less than 2%.

The solute reduction in the NaCl - clay solutions are summarized in Table 8. The maximum reduction occurred at a clay loading of 100 mg/L, with a solute reduction of 32.5%. It is important to note that none of the NaCl - clay solutions ever reached steady

state conditions. This may be due to the extremely low concentrations of salt in solution (14 to 18 mg/L TDS), since the efficiencies of clay membranes increase as solute concentration decreases, or due to the relatively low volume of solution filtered.

**Table 8 -** Maximum effluent solute reduction in binary salt experiments

Analyte	Suspended Clay Content (mg/L)						
	5	10	15	25	50	75	100
Cl <sup>-</sup>	0%	0%	0%	7.5%	13.4%	17.4%	32.5%
Na <sup>+</sup>	0%	0%	0%	7.5%	13.4%	17.4%	32.5%

For the tap water - clay solutions, there were only minor variations in the concentrations of major species for the solutions with TSS levels of 102 mg/L and 282 mg/L (Table 9). Although there was a slight decrease in the concentrations of the major species, neither was as significant as the decreases for the solution with a TSS concentration of 425 mg/L. The TDS in the tap water used in each of the filter runs was approximately 264 mg/L, approximately ten times higher than the TDS levels of the NaCl - clay solutions.

The concentration of major species in filtrate as a function of the volume of solution filtered for the 282 mg/L clay - tap water solution can be seen in Figure 42. This trend of fairly constant species concentrations was very similar for the 102 mg/L clay - tap water solution. The trends exhibited by the 425 mg/L clay - tap water solution were very different from the previous solutions in that a definite membrane-like pattern, similar to that of McKelvery and Milne (1962), could be seen.

**Table 9 -** Maximum effluent solute reduction in tap water experiments

Analyte	Suspended Clay Content (mg/L)		
	102	282	425
Na <sup>+</sup>	0.1%	3.8%	5.0%
K <sup>+</sup>	1.0%	4.3%	8.0%
Ca <sup>2+</sup>	0.6%	1.2%	8.6%
Mg <sup>2+</sup>	0%	0%	10.0%
Cl <sup>-</sup>	3.5%	4.8%	9.2%
F <sup>-</sup>	1.4%	1.3%	0.5%
NO <sub>3</sub> <sup>-</sup>	1.7%	2.6%	5.2%
Alkalinity as CaCO <sub>3</sub>	0%	2.0%	4.0%
SO <sub>4</sub> <sup>2-</sup>	0%	1.6%	12.1%
Aluminum	-45%	-1180%	-258%

Figures 43 - 47 show the concentrations of the major anions as a function of filtrate volume for the 425 mg/L clay - tap water solution. Each of the anions appear to be retarded at different rates during filtration (Figures 43-47). The anions that exhibited the greatest decreases due to filtration were HCO<sub>3</sub><sup>-</sup>, SO<sub>4</sub><sup>2-</sup>, and Cl<sup>-</sup> (Figures 43-47). All of the anions exhibit different rates and amounts of solute rejection due to the clay layer on the filter paper. Both Cl<sup>-</sup> and SO<sub>4</sub><sup>2-</sup> experienced the greatest amount of rejection by the membrane after 200 mL of the solution had been filtered, returning to true concentration levels at the 400 to 600 mL mark. The levels of HCO<sub>3</sub><sup>-</sup> for this solution dropped 4.0% at the 300 mL point and never returned to the original, or true, concentration. NO<sub>3</sub><sup>-</sup> levels dropped 5.2% after 700 mL of the solution had been filtered and returned to the original level after 950 mL had passed (Figure 46). Interestingly, F<sup>-</sup> levels never significantly changed during the filter run (Figure 47).

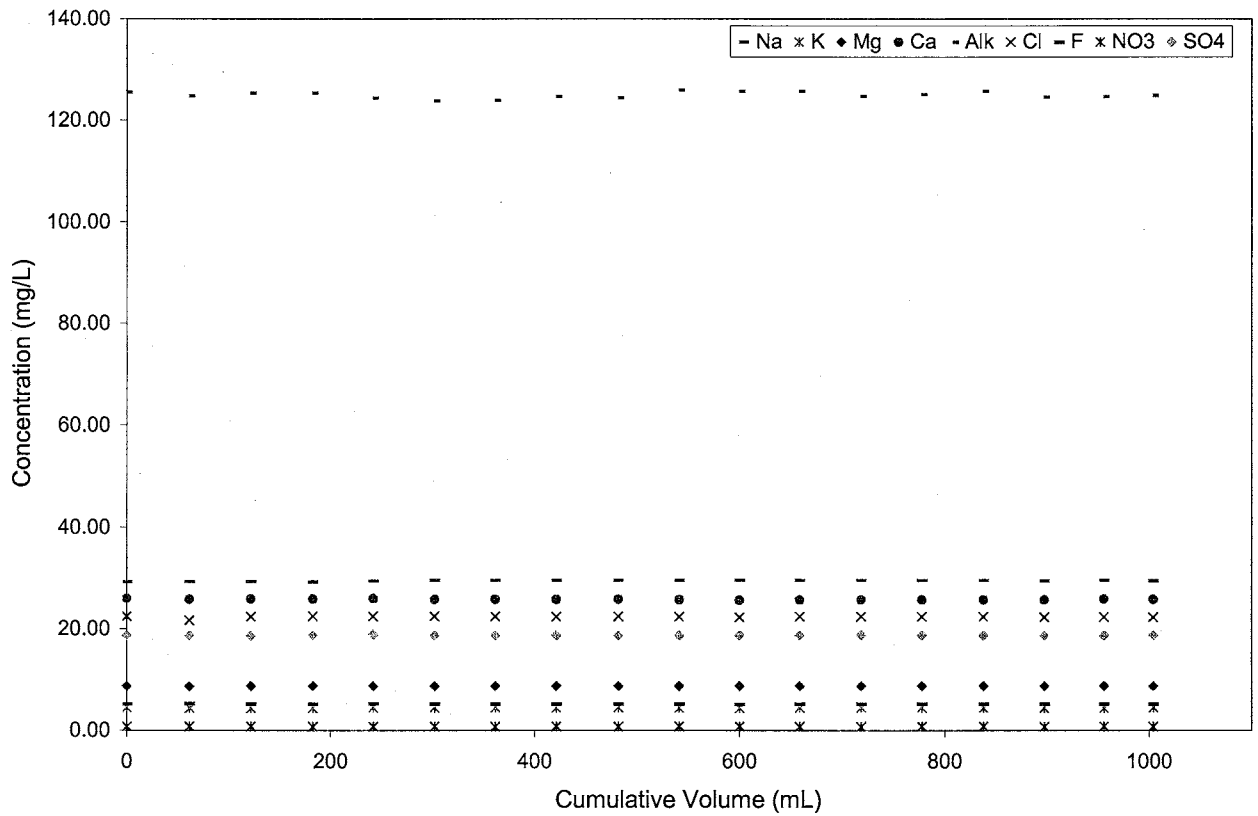


**Figure 42 -** Results of tap water experiment with 282 mg/L of suspended clay. This figure suggests that solute sieving effects were not important during this filtration. Symbols are larger than error bars of two standard deviations. True dissolved concentrations are denoted by the data point for “zero volume filtered.”

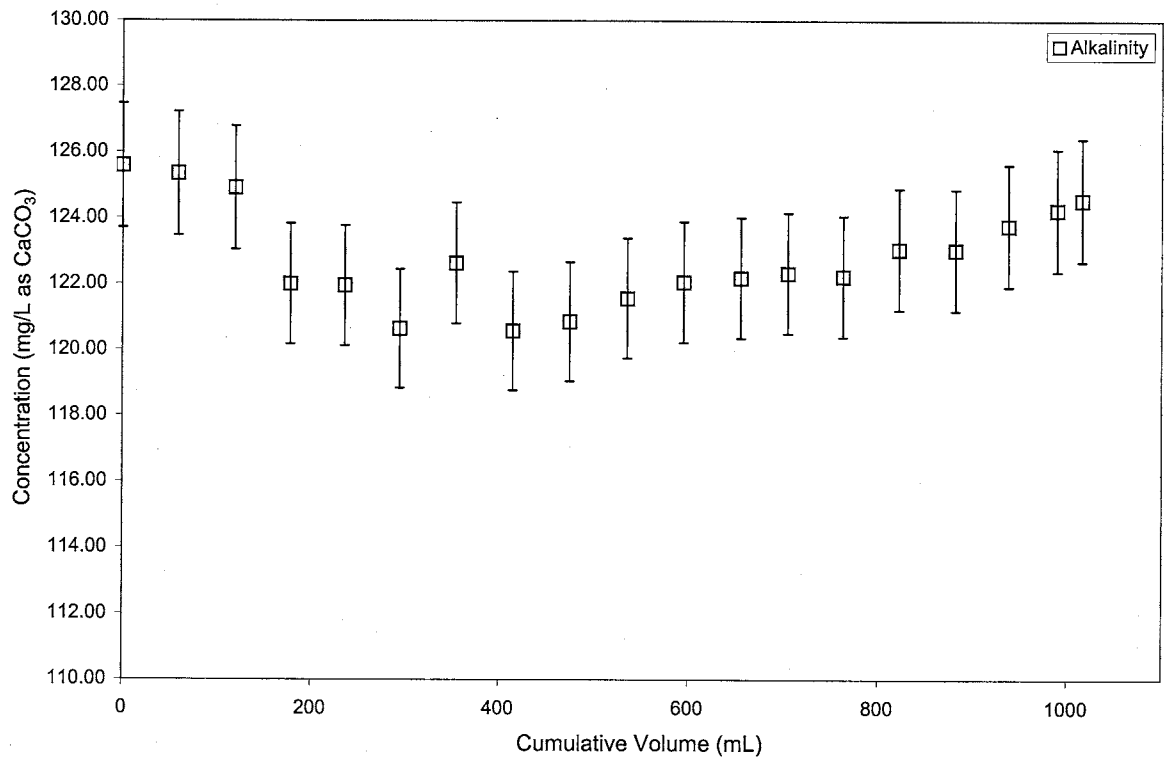


**Figure 43 -** Results of tap water experiment with 425 mg/L of suspended clay. Error bars represent an analytical uncertainty of two standard deviations. True dissolved concentrations are denoted by the data point for “zero volume filtered.”

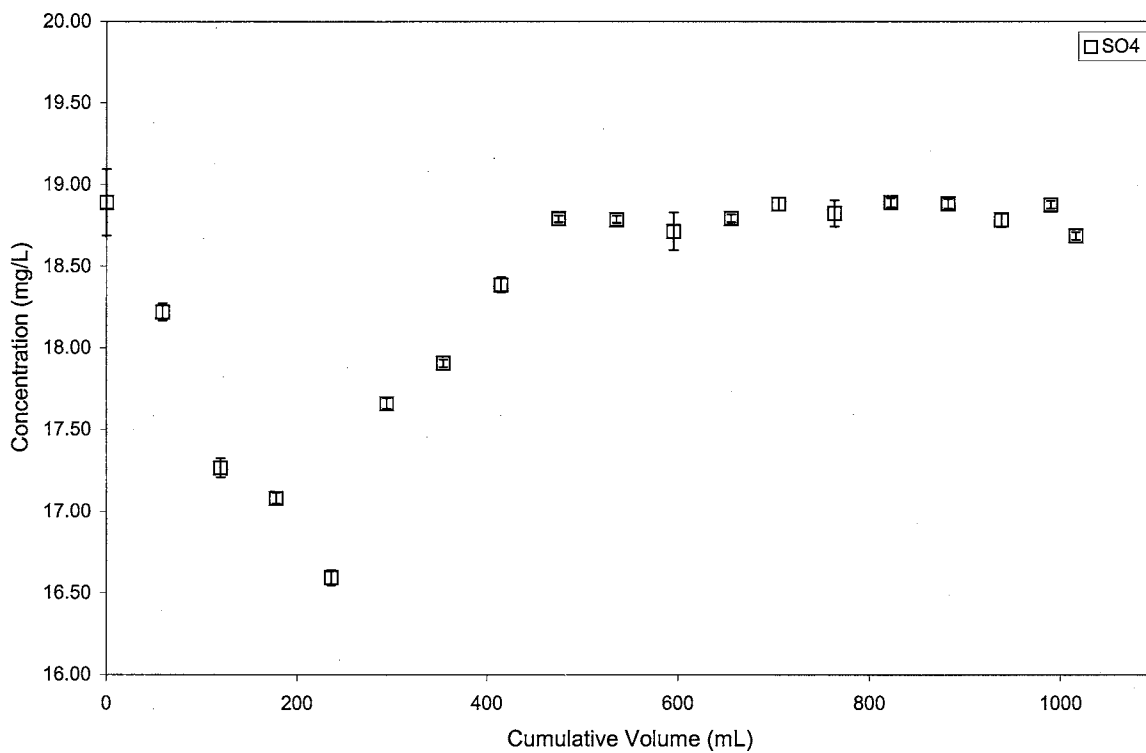


**Figure 44 -** Results of tap water experiment with 425 mg/L of suspended clay. Error bars represent an analytical uncertainty of two standard deviations. True dissolved concentrations are denoted by the data point for “zero volume filtered.”

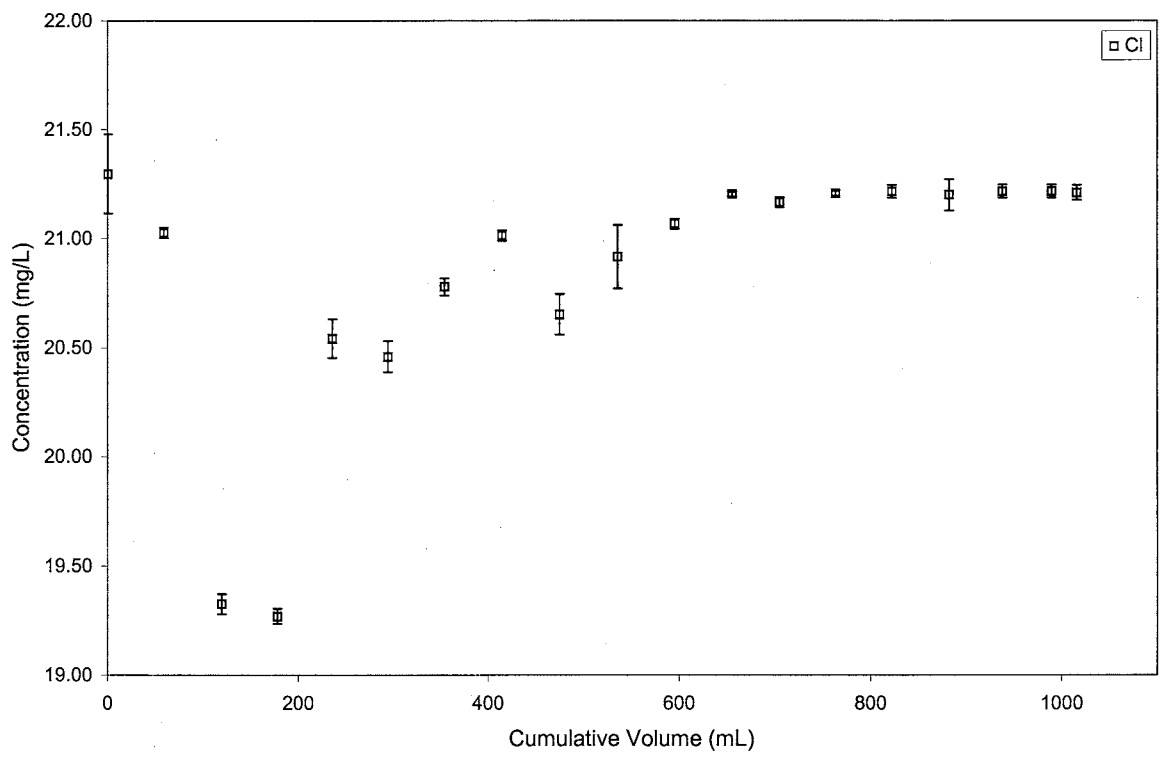


**Figure 45 -** Results of tap water experiment with 425 mg/L of suspended clay. Error bars represent an analytical uncertainty of two standard deviations. True dissolved concentrations are denoted by the data point for “zero volume filtered.”

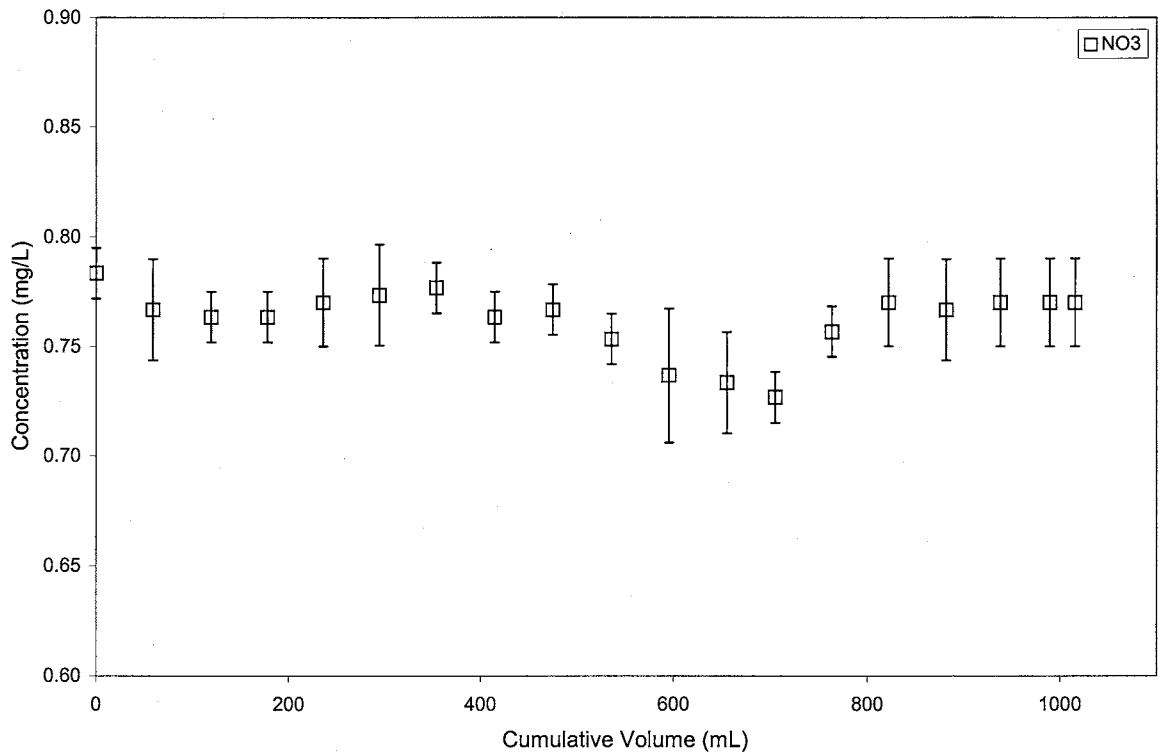


**Figure 46 -** Results of tap water experiment with 425 mg/L of suspended clay. Error bars represent an analytical uncertainty of two standard deviations. True dissolved concentrations are denoted by the data point for “zero volume filtered.”



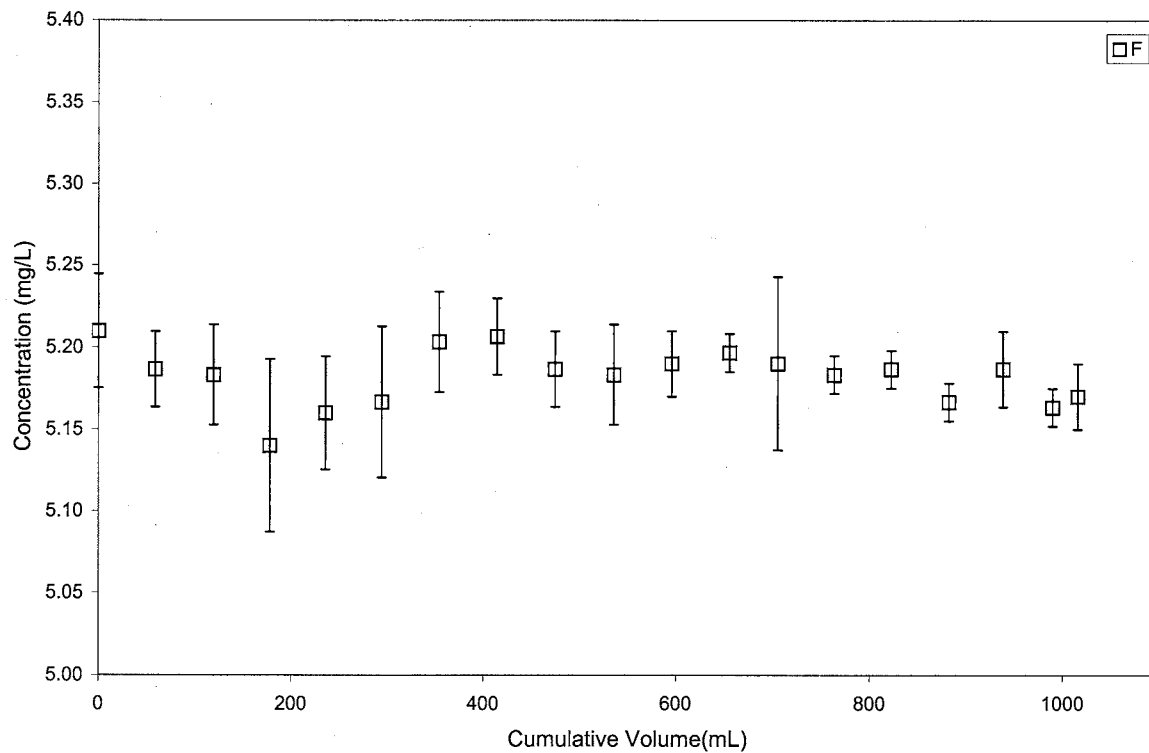
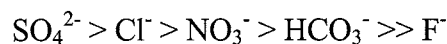
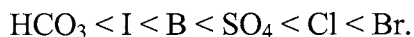


**Figure 47 -** Results of tap water experiment with 425 mg/L of suspended clay. Error bars represent an analytical uncertainty of two standard deviations. True dissolved concentrations are denoted by the data point for “zero volume filtered.”

From these results, it would appear that the following series would best describe the affinity of major anions to be retained by the bentonite membrane:



This trend is somewhat different than that noted by Briggs (1906). As stated earlier, Briggs (1906) found that the membrane effect during the filtration of waters with high clay loads was greatest for the complex anions of  $\text{SO}_4^{2-}$ ,  $\text{HCO}_3^-$ , and  $\text{NO}_3^-$ , and insignificant for simple ions such as  $\text{Cl}^-$ . The results from this study do confirm Briggs' contention that filtering waters with high clay loads will tend to underestimate the concentrations of polyatomic ions. However, the fact that  $\text{Cl}^-$  levels also seem to be subject to this effect differs with Briggs' (1906) conclusions. This is probably due to differing membrane properties of smectite and the kaolinite used by Briggs (1906). Kharaka and Berry (1973) found that the retardation sequence for anions at room temperature were variable during high pressure geological membrane experiments, but at 70°C, the following retardation sequence was generally noted:



Kharaka and Berry (1973) noted that the retardation sequence for anions was most strongly affected by temperature.

Figures 48 - 51 show the concentrations of the major cations as a function of the volume of solution filtered for the 425 mg/L clay - tap water solution. Again, all of the major cation species exhibited different rates and amounts of rejection by the bentonite membrane.

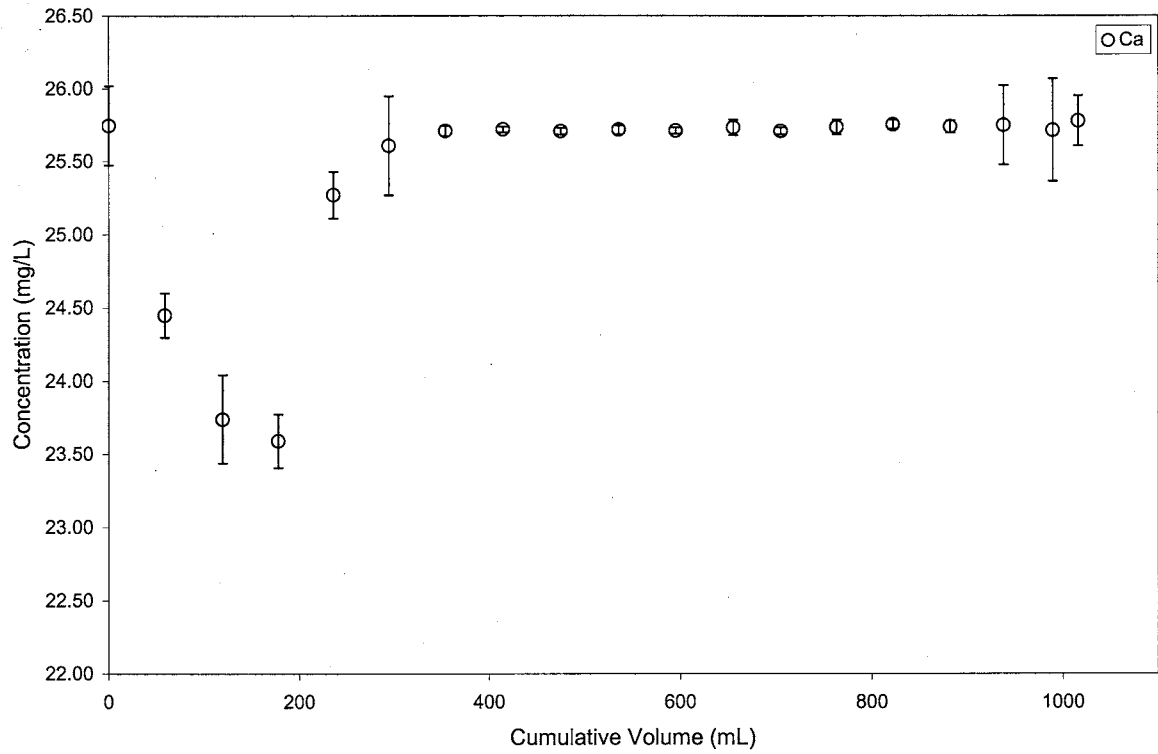


**Figure 48 -** Results of tap water experiment with 425 mg/L of suspended clay. Error bars represent an analytical uncertainty of two standard deviations. True dissolved concentrations are denoted by the data point for “zero volume filtered.”

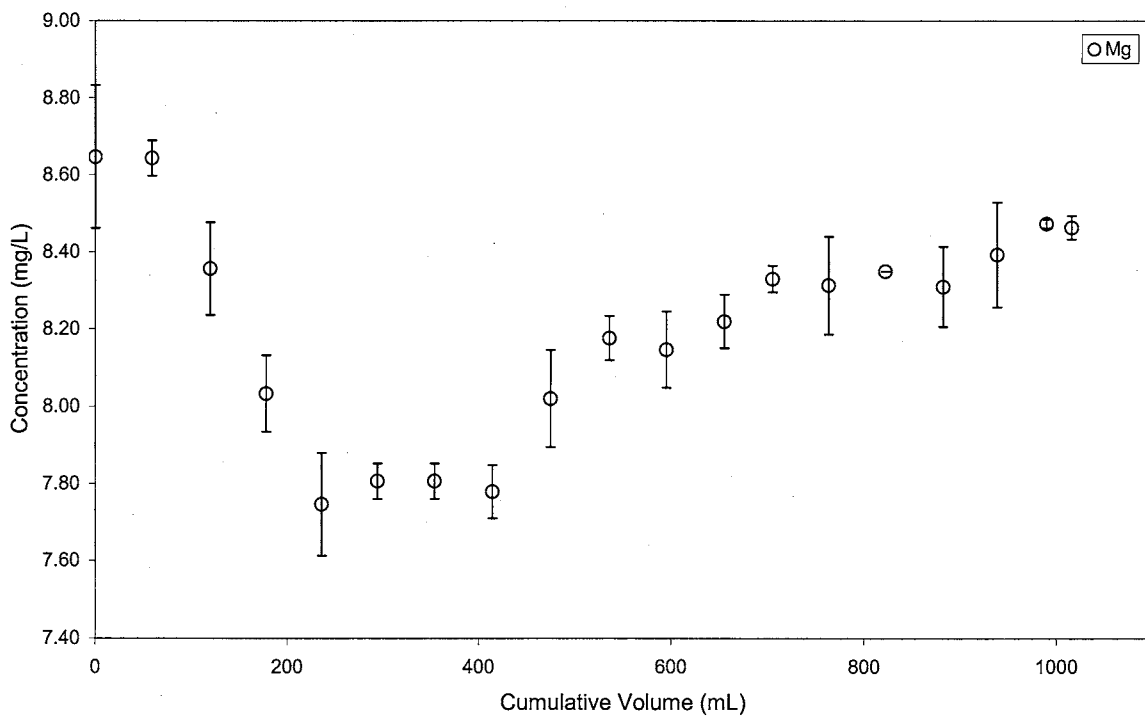


**Figure 49 -** Results of tap water experiment with 425 mg/L of suspended clay. Error bars represent an analytical uncertainty of two standard deviations. True dissolved concentrations are denoted by the data point for “zero volume filtered.”

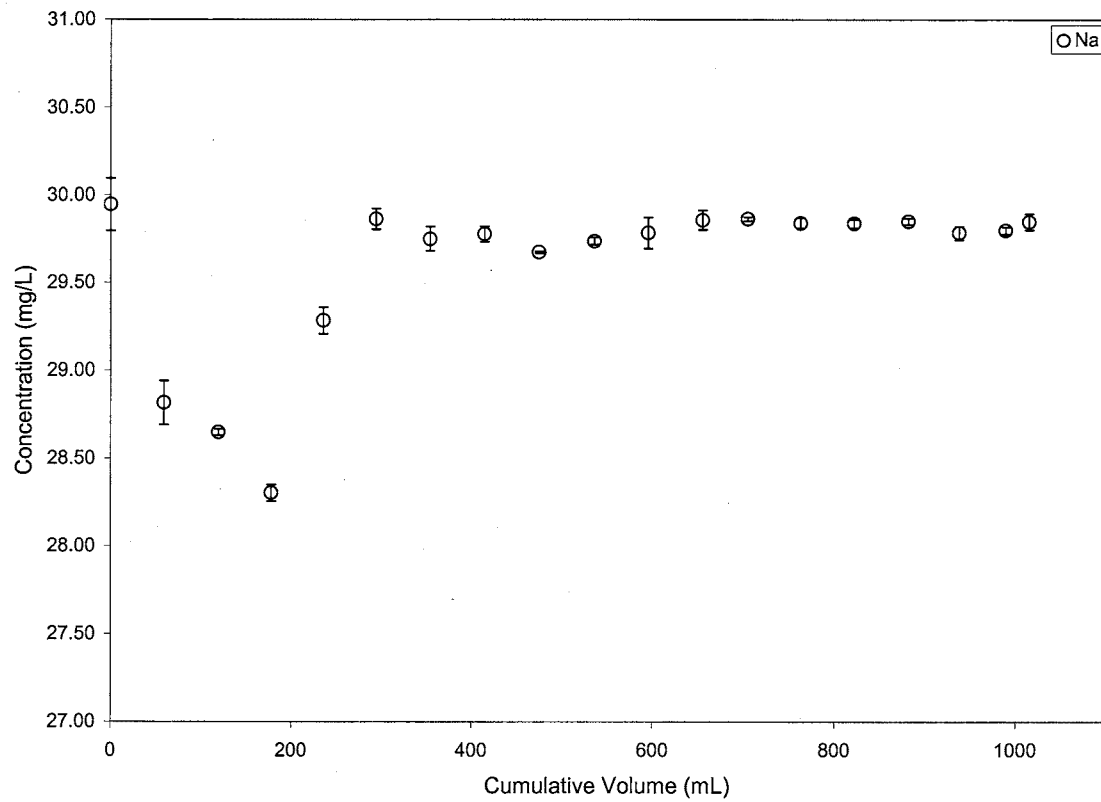


**Figure 50 -** Results of tap water experiment with 425 mg/L of suspended clay. Error bars represent an analytical uncertainty of two standard deviations. True dissolved concentrations are denoted by the data point for “zero volume filtered.”

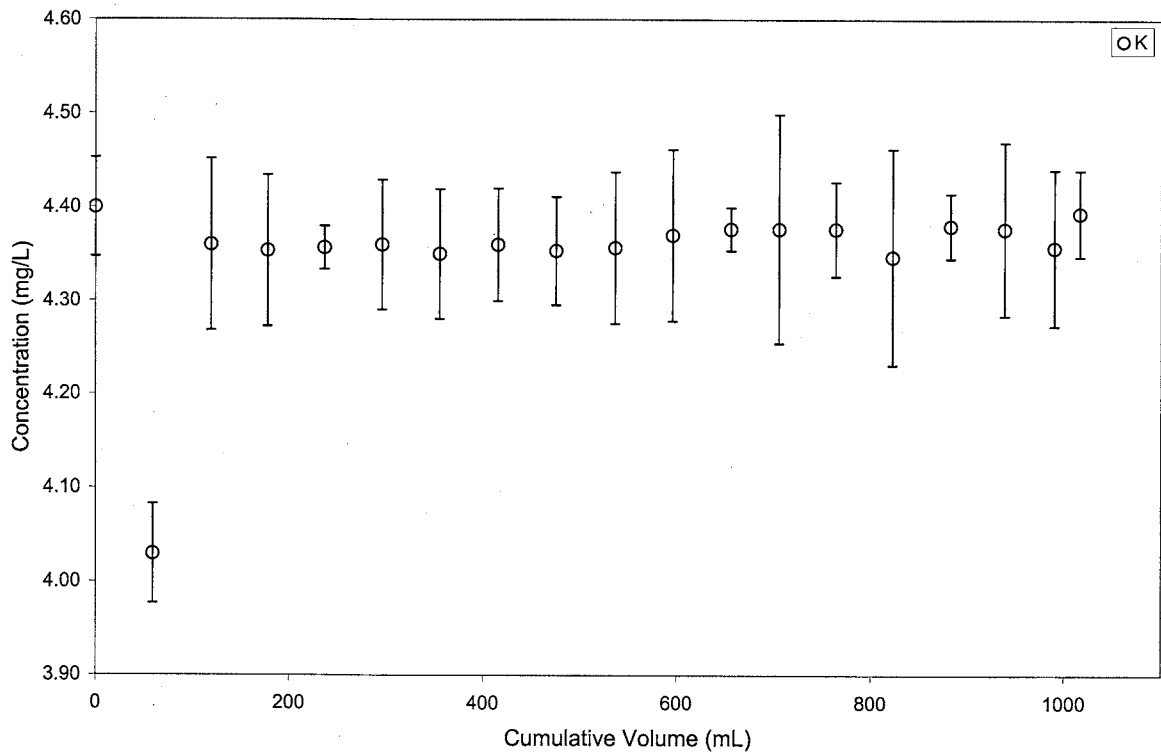
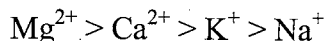
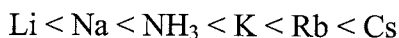


**Figure 51 -** Results of tap water experiment with 425 mg/L of suspended clay. Error bars represent an analytical uncertainty of two standard deviations. True dissolved concentrations are denoted by the data point for “zero volume filtered.”

The divalent cations  $\text{Ca}^{2+}$  and  $\text{Mg}^{2+}$  exhibited the largest concentration drop of any of the major cations with concentration decreases of 8.6% and 10.0%, respectively. The monovalent cations  $\text{Na}^+$  and  $\text{K}^+$  showed decreases of 5.0% and 8.0%. Based on these results, the following series best describes the affinity of the bentonite membrane to reject cation species during filtration:



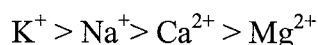
Based on this series, it appears that divalent cations are much more susceptible to this membrane effect than monovalent cations. This observation is very similar to that made by Loeb (1964) during early reverse osmosis experiments; Loeb (1964) showed that divalent cations in solution were rejected to a much greater degree than monovalent cations (Figure 6). Kharaka and Berry (1973) found that the retardation sequences for monovalent and divalent cations at laboratory temperature during high pressure geological membrane experiments were generally:



Kharaka and Berry (1973) noted that this retardation sequence was affected by compaction pressure, flow pressure, the forces of attraction between the cations and the electrical sites on the surface of the clay particles, the forces of repulsion between the cations and the streaming potential, and the drag due to the passage of the water through the membrane.

Briggs (1906) examined this effect with Na-based salts only. He stated that the major cause of this effect was the size and charge of the salts' anions. If the ionic radii of

the cations were the sole factor determining the retention of cations by the clay membrane, then the following series would have to hold true:



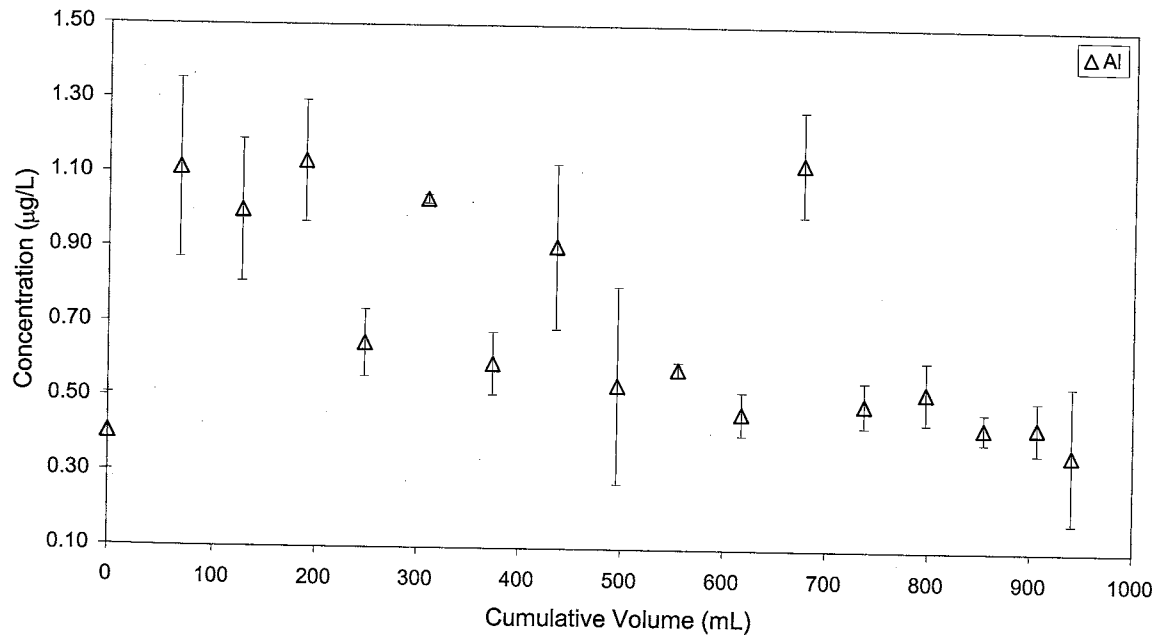
Since this is not the case, the valence may determine the affinity of the membrane to retain certain cations.

Figures 52 through 54 show the concentration of Al as a function of sample volume filtered for the three clay - tap water solutions. The three figures confirm some long held beliefs regarding the variation of Al concentrations due to filtration and present some interesting new concepts.

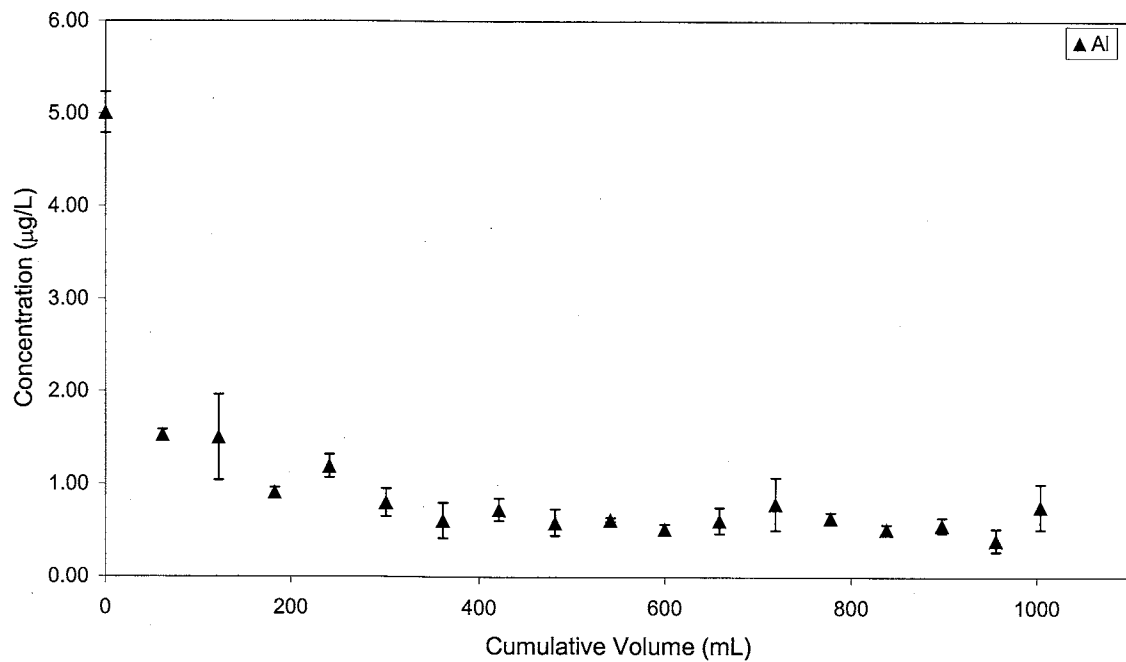
Figure 52 shows the variation of Al levels with respect to the amount of solution filtered for the 102 mg/L clay - tap water solution. Note that the concentration of Aluminum in each aliquot is consistently higher than that in the original solution for the first 800 mL of filtrate. After 800 mL of the solution has been filtered, the Aluminum concentration in the filtrate begins to return to that of the original solution. In this case, it appears as though the passage of colloidal clay through the filter paper is the cause for the Al concentration profile seen in Figure 52.

Figure 53 shows the variation of Al concentration as a function of the amount of solution filtered for the 284 mg/L clay - tap water solution. The concentration of Al in each aliquot is consistently higher than that in the original solution. The Al concentrations in the first few aliquots are significantly higher than the actual concentration. However, after some 400 mL of the solution has been filtered, the Al levels return to concentrations extremely close to that of the blank solution.





**Figure 52 -** Results of tap water experiment with 102 mg/L of suspended clay. Error bars represent an analytical uncertainty of two standard deviations. True dissolved concentration is denoted by the data point for “zero volume filtered.”



**Figure 53 -** Results of tap water experiment with 282 mg/L of suspended clay. Error bars represent an analytical uncertainty of two standard deviations. True dissolved concentration is denoted by the data point for “zero volume filtered.”

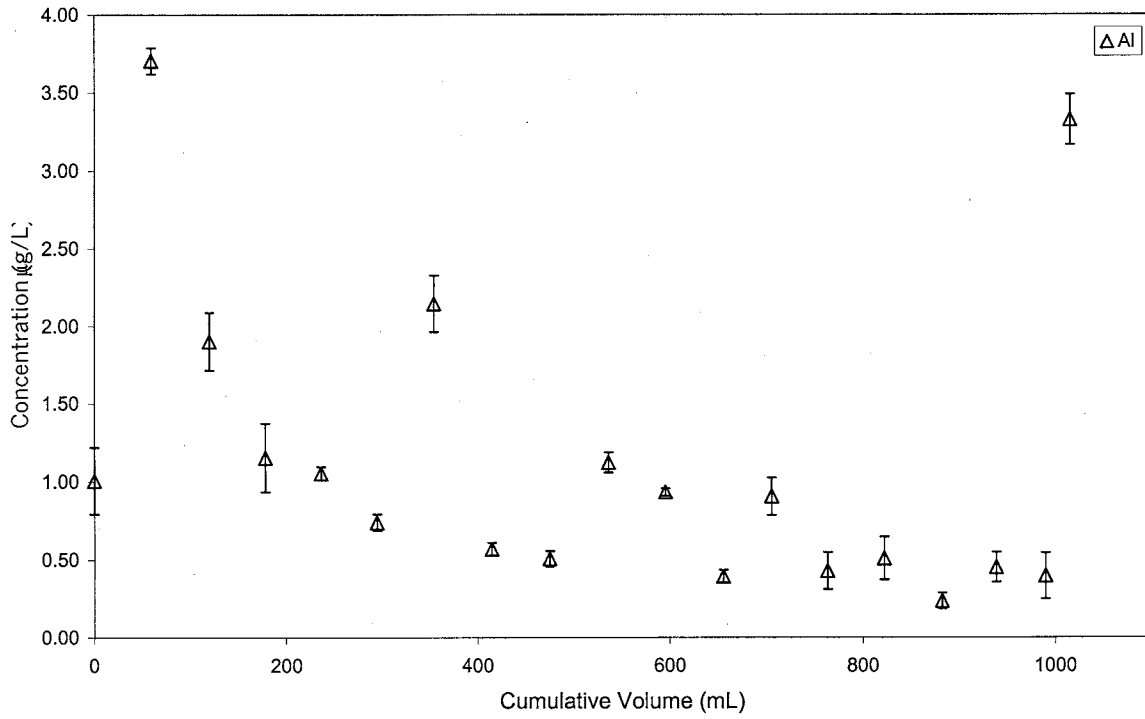


**Figure 54 -** Results of tap water experiment with 425 mg/L of suspended clay. Error bars represent an analytical uncertainty of two standard deviations. True dissolved concentration is denoted by the data point for “zero volume filtered.”

Perhaps the most interesting results of this study are shown in Figure 54. Figure 52 contains the Al concentration profile for the filtration of the 425 mg/L clay - tap water

solution. In this case, it seems as though there are two different mechanisms competing. On one hand, the passage of colloidal clay through the filter raises the Al concentrations above the true concentration for initial portions of the solution. However, as more of the clay accumulates onto the filter, the Al levels fall significantly below that of the blank solution. This drop seems to indicate that solute sieving may be taking place. The last aliquot filtered is significantly higher than the true solution concentration. This may be due to the passage of clay particles through the filter or could represent some type of breakthrough concentration for this filter run.

The filtrate aliquots produced from the Rio Grande and Rio Puerco samples yielded results similar to those of the NaCl - clay solutions. The solute concentrations of the first few filtrate aliquots decreased rapidly and settled out after the first 200 mL (Figures 55 - 68). A significant amount of clay from the Rio Grande sample passed through the 0.45  $\mu\text{m}$  filter as the first 150 mL of sample was filtered. As a layer of sediments accumulated onto the filter, the passage of clay along with the filtrate stopped. There was no visible trace of sediment in any of the filtrate aliquots produced from the Rio Puerco water.

Both samples showed a significant decrease in the concentration of all major species during the first few aliquots. This trend was accompanied by a significant decrease in the flow rate of the filtrate during these first aliquots. As both samples were filtered, one could notice a significant increase in the amount of sediments close to the

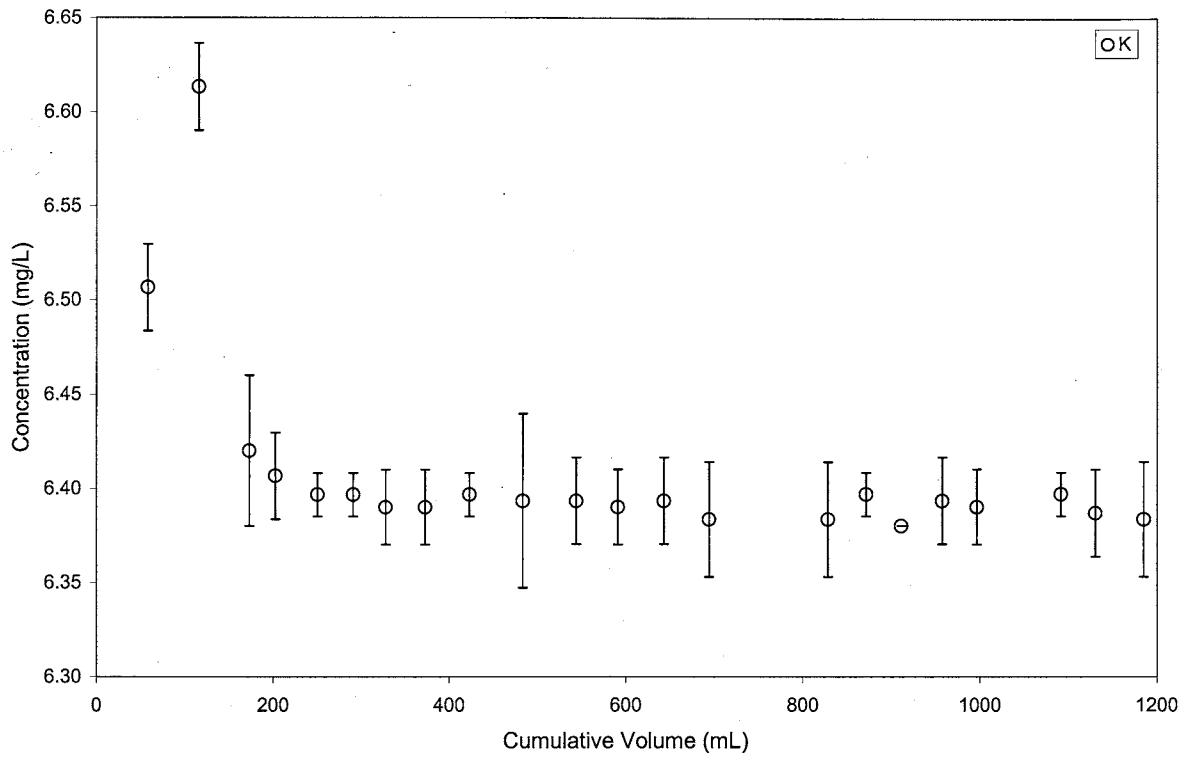


**Figure 55 -** Plot of filtrate concentration as function of sample filtered for Rio Grande water sample with a suspended solids concentration of 4,100 mg/L. Error bars represent an analytical uncertainty of two standard deviations.

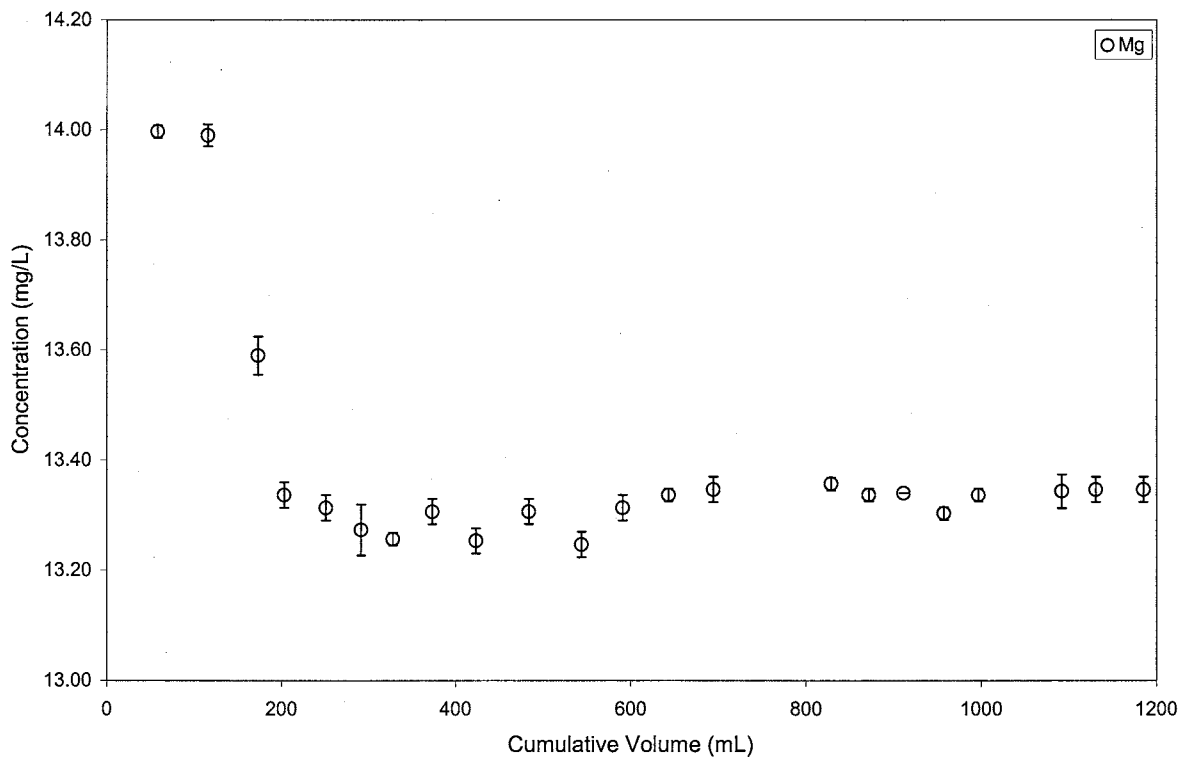


**Figure 56 -** Plot of filtrate concentration as function of sample filtered for Rio Grande water sample with a suspended solids concentration of 4,100 mg/L. Error bars represent an analytical uncertainty of two standard deviations.

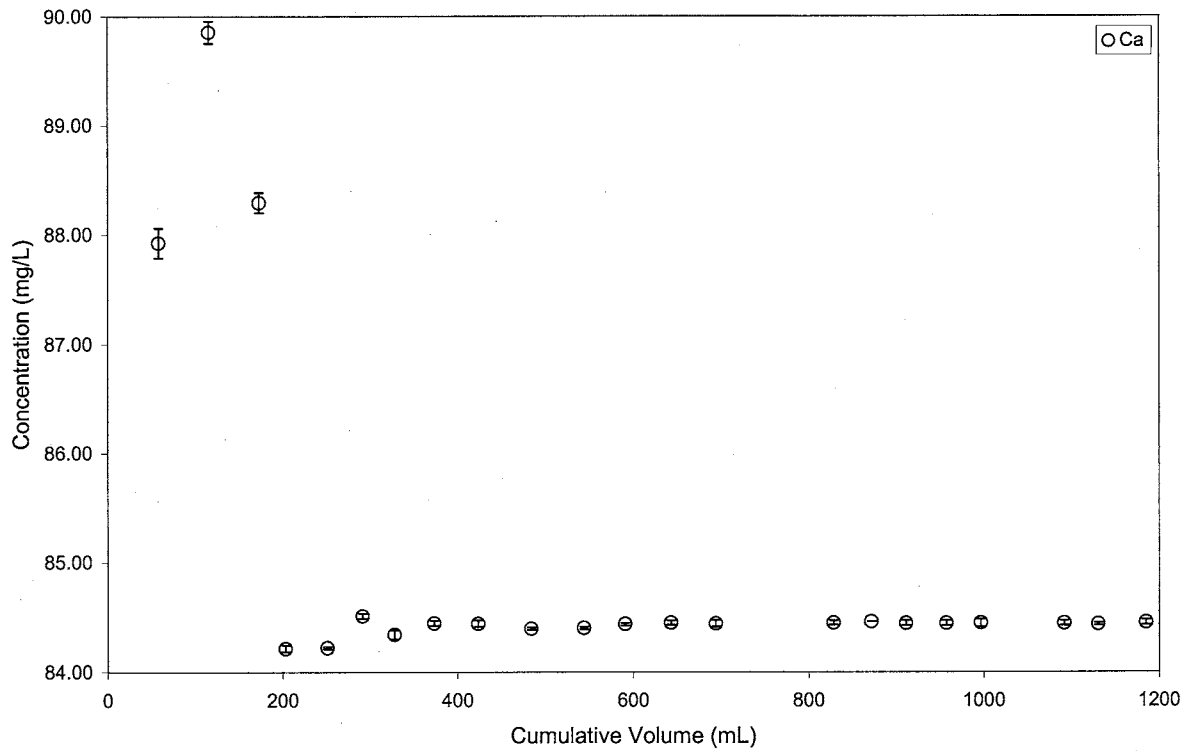


**Figure 57 -** Plot of filtrate concentration as function of sample filtered for Rio Grande water sample with a suspended solids concentration of 4,100 mg/L. Error bars represent an analytical uncertainty of two standard deviations.

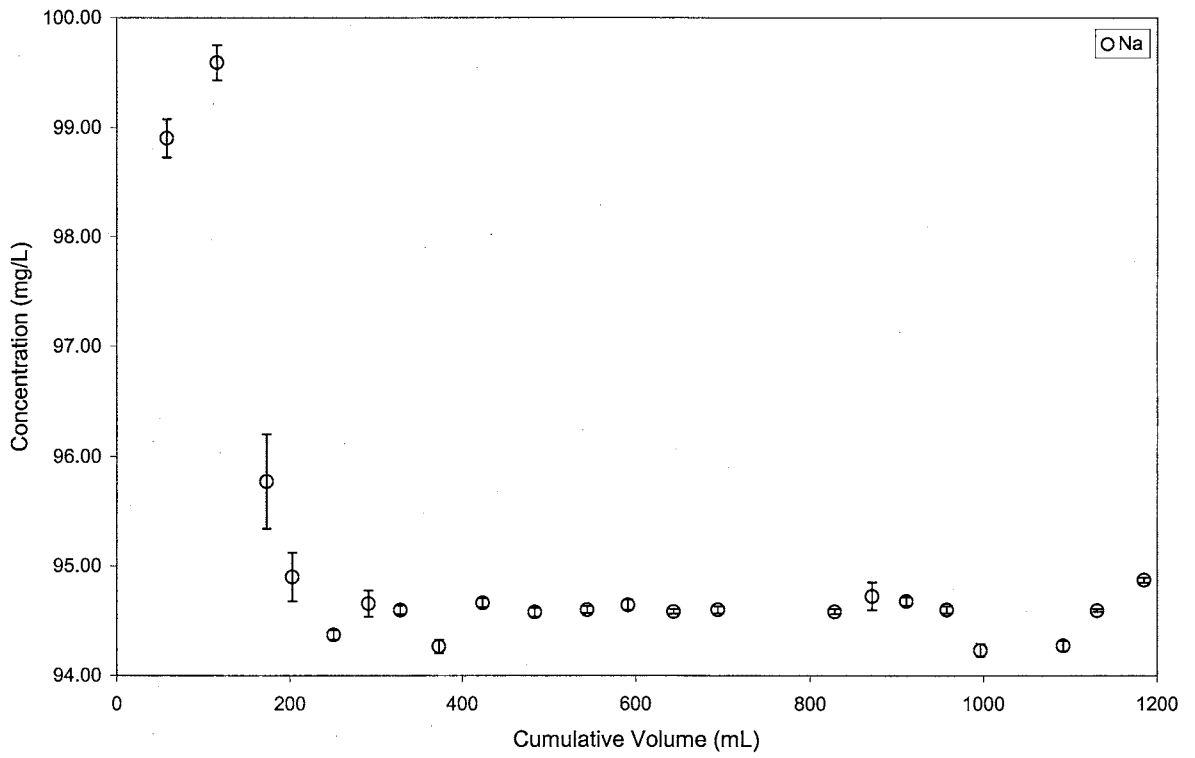


**Figure 58 -** Plot of filtrate concentration as function of sample filtered for Rio Grande water sample with a suspended solids concentration of 4,100 mg/L. Error bars represent an analytical uncertainty of two standard deviations.



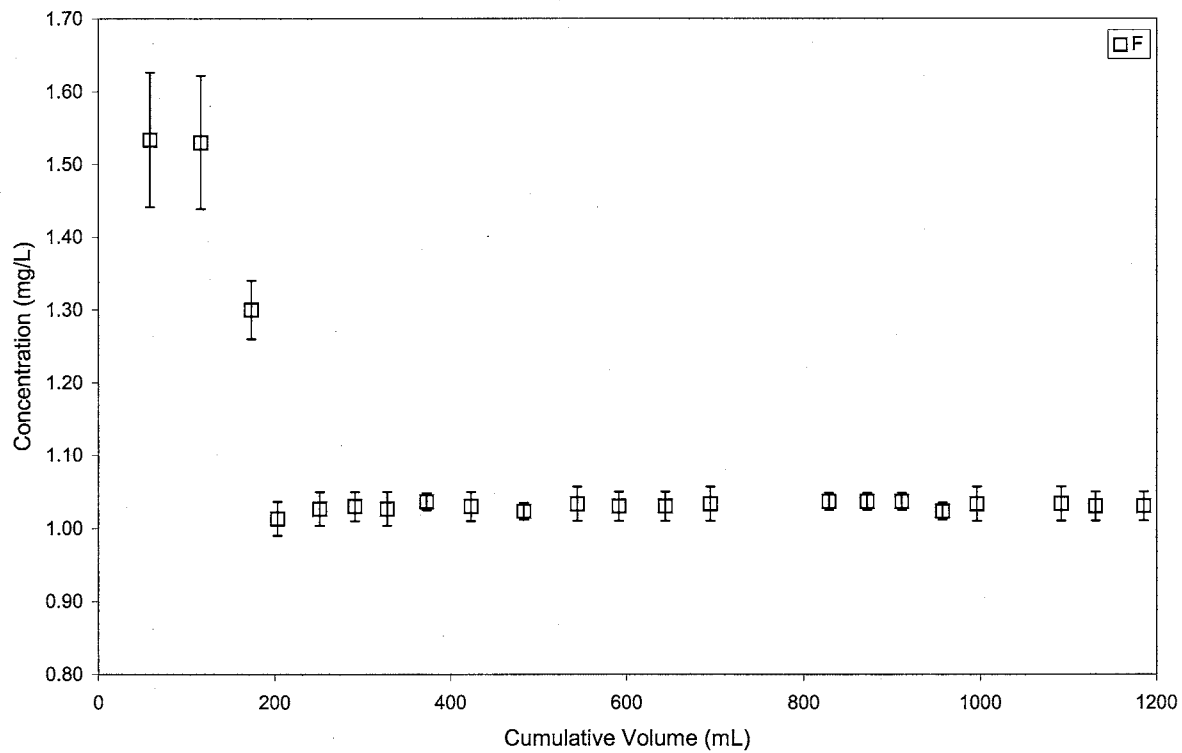


**Figure 59** - Plot of filtrate concentration as function of sample filtered for Rio Grande water sample with a suspended solids concentration of 4,100 mg/L. Error bars represent an analytical uncertainty of two standard deviations.

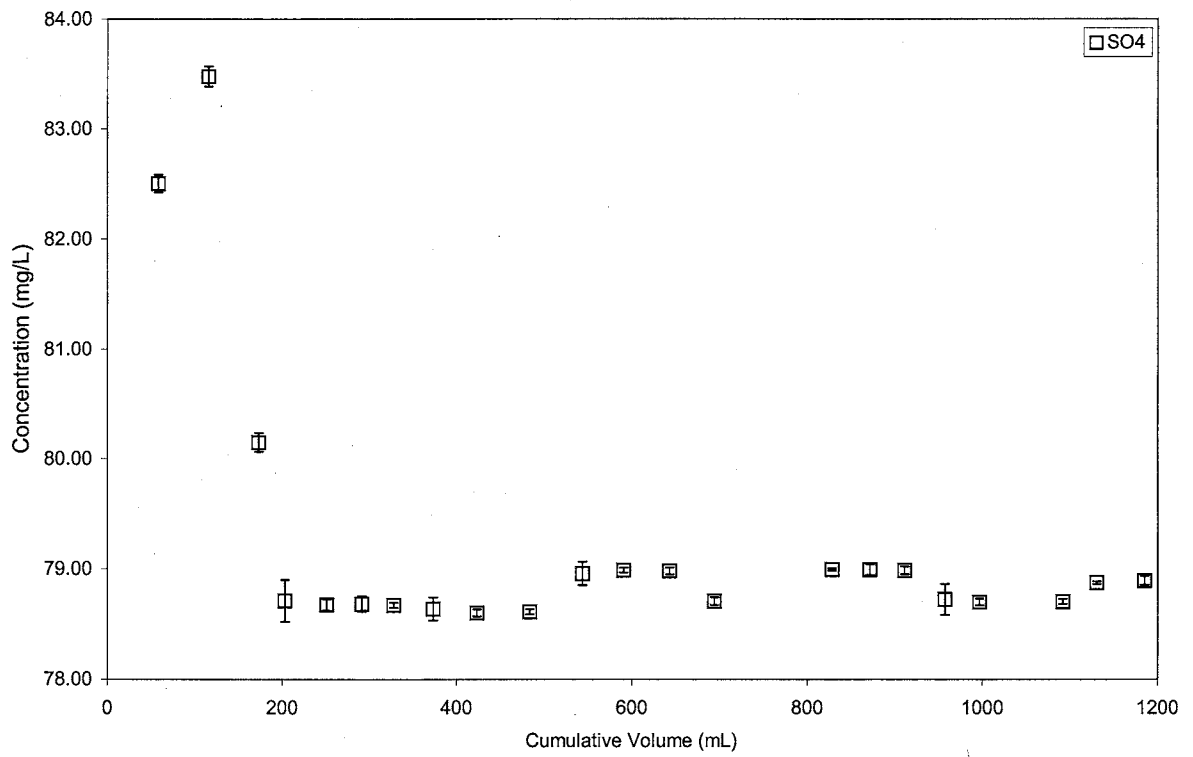


**Figure 60 -** Plot of filtrate concentration as function of sample filtered for Rio Grande water sample with a suspended solids concentration of 4,100 mg/L. Error bars represent an analytical uncertainty of two standard deviations.

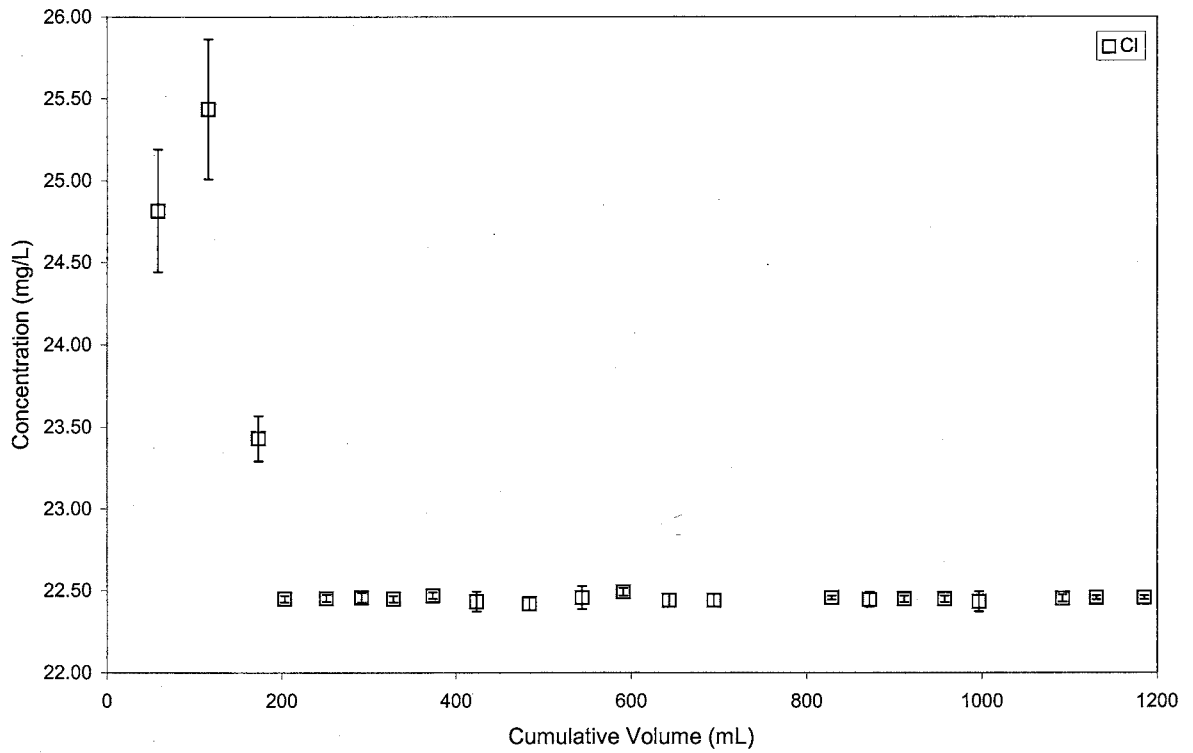


**Figure 61 -** Plot of filtrate concentration as function of sample filtered for Rio Grande water sample with a suspended solids concentration of 4,100 mg/L. Error bars represent an analytical uncertainty of two standard deviations.

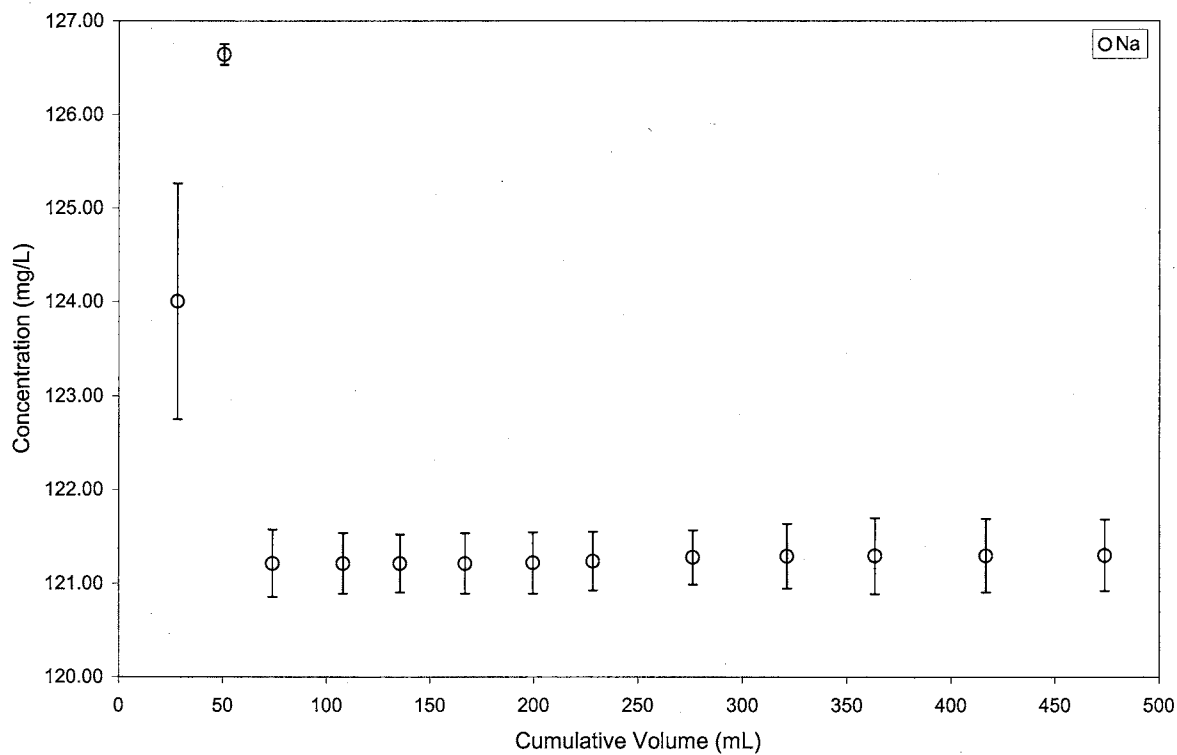


**Figure 62 -** Plot of filtrate concentration as function of sample filtered for Rio Puerco water sample with a suspended solids concentration of 32,100 mg/L. Error bars represent an analytical uncertainty of two standard deviations.

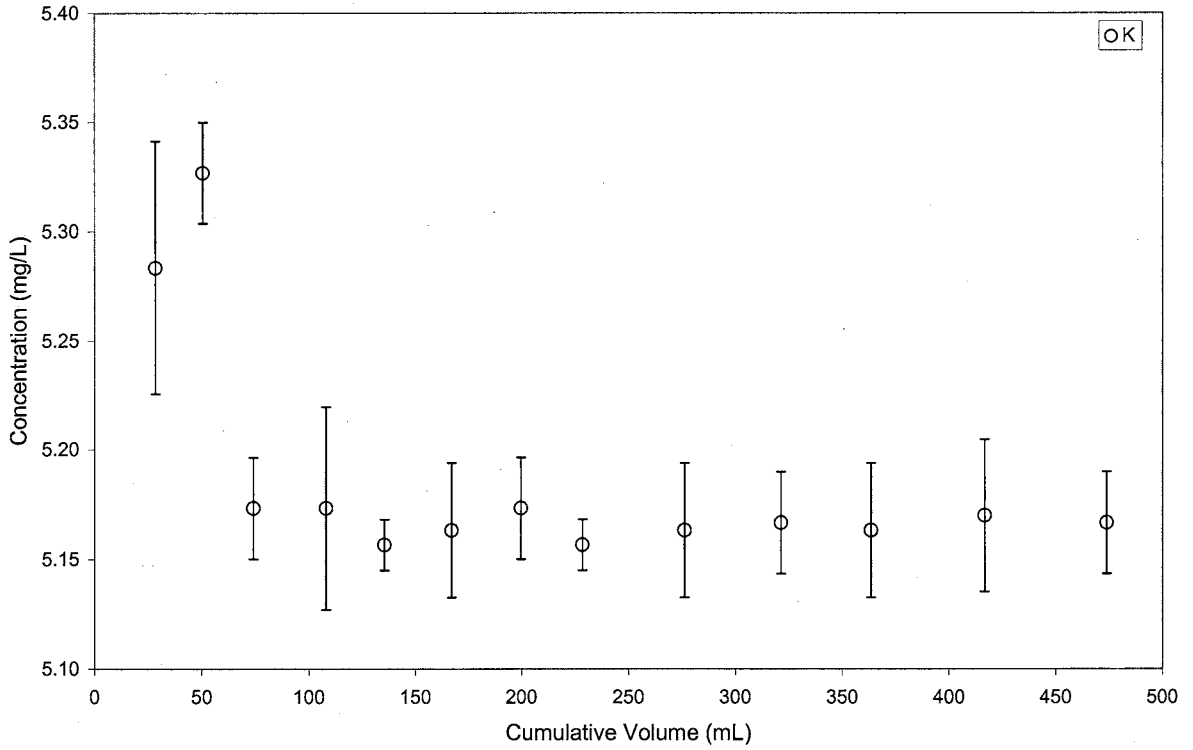


**Figure 63 -** Plot of filtrate concentration as function of sample filtered for Rio Puerco water sample with a suspended solids concentration of 32,100 mg/L. Error bars represent an analytical uncertainty of two standard deviations.

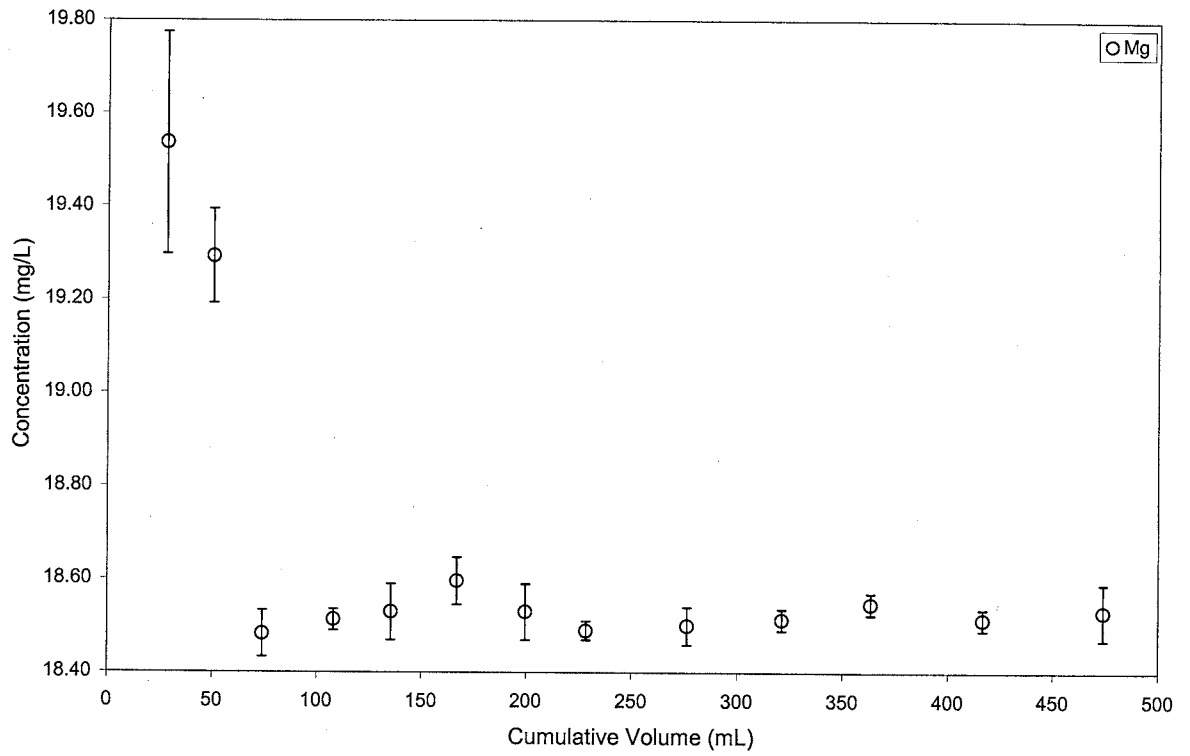


**Figure 64 -** Plot of filtrate concentration as function of sample filtered for Rio Puerco water sample with a suspended solids concentration of 32,100 mg/L. Error bars represent an analytical uncertainty of two standard deviations.

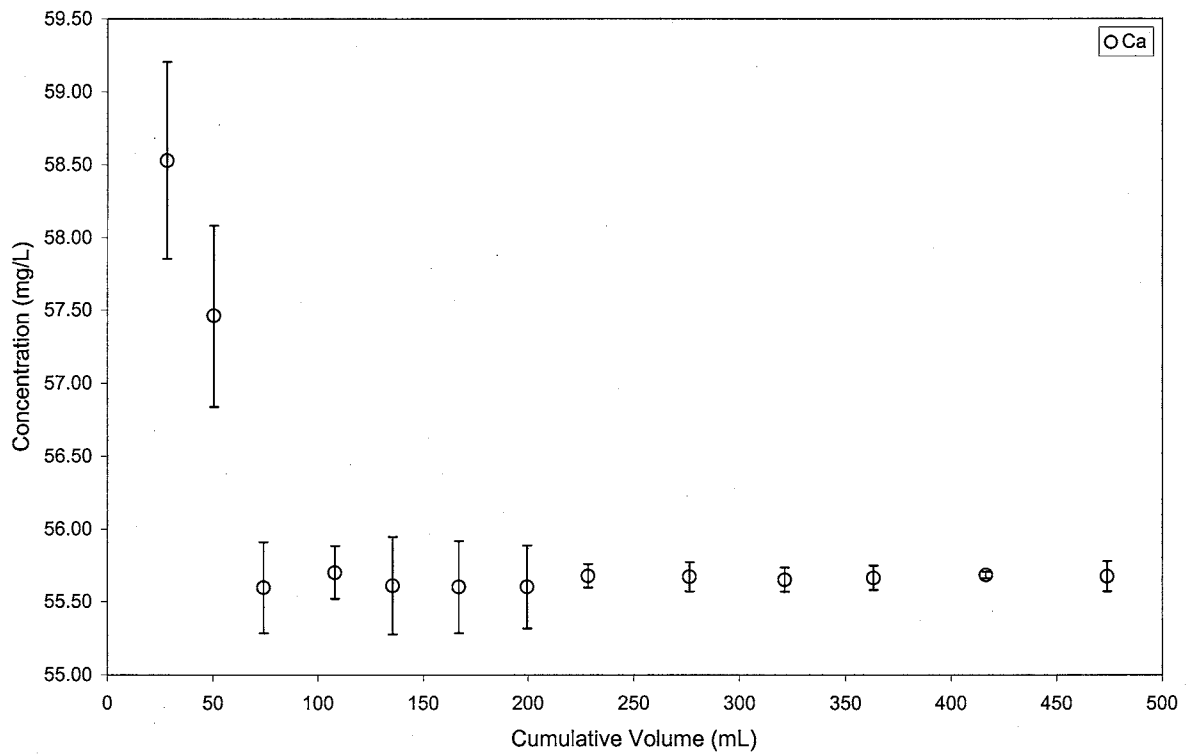


**Figure 65 -** Plot of filtrate concentration as function of sample filtered for Rio Puerco water sample with a suspended solids concentration of 32,100 mg/L. Error bars represent an analytical uncertainty of two standard deviations.

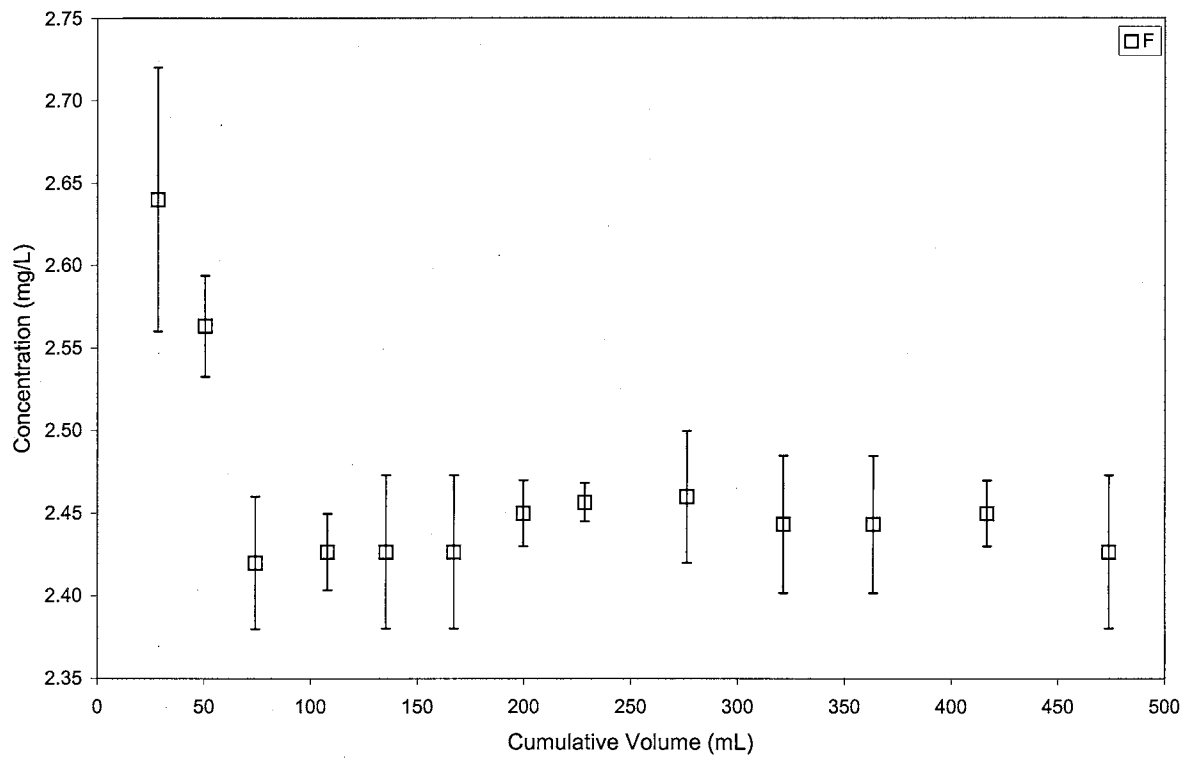


**Figure 66 -** Plot of filtrate concentration as function of sample filtered for Rio Puerco water sample with a suspended solids concentration of 32,100 mg/L. Error bars represent an analytical uncertainty of two standard deviations.



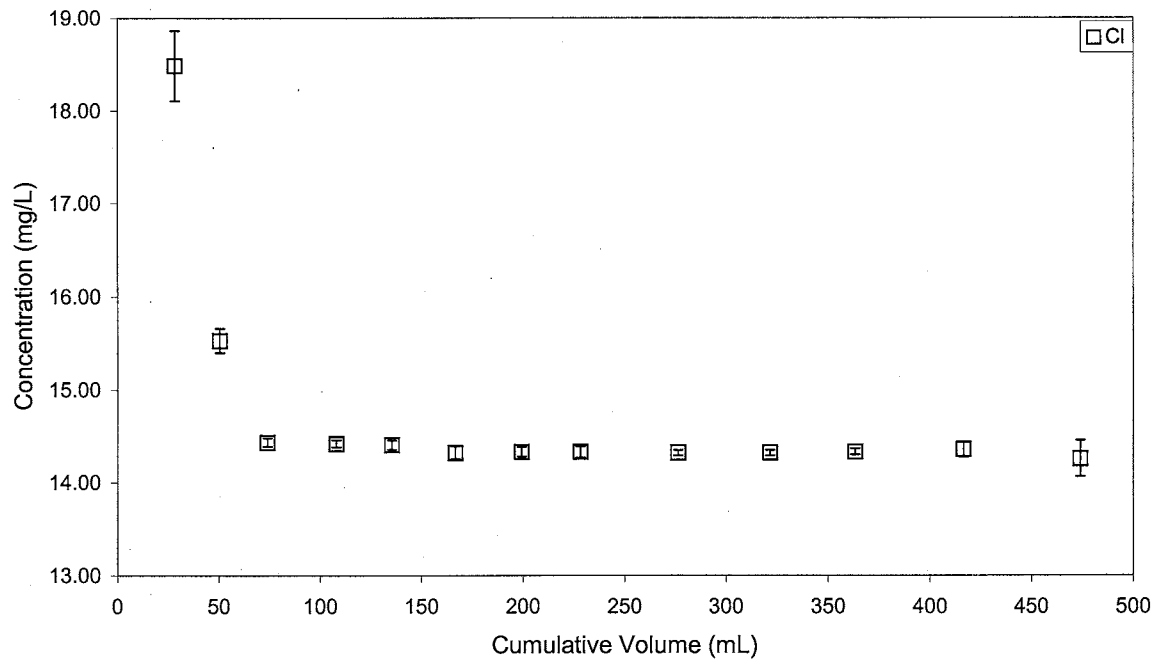


**Figure 67 -** Plot of filtrate concentration as function of sample filtered for Rio Puerco water sample with a suspended solids concentration of 32,100 mg/L. Error bars represent an analytical uncertainty of two standard deviations.

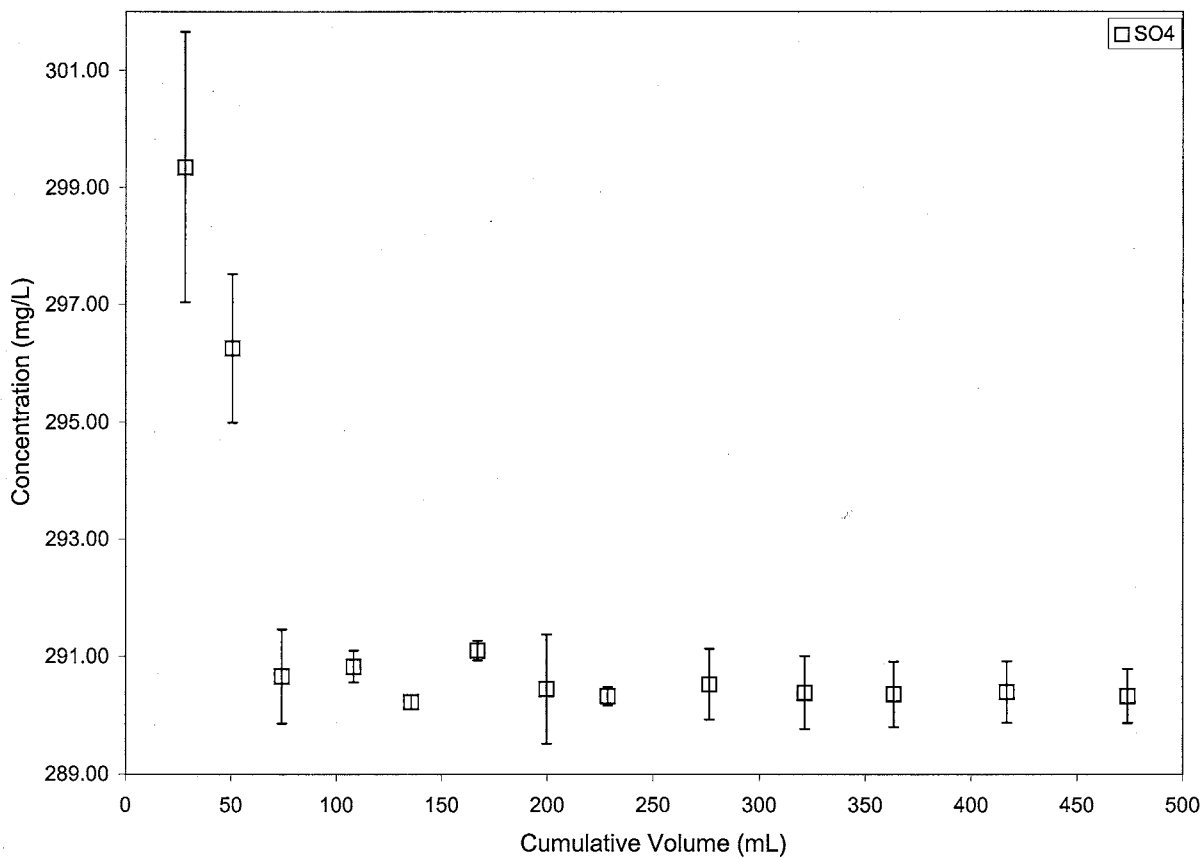


**Figure 68 -** Plot of filtrate concentration as function of sample filtered for Rio Puerco water sample with a suspended solids concentration of 32,100 mg/L. Error bars represent an analytical uncertainty of two standard deviations.

filter medium. This increase in sediment concentration near the filter medium was accompanied by a visible decrease in sediments at the top of the filter cell. By definition, these observations are indicative of the formation of a concentration polarization layer of sediments during filtration.

**Table 10 -** Maximum effluent solute reduction in river water filtration experiments

Analyte	Rio Puerco (TSS = 32,100 mg/L)	Rio Grande (TSS = 4,100 mg/L)
Na <sup>+</sup>	2.2%	4.8%
K <sup>+</sup>	1.9%	2.0%
Ca <sup>2+</sup>	4.6%	4.1%
Mg <sup>2+</sup>	5.7%	5.4%
Cl <sup>-</sup>	9.0%	9.0%
F <sup>-</sup>	23.0%	31%
SO <sub>4</sub> <sup>2-</sup>	3.3%	4.7%

X-ray diffraction analysis of the sediments from the Rio Grande showed that the sediments were primarily composed of 90% quartz (SiO<sub>2</sub>) and 6.0% diopside (CaMg(SiO<sub>3</sub>)<sub>2</sub>). Using the same method, the sediments from the Rio Puerco sample were determined to be comprised of 20% illite (K<sub>0.7</sub>Al<sub>2</sub>(Si,Al)<sub>4</sub>O<sub>10</sub>(OH)<sub>2</sub>), 74% quartz (SiO<sub>2</sub>), and 21% clinopyroxene, titanian, aluminan (Ca(Ti,Mg,Al)(Si,Al)<sub>2</sub>O<sub>6</sub>).

Whitworth et al. (1999) did show that crushed quartz sand does exhibit solute sieving properties. The large amount of sediments in the Rio Grande sample (4,100 mg/L) most likely amplified these properties. The fact that the Rio Grande sediments did not contain a significant amount of clay minerals was not too surprising, as the stretch of the river from Cochiti Reservoir to Bernardo is fairly sandy and drains the urban

watershed of Albuquerque, as well as farmland throughout the Middle Rio Grande Valley.

The Rio Puerco sediments do contain significant levels of illite. Illite is a mica-like clay mineral, which is the chief constituent of many types of shales. A significant portion of the land that the Rio Puerco drains are composed of shale and shale outcrops. Thus, one would expect the sediments from the Rio Puerco sample to contain significant levels of clays. This large amount of illite present in the layer of sediments may be the chief reason for the effectiveness of these sediments as a solute sieve.

Perhaps the most dramatic evidence that sediments, which accumulate onto the 0.45  $\mu\text{m}$  filter, do act as a prefilter can be seen in Figure 69 and Figure 70. Figure 69 is a scanning electron microscope (SEM) photograph of an unused 0.45  $\mu\text{m}$  MFS filter at 2500 times magnification. Note the fibrous and porous nature of the filter. It is easy to see how a significant amount of colloidal particles could pass through this type of filter during the initial phases of filtration.

Figure 70 provides a sharp contrast to that of 69. Figure 70 is an SEM photograph of the sediments deposited onto a 0.45  $\mu\text{m}$  filter after 500 mL of water from the Rio Grande had been filtered. At a 500 times magnification level, no portion of the filter paper is visible. Material such as sand grains, detrital calcite, bacteria, clay particles, and plants have been deposited on the filter paper. If any more of the water sample were to be filtered, the solution would definitely have to pass through this layer of sediments. Interestingly, each of the particles shown in Figure 70 has been shown to act as either trace metal scavengers, or solute sieves. Stenkamp and Benjamin (1994) showed that

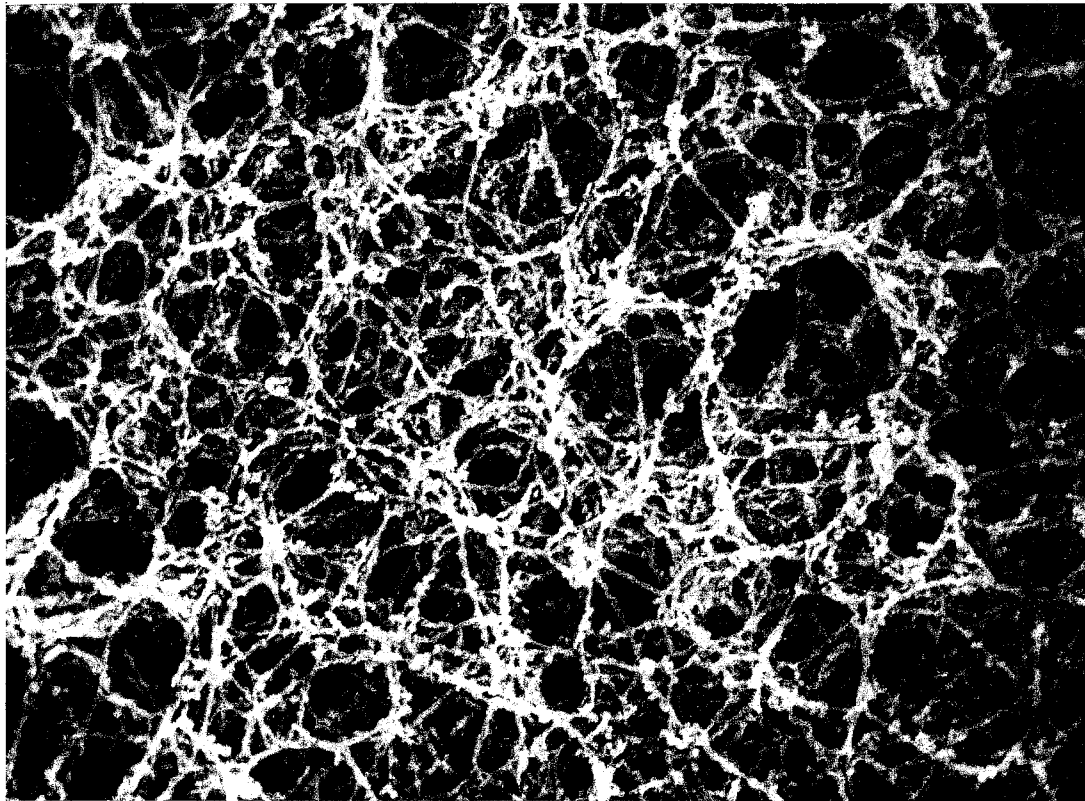


**Figure 69 -** Scanning Electron Microscope (SEM) photograph of an unused 0.45  $\mu\text{m}$  MFS filter 2500 times magnification



**Figure 70 -** Scanning Electron Microscope (SEM) photograph of a 0.45 µm MFS filter at 500 times magnification after approximately 500 mL of Rio Grande water has been filtered.

water treatment systems that have filter beds containing iron oxide coated sands are quite effective at reducing trace metal concentrations. Coffee and Gallagher (1990) showed that manganese oxide coated sand can also act as an effective trace metal scavenger. Rayson et al. (1996) showed that filters composed of immobilized humic substances retain heavy metals. Thus, the accretion of these types of material onto a filter during sample preparation greatly increases the probability that the concentrations of certain species in the filtrate are not an accurate representation of actual dissolved concentrations in the whole water samples.

One can see that there are a number of different mechanisms that may affect this type of filtration. Figure 71 presents a conceptual image of the processes that may be occurring during filtration. The suspended sediments in a water sample can be classified as either mobile or immobile particles during filtration. Large particles cannot pass through the filter pores and build up on the surface of the filter. As these large particles accumulate onto the filter, they also trap some smaller particles. Both of these types of particles can be termed immobile particles. Particles capable of passing through the filter pores and are not trapped by the larger immobile particles can be thought of as mobile particles.

Metals in solution can sorb onto either mobile or immobile particles. If metals in solution sorb onto the immobile particles, the concentrations of these metals, as measured in the filtrate, will be considerably lower than that actually in solution. However, if these trace metals sorb onto the immobile particles, which may also be composed of these trace

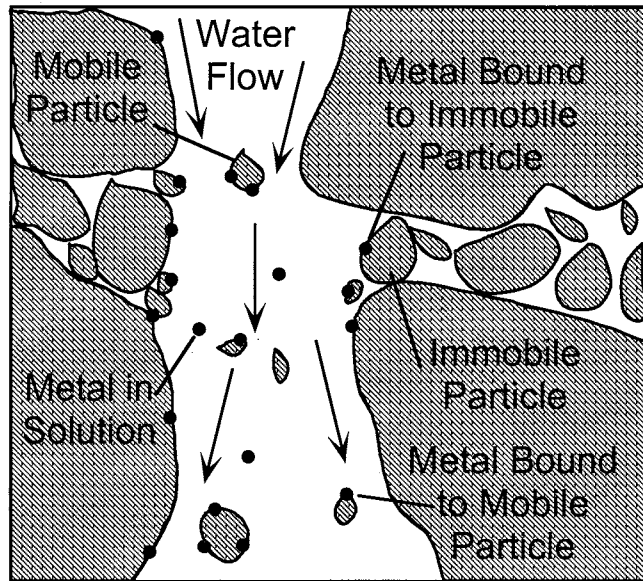


**Figure 71 -** A Conceptual Image of the Processes that may be occurring during Filtration (modified from Corapcioglu and Jiang, 1991)



metals, the concentrations of these metals in the filtrate will be considerably higher than that actually in solution.

### Chemical Analysis of Dialysis and Centrifugation Samples

Both dialysis and centrifugation have been touted as alternatives to filtration of natural waters in order to eliminate the problems associated with contamination and filtration artifacts. Figures 72 - 78 compare the analysis of filtrate from the NaCl - clay solutions treated by filtration, dialysis, and centrifugation. The values for Na<sup>+</sup> and Cl<sup>-</sup> for the filtered samples were determined using a weighted mean for each aliquot analyzed in each of the filter runs. The centrifugation and dialysis of the majority of the solutions were carried out with no apparent problems. However, the first two solutions subjected to dialysis were definitely exposed to possible sources of contamination. The 75 mg/L and 15 mg/L clay - NaCl solutions were the first two solutions placed in the dialysis cell used in this study (Figure 21). These first two cells were constructed with a metal hook and piece of string rather than the plastic fitting and nylon fishing line seen in Figure 21. After approximately five days of dialysis, the string began to fall apart, and a noticeable amount of rust could be seen on the metal hook.

A comparison of the three solid-liquid separation methods for the 5 mg/L clay - NaCl solution can be seen in Figure 72. Due to the very low suspended clay concentration, there is no noticeable difference in solute concentrations for each of the three methods. All of the solutes analyzed fall within two standard deviations of the true Na<sup>+</sup> and Cl<sup>-</sup> concentrations.

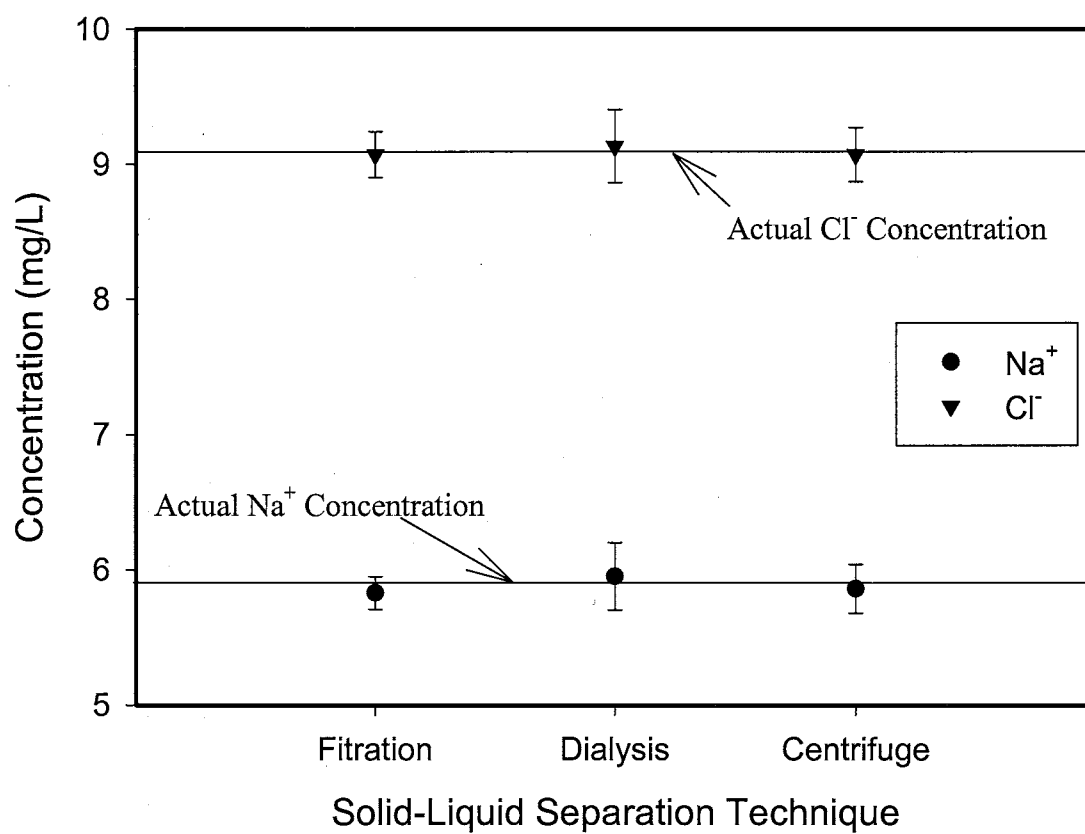


**Figure 72 -** Plot comparing solution concentration as a function of separation method for a NaCl solution with a suspended clay concentration of 5 mg/L. Solid line indicates actual solution concentration before addition of clay. Error bars represent an analytical uncertainty of two standard deviations.

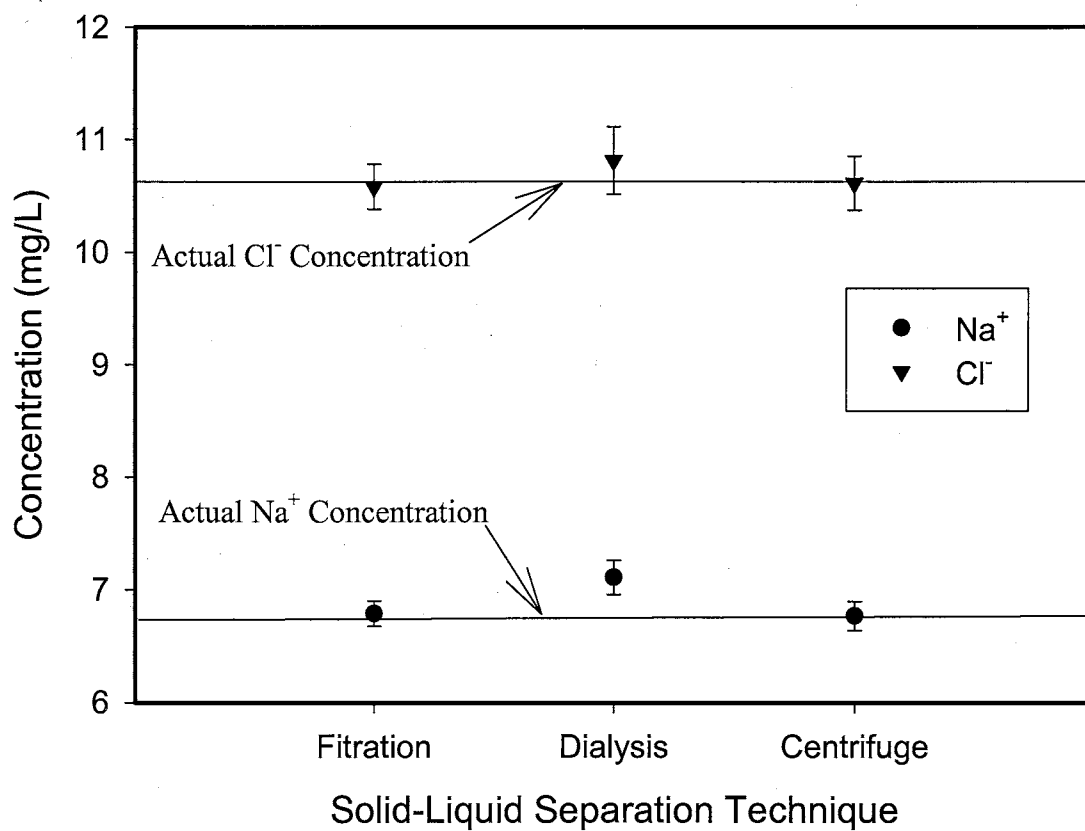


**Figure 73 -** Plot comparing solution concentration as a function of separation method for a NaCl solution with a suspended clay concentration of 10 mg/L. Solid line indicates actual solution concentration before addition of clay. Error bars represent an analytical uncertainty of two standard deviations.

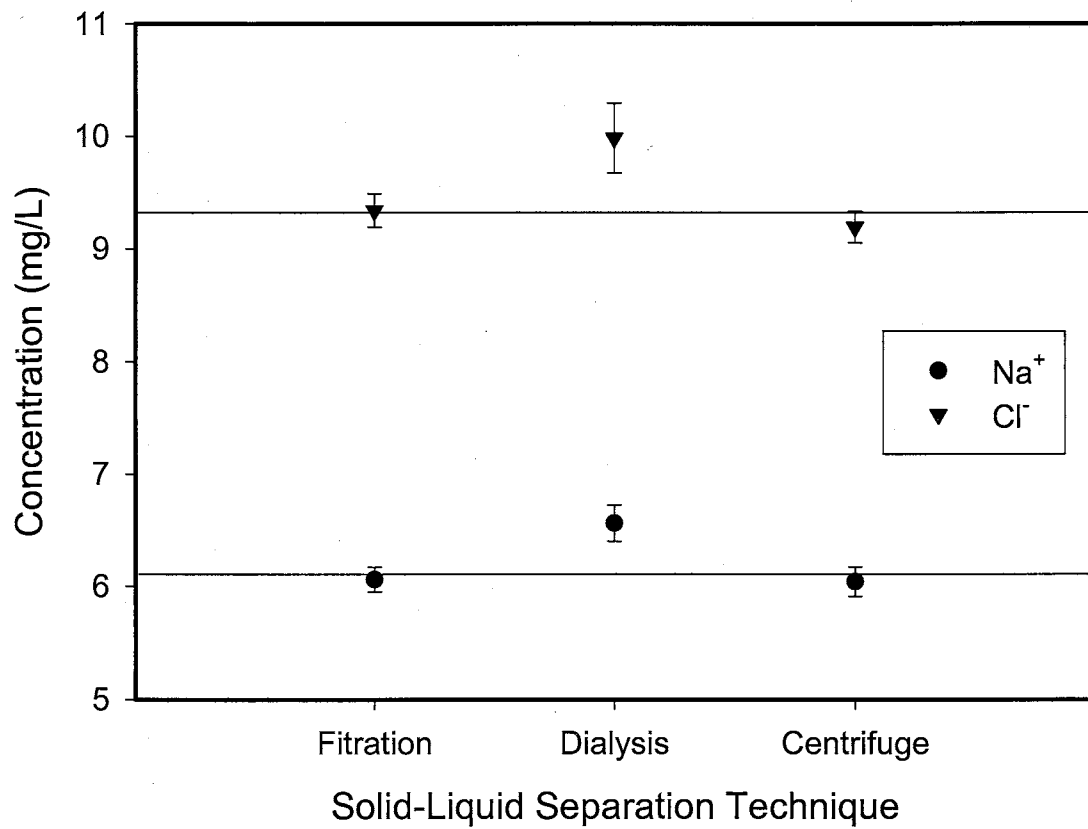


**Figure 74 -** Plot comparing solution concentration as a function of separation method for a NaCl solution with a suspended clay concentration of 15 mg/L. Solid line indicates actual solution concentration before addition of clay. Error bars represent an analytical uncertainty of two standard deviations.

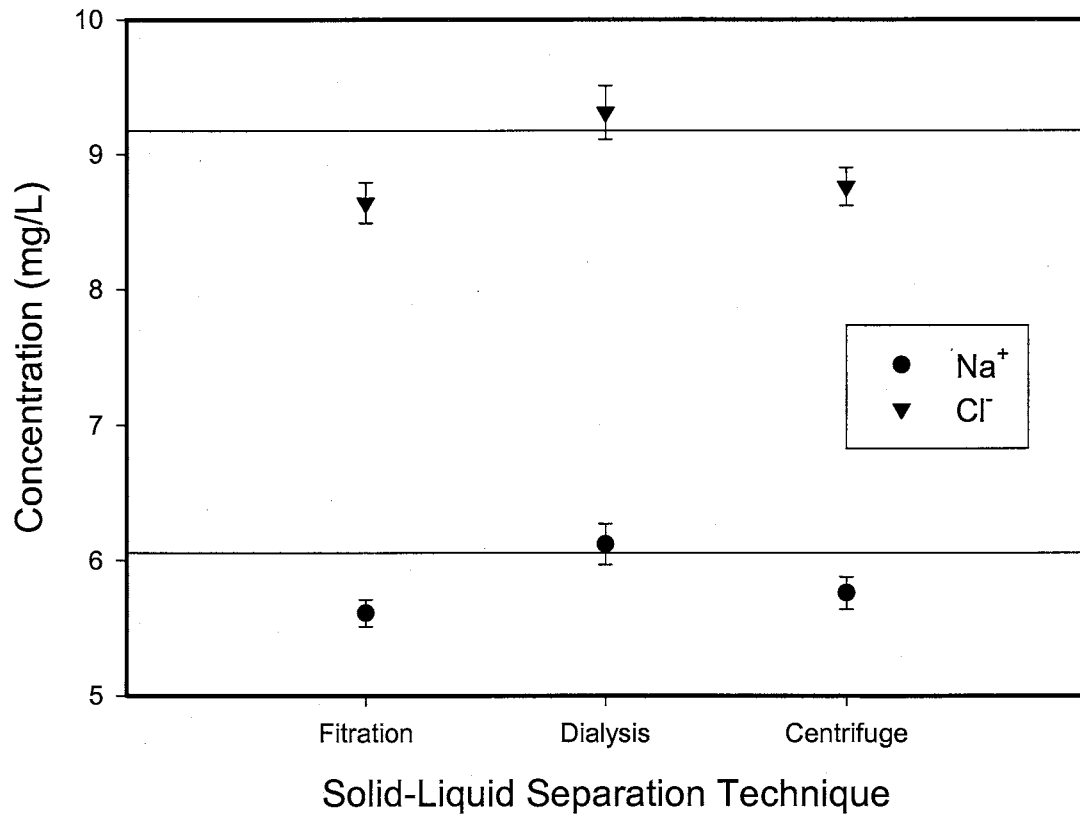


**Figure 75 -** Plot comparing solution concentration as a function of separation method for a NaCl solution with a suspended clay concentration of 25 mg/L. Solid line indicates actual solution concentration before addition of clay. Error bars represent an analytical uncertainty of two standard deviations.

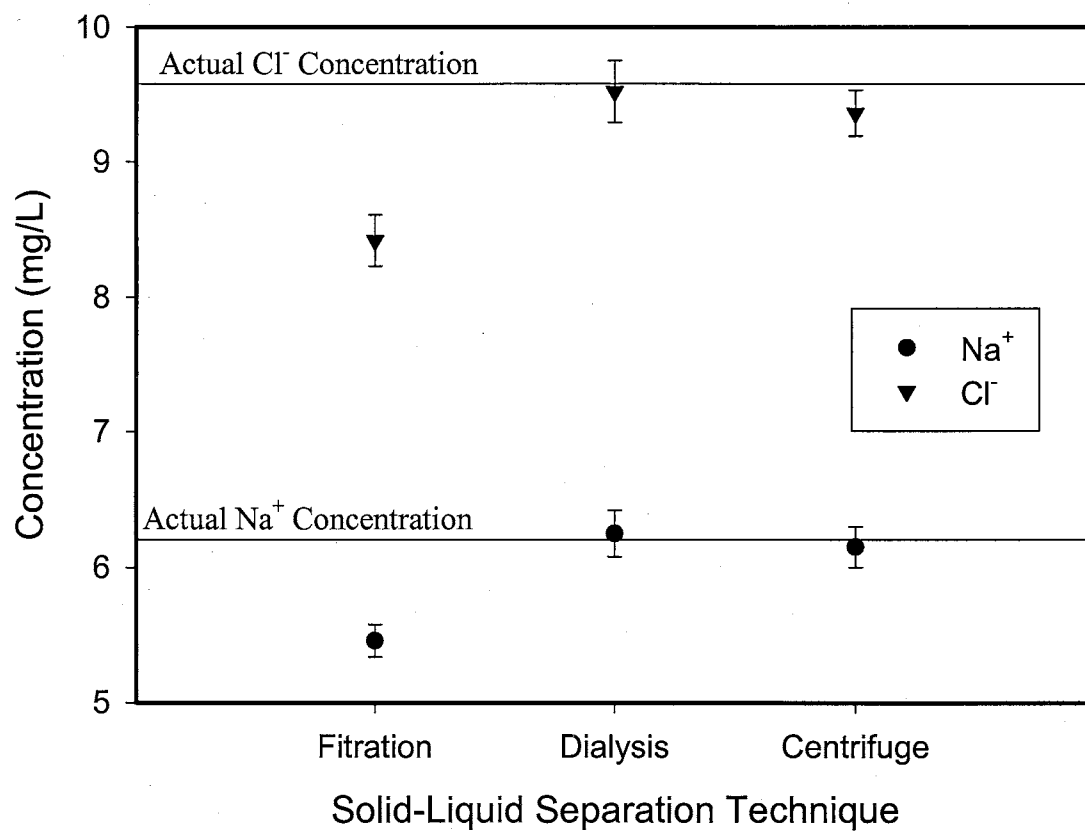


**Figure 76 -** Plot comparing solution concentration as a function of separation method for a NaCl solution with a suspended clay concentration of 50 mg/L. Solid line indicates actual solution concentration before addition of clay. Error bars represent an analytical uncertainty of two standard deviations.

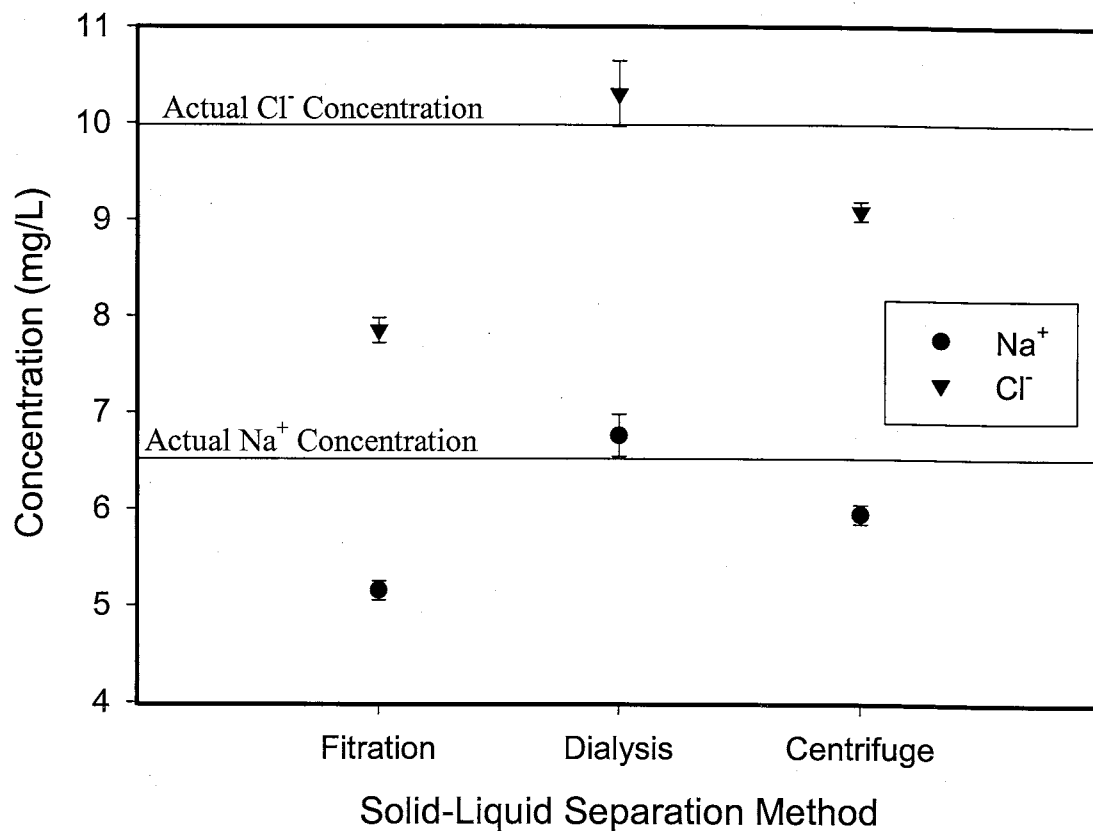


**Figure 77 -** Plot comparing solution concentration as a function of separation method for a NaCl solution with a suspended clay concentration of 75 mg/L. Solid line indicates actual solution concentration before addition of clay. Error bars represent an analytical uncertainty of two standard deviations.

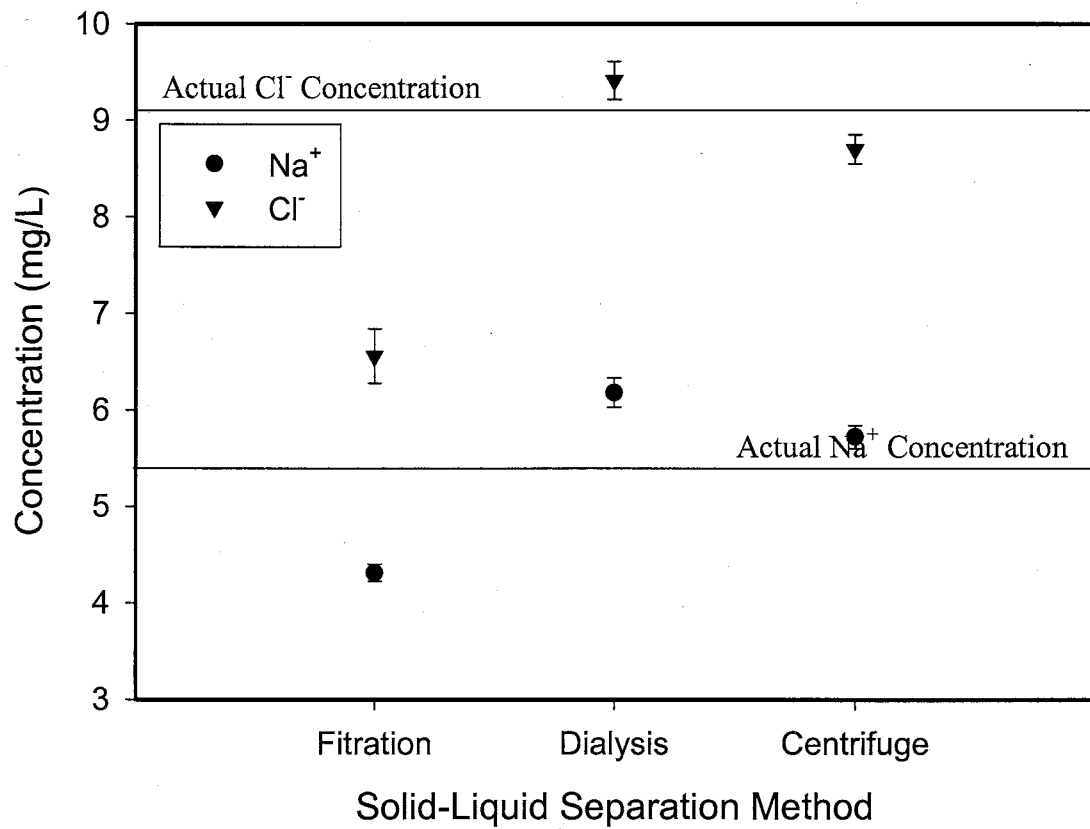


**Figure 78 -** Plot comparing solution concentration as a function of separation method for a NaCl solution with a suspended clay concentration of 100 mg/L. Solid line indicates actual solution concentration before addition of clay. Error bars represent an analytical uncertainty of two standard deviations.



Figure 73 compares the results of these three methods as applied to the 10 mg/L clay - NaCl solution. With the exception of  $\text{Na}^+$  determined from the solution treated by dialysis, all samples fell within two standard deviations of the actual solution concentrations. The high level of  $\text{Na}^+$  in the dialyzed sample may be due to contamination, as it is extremely unlikely that any appreciable amount of clay particles could have passed through the dialysis tubing (MWCO of 5000 daltons).

Figure 74 is a comparison of the three different separation methods for the 15 mg/L clay - NaCl solution. As stated earlier, the dialysis cell for this solution was exposed to some contamination. In all likelihood, this is the cause of the high  $\text{Na}^+$  and  $\text{Cl}^-$  levels for the dialyzed sample. Again, both the filtered and centrifuged solutions are reasonably close to the actual solution concentration for this case.

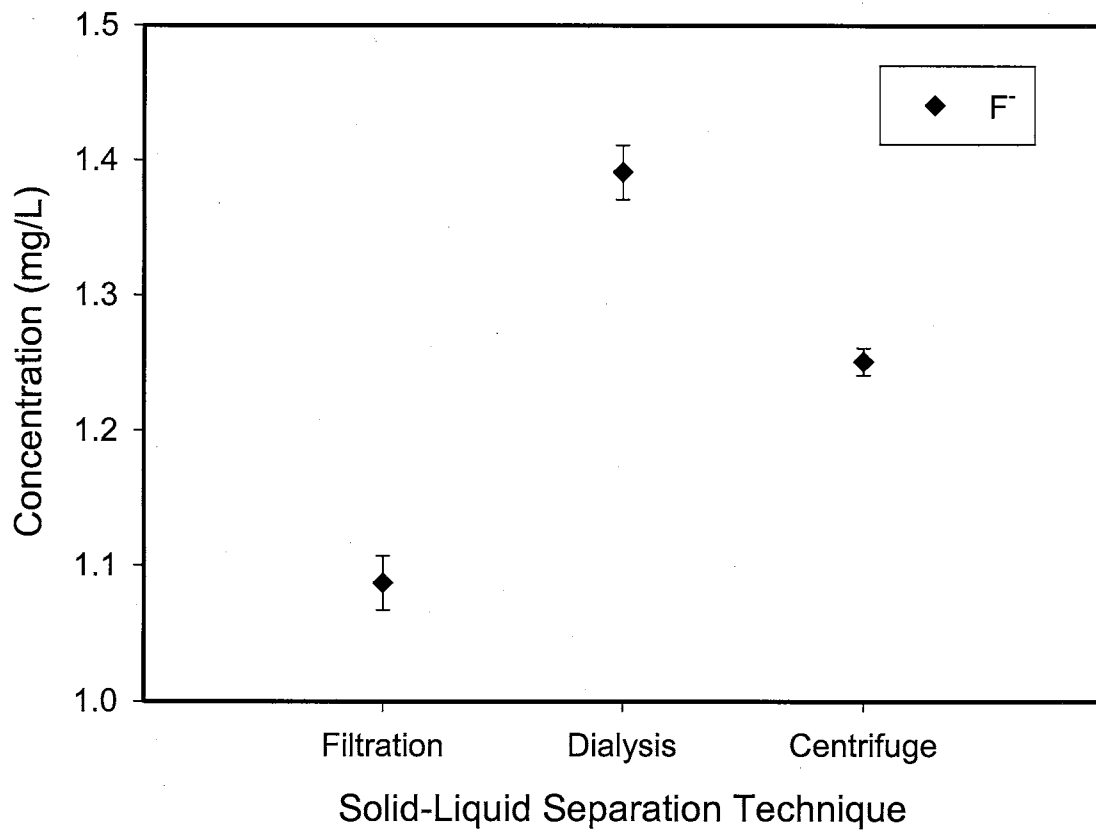
The comparison of separation methods for the 25 mg/L clay - NaCl solution can be seen in Figure 75. In this case, dialysis seems to have performed as the best separation method. The dialyzed sample is the only solution that is within two standard deviations of the actual concentration. The concentrations of both the filtered and centrifuged solutions are significantly lower than that of the blank solution.

Figure 76 compares each of the solid - liquid separation methods for the 50 mg/L clay - NaCl solution. Again, the concentrations for the sample that underwent dialysis are the closest to that of the blank solution. The  $\text{Na}^+$  levels for the centrifuged solution are within two standard deviations of the actual concentration. However, the  $\text{Cl}^-$  concentration for the centrifuged solution is significantly below that of the blank solution. The  $\text{Na}^+$  and  $\text{Cl}^-$  concentrations of the filtered solutions are significantly lower than that of the blank solution.

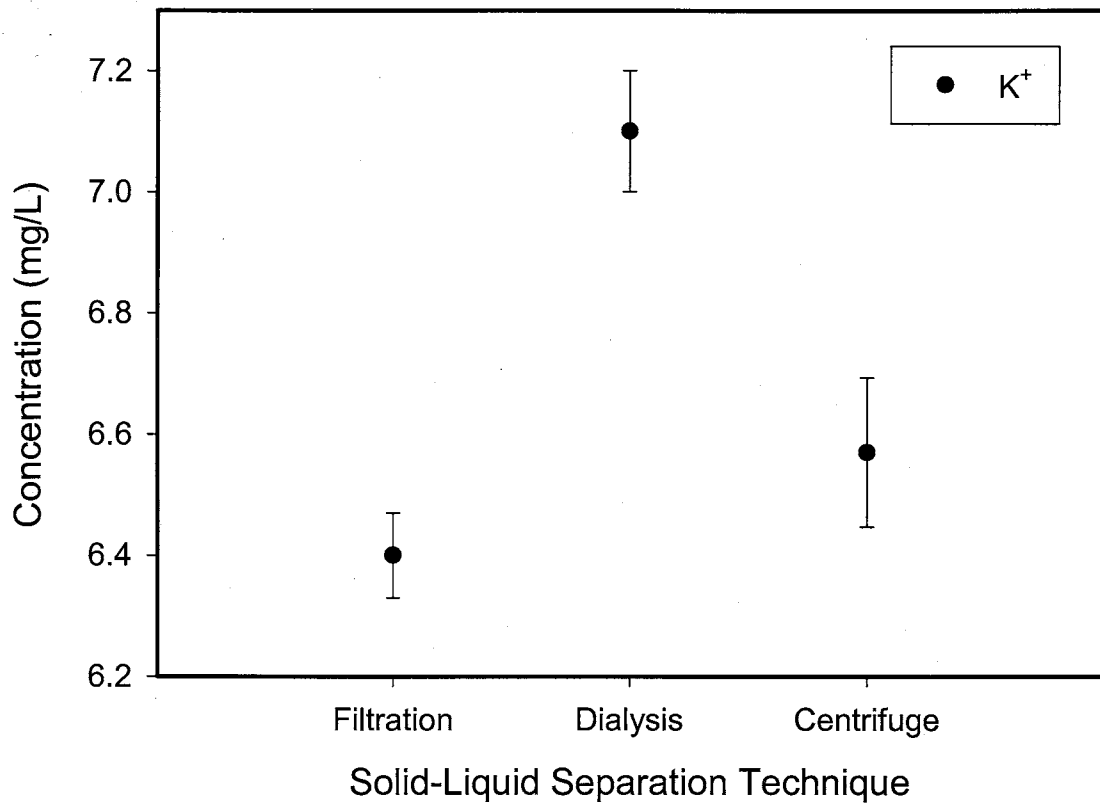
The results for the 75 mg/L clay - NaCl solution can be seen in Figure 77. The dialysis cell containing this solution was exposed to a significant amount of contamination due to the string and metal hook used in the construction of the cell. Because of this contamination, the concentrations of  $\text{Na}^+$  and  $\text{Cl}^-$  for the dialyzed solution are higher than two standard deviations from the concentrations of the blank solution. In this case, the  $\text{Na}^+$  and  $\text{Cl}^-$  concentrations of the filtered and centrifuged solutions are significantly lower than that of the blank solution.

Figure 78 contains the results for the 100 mg/L clay - NaCl solution. Again, the sample subjected to dialysis shows the closest agreement to the actual solution concentration. Although the centrifuged sample is significantly lower than the actual solution concentration, it is still much closer to the actual solution concentration than the filtered sample. Both the  $\text{Na}^+$  and  $\text{Cl}^-$  concentrations for the filtered sample are far below that of the blank solution.

Figures 79 - 88 are plots comparing the solid - liquid separation methods of dialysis, centrifugation, and filtration for the Rio Grande and Rio Puerco samples. In almost every instance, for both cations and anions, the following trend holds true: the sample which was dialyzed has the highest solute concentration of the three methods; typically, the sample analyzed after centrifugation has the next highest solute concentration; and the lowest solute concentrations were those which were treated via filtration. There are only two exceptions to this trend. For the Rio Grande sample, the



**Figure 79 -** Plot comparing solution concentration as a function of separation method for a water sample from the Rio Grande with a suspended solids concentration of 4,100 mg/L. Error bars represent an analytical uncertainty of two standard deviations.



**Figure 80 -** Plot comparing solution concentration as a function of separation method for a water sample from the Rio Grande with a suspended solids concentration of 4,100 mg/L. Error bars represent an analytical uncertainty of two standard deviations.

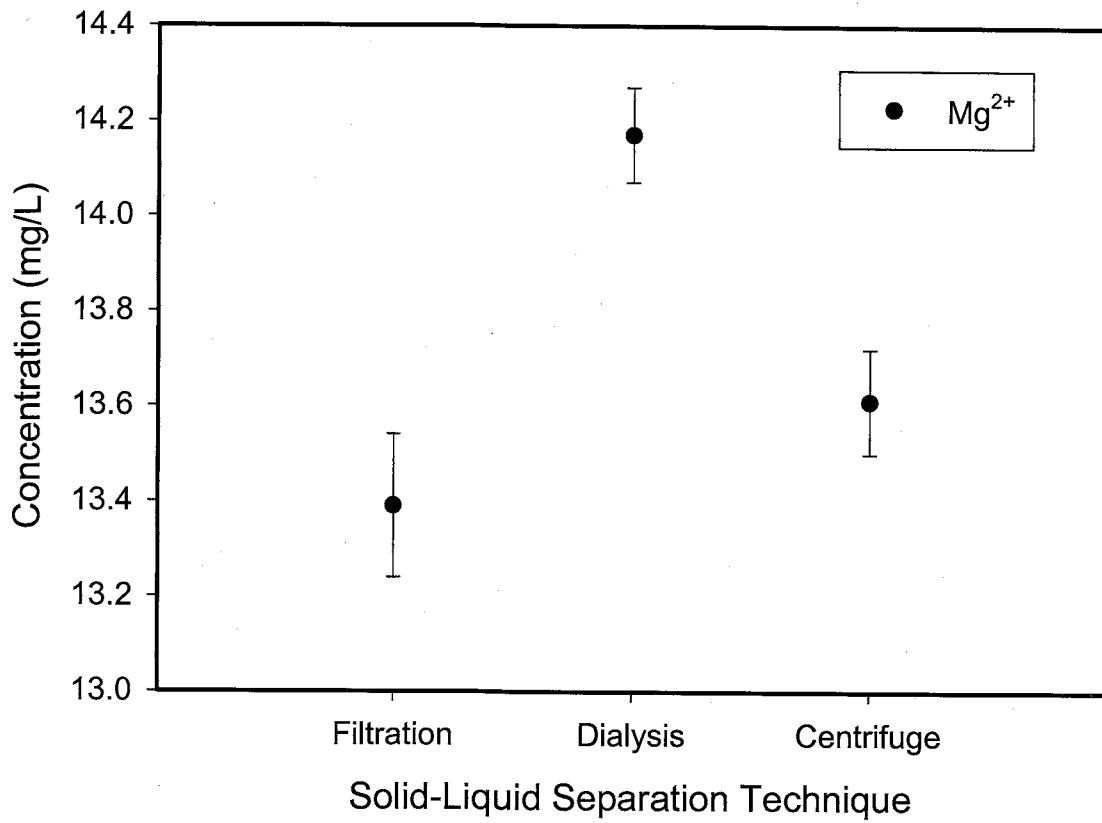


**Figure 81 -** Plot comparing solution concentration as a function of separation method for a water sample from the Rio Grande with a suspended solids concentration of 4,100 mg/L. Error bars represent an analytical uncertainty of two standard deviations.

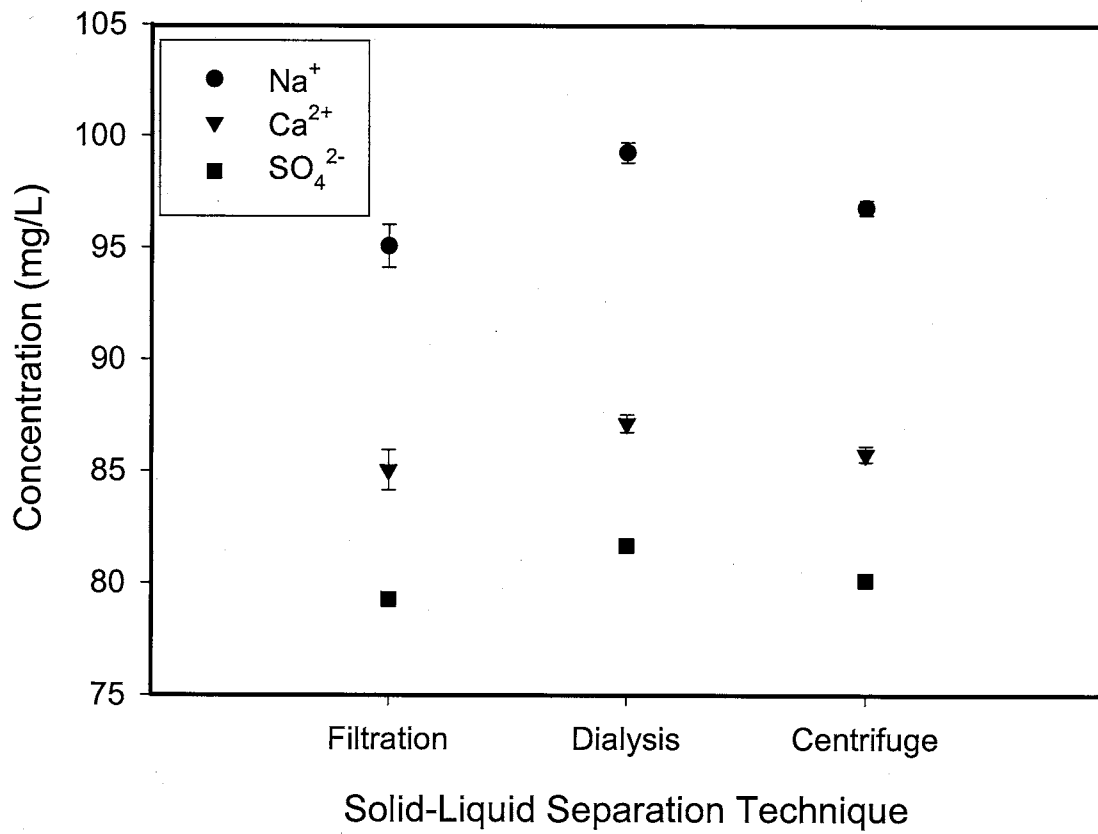


**Figure 82 -** Plot comparing solution concentration as a function of separation method for a water sample from the Rio Grande with a suspended solids concentration of 4,100 mg/L. Error bars represent an analytical uncertainty of two standard deviations.

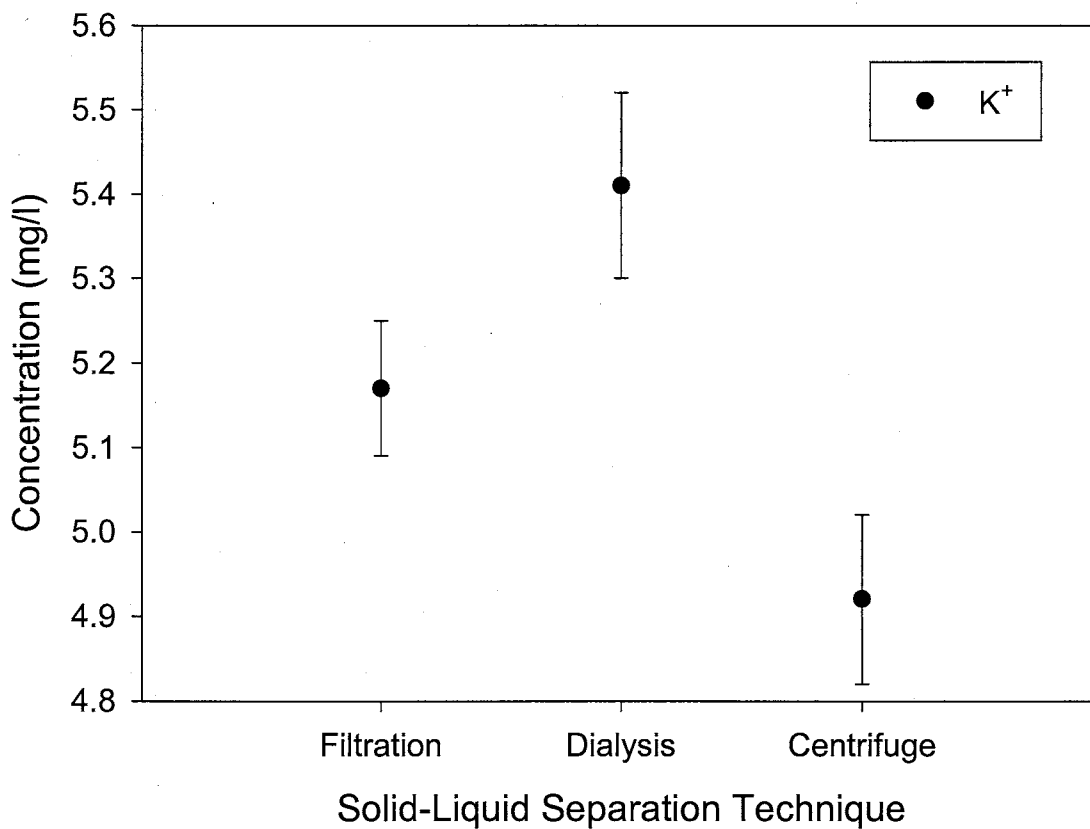


**Figure 83 -** Plot comparing solution concentration as a function of separation method for a water sample from the Rio Grande with a suspended solids concentration of 4,100 mg/L. Error bars represent an analytical uncertainty of two standard deviations.

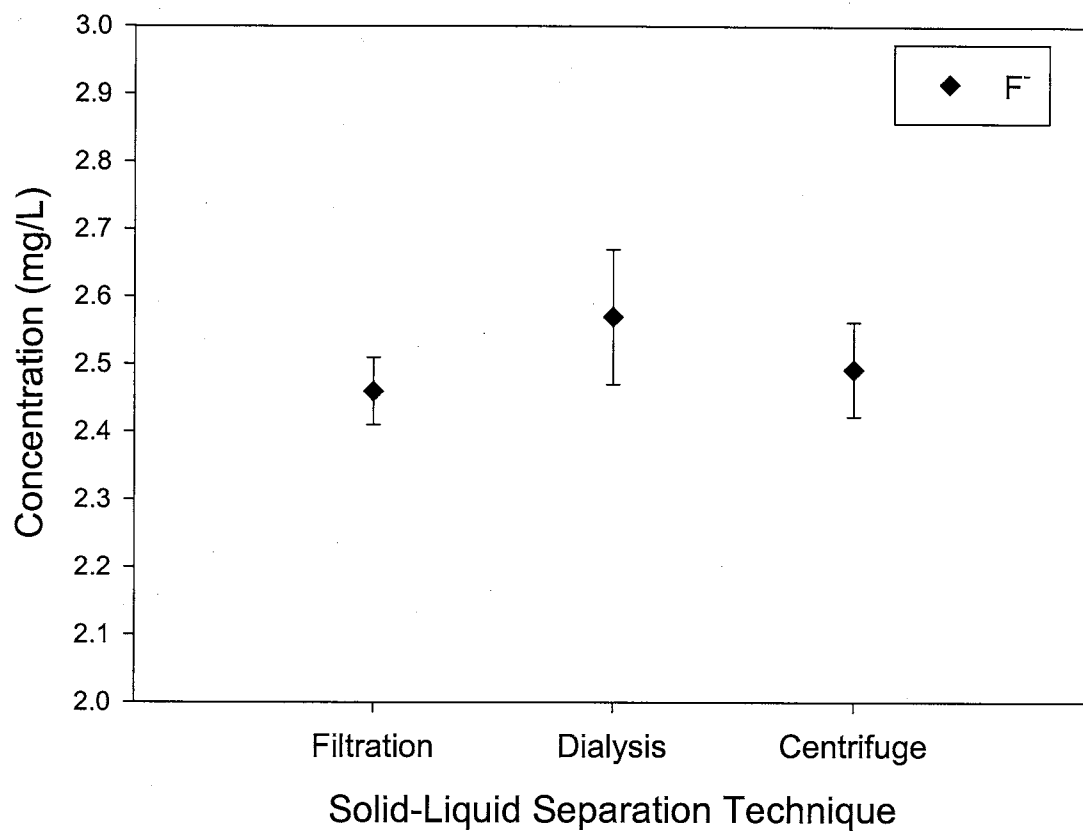


**Figure 84 -** Plot comparing solution concentration as a function of separation method for a water sample from the Rio Puerco with a suspended solids concentration of 32,100 mg/L. Error bars represent an analytical uncertainty of two standard deviations.



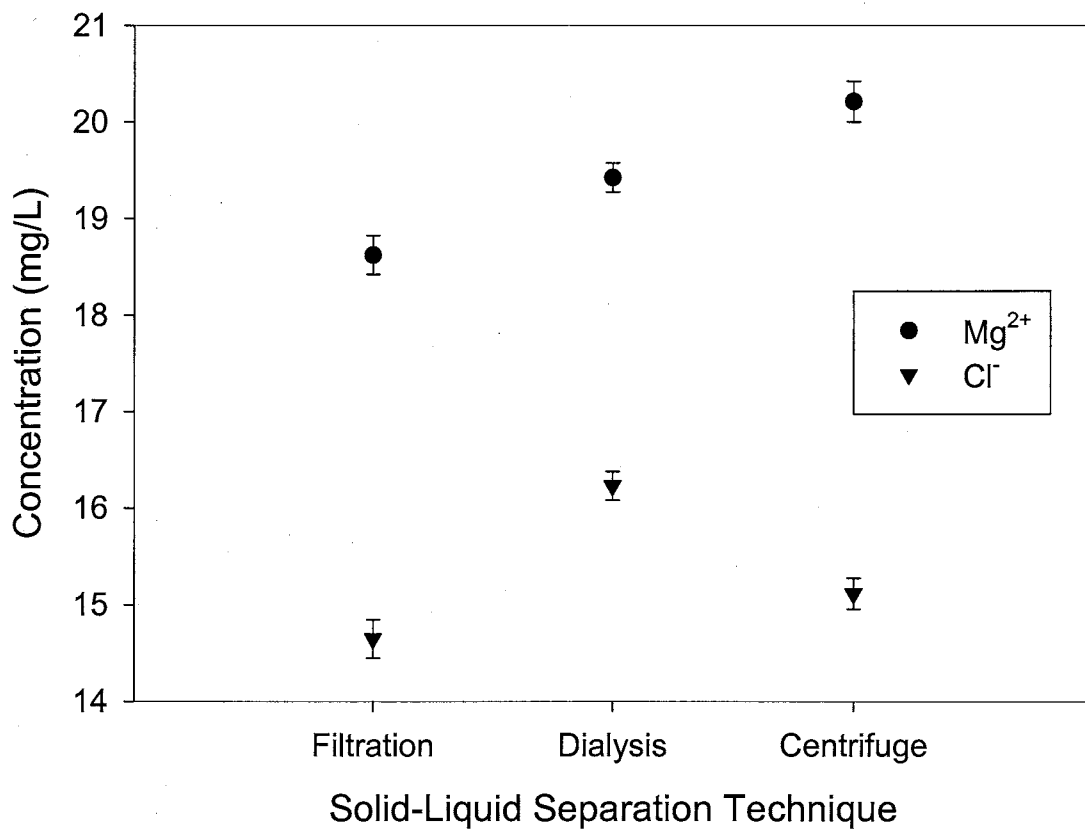


**Figure 85 -** Plot comparing solution concentration as a function of separation method for a water sample from the Rio Puerco with a suspended solids concentration of 32,100 mg/L. Error bars represent an analytical uncertainty of two standard deviations.

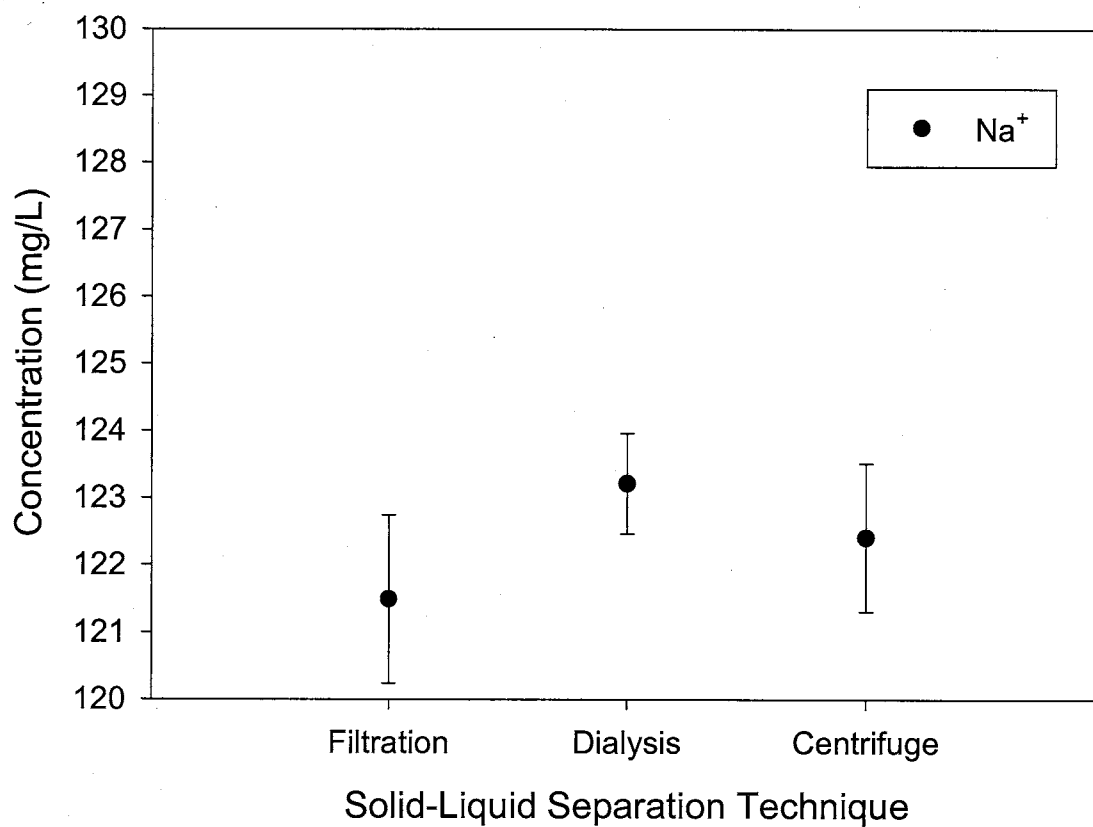


**Figure 86 -** Plot comparing solution concentration as a function of separation method for a water sample from the Rio Puerco with a suspended solids concentration of 32,100 mg/L. Error bars represent an analytical uncertainty of two standard deviations.

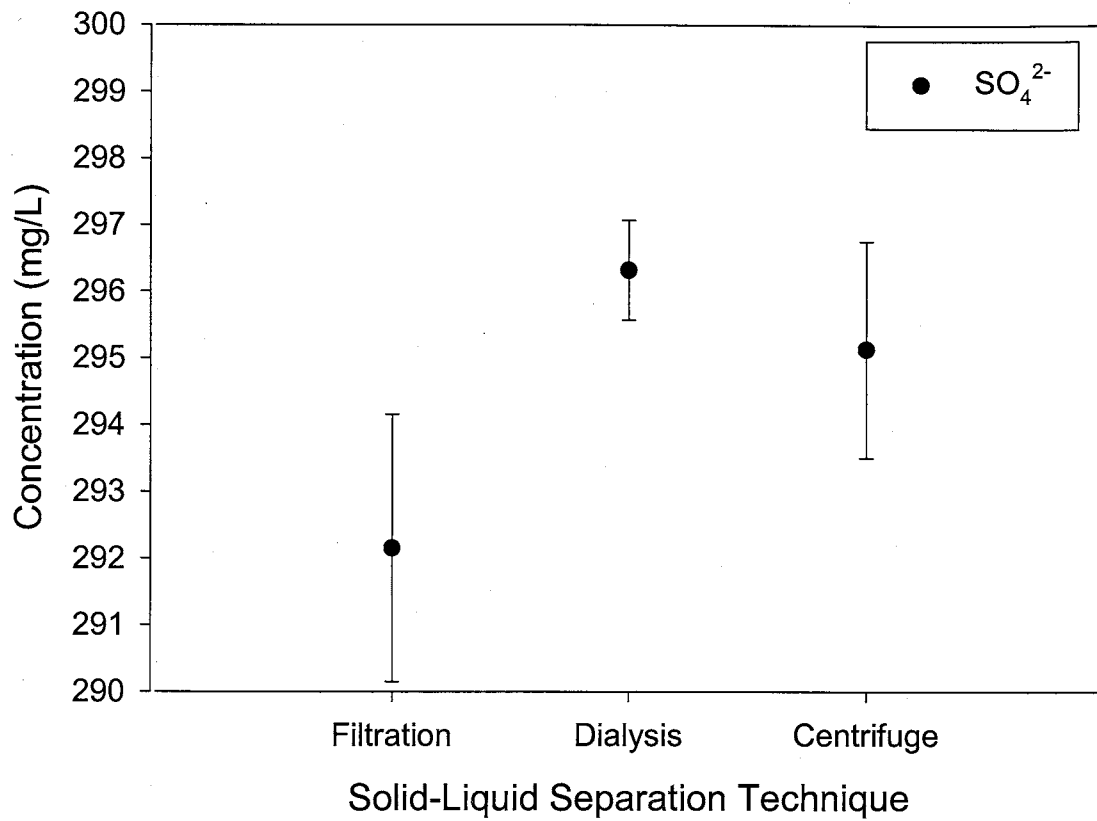


**Figure 87 -** Plot comparing solution concentration as a function of separation method for a water sample from the Rio Puerco with a suspended solids concentration of 32,100 mg/L. Error bars represent an analytical uncertainty of two standard deviations.

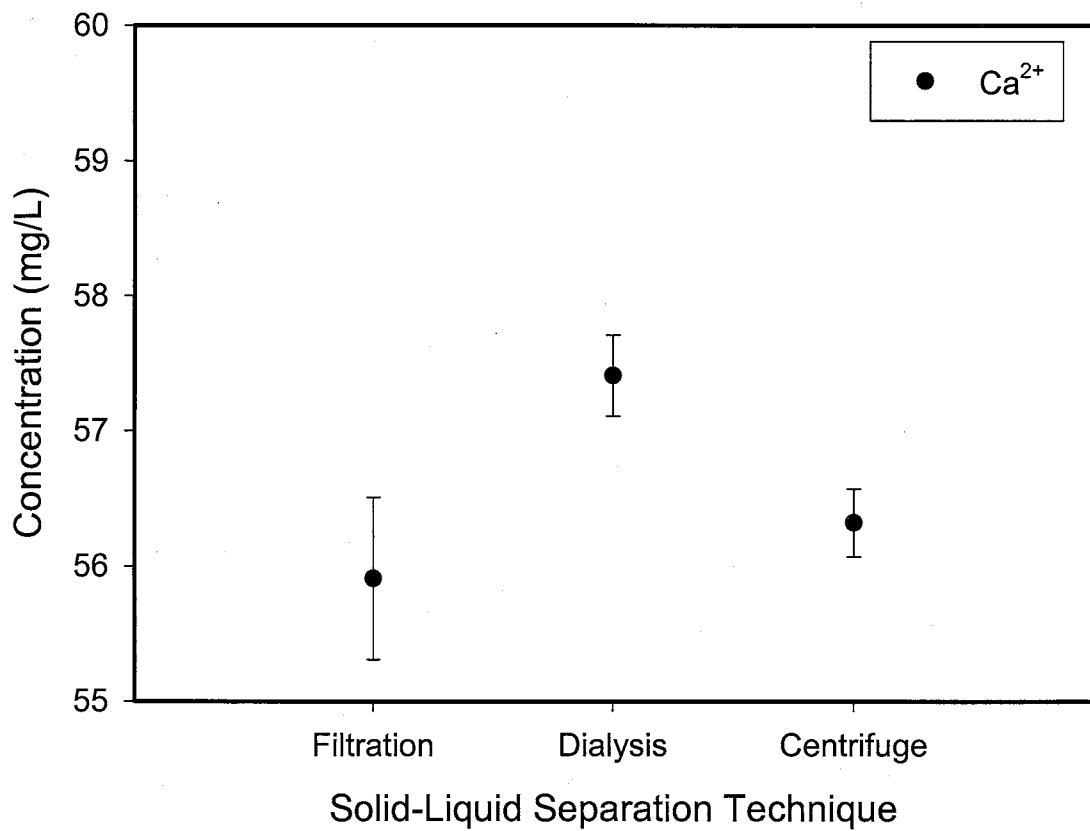


**Figure 88 -** Plot comparing solution concentration as a function of separation method for a water sample from the Rio Puerco with a suspended solids concentration of 32,100 mg/L. Error bars represent an analytical uncertainty of two standard deviations.

levels of  $K^+$  of the solution treated via centrifugation was lower than that treated by filtration (Figure 83). For the Rio Puerco sample, the  $Mg^{2+}$  concentration for the sample treated via centrifugation was higher than that treated with dialysis (Figure 85).

**Table 12 -** Maximum effluent solute reduction as a function of separation method.

Suspended Clay (mg/L)	Percent Difference from True (Known) Concentration		
	Separation Method	$Na^+$	$Cl^-$
5	Dialysis	-1.19	0.08
	Filtration	0.85	-0.55
	Centrifuge	0.34	0.11
10	Dialysis	-5.02	-1.89
	Filtration	-0.34	0.29
	Centrifuge	-0.02	-0.07
15	Dialysis	-8.25	-6.85
	Filtration	0.01	-0.01
	Centrifuge	0.33	1.61
25	Dialysis	-0.49	0.85
	Filtration	7.89	8.01
	Centrifuge	5.92	6.71
50	Dialysis	-1.13	0.21
	Filtration	11.60	11.70
	Centrifuge	0.45	1.89
75	Dialysis	-4.48	-3.31
	Filtration	20.39	21.29
	Centrifuge	8.19	8.91
100	Dialysis	-1.98	-0.86
	Filtration	28.93	29.70
	Centrifuge	5.59	6.75

**Table 34 -** Comparison of Analyte Concentrations as a Function of Separation Method for Rio Grande and Rio Puerco Samples

Sample	TSS (mg/L)	Separation Method	% Difference in Concentration Determined via Dialysis						
			$K^+$	$Na^+$	$Ca^{2+}$	$Mg^{2+}$	$F^-$	$Cl^-$	$SO_4^{2-}$
Rio Grande	4,100	Filtration	9.85	4.21	2.39	5.48	21.87	3.08	2.94
		Centrifuge	7.47	2.49	1.56	3.95	10.06	2.34	1.90
Rio Puerco	32,100	Filtration	4.46	1.39	2.61	4.14	4.14	9.71	5.48
		Centrifuge	9.06	0.65	1.90	-4.07	3.04	6.84	0.40

## IMPLICATIONS AND FUTURE WORK

At first glance, a topic such as the filtration of natural water samples prior to analysis does not seem very consequential. However, from the results of the current study, one can see that the impact of filtering water samples with high sediment loads may have an adverse impact upon subsequent chemical analysis of the filtrate.

The original intent of this study was to explore the possibility that filtering natural waters with high clay loads may cause a solute sieving effect due to the accumulation of clay minerals on the surface of the filter used. However, as the study progressed, it became evident that this phenomenon was not the only one occurring during filtration.

The mathematical model of cake filtration may be able to accurately describe and predict the clogging rates for filters first noted by Laxen and Chandler (1982). Most studies examining the effect of filtration on the chemical analysis of natural waters simply stated that the clogging of the filters used became more pronounced as the amount of water filtered increased. As shown in this study, the time-discharge data of the dilute suspensions used in this study appears to fit very well with the mathematical model of cake filtration.

Although the time-discharge data for the slurries synthesized in the lab matched very well with the cake filtration model, the variation of the size and density of suspended particles in natural waters may tend to disrupt this fit. A variety of suspended particles, from bacteria to plant life to clay minerals, can accumulate onto the filter during sample preparation. The heterogeneity of these particles may eventually show that the cake filtration model cannot accurately describe the clogging rates of filters. However,

the cake filtration model is an excellent place to begin further examination of filter clogging rates and filter capacities and may explain the clogging rates noted by Horowitz et al. (1996).

One interesting finding of this study involves the fact that high clay loads in natural waters may be causing a membrane to form during filtration. Despite the number of recent studies on the topic of filtering natural waters, Briggs' study (1906) may be the most accurate regarding the filtration of natural water samples prior to analysis. The data from the current study coupled with Briggs' work (1906) definitely indicate the need for more research along these lines.

This study's last major finding involves the effectiveness of different solid-liquid separation methods in the preparation of natural waters for chemical analysis. The data for the clay - NaCl solutions indicate that dialysis may be a more effective method of sample preparation than either filtration or centrifugation. However, the biggest shortcoming of dialysis involves the rather lengthy amount of time it takes for a water sample to come to equilibrium within the dialysis cell. Despite this drawback, dialysis should definitely be considered as a viable option when preparing water samples with high concentrations of suspended solids for analysis.

The findings of this study bring to mind the potential for low-cost, viable studies that would combine skills from various disciplines. Consider, for example, the uses of water quality data after chemical analyses are complete and reported. Water quality data may be used for regulatory purposes, total maximum discharge limit (TMDL) monitoring, ground and surface water geochemical modeling, water quality modeling for watershed protection, or as a planning tool for future regional development.

If water quality data were to be used as input to geochemical models such as MINTEQ or PHREEQEC, how would the potential effect of filtration artifacts or solute sieving affect the results of these modeling efforts? Depending on the purpose of utilizing these geochemical models, the effects detailed in this study could be very significant and should be studied further, as the effects detailed in this study may affect the saturation indices of certain minerals, the precipitation of minerals during the mixing of two different waters, or the solubility and subsequent transport of trace metal contaminants.

Consider the potential of filtration artifacts on drinking water standards. The Environmental Protection Agency (EPA) is currently considering lowering the maximum allowable arsenic concentration in drinking water from 50 ppb to 10 ppb. If the concentration of arsenic is affected by either colloidal particles passing through a filter or solute sieving, the ramifications could be very costly from both a monitoring and treatment perspective. For example, if iron oxide colloids present in a water sample were to pass through a 0.45  $\mu\text{m}$  filter, the resulting analysis could show a false high level of arsenic present in the water, which would result in costly required treatment. On the other hand, if arsenic concentrations in excess of 10 ppb were present in a water with a high sediment load, the pre-filtering, or membrane effect, described in the current study could cause an erroneous low concentration of arsenic to be present; this situation would not require any treatment from a regulatory perspective, but might cause adverse health effects for the community that uses this water supply.

What about the effects of filtration on regulatory aspects of water management? The effects of filtration of water samples may be allowing levels of trace metal



contaminants in the environment to be reported at lower than actual levels. This under-reporting could be significant in the areas of ground water remediation, watershed protection, and planning for regional development.

Consider the use of water quality data in traditional geological studies. A classic exercise in geology is the calculation of the amount of dissolved salts transported by rivers to the ocean. For example, if 5% of the rivers used in this geological mass balance contained high amounts of suspended sediments such as clay or iron oxide particles, which decreased the measured concentrations dissolved solids by just 5%, the loading of magnesium and calcium transported to the world's ocean would decrease by  $1.25 \times 10^{20}$  g, assuming a total of  $5 \times 10^{22}$  g of dissolved salts present in the world's oceans. Granted, this figure is a gross approximation, but it does serve to illustrate the ramifications of a systematic error in measurement that filtration may introduce into the chemical analysis of natural water samples. A variation such as this in a global geochemical budget would cause us to re-examine geological models used to describe the erosion rates of continental features, the age of the oceans themselves, and depositional rates of mineral deposits on the ocean floor.

## CONCLUSIONS

In this study, we present a comparison of solid-liquid separation techniques applied to natural water samples, a conceptual model of membrane effects that may be occurring during certain instances of filtration of natural water samples, and a mathematical model to describe the clogging rates of natural water samples undergoing filtration with a 0.45  $\mu\text{m}$  filter.

First, based on experimental results, there is ample evidence to support the use of dialysis and centrifugation as effective techniques for treating natural water samples prior to chemical analysis. Both laboratory and field data show that sediment-laden waters treated via dialysis yield consistently reproducible dissolved solids concentrations. Laboratory data show that, under controlled circumstances, dialysis is capable of yielding concentrations of dissolved species within 2% of actual values. Centrifugation, while more convenient in a laboratory setting, yielded concentrations within 8% of actual values for synthesized water samples.

Secondly, results of this study also suggest that, under certain circumstances, hyperfiltration of natural water samples may occur during treatment with a 0.45  $\mu\text{m}$  filter. Hyperfiltration may be caused by the rapid accretion of certain sediments onto the filter as the sample is being treated prior to analysis. Results show that waters with high suspended clay loads could be susceptible to this effect. There is a marked similarity between the results of this study and experiments designed to examine membrane properties of certain geologic media. While this similarity was only studied from a qualitative perspective, it may be possible to quantify this effect with respect to the

amount of suspended sediment present in natural waters, as well as with respect to the mineralogy of suspended sediments present in natural bodies of water.

Finally, the classical filter cake model employed within the chemical engineering discipline, shows a great deal of promise to describe clogging rates noted during the use of a 0.45 mm filter to treat natural water samples. The linear relationship between the inverse instantaneous flow rate and cumulative volume of solution filtered described by the filter cake model held true for all but one of the samples examined in this study. The resistances due to the 0.45  $\mu\text{m}$  filters ( $R_m$ ) and the filter cakes ( $\alpha$ ) calculated during the current study were comparable to resistance values obtained during industrial and laboratory scale studies.

The phenomena reported in this paper could help to evaluate the significance of colloid and sediment presence in water sampling activities. Furthermore, approaches such as those described in this paper would be useful in analyzing the importance of sampling protocol during the collection of natural water samples.

## REFERENCES CITED

- Akers R. J. and Ward, A. S., Liquid filtration theory and filtration pretreatment *in* Filtration Principles and Practices - Part I. Orr, C. (ed.), Marcel Drekker, Inc., New York, 1977.
- American Public Health Association, American Water Works Association, and Water Pollution Control Federation, 1992, Standard Methods for the Examination of Water and Wastewater, 17th edition; American Water Works Association, Washington, D.C., 1989.
- American Society for Testing and Materials, Annual Book of ASTM Standards, Vol. 11.01, Water (I); American Society for Testing and Materials; Philadelphia, PA, 1995.
- Armstrong, F. A. J., 1958, Inorganic suspended matter in seawater, *Journal of Marine Research*, v. 17, 23-34.
- Atkins, P., Physical Chemistry - Fifth Edition. W. H. Freeman and Company, New York, 1994.
- Batley, B. E. and Gardner, D., 1977, Sampling and storage of natural waters for trace metal analysis, *Water Research*, v. 41, 745-756.
- Benes, P. and Steinnes, E., 1974, In situ dialysis for the determination of the state of trace elements in natural waters, *Water Research*, v. 8, 947-953.
- Benoit, G., 1994, Clean technique measurement of Pb, Ag, and Cd in freshwater: a redefinition of metal pollution, *Environmental Science and Technology*, v. 28, 1987-1991
- Blatt, W. F.; Dravid, A.; Michaels, A. S.; and Nelsen, L.; Solute polarization and cake formation in membrane ultrafiltration: causes, consequences, and control techniques *in* Membrane Science and Technology - Industrial, Biological, and Waste Treatment Processes, Plenum Press, New York, 1970.
- Bowen, W. R. and Jenner, F., 1996, Dynamic ultrafiltration model for charged colloidal dispersions: a Wigner-Seitz cell approach, *Chemical Engineering Science*, v. 50 (11), 1707-1736.
- Bowen, W. R. and Williams, P. M., 1996, Dynamic ultrafiltration model for proteins: a colloidal interaction approach, *Biotechnology and Bioengineering*, v. 50, 125-135.

- Briggs, L. J., 1902, Filtration of suspended clay from soil solutions, US Bureau of Soils Bulletin, no. 19, 31-40.
- Carman, P. C., 1937, Fundamental principles of industrial filtration, Transactions of the Institute of Chemical Engineers (London), v. 58.
- Coffey, B. M.; Gallagher, D. I.; and Knocke, W. R.; 1990, Journal of Environmental Engineering, v. 119 (4), 679-694.
- Cooney, D. O., 1980, Interference of contaminants from membrane filters in ultraviolet spectrophotometry, Analytical Chemistry, v. 52, 1068-1071.
- Coplen, T. B. and Hanshaw, B. B., 1973, Ultrafiltration by a compacted clay membrane, I. Oxygen and hydrogen isotopic fractionation, *Geochemica et Cosmochemica Acta*, v. 37, 2295-2310.
- Counts, M. E., 1975, Adsorption of Heavy Metal Ions on Mineral Surfaces. Virginia Polytechnic Institute and State University Ph.D. Dissertation.
- Corapcioglu, M. Y. and Jiang, S., 1991, Colloid-facilitated ground water contaminant transport, *Water Resources Research*, v. 29, no. 7, 2215-2226.
- Danielson, L. G., 1981, On the use of filters for distinguishing between dissolved and particulate fractions in natural waters, *Water Resources Research*, v. 16, 179-182.
- Denisov, G. A., 1994, Theory of concentration polarization in cross-flow ultrafiltration: gel-layer model and osmotic-pressure model, *Journal of Membrane Science*, v. 91, 173-187.
- Dickey, G. D., *Filtration*. Reinhold Publishing Company, New York, 1960.
- Ding, L. H.; Jaffrin, M. Y.; and Defosse, M.; 1993, Concentration polarization formation in ultrafiltration of blood and plasma, *Journal of Membrane Science*, v. 84, 293- 301.
- Fane, A. G.; Fell, C. J. D.; and Waters, A. G.; 1981, The relationship between membrane surface pore characteristics and flux for ultrafiltration membranes, *Journal of Membrane Science*, v. 9, 245.
- Fritz, S. J. and Eady, C. D., 1985, Hyperfiltration-induced precipitation of calcite, *Geochemica et Cosmochemica Acta*, v. 49, 761-768.
- Fritz, S. J. and Marine, I. W., 1983, Experimental support for a predictive osmotic model of clay membranes, *Geochemica et Cosmochemica Acta*, v. 47, 1515-1522.

- Goldberg, E. D., Baker, M., and Fox, D. L., 1952, Microfiltration in oceanographic research - I. Marine sampling with the molecular filter, *Journal of Marine Research*, v. 11, 197-202
- Grace, H. P., 1953, Resistance and compressibility of filter cakes - part I, *Chemical Engineering Progress*, v. 44, 318 - 330.
- Grace, H. P., 1953, Resistance and compressibility of filter cakes - part II, *Chemical Engineering Progress*, v. 44, 367-380.
- Grasshoff, K., 1976, *Methods of Seawater Analysis*. Verlag Chemie, Weinheim.
- Grim, R. E., 1968, *Clay Mineralogy*, Second Edition. McGraw-Hill Publishers, New York.
- Grolimund, D.; Borkovec, M.; Barmettler, K.; and Sticher, H.; 1996, Colloid-facilitated transport of strongly sorbing contaminants in natural porous media: a laboratory column study, *Environmental Science and Technology*, v. 30 (10), 3118-3123.
- Happel, J., 1958, Viscous flow in multiparticle systems: slow motion of fluids relative to beds of spherical particles, *AIChE Journal*, v. 4 (2), 197-201.
- Happel, J. and Brenner, H., *Low Reynolds Number Hydrodynamics*. Prentice-Hall, Englewood Cliffs, NJ, 1965
- Horowitz, A. J.; Elrick, K. A.; and Colberg, M. R.; 1992, The effect of membrane filtration artifacts on dissolved trace element concentrations, *Water Research*, v. 26 (6), 753-763.
- Horowitz, A. J.; Lum, K. R.; Garbarino, J. R.; Hall, G. E. M.; Lemieux, C.; Demas, C. R.; 1996, Problems associated with using filtration to define dissolved trace element concentrations in natural water samples, *Environmental Science and Technology*, v. 30 (3), 954-963.
- Horowitz, A. J.; Demas, C. R.; Fitzgerald, K. K.; Miller, T. L.; Rickert, D. A.; U.S. Geological Survey protocol for the collection and processing of surface-water samples for the subsequent determination of inorganic constituents in filtered water. Open-File Report No. 94-539; U.S. Geological Survey, 1994.
- Houi, D. and Lenormand, R., 1986, Particle accumulation at the surface of a filter, *Filtration and Separation*, 238-247.
- Hunter, R. J., 1993, *Introduction to Modern Colloid Science*, Oxford Science Publications, Oxford, U.K.

- Jardine, P.; Zelazny, L.; Evans, A.; 1986, Solution aluminum anomalies resulting from various filtering materials, *Soil Science Society of America Journal*, v. 50, 891-894.
- Katalsky, A. and Curran, P. F., *Non-equilibrium thermodynamics in biophysics*. Harvard University Press, 1962.
- Kemper, W. D. and Rollins, J. B., 1966, Osmotic efficiency coefficients across compacted clays, *Soil Science Society of America Proceedings*, v. 30, 529-534.
- Kennedy, V. C.; Jones, B. F.; and Zellweger, G. W., 1974, Filter pore size effects on the analysis of Al, Fe, Mn, and Ti in water, *Water Resources Research*, v. 10, 785-790.
- Kharaka, Y. K. and Berry, F. A. F., 1973, Simultaneous flow of water and solutes through geologic membranes, I. Experimental Investigation, *Geochemica et Cosmochemica Acta*, v. 37, 2577-2603.
- Kharaka, Y. K. and Smalley, W. C., 1976, Flow of water and solutes through compacted clays. *American Association of Petroleum Geologists Bulletin*, v. 60, 973-980
- Kottwitz, F. A. and Boylan, D. R., 1958, Confirmed experimentally that compression-permeability measurements of cake properties can be used successfully to predict filtration performance, *American Institute of Chemical Engineers Journal*, v. 4, 175-188.
- Kozeny, J., 1927, *Über kapillare leitung des wassers im bodem*, *Sitzber Akad Wiss. Wein, Math. Naturw. Klasse*, v. 136.
- Laxen, D. P. and Chandler, I. M., 1992, Comparison of filtration techniques for size distribution in freshwaters, *Analytical Chemistry*, v. 54, 1350-1355.
- Laxen, D. and Harrison, R., 1981, A scheme for the physico-chemical speciation of trace metals in freshwater samples, *The Science of the Total Environment*, v. 19, 59-82.
- Le, M. S. and Howell, J. A., 1984, Alternative model for ultrafiltration, *Chemical Engineering Research Design*, v. 62, 373-380.
- Liu, S.; Carney, C.; and Hurwitz, A.; 1977, Adsorption as a possible limit in solubility determination, *Journal of Pharmacy and Pharmacology*, v. 29, 319-321.
- Loeb, S and Sourirajin, S.; 1963, *Advan. Chem. Ser.* 38, 117.
- Lu, W. M. and Hwang, K. J., 1995, Cake formation in 2-d cross-flow filtration, *AIChE Journal*, v. 41 (6), 1443-1455.

- Lu, W. M. and Hwang, K. J., 1993, Mechanism of cake formation in constant pressure filtration, *Separation Technology*, v. 3, 122-131.
- Mackeley, M. R. and Sherman, N. E., 1992, Crossflow cake filtration mechanisms and kinetics, *Chemical Engineering Science*, v. 47, 3067-3084.
- Marine, I. W. and Fritz, S. J., 1981, Osmotic model to explain anomalous hydraulic heads, *Water Resources Research*, v. 17, 73-82.
- Marshall, C. E. and Krinbull, C. A., 1942, *Journal of Physical Chemistry*, v. 46, 1077.
- Matsuura, T., 1994, *Synthetic Membranes and Membrane Separation Processes*. CRC Press, Boca Raton.
- McKelvey, J. G. and Milne, I. H., 1962, The flow of salt solutions through compacted clay, *Clays and Clay Minerals*, v. 9, 248-259.
- Meadows, J. W.; Smith, C. F.; Coles, D. G.; Maynard, L; and Dellis, I.; 1978, Sampling natural waters: are filtered samples true solutions? *in* Environmental chemistry and cycling processes. Adriano, D. C. and Brisbin, I. L., eds. Technical Information Center, U. S. Department of Energy.
- Mora, S. J. and Harrison, R. M., 1983, The use of physical separation techniques in trace metal speciation studies, *Water Resources Research*, v. 17, 723-733.
- Nrigau, J. O.; Lawson, G.; Wong, H. K. T.; and Azcue, J. M.; 1993, A protocol for minimizing contamination in the analysis of trace metals in Great Lakes waters, *Journal of Great Lakes Research*, v. 19 (1), 175-182.
- Olsen, H. W., 1969, Simultaneous fluxes of liquid and charge in saturated kaolinite, *Soil Science Society of America Proceedings*, v. 33, 338-344.
- Perry, R. H., 1969, *Chemical Engineer's Handbook*, Fifth Edition. McGraw-Hill Publishers, New York.
- Pires, E. C.; Springer, A. M.; and Kumar, V.; 1989, A new technique for specific filtration resistance measurement, *Tappi Journal*, v. 72, 149-154.
- Reinhanian, H.; Robertson, C. R.; and Michaels, A. S.; 1983, Mechanisms of polarization and fouling of ultrafiltration membranes by proteins, *Journal of Membrane Science*, v. 16, 237-258.
- Rietema, K., 1953, Stabilizing effects in compressible filter cakes, *Chemical Engineering Science*, v. 2, 88-102.



- Robertson, D. E., 1968, The role of contamination in trace metal analysis of seawater, *Analytical Chemistry*, v. 40, 1067-1072.
- Romero, C. A. and Davis, R. H., 1988, Global model of crossflow microfiltration based on hydrodynamic particle diffusion, *Journal of Membrane Science*, v. 39, 157-170.
- Romero, C. A. and Davis, R. H., 1990, Transient model of crossflow microfiltration, *Chemical Engineering Science*, v. 45, 13-27.
- Ruth, B. F., Montillion, G. H., Montonna, R. E., 1935, Studies in filtration, *Industrial Engineering Chemistry*, v. 27, 708-720.
- Ruth, B. F., 1946, Correlation of filtration theory with industrial practice, *Industrial Engineering Chemistry*, v. 38, 564-577.
- Saltonstall, C. W., 1992, Separations with dialysis and ultrafiltration: Theoretical and practical considerations, American Biotechnology Laboratory,
- Schmitz, P.; Gouverneur, C.; Houi, D.; and Madianos, M.; 1990, Theoretical model at pore scale for particle deposition on a crossflow microfiltration membrane *in* Proceedings of the World Filtration Congress, Nice, France.
- Schramm, L. L., The language of colloid and interface science. American Chemical Society, Washington, D. C., 1993.
- Sharma, M. M. and Lei, Z., 1991, A model for clay filter cake properties, *Colloids Surf.*, v. 56.
- Shaw, D. J., 1989, Introduction to Colloid and Surface Chemistry, Third Edition. Butterworths, London, U.K.
- Sheldon, R. W. and Sutcliffe, W. H., 1969, Retention of marine particles by screens and filters, *Limnology and Oceanography*, v. 14, 441-444.
- Sheldon, R. W., 1972, Size separation of marine seston by membrane and glass-fiber filters, *Limnology and Oceanography*, v. 17, 495-498.
- Song, L. and Elimelech, M., 1995, Theory of concentration polarization in crossflow filtration, *J. Chem. Soc. Faraday Trans.*, v. 91 (19), 3389-3398.
- Sorvall, 1968, Sorvall Relative Centrifuge Chart.  
Spectra-Por Corporation, 1994, Technical Specification Sheet for RC-1 Spectra-Por Dialysis Tubing.

- Spencer, D. W. and Mannheim, F. T., 1969, Ash content and composition of Millipore HA filters, USGS Professional Paper 650-D, D288-D290.
- Sperry, D. R., 1916, The principles of filtration - part I, Chemical and Metallurgical Engineering, v. 15, 198-203.
- Sperry, D. R., 1917, The principles of filtration - part II, Chemical and Metallurgical Engineering, v. 17, 161-165.
- Stenkamp, V. S. and Benjamin, M. M., 1994, Effect of iron oxide coating on sand filtration, Journal of the American Water Works Association, v. 86, 37-50.
- Stumm, W. and Billinski, H., 1973, Trace metals in natural waters: difficulties of interpretation arising from our ignorance of their speciation *in* Advances in Water Pollution Research, Jenkins, S. (ed.), Pergamon Press, Oxford, UK
- Stumm, W. and Morgan, J. J., 1981, Aquatic Chemistry, Second Edition. Wiley-Interscience, New York
- Tassopoulos, M.; O'Brien, J. A.; and Rosner, D. E.; 1989, Simulation of microstructure/mechanism relationships in particle deposition, AIChE Journal, v. 35 (6), 967-979.
- Tiller, F. M., 1953, The role of porosity in filtration - part I, Chemical Engineering Progress, v. 49, 467-471.
- Tiller, F. M., 1955, The role of porosity in filtration - part II. Analytical equations for constant rate filtration, Chemical Engineering Progress, v. 51, 282-293.
- Tiller, F. M., 1958, The role of porosity in filtration - numerical methods for constant rate and constant pressure filtration based on Kozeny's law, Chemical Engineering Progress, v. 49 (9), 467-482.
- Tiller, F. M. and Cooper, H., 1960, The role of porosity in filtration: IV. Constant pressure filtration, AIChE Journal, v. 6 (4), 595-611.
- Tiller, F. M., 1990, Tutorial: interpretation of filtration data I, Fluid/Particle Separation Journal, v. 3 (2), 85-94.
- Tiller, F. M., Hsyung, N. B., Cong, D. Z., 1995, Role of porosity in filtration: XII – Filtration with sedimentation, AIChE Journal, v. 41, 1153-1164.
- Vajda, T. and Toros, R., 1990, A modern theory of filtration and its application in the optimization of the operation of various filters. Part I, International Chemical Engineering, v. 30 (4), 767-775.

- Wagemann, R. and Graham, B., 1974, Membrane and glass fiber filter contamination in chemical analysis of freshwater, *Water Research*, v. 8, 407-412.
- Wagemann, R. and Brunskill, G. J., 1975, The effect of filter pore size on analytical concentrations of some trace elements in filtrates of natural water, *International Journal of Environmental and Analytical Chemistry*, v. 4, 75.
- Walsh, M.; Knapp, L.; and Jenkins, T.; 1988, Evaluation of disposable membrane filter units for sorptive losses and sample contamination, *Environmental Technology Letters*, v. 9, 45-52.
- Whitworth, T. M. and Fritz, S. J., 1994, Electrolyte-induced solute permeability effects in compacted smectite membranes, *Applied Geochemistry*, v. 9, 533-546.
- Whitworth, T. M., Haneberg, W. C., Mozley, P. S., and Goodwin, L. B., 1999, Solute sieving on pulverized quartz sand – experimental results and implications for the membrane behavior of fault gouge, *Special Penrose Conference, American Geophysical Monograph Series volume 113*, 149-159.
- Whitehouse, B. G.; Petrick, G.; and Ehrhardt, M.; 1986, Crossflow filtration of colloids from Baltic sea water, *Water Research*, v. 20 (12), 1599-1601.
- Wijimans, J. G.; Nakao, S.; Smolders, C. A.; van den Berg, J. W.; and Troelstra, F. R., 1985, Hydrodynamic resistance of concentration polarization boundary layers in ultrafiltration, *Journal of Membrane Science*, v. 22, 117-135.
- Xu-Jiang, Y.; Dodds, J.; and Leclerc, D.; 1995, Cake characteristics in crossflow and dead-end microfiltration, *Filtration and Separation*, September, 795-798.
- Young, A. and Low, P. F., 1965, Osmosis in argillaceous rocks, *American Association of Petroleum Geology*

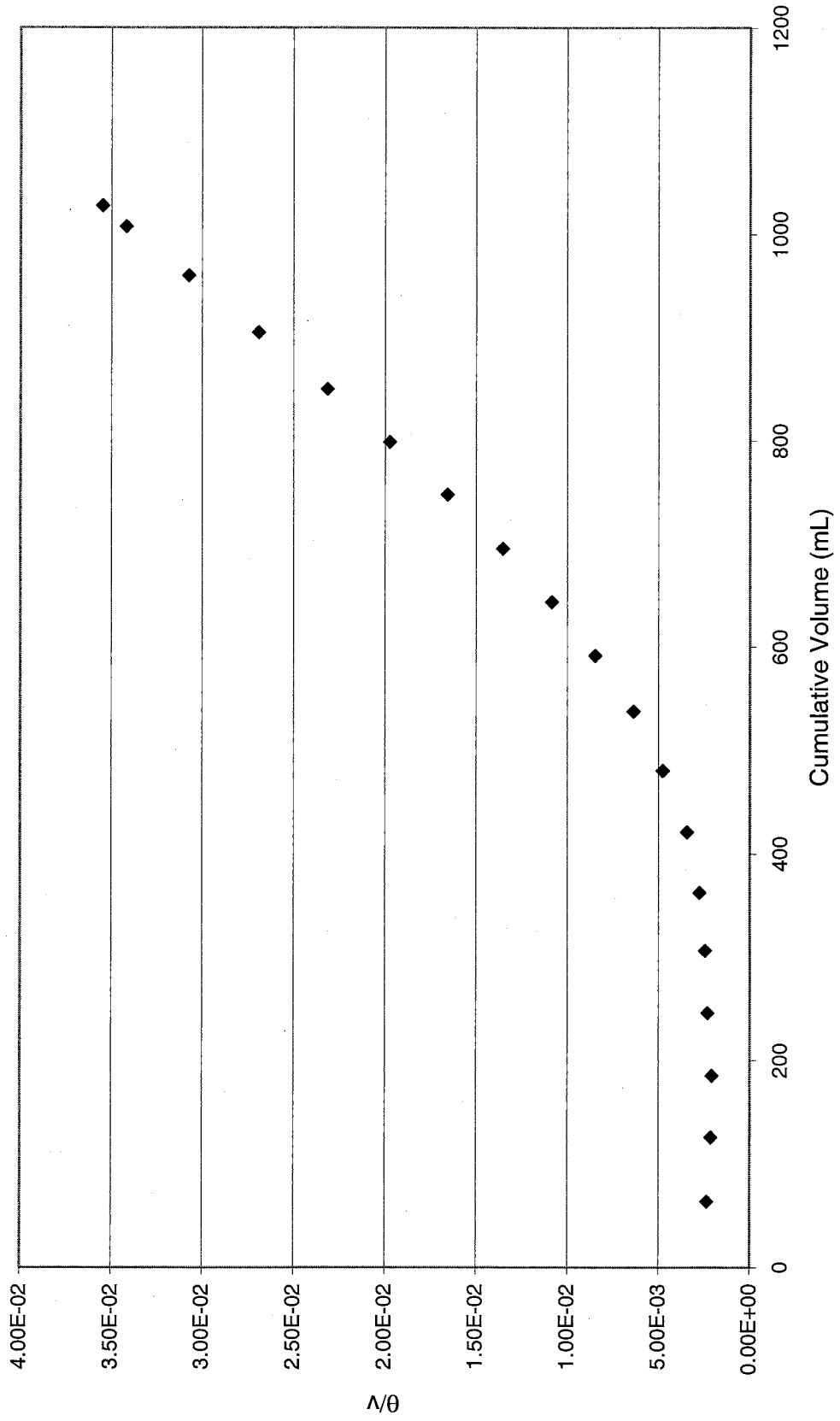
**APPENDIX A**

**Filter Resistance Data**

Filter Resistance Calculations							
Sample Number	Suspended solids (mg/L)	Pressure (psi)	Pressure (Pa)	L (inch)	L (cm)	L (m)	
95-196	5	65	4.48E+05	0.00075	1.91E-03	1.91E-05	
95-192	10	65	4.48E+05	0.002	5.08E-03	5.08E-05	
95-188	15	65	4.48E+05	0.0023	5.84E-03	5.84E-05	
95-180	25	65	4.48E+05	0.003	7.62E-03	7.62E-05	
95-174	50	65	4.48E+05	0.005	1.27E-02	1.27E-04	
95-166	75	65	4.48E+05	0.0065	1.65E-02	1.65E-04	
95-162	100	100	6.89E+05	0.007	1.78E-02	1.78E-04	
95-210	102.45	85	5.86E+05	0.008	2.03E-02	2.03E-04	
95-214	281.5	80	5.52E+05	0.012	3.05E-02	3.05E-04	
95-212	424.9	85	5.86E+05	0.021	5.33E-02	5.33E-04	
95-202	4100	65	4.48E+05	0.1245	3.16E-01	3.16E-03	
95-208	32100	100	6.89E+05	2.5	6.35E+00	6.35E-02	
Sample Number	Slope (min/mL <sup>2</sup> )	Slope (s/m <sup>6</sup> )	Y intercept (min/mL)	Y intercept (s/m <sup>3</sup> )	Filtrate Volume (mL)	r <sub>s</sub> (g/cm <sup>3</sup> )	
95-196	6.62E-05	3.97E+09	-3.29E-02	-1.97E+06	1028.003	2.17	
95-192	1.30E-04	7.79E+09	-4.96E-02	-2.97E+06	1016.26	2.17	
95-188	2.44E-04	1.46E+10	-5.89E-02	-3.54E+06	1024.22	2.17	
95-180	6.59E-05	3.96E+09	-1.34E-02	-8.02E+05	1042.44	2.17	
95-174	1.52E-04	9.15E+09	-2.12E-02	-1.27E+06	1033.32	2.17	
95-166	6.01E-04	3.61E+10	-2.65E-02	-1.59E+06	1036.11	2.17	
95-162	1.40E-04	8.38E+09	-2.40E-02	-1.44E+06	1068.37	2.17	
95-210	2.65E-05	1.59E+09	1.75E-04	1.05E+04	940.67	2.17	
95-214	1.41E-04	8.46E+09	-2.13E-02	-1.28E+06	983.25	2.17	
95-212	2.79E-04	1.67E+10	-2.21E-02	-1.33E+06	1015.65	2.17	
95-202	4.53E-03	2.72E+11	-5.28E-01	-3.17E+07	1206.27	2.5	
95-208	1.26E-01	7.55E+12	-4.47E+00	-2.68E+08	473.87	2.25	
Sample Number	w <sub>c</sub> (g)	v (dimensionless)	a (m <sup>-2</sup> )	R <sub>m</sub> (m <sup>-1</sup> )	Correlation	Covariance	Porosity
95-196	5.00E-03	2.30E-03	1.60E+15	Neg. slope	9.99E-01	8.54E-01	1.26E-01
95-192	1.00E-02	4.61E-03	1.57E+15	Neg. slope	9.99E-01	4.03E+00	9.43E-02
95-188	1.50E-02	6.91E-03	1.96E+15	Neg. slope	1.00E+00	1.00E+01	1.23E-01
95-180	2.50E-02	1.15E-02	3.19E+14	Neg. slope	9.99E-01	1.99E+00	1.57E-01
95-174	5.00E-02	2.30E-02	3.68E+14	Neg. slope	9.99E-01	6.75E+00	1.89E-01
95-166	7.50E-02	3.46E-02	9.69E+14	Neg. slope	9.99E-01	3.02E+01	2.18E-01
95-162	1.00E-01	4.61E-02	2.60E+14	Neg. slope	9.99E-01	4.81E+00	2.69E-01
95-210	1.02E-01	4.72E-02	4.09E+13	6.62E+09	9.97E-01	1.08E+00	2.42E-01
95-214	2.82E-01	1.30E-01	7.45E+13	Neg. slope	9.99E-01	5.49E+00	4.42E-01
95-212	4.25E-01	1.96E-01	1.04E+14	Neg. slope	1.00E+00	7.49E+00	3.82E-01
95-202	4.10E+00	1.64E+00	1.54E+14	Neg. slope	9.95E-01	3.72E+01	5.39E-01
95-208	3.21E+01	1.43E+01	7.56E+14	Neg. slope	1.00E+00	7.32E+02	2.34E-01

5 mg/L Clay Solution									
Sample No.	Mass Bottle (g)	Mass Sample + Btl (g)	Mass Sample (g)	Time Required (min)	Flow Rate (mL/min)	Pressure (psi)	Cumulative Time (min)	Cumulative Volume (mL)	θ/v
95-196-1	11.55	72.27	60.72	blank	blank	blank	blank	blank	blank
95-196-1A	10.91	73.40	62.49	blank	blank	blank	blank	blank	blank
95-196-2	9.75	73.36	63.61	0.15	424.07	65.00	0.15	63.61	2.358E-03
95-196-3	9.74	71.87	62.13	0.12	532.54	65.00	0.27	125.74	2.121E-03
95-196-4	9.75	69.34	59.59	0.12	510.77	65.00	0.38	185.33	2.068E-03
95-196-5	9.90	70.57	60.67	0.18	330.93	65.00	0.57	246.00	2.304E-03
95-196-6	9.76	70.09	60.33	0.18	329.07	65.00	0.75	306.33	2.448E-03
95-196-7	9.72	65.95	56.23	0.25	224.92	65.00	1.00	362.56	2.758E-03
95-196-8	9.75	68.19	58.44	0.45	129.87	65.00	1.45	421.00	3.444E-03
95-196-9	9.74	69.30	59.56	0.85	70.07	65.00	2.30	480.56	4.786E-03
95-196-10	9.74	66.81	57.07	1.13	50.36	65.00	3.43	537.63	6.386E-03
95-196-11	9.75	63.54	53.79	1.58	33.97	65.00	5.02	591.42	8.482E-03
95-196-12	9.72	61.71	51.99	1.97	26.44	65.00	6.98	643.41	1.085E-02
95-196-13	9.79	61.28	51.49	2.42	21.31	65.00	9.40	694.90	1.353E-02
95-196-14	9.79	62.31	52.52	2.98	17.60	65.00	12.38	747.42	1.657E-02
95-196-15	9.77	60.97	51.20	3.38	15.13	65.00	15.77	798.62	1.974E-02
95-196-16	9.94	61.63	51.69	3.92	13.20	65.00	19.68	850.31	2.315E-02
95-196-17	9.75	64.75	55.00	4.67	11.79	65.00	24.35	905.31	2.690E-02
95-196-18	9.78	64.89	55.11	5.17	10.67	65.00	29.52	960.42	3.073E-02
95-196-19	9.76	57.10	47.34	4.93	9.60	65.00	34.45	1007.76	3.418E-02
95-196-20	9.79	30.03	20.24	2.03	9.95	65.00	36.48	1028.00	3.549E-02
STOP									
95-196-D	Sample drawn for dialysis cell								
95-196-C	Sample drawn for centrifuge								

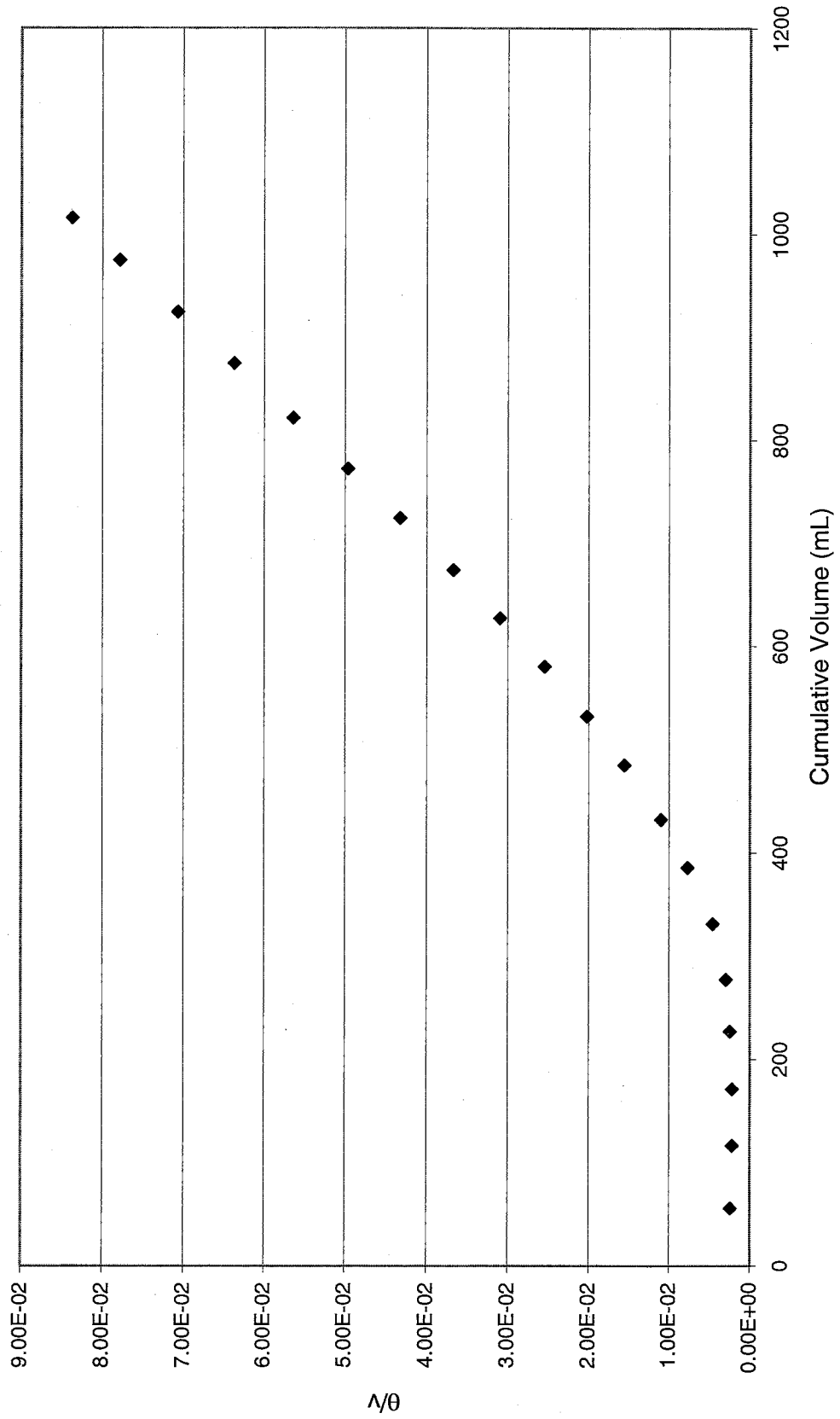
# 5 mg/L Clay Solution



10 mg/L Clay Solution										
Sample No.	Mass Bottle (g)	Mass Sample + Btl (g)	Mass Sample (g)	Time Required (min)	Flow Rate (mL/min)	Pressure (psi)	Cumulative Time (min)	Cumulative Volume (mL)	$\theta/v$	
95-192-1	11.04	76.25	65.21	blank	blank	blank	blank	blank	blank	
95-192-1A	10.89	63.98	53.09	blank	blank	blank	blank	blank	blank	
95-192-2	9.79	65.36	55.57	0.13	416.78	65.00	0.13	55.57	2.399E-03	
95-192-3	9.72	70.39	60.67	0.12	520.03	65.00	0.25	116.24	2.151E-03	
95-192-4	9.80	64.38	54.58	0.12	467.83	65.00	0.37	170.82	2.147E-03	
95-192-5	9.83	65.79	55.96	0.18	305.24	65.00	0.55	226.78	2.425E-03	
95-192-6	9.91	60.18	50.27	0.27	188.51	65.00	0.82	277.05	2.948E-03	
95-192-7	9.82	64.01	54.19	0.70	77.41	65.00	1.52	331.24	4.579E-03	
95-192-8	9.98	64.49	54.51	1.47	37.17	65.00	2.98	385.75	7.734E-03	
95-192-9	9.80	56.41	46.61	1.78	26.14	65.00	4.77	432.36	1.102E-02	
95-192-10	9.77	62.30	52.53	2.78	18.87	65.00	7.55	484.89	1.557E-02	
95-192-11	9.97	57.17	47.20	3.22	14.67	65.00	10.77	532.09	2.023E-02	
95-192-12	9.87	57.96	48.09	4.03	11.92	65.00	14.80	580.18	2.551E-02	
95-192-13	9.78	56.65	46.87	4.63	10.12	65.00	19.43	627.05	3.099E-02	
95-192-14	9.77	56.40	46.63	5.33	8.74	65.00	24.77	673.68	3.676E-02	
95-192-15	9.75	60.49	50.74	6.57	7.73	65.00	31.33	724.42	4.325E-02	
95-192-16	9.73	57.71	47.98	7.03	6.82	65.00	38.37	772.40	4.967E-02	
95-192-17	9.77	59.42	49.65	8.00	6.21	65.00	46.37	822.05	5.640E-02	
95-192-18	9.74	62.83	53.09	9.40	5.65	65.00	55.77	875.14	6.372E-02	
95-192-19	9.77	59.55	49.78	9.63	5.17	65.00	65.40	924.92	7.071E-02	
95-192-20	9.73	60.13	50.40	10.53	4.78	65.00	75.93	975.32	7.785E-02	
95-192-21	9.78	50.72	40.94	9.15	4.47	65.00	85.08	1016.26	8.372E-02	
STOP										
95-192-D	Sample drawn for dialysis cell									
95-192-C	Sample drawn for centrifuge									

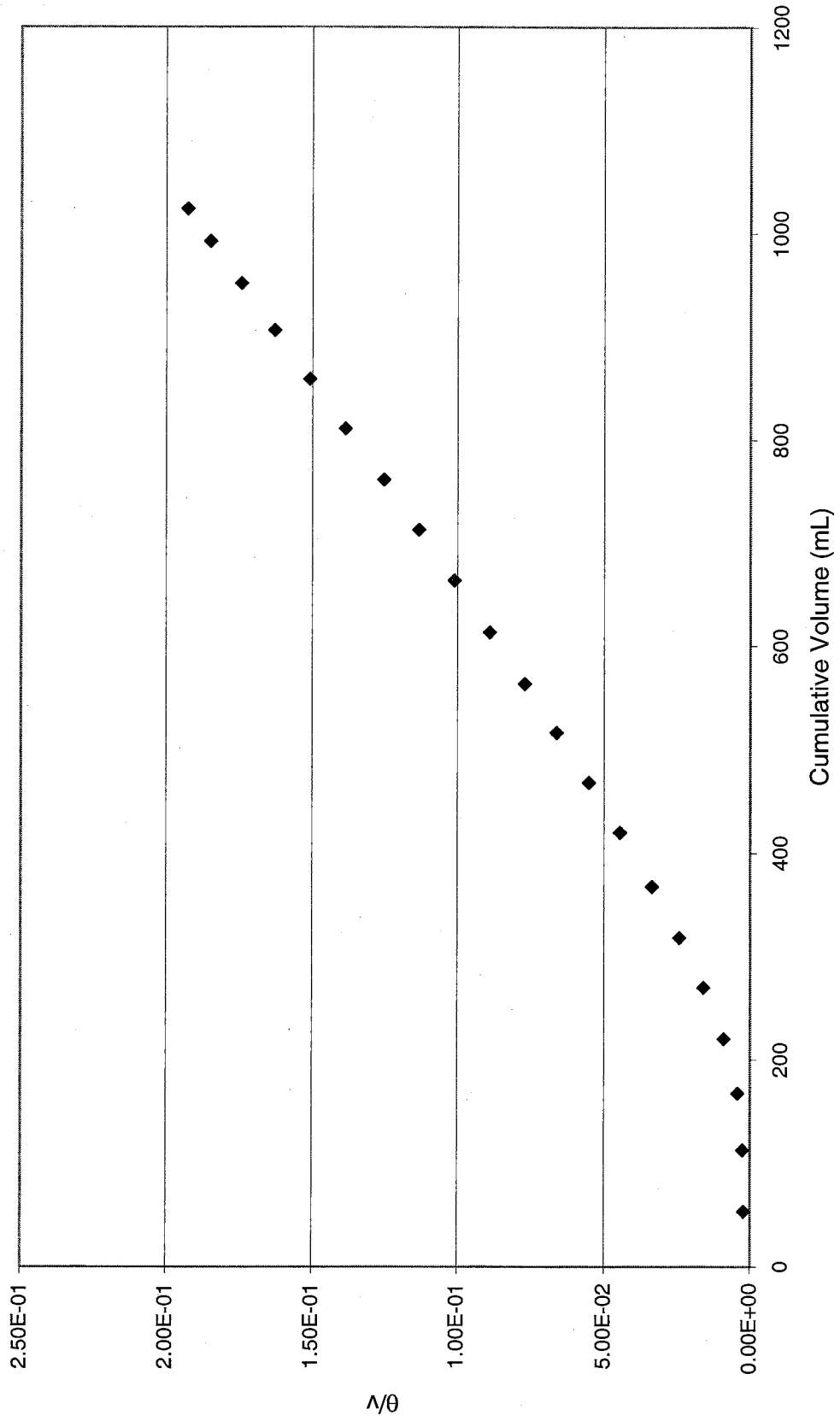


# 10 mg/L Clay Solution



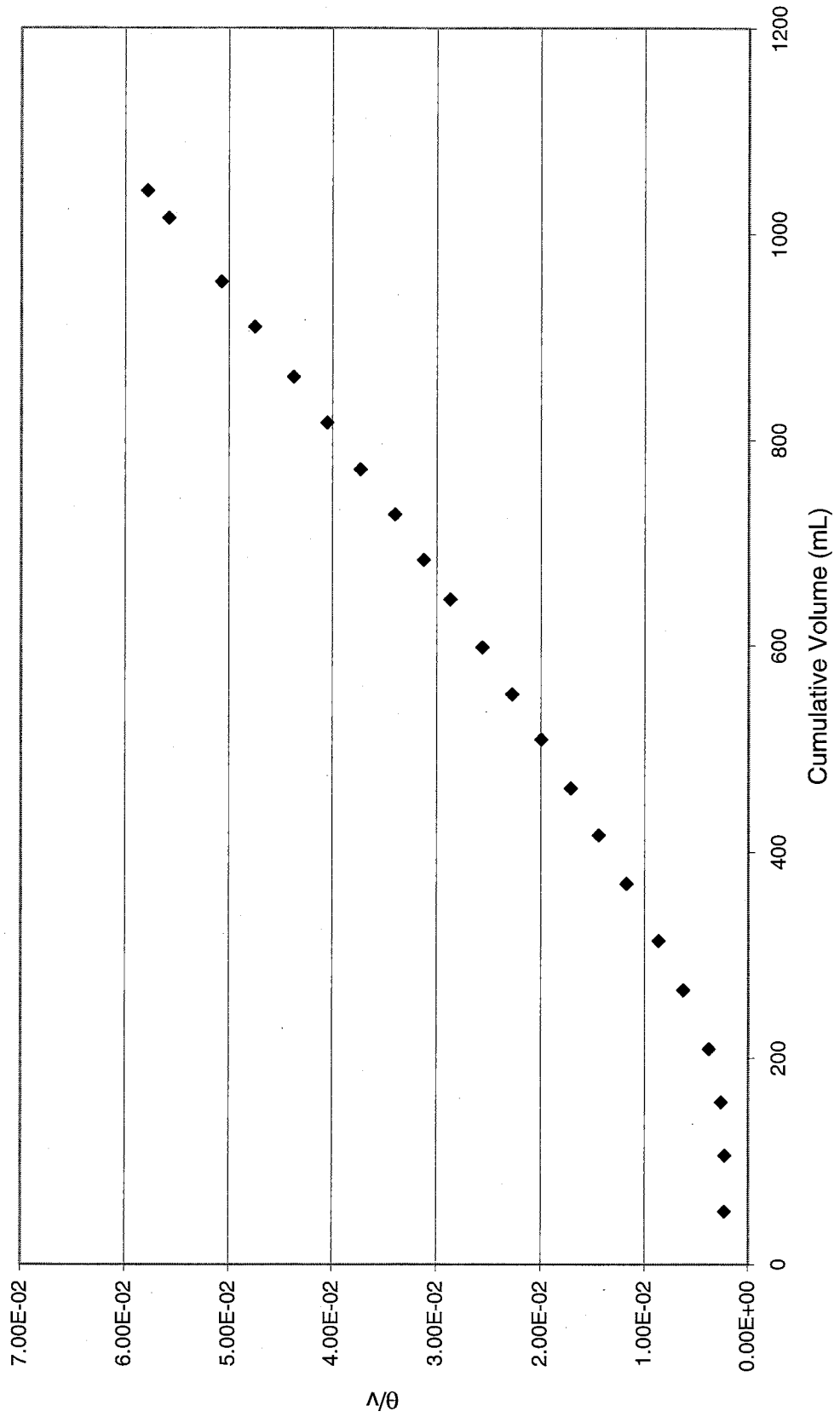
15 mg/L Clay Solution									
Sample No.	Mass Bottle (g)	Mass Sample + Btl (g)	Mass Sample (g)	Time Required (min)	Flow Rate (mL/min)	Pressure (psi)	Cumulative Time (min)	Cumulative Volume (mL)	$\theta/v$
95-188-1	10.91	71.65	60.74	blank	blank	blank	blank	blank	blank
95-188-1A	11.59	69.76	58.17	blank	blank	blank	blank	blank	blank
95-188-2	9.74	63.08	53.34	0.12	457.20	65.00	0.12	53.34	2.187E-03
95-188-3	9.73	68.98	59.25	0.17	355.50	65.00	0.28	112.59	2.517E-03
95-188-4	9.78	64.57	54.79	0.42	131.50	65.00	0.70	167.38	4.182E-03
95-188-5	9.72	62.55	52.83	1.28	41.17	65.00	1.98	220.21	9.007E-03
95-188-6	9.73	59.45	49.72	2.35	21.16	65.00	4.33	269.93	1.605E-02
95-188-7	9.80	58.07	48.27	3.42	14.13	65.00	7.75	318.20	2.436E-02
95-188-8	9.74	59.22	49.48	4.68	10.57	65.00	12.43	367.68	3.382E-02
95-188-9	9.75	62.03	52.28	6.33	8.25	65.00	18.77	419.96	4.469E-02
95-188-10	9.96	58.13	48.17	7.08	6.80	65.00	25.85	468.13	5.522E-02
95-188-11	9.74	58.14	48.40	8.33	5.81	65.00	34.18	516.53	6.618E-02
95-188-12	9.76	56.75	46.99	9.28	5.06	65.00	43.47	563.52	7.713E-02
95-188-13	9.95	59.61	49.66	11.13	4.46	65.00	54.60	613.18	8.904E-02
95-188-14	9.75	59.83	50.08	12.50	4.01	65.00	67.10	663.26	1.012E-01
95-188-15	9.73	59.14	49.41	13.67	3.62	65.00	80.77	712.67	1.133E-01
95-188-16	9.74	58.49	48.75	14.70	3.32	65.00	95.47	761.42	1.254E-01
95-188-17	9.77	59.37	49.60	16.93	2.93	65.00	112.40	811.02	1.386E-01
95-188-18	9.76	57.89	48.13	17.22	2.80	65.00	129.62	859.15	1.509E-01
95-188-19	9.73	57.17	47.44	18.05	2.63	65.00	147.67	906.59	1.629E-01
95-188-20	9.75	55.40	45.65	18.32	2.49	65.00	165.98	952.24	1.743E-01
95-188-21	9.74	50.51	40.77	17.58	2.32	65.00	183.57	993.01	1.849E-01
95-188-22	9.76	40.97	31.21	13.73	2.27	65.00	197.30	1024.22	1.926E-01
STOP									
95-188-D	Sample drawn for dialysis cell								
95-188-C	Sample drawn for centrifuge								

# 15 mg/L Clay Solution



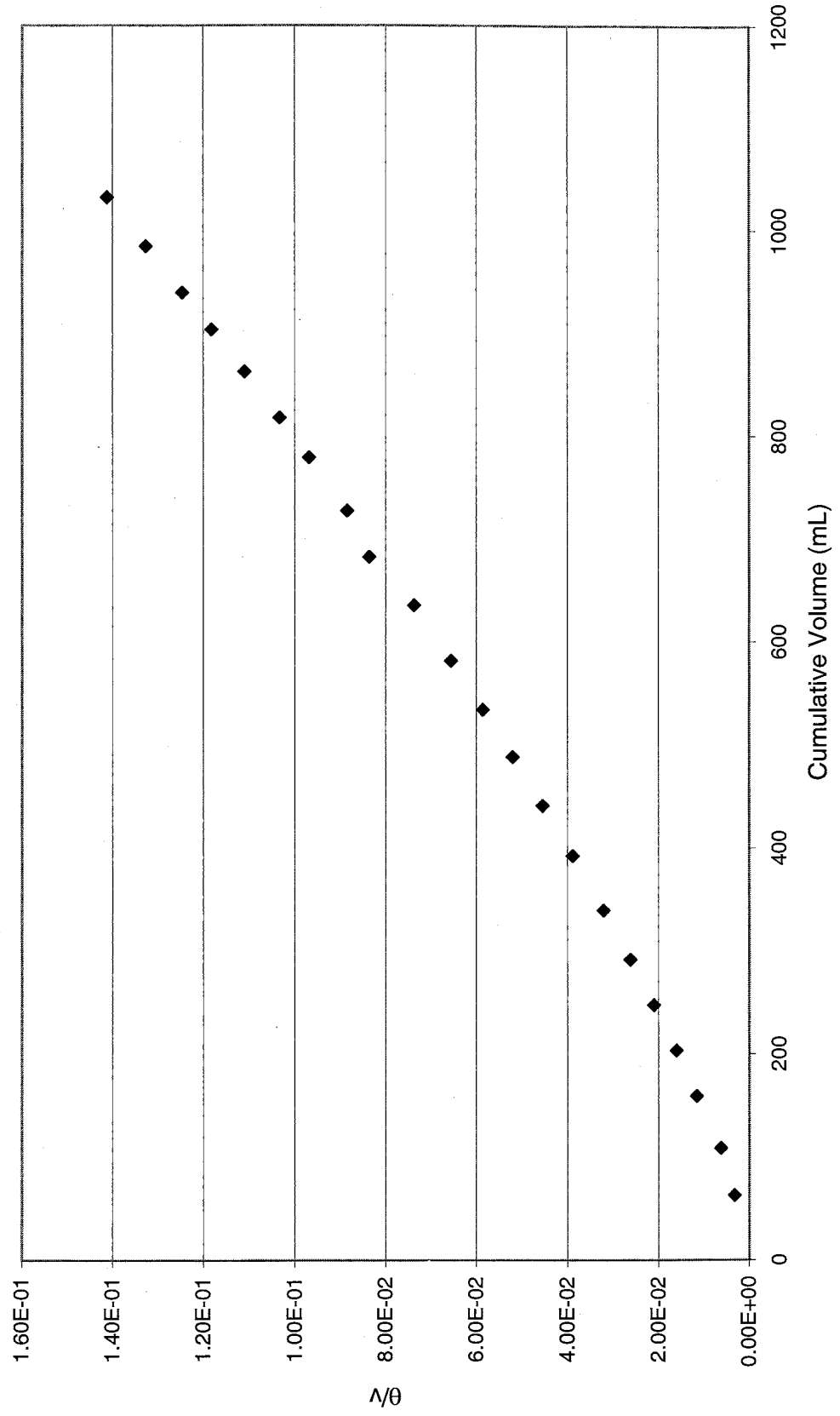
25 mg/L Clay Solution									
Sample No.	Mass Bottle (g)	Mass Sample + Btl (g)	Mass Sample (g)	Time Required (min)	Flow Rate (mL/min)	Pressure (psi)	Cumulative Time (min)	Cumulative Volume (mL)	$\theta/v$
95-180-1	10.28	61.86	51.58	blank	blank	blank	blank	blank	blank
95-180-1A	10.26	60.26	50.00	blank	blank	blank	blank	blank	blank
95-180-2	10.31	61.33	51.02	0.12	437.31	65.00	0.12	51.02	2.287E-03
95-180-3	10.19	64.54	54.35	0.12	452.92	65.00	0.24	105.37	2.246E-03
95-180-4	10.32	61.96	51.64	0.17	303.76	65.00	0.41	157.01	2.590E-03
95-180-5	10.36	62.17	51.81	0.38	136.34	65.00	0.79	208.82	3.767E-03
95-180-6	10.21	67.40	57.19	0.88	64.99	65.00	1.67	266.01	6.265E-03
95-180-7	10.17	58.04	47.87	1.05	45.59	65.00	2.72	313.88	8.655E-03
95-180-8	10.26	65.69	55.43	1.62	34.22	65.00	4.34	369.31	1.174E-02
95-180-9	10.36	57.39	47.03	1.67	28.16	65.00	6.01	416.34	1.443E-02
95-180-10	10.35	55.77	45.42	1.90	23.91	65.00	7.91	461.76	1.712E-02
95-180-11	10.26	57.42	47.16	2.27	20.78	65.00	10.18	508.92	2.000E-02
95-180-12	10.40	54.34	43.94	2.42	18.16	65.00	12.60	552.86	2.278E-02
95-180-13	10.33	55.61	45.28	2.75	16.47	65.00	15.35	598.14	2.566E-02
95-180-14	10.34	56.99	46.65	3.17	14.72	65.00	18.52	644.79	2.872E-02
95-180-15	10.22	48.45	38.23	2.83	13.51	65.00	21.35	683.02	3.125E-02
95-180-16	10.26	54.49	44.23	3.40	13.01	65.00	24.75	727.25	3.403E-02
95-180-17	10.39	54.18	43.79	4.02	10.89	65.00	28.77	771.04	3.731E-02
95-180-18	9.68	55.27	45.59	4.32	10.55	65.00	33.09	816.63	4.052E-02
95-180-19	10.28	55.18	44.90	4.60	9.76	65.00	37.69	861.53	4.374E-02
95-180-20	10.26	58.86	48.60	5.55	8.76	65.00	43.24	910.13	4.751E-02
95-180-21	10.3	54.15	43.85	5.15	8.51	65.00	48.39	953.98	5.072E-02
95-180-22	10.26	72.00	61.74	8.30	7.44	65.00	56.69	1015.72	5.581E-02
95-180-23	9.71	36.43	26.72	3.62	7.38	65.00	60.31	1042.44	5.785E-02
STOP									
95-180-D	Sample drawn for dialysis cell								
95-180-C	Sample drawn for centrifuge								

# 25 mg/L Clay Solution



50 mg/L Clay Solution									
Sample No.	Mass Bottle (g)	Mass Sample + Btl (g)	Mass Sample (g)	Time Required (min)	Flow Rate (mL/min)	Pressure (psi)	Cumulative Time (min)	Cumulative Volume (mL)	θ/v
95-174-1	10.27	61.33	51.06	blank	blank	blank	blank	blank	blank
95-174-1A	10.23	60.23	50.00	blank	blank	blank	blank	blank	blank
95-174-2	10.36	72.79	62.43	0.20	312.15	65.00	0.20	62.43	3.204E-03
95-174-3	10.23	56.07	45.84	0.47	97.53	65.00	0.67	108.27	6.188E-03
95-174-4	10.30	61.00	50.70	1.17	43.33	65.00	1.84	158.97	1.157E-02
95-174-5	10.29	54.49	44.20	1.42	31.13	65.00	3.26	203.17	1.605E-02
95-174-6	10.31	54.52	44.21	1.95	22.67	65.00	5.21	247.38	2.106E-02
95-174-7	10.32	54.49	44.17	2.45	18.03	65.00	7.66	291.55	2.627E-02
95-174-8	10.20	57.98	47.78	3.25	14.70	65.00	10.91	339.33	3.215E-02
95-174-9	10.36	63.38	53.02	4.35	12.19	65.00	15.26	392.35	3.889E-02
95-174-10	10.33	59.05	48.72	4.77	10.21	65.00	20.03	441.07	4.541E-02
95-174-11	10.25	57.65	47.40	5.37	8.83	65.00	25.40	488.47	5.200E-02
95-174-12	10.37	56.21	45.84	5.90	7.77	65.00	31.30	534.31	5.858E-02
95-174-13	10.33	57.67	47.34	6.85	6.91	65.00	38.15	581.65	6.559E-02
95-174-14	10.35	64.33	53.98	8.73	6.18	65.00	46.88	635.63	7.375E-02
95-174-15	10.28	57.39	47.11	10.22	4.61	65.00	57.10	682.74	8.363E-02
95-174-16	10.35	55.35	45.00	7.28	6.18	65.00	64.38	727.74	8.847E-02
95-174-17	10.31	62.58	52.27	11.17	4.68	65.00	75.55	780.01	9.686E-02
95-174-18	10.31	49.01	38.70	9.07	4.27	65.00	84.62	818.71	1.034E-01
95-174-19	10.30	55.39	45.09	11.30	3.99	65.00	95.92	863.80	1.110E-01
95-174-20	10.43	51.41	40.98	11.05	3.71	65.00	106.97	904.78	1.182E-01
95-174-21	10.39	46.35	35.96	10.28	3.50	65.00	117.25	940.74	1.246E-01
95-174-22	10.39	55.45	45.06	13.52	3.33	65.00	130.77	985.80	1.327E-01
95-174-23	10.37	57.89	47.52	15.20	3.13	65.00	145.97	1033.32	1.413E-01
STOP									
95-174-D	Sample drawn for dialysis cell								
95-174-C	Sample drawn for centrifuge								

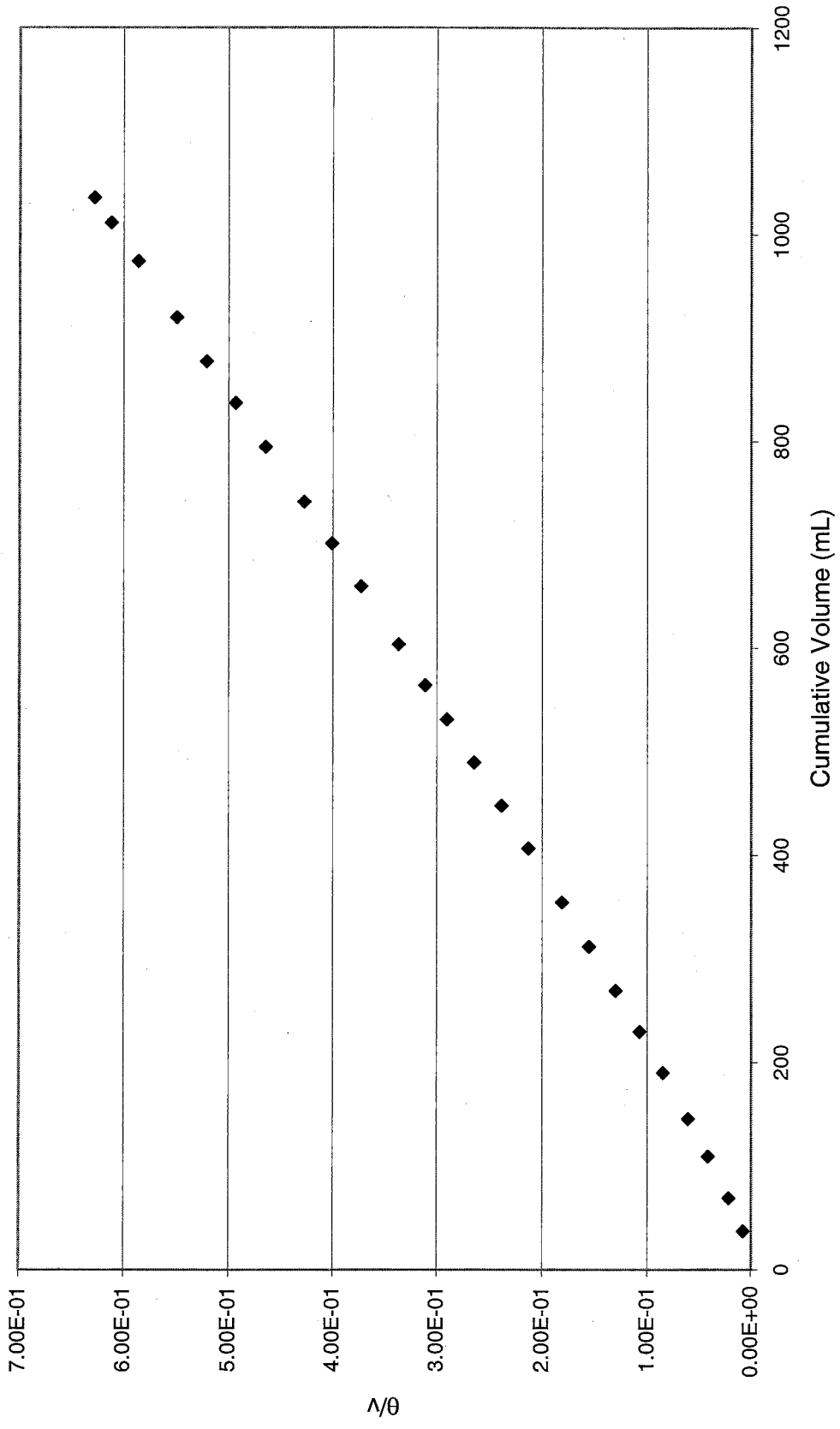
# 50 mg/L Clay Solution



75 mg/L Clay Solution										
Sample No.	Mass Bottle (g)	Mass Sample + Btl (g)	Mass Sample (g)	Time Required (min)	Flow Rate (mL/min)	Pressure (psi)	Cumulative Time (min)	Cumulative Volume (mL)	θ/v	
95-166-1	9.74	74.96	65.22	blank	blank	blank	blank	blank	blank	
95-166-2	9.69	46.72	37.03	0.28	130.85	65.00	0.28	37.03	7.642E-03	
95-166-3	9.72	41.60	31.88	1.20	26.57	65.00	1.48	68.91	2.152E-02	
95-166-4	9.90	50.06	40.16	3.03	13.25	65.00	4.51	109.07	4.138E-02	
95-166-5	9.73	46.06	36.33	4.28	8.49	65.00	8.79	145.40	6.047E-02	
95-166-6	9.92	54.38	44.46	7.33	6.07	65.00	16.12	189.86	8.492E-02	
95-166-7	9.74	49.23	39.49	8.50	4.65	65.00	24.62	229.35	1.074E-01	
95-166-8	9.89	49.54	39.65	10.47	3.79	65.00	35.09	269.00	1.305E-01	
95-166-9	9.70	52.38	42.68	13.47	3.17	65.00	48.56	311.68	1.558E-01	
95-166-10	9.88	52.68	42.80	15.78	2.71	65.00	64.34	354.48	1.815E-01	
95-166-11	9.74	62.07	52.33	22.38	2.34	65.00	86.72	406.81	2.132E-01	
95-166-12	9.78	50.96	41.18	20.20	2.04	65.00	106.92	447.99	2.387E-01	
95-166-13	9.70	51.22	41.52	22.57	1.84	65.00	129.49	489.51	2.645E-01	
95-166-14	9.69	51.27	41.58	24.77	1.68	65.00	154.26	531.09	2.905E-01	
95-166-15	9.74	42.65	32.91	21.25	1.55	65.00	175.51	564.00	3.112E-01	
95-166-16	9.69	49.13	39.44	27.71	1.42	65.00	203.22	603.44	3.368E-01	
95-166-17	9.72	65.56	55.84	42.70	1.31	65.00	245.92	659.28	3.730E-01	
95-166-18	9.88	51.61	41.73	35.18	1.19	65.00	281.10	701.01	4.010E-01	
95-166-19	9.72	50.10	40.38	35.98	1.12	65.00	317.08	741.39	4.277E-01	
95-166-20	9.90	63.04	53.14	52.07	1.02	65.00	369.15	794.53	4.646E-01	
95-166-21	9.71	52.40	42.69	43.77	0.98	65.00	412.92	837.22	4.932E-01	
95-166-22	9.65	49.98	40.33	44.12	0.91	65.00	457.04	877.55	5.208E-01	
95-166-23	9.64	52.39	42.75	48.62	0.88	65.00	505.66	920.30	5.495E-01	
95-166-24	9.68	63.79	54.11	65.58	0.83	65.00	571.24	974.41	5.862E-01	
95-166-25	9.68	47.08	37.40	48.12	0.78	65.00	619.36	1011.81	6.121E-01	
95-166-26	9.62	33.92	24.30	31.38	0.77	65.00	650.75	1036.11	6.281E-01	
STOP										
95-166-D	Sample drawn for dialysis cell									
95-166-C	Sample drawn for centrifuge									

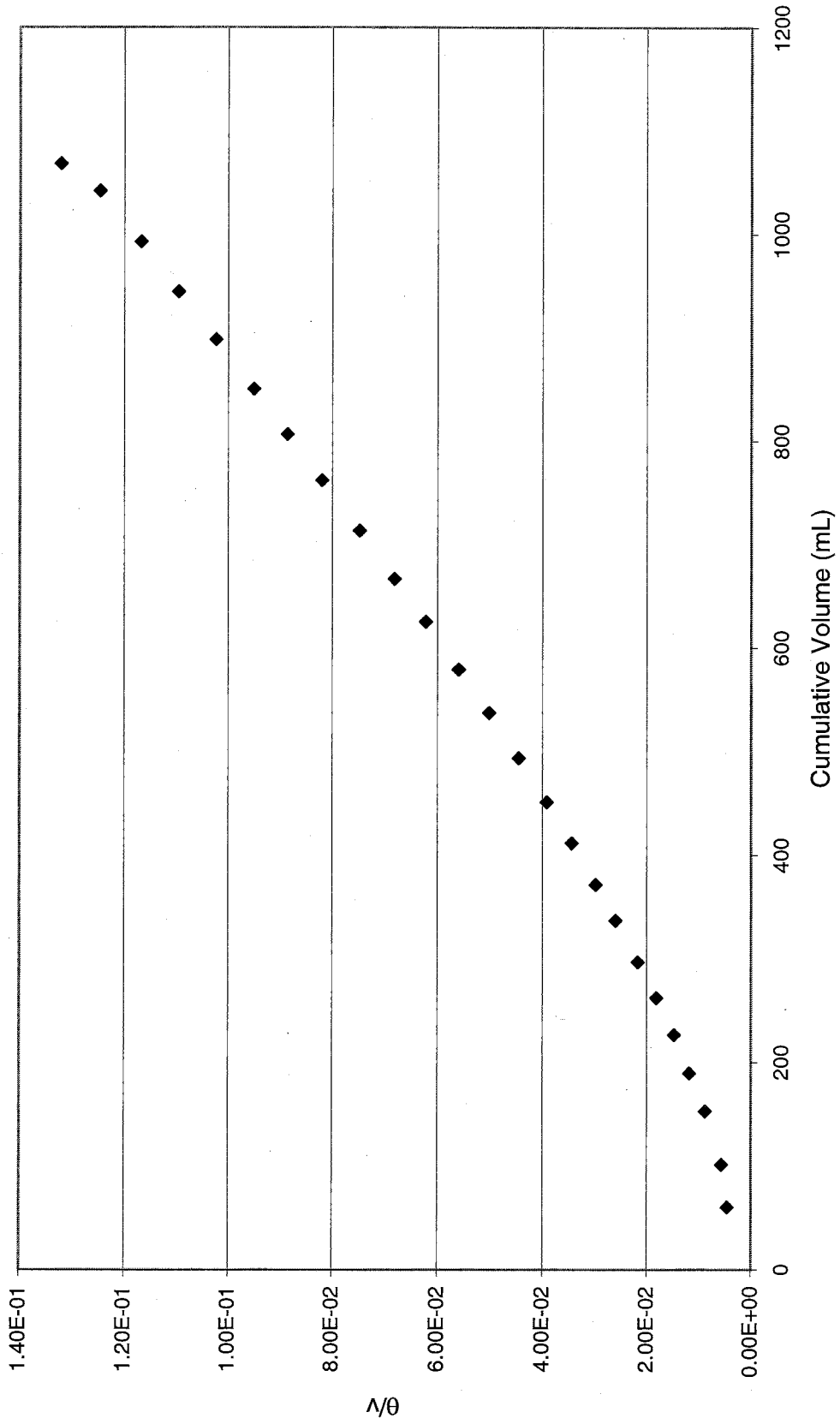


# 75 mg/L Clay Solution



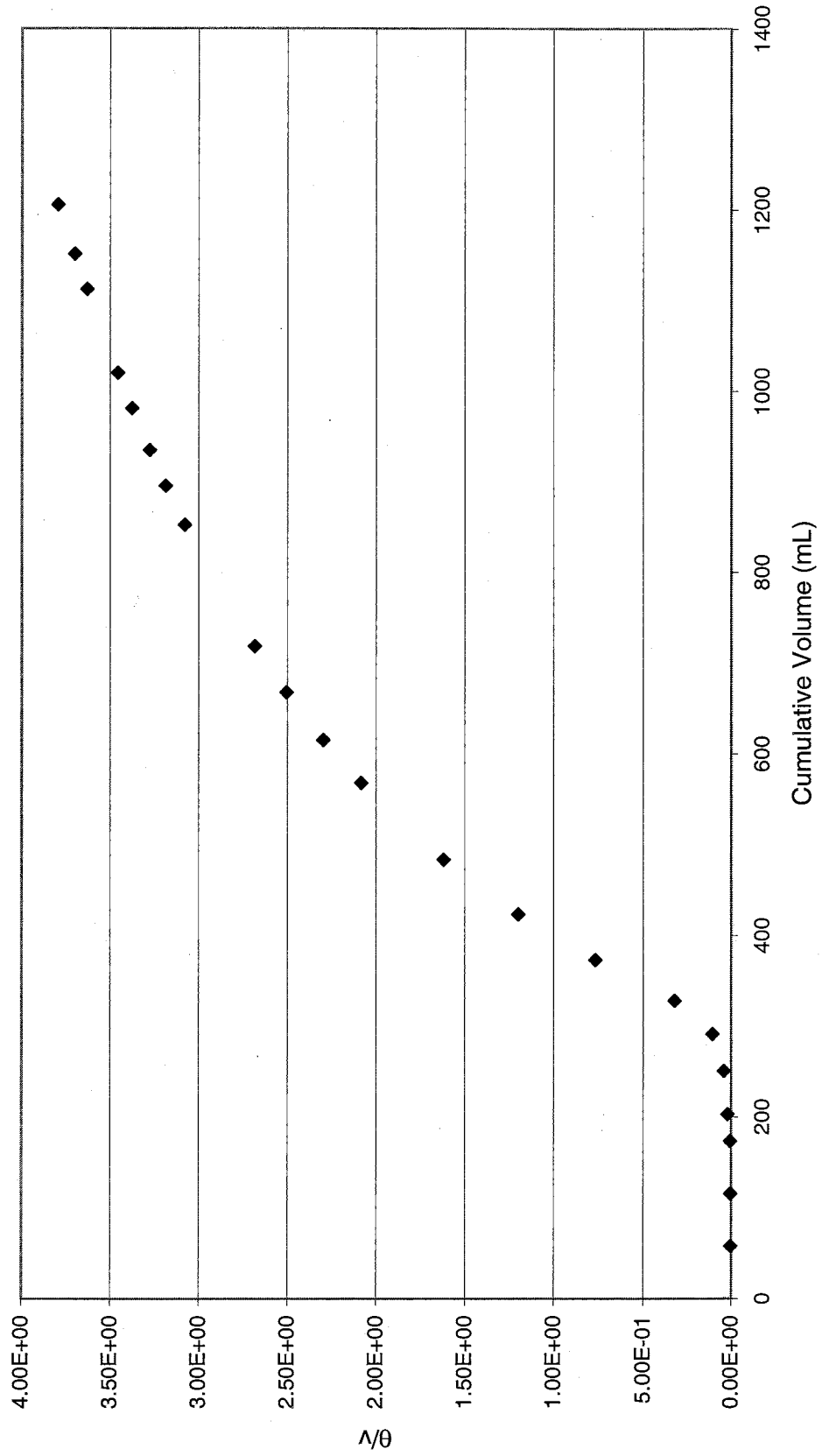
100 mg/L Clay Solution									
Sample No.	Mass Bottle (g)	Mass Sample + Btl (g)	Mass Sample (g)	Time Required (min)	Flow Rate (mL/min)	Pressure (psi)	Cumulative Time (min)	Cumulative Volume (mL)	θ/v
95-162-1	9.68	75.00	65.32	0.00	blank	blank	blank	blank	blank
95-162-2	9.88	70.03	60.15	0.27	222.78	100.00	0.27	60.15	4.489E-03
95-162-3	9.80	50.87	41.07	0.30	136.90	100.00	0.57	101.22	5.631E-03
95-162-4	9.89	61.55	51.66	0.77	67.09	100.00	1.34	152.88	8.765E-03
95-162-5	9.88	46.62	36.74	0.90	40.82	100.00	2.24	189.62	1.181E-02
95-162-6	9.91	46.92	37.01	1.10	33.65	100.00	3.34	226.63	1.474E-02
95-162-7	9.71	45.30	35.59	1.42	25.06	100.00	4.76	262.22	1.815E-02
95-162-8	9.70	44.38	34.68	1.68	20.64	100.00	6.44	296.90	2.169E-02
95-162-9	9.73	49.73	40.00	2.30	17.39	100.00	8.74	336.90	2.594E-02
95-162-10	9.73	44.50	34.77	2.33	14.92	100.00	11.07	371.67	2.978E-02
95-162-11	9.74	49.75	40.01	3.10	12.91	100.00	14.17	411.68	3.442E-02
95-162-12	9.73	49.28	39.55	3.53	11.19	100.00	17.70	451.23	3.923E-02
95-162-13	9.76	52.25	42.49	4.30	9.88	100.00	22.00	493.72	4.457E-02
95-162-14	9.73	53.17	43.44	5.00	8.69	100.00	27.00	537.16	5.027E-02
95-162-15	9.72	51.47	41.75	5.42	7.70	100.00	32.42	578.91	5.601E-02
95-162-16	9.72	55.79	46.07	6.50	7.09	100.00	38.92	624.98	6.228E-02
95-162-17	9.70	51.29	41.59	6.52	6.38	100.00	45.44	666.57	6.817E-02
95-162-18	9.71	56.33	46.62	7.92	5.89	100.00	53.36	713.19	7.482E-02
95-162-19	9.72	58.57	48.85	9.12	5.36	100.00	62.48	762.04	8.199E-02
95-162-20	9.69	54.53	44.84	9.00	4.98	100.00	71.48	806.88	8.859E-02
95-162-21	9.68	53.61	43.93	9.38	4.68	100.00	80.86	850.81	9.504E-02
95-162-22	9.82	57.68	47.86	11.10	4.31	100.00	91.96	898.67	1.023E-01
95-162-23	9.87	56.19	46.32	11.58	4.00	100.00	103.54	944.99	1.096E-01
95-162-24	9.79	58.09	48.30	12.48	3.87	100.00	116.02	993.29	1.168E-01
95-162-25	9.72	58.57	48.85	13.92	3.51	100.00	129.94	1042.14	1.247E-01
95-162-26	9.71	35.94	26.23	11.28	2.33	100.00	141.22	1068.37	1.322E-01
STOP									
95-162-D	Sample drawn for dialysis cell								
95-162-C	Sample drawn for centrifuge								

# 100 mg/L Clay Solution



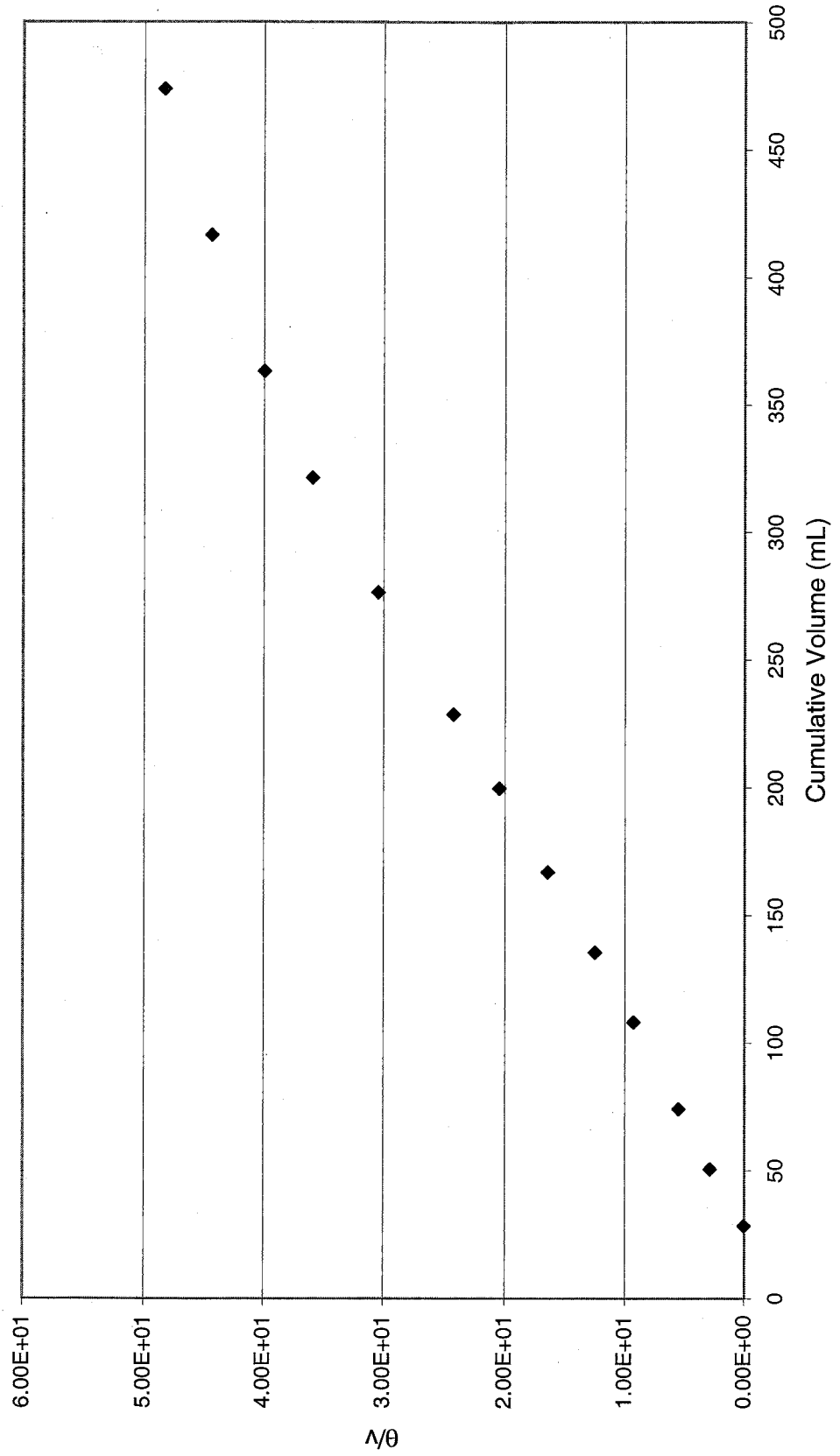
Rio Grande Sample - 4,100 mg/L Total Suspended Solids										
Sample No.	Mass Bottle (g)	Mass Sample + Btl (g)	Mass Sample (g)	Time Required (min)	Flow Rate (mL/min)	Pressure (psi)	Cumulative Time (min)	Cumulative Volume (mL)	θ/v	
95-202-1	10.90	68.72	57.82	0.18	321.2222	45	0.18	57.82	3.113E-03	
95-202-2	11.05	68.87	57.82	0.20	289.1000	45	0.38	115.64	3.286E-03	
95-202-3	11.55	69.12	57.57	0.37	155.5946	45	0.75	173.21	4.330E-03	
95-202-4	11.09	40.69	29.60	3.05	9.7049	45	3.8	202.81	1.874E-02	
95-202-5	10.91	58.80	47.89	6.28	7.6258	65	10.08	250.70	4.021E-02	
95-202-6	11.70	52.15	40.45	20.12	2.0104	65	30.2	291.15	1.037E-01	
95-202-7	10.91	47.64	36.73	74.70	0.4917	65	104.9	327.88	3.199E-01	
95-202-8	11.58	56.53	44.95	180.75	0.2487	65	285.65	372.83	7.662E-01	
95-202-9	11.70	62.14	50.44	221.85	0.2274	65	507.5	423.27	1.199E+00	
95-202-10	11.07	71.39	60.32	275.58	0.2189	65	783.08	483.59	1.619E+00	
95-202-11	11.52	96.06	84.54	401.53	0.2105	65	1184.613	568.13	2.085E+00	
95-202-12	11.81	58.97	47.16	229.90	0.2051	65	1414.513	615.29	2.299E+00	
95-202-13	11.06	63.43	52.37	258.40	0.2027	65	1672.913	667.66	2.506E+00	
95-202-14	10.88	61.56	50.68	255.13	0.1986	65	1928.043	718.34	2.684E+00	
95-202-15	11.53	76.00	134.08	696.67	0.1925	65	2624.713	852.42	3.079E+00	
95-202-16	10.89	54.00	43.11	228.20	0.1889	65	2852.913	895.53	3.186E+00	
95-202-17	11.59	51.01	39.42	210.30	0.1874	65	3063.213	934.95	3.276E+00	
95-202-18	11.07	57.39	46.32	249.85	0.1854	65	3313.063	981.27	3.376E+00	
95-202-19	11.06	50.33	39.27	214.28	0.1833	65	3527.343	1020.54	3.456E+00	
95-202-20	11.77	75.67	92.45	513.93	0.1799	65	4041.273	1112.99	3.631E+00	
95-202-21	11.59	50.40	38.81	220.55	0.1760	65	4261.823	1151.80	3.700E+00	
95-202-22	11.79	66.26	54.47	315.68	0.1725	65	4577.503	1206.27	3.795E+00	
STOP										
95-202-D	Sample drawn for dialysis cell									
95-202-C	Sample drawn for centrifuge									

Rio Grande Sample  
TSS = 4,100 mg/L



Rio Puerco Sample - 32,100 mg/L Total Suspended Solids										
Sample No.	Mass Bottle (g)	Mass Sample + Btl (g)	Mass Sample (g)	Time Required (min)	Flow Rate (mL/min)	Pressure (psi)	Cumulative Time (min)	Cumulative Volume (mL)	$\theta/v$	
95-208-1	11.10	39.33	28.23	0.91	30.98	100	0.91	28.23	3.227E-02	
95-208-2	11.08	33.37	22.29	144.42	0.15	100	145.33	50.52	2.877E+00	
95-208-3	11.09	34.64	23.55	261.87	0.09	100	407.19	74.07	5.497E+00	
95-208-4	11.07	45.01	33.94	597.48	0.06	100	1004.68	108.01	9.302E+00	
95-208-5	11.11	38.56	27.45	689.75	0.04	100	1694.43	135.46	1.251E+01	
95-208-6	10.92	42.40	31.48	1053.35	0.03	100	2747.78	166.94	1.646E+01	
95-208-7	10.91	43.49	32.58	1338.78	0.02	100	4086.56	199.52	2.048E+01	
95-208-8	10.91	39.86	28.95	1459.30	0.02	100	5545.86	228.47	2.427E+01	
95-208-9	11.08	58.89	47.81	2869.90	0.02	100	8415.76	276.28	3.046E+01	
95-208-10	11.06	56.13	45.07	3137.27	0.01	100	11553.03	321.35	3.595E+01	
95-208-11	10.92	52.85	41.93	2966.33	0.01	100	14519.36	363.28	3.997E+01	
95-208-12	10.98	64.35	53.37	3983.66	0.01	100	18503.02	416.65	4.441E+01	
95-208-13	11.02	68.24	57.22	4408.57	0.01	100	22911.59	473.87	4.835E+01	
STOP										
95-208-D	Sample drawn for dialysis cell									
95-208-C	Sample drawn for centrifuge									

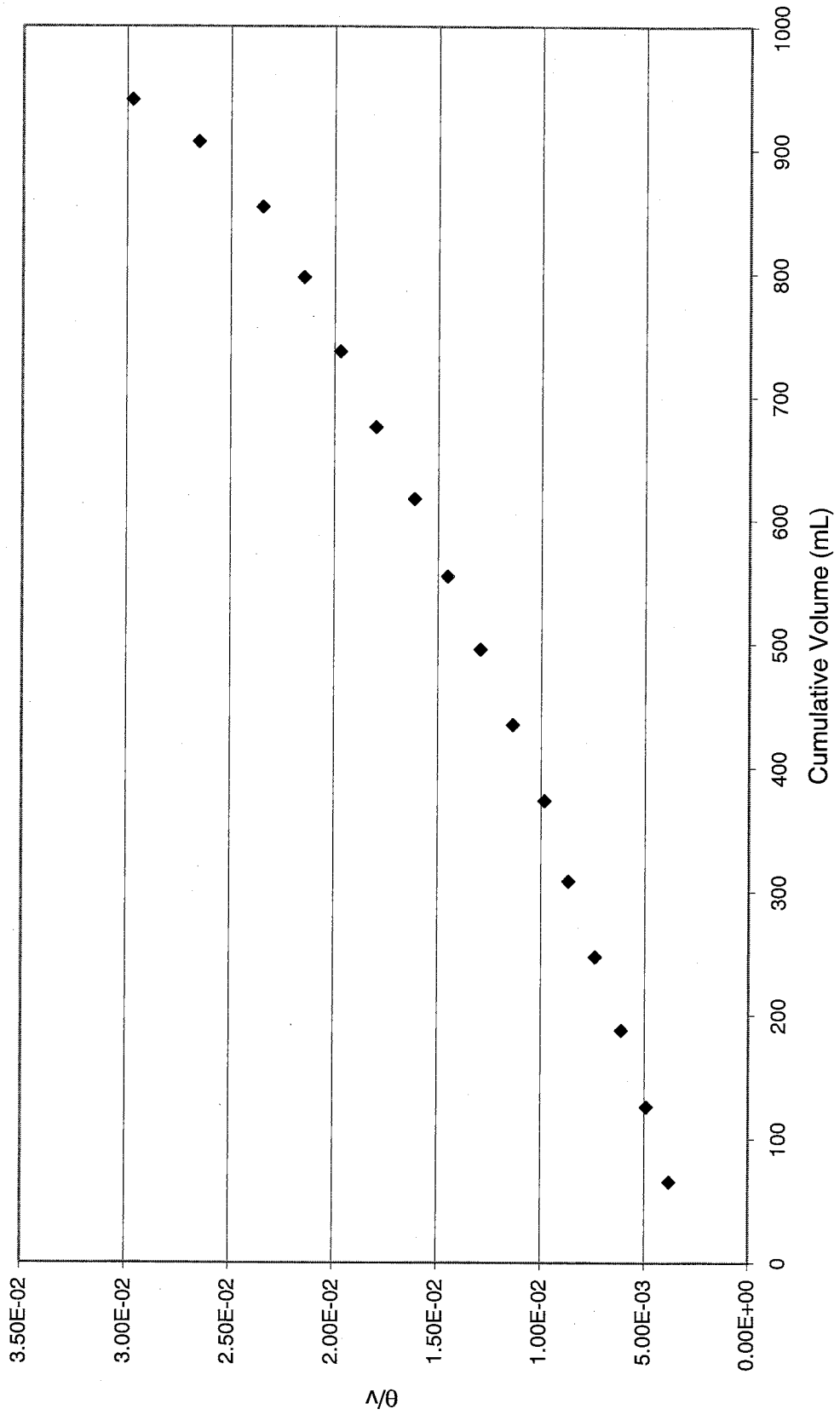
Rio Puerco Sample  
TSS = 32,100 mg/L



102.45 mg/L Clay Solution									
Sample No.	Mass Bottle (g)	Mass Sample + Btl (g)	Mass Sample (g)	Time Required (min)	Flow Rate (mL/min)	Pressure (psi)	Cumulative Time (min)	Cumulative Volume (mL)	$\theta/v$
95-210-1	9.89	75.39	65.50	0.25	262.00	85	0.25	65.50	3.817E-03
95-210-2	9.71	70.23	60.52	0.37	163.57	85	0.62	126.02	4.920E-03
95-210-3	9.79	71.61	61.82	0.53	116.64	85	1.15	187.84	6.122E-03
95-210-4	9.80	69.25	59.45	0.68	87.43	85	1.83	247.29	7.400E-03
95-210-5	9.68	70.92	61.24	0.85	72.05	85	2.68	308.53	8.686E-03
95-210-6	9.68	74.61	64.93	1.00	64.93	85	3.68	373.46	9.854E-03
95-210-7	9.95	71.28	61.33	1.27	48.29	85	4.95	434.79	1.138E-02
95-210-8	9.75	70.52	60.77	1.47	41.34	85	6.42	495.56	1.296E-02
95-210-9	9.80	68.91	59.11	1.65	35.82	85	8.07	554.67	1.455E-02
95-210-10	9.76	72.37	62.61	1.90	32.95	85	9.97	617.28	1.615E-02
95-210-11	9.69	68.15	58.46	2.20	26.57	85	12.17	675.74	1.801E-02
95-210-12	9.75	71.23	61.48	2.37	25.94	85	14.54	737.22	1.972E-02
95-210-13	9.73	69.81	60.08	2.58	23.29	85	17.12	797.30	2.147E-02
95-210-14	9.69	66.75	57.06	2.92	19.54	85	20.04	854.36	2.346E-02
95-210-15	9.72	62.17	52.45	4.03	13.01	85	24.07	906.81	2.654E-02
95-210-16	9.71	43.57	33.86	3.91	8.65	85	27.98	940.67	2.975E-02

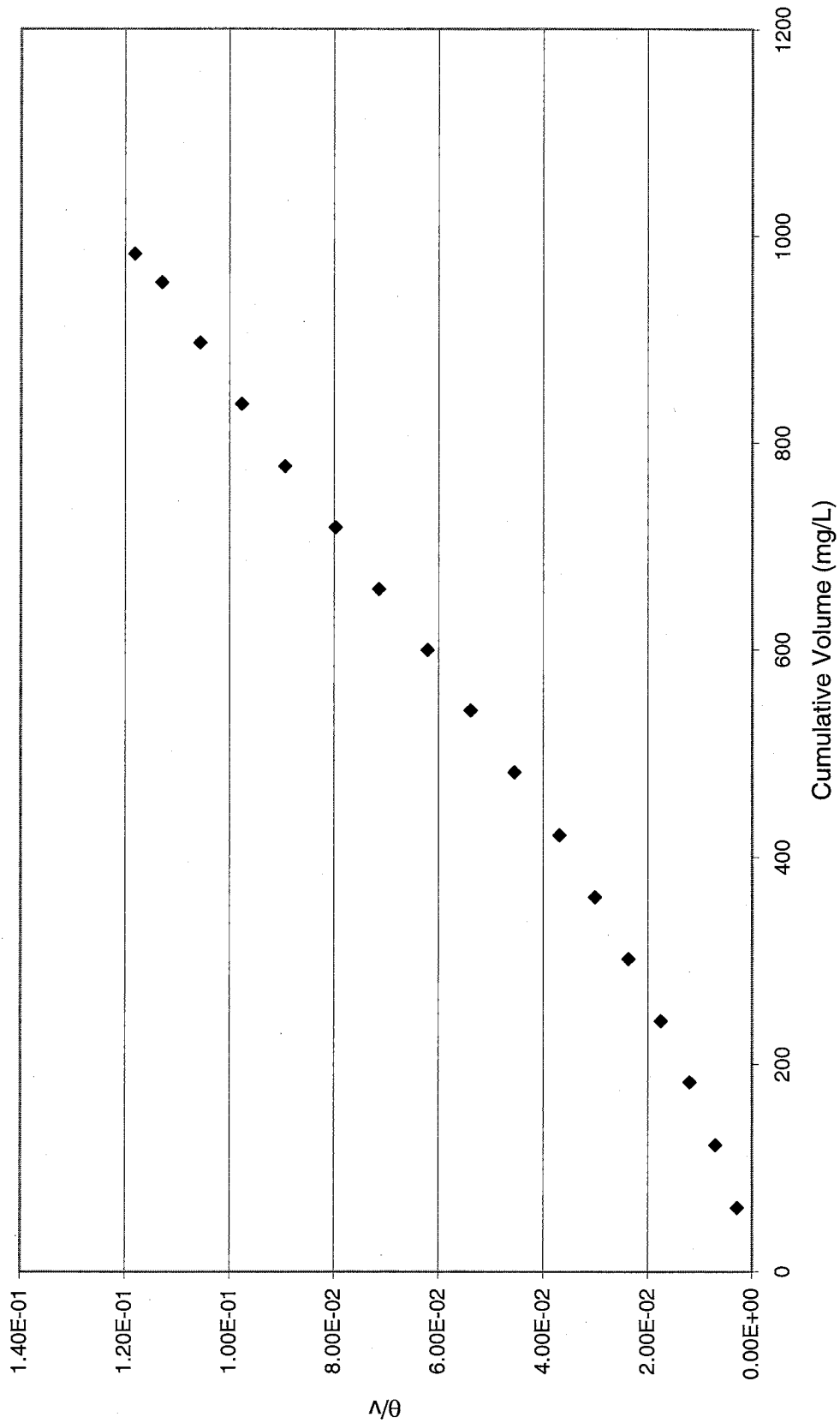


# 102.45 mg/L Multicomponent Clay Solution



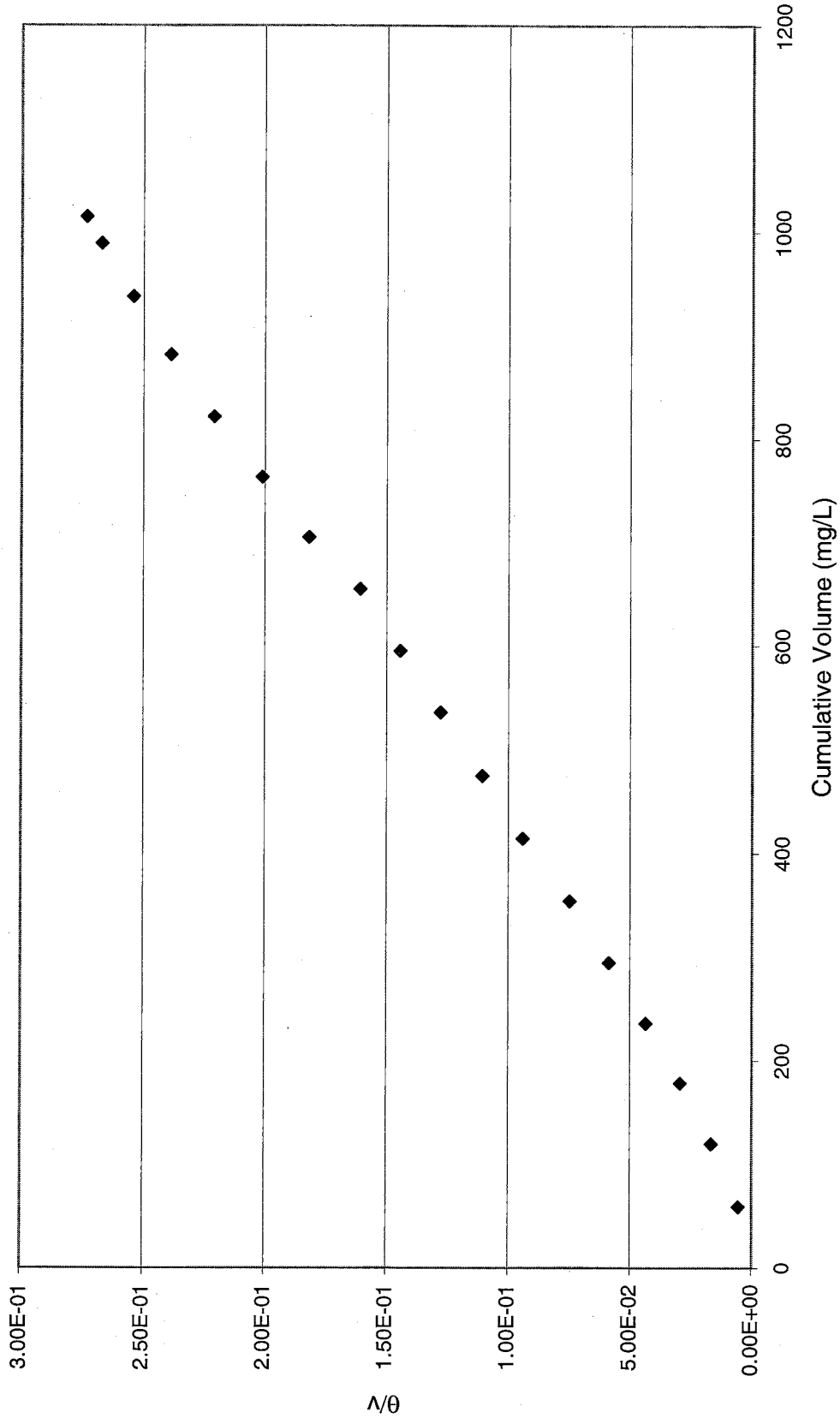
281.5 mg/L Clay Solution									
Sample No.	Mass Bottle (g)	Mass Sample + Btl (g)	Mass Sample (g)	Time Required (min)	Flow Rate (mL/min)	Pressure (psi)	Cumulative Time (min)	Cumulative Volume (mL)	$\theta/v$
95-214-2	10.34	71.82	61.48	0.17	361.65	80	0.17	61.48	2.765E-03
95-214-3	10.42	70.77	60.35	0.68	88.75	80	0.85	121.83	6.977E-03
95-214-4	9.74	70.4	60.66	1.33	45.61	80	2.18	182.49	1.195E-02
95-214-5	10.41	69.65	59.24	2.05	28.90	80	4.23	241.73	1.750E-02
95-214-6	10.39	70.56	60.17	2.93	20.54	80	7.16	301.90	2.372E-02
95-214-7	10.33	69.84	59.51	3.72	16.00	80	10.88	361.41	3.010E-02
95-214-8	10.43	70.31	59.88	4.67	12.82	80	15.55	421.29	3.691E-02
95-214-9	10.38	70.81	60.43	6.42	9.41	80	21.97	481.72	4.561E-02
95-214-10	10.48	70.09	59.61	7.25	8.22	80	29.22	541.33	5.398E-02
95-214-11	10.47	68.88	58.41	8.07	7.24	80	37.29	599.74	6.218E-02
95-214-12	10.47	69.18	58.71	9.75	6.02	80	47.04	658.45	7.144E-02
95-214-13	10.36	70.09	59.73	10.23	5.84	80	57.27	718.18	7.974E-02
95-214-14	10.46	69.94	59.48	12.22	4.87	80	69.49	777.66	8.936E-02
95-214-15	10.41	70.63	60.22	12.35	4.88	80	81.84	837.88	9.768E-02
95-214-16	10.48	69.89	59.41	12.93	4.59	80	94.77	897.29	1.056E-01
95-214-17	10.26	68.53	58.27	13.17	4.42	80	107.94	955.56	1.130E-01
95-214-18	10.4	38.09	27.69	8.28	3.34	80	116.22	983.25	1.182E-01

# 281.50 mg/L Multicomponent Clay Solution



421 mg/L Clay Solution									
Sample No.	Mass Bottle (g)	Mass Sample + Btl (g)	Mass Sample (g)	Time Required (min)	Flow Rate (mL/min)	Pressure (psi)	Cumulative Time (min)	Cumulative Volume (mL)	q/v
95-212-2	9.78	68.74	58.96	0.32	184.25	85	0.32	58.96	5.427E-03
95-212-3	9.80	70.32	60.52	1.67	36.24	85	1.99	119.48	1.666E-02
95-212-4	9.73	68.32	58.59	3.25	18.03	85	5.24	178.07	2.943E-02
95-212-5	9.99	67.83	57.84	5.05	11.45	85	10.29	235.91	4.362E-02
95-212-6	9.70	68.31	58.61	7.00	8.37	85	17.29	294.52	5.871E-02
95-212-7	9.72	69.33	59.61	9.22	6.47	85	26.51	354.13	7.486E-02
95-212-8	9.80	70.13	60.33	12.53	4.81	85	39.04	414.46	9.419E-02
95-212-9	9.73	70.11	60.38	13.52	4.47	85	52.56	474.84	1.107E-01
95-212-10	9.77	70.78	61.01	15.95	3.83	85	68.51	535.85	1.279E-01
95-212-11	9.74	69.20	59.46	17.40	3.42	85	85.91	595.31	1.443E-01
95-212-12	9.76	69.68	59.92	19.48	3.08	85	105.39	655.23	1.608E-01
95-212-13	9.80	59.62	49.82	22.87	2.18	85	128.26	705.05	1.819E-01
95-212-14	9.97	68.28	58.31	25.20	2.31	85	153.46	763.36	2.010E-01
95-212-15	9.77	68.48	58.71	28.13	2.09	85	181.59	822.07	2.209E-01
95-212-16	9.73	69.72	59.99	28.97	2.07	85	210.56	882.06	2.387E-01
95-212-17	9.91	66.10	56.19	28.02	2.01	85	238.58	938.25	2.543E-01
95-212-18	9.75	61.13	51.38	25.91	1.98	85	264.49	989.63	2.673E-01
95-212-19	9.74	35.76	26.02	13.22	1.97	85	277.71	1015.65	2.734E-01

# 425 mg/L Multicomponent Clay Solution



**APPENDIX B**

**Chemical Analyses**

5 mg/L Clay Solution												
Sample Number	Cumulative Volume Filtered (mL)	Na (mg/L)					Cl (mg/L)					
		1	2	3	Avg	Two Std Deviation	1	2	3	Avg	Two Std Deviation	
95-196-1	0.00	5.88	5.76	5.90	5.85	0.15	9.08	9.05	9.12	9.08	0.07	
95-196-2	63.61	5.90	5.88	5.94	5.91	0.06	9.10	9.11	9.10	9.10	0.01	
95-196-3	125.74	5.92	5.90	5.94	5.92	0.04	9.11	9.14	9.11	9.12	0.03	
95-196-4	185.33	5.78	5.81	5.78	5.79	0.03	9.08	9.06	9.08	9.07	0.02	
95-196-5	246.00	5.87	5.88	5.87	5.87	0.01	9.07	9.09	9.08	9.08	0.02	
95-196-6	306.33	5.73	5.73	5.75	5.74	0.02	9.07	9.05	9.07	9.06	0.02	
95-196-7	362.56	5.77	5.80	5.80	5.79	0.03	9.07	9.08	9.08	9.08	0.01	
95-196-8	421.00	5.84	5.85	5.84	5.84	0.01	9.09	9.10	9.07	9.09	0.03	
95-196-9	480.56	5.85	5.86	5.83	5.85	0.03	9.08	9.07	9.08	9.08	0.01	
95-196-10	531.63	5.82	5.81	5.80	5.81	0.02	9.07	9.10	9.03	9.07	0.07	
95-196-11	585.42	5.87	5.88	5.87	5.87	0.01	9.06	9.02	9.10	9.06	0.08	
95-196-12	637.41	5.85	5.85	5.84	5.85	0.01	9.06	9.02	9.09	9.06	0.07	
95-196-13	688.92	5.81	5.79	5.82	5.81	0.03	9.05	9.00	9.07	9.04	0.07	
95-196-14	741.44	5.87	5.89	5.88	5.88	0.02	9.07	9.07	9.08	9.07	0.01	
95-196-15	792.64	5.74	5.70	5.76	5.73	0.06	9.06	9.04	9.05	9.05	0.02	
95-196-16	844.33	5.76	5.70	5.80	5.75	0.10	9.07	9.10	9.09	9.09	0.03	
95-196-17	899.33	5.87	5.82	5.88	5.86	0.06	9.07	9.10	9.07	9.08	0.03	
95-196-18	954.44	5.86	5.84	5.83	5.84	0.03	9.08	9.09	9.06	9.08	0.03	
95-196-19	1001.78	5.80	5.80	5.78	5.79	0.02	9.06	9.04	9.06	9.05	0.02	
95-196-20	1022.02	5.89	5.90	5.90	5.90	0.01	9.08	9.10	9.09	9.09	0.02	
STOP												

Sample Number	Cumulative Volume Filtered (mL)	10 mg/L Clay Solution									
		Na (mg/L)					Cl (mg/L)				
		1	2	3	Avg	Two Std Deviation	1	2	3	Avg	Two Std Deviation
95-192-1	0.00	6.77	6.76	6.77	6.77	0.01	10.61	10.65	10.62	10.63	0.04
95-192-2	55.57	6.76	6.78	6.75	6.76	0.03	10.63	10.59	10.67	10.63	0.08
95-192-3	116.24	6.75	6.75	6.74	6.75	0.01	10.64	10.65	10.60	10.63	0.05
95-192-4	170.82	6.79	6.78	6.78	6.78	0.01	10.58	10.60	10.58	10.59	0.02
95-192-5	226.38	6.82	6.80	6.83	6.82	0.03	10.58	10.58	10.59	10.58	0.01
95-192-6	276.65	6.84	6.86	6.85	6.85	0.02	10.57	10.55	10.57	10.56	0.02
95-192-7	330.84	6.79	6.80	6.80	6.80	0.01	10.56	10.57	10.56	10.56	0.01
95-192-8	385.35	6.79	6.79	6.77	6.78	0.02	10.58	10.64	10.58	10.60	0.07
95-192-9	431.96	6.82	6.80	6.83	6.82	0.03	10.58	10.58	10.70	10.62	0.14
95-192-10	484.49	6.83	6.83	6.80	6.82	0.03	10.57	10.60	10.58	10.58	0.03
95-192-11	531.69	6.73	6.73	6.75	6.74	0.02	10.56	10.57	10.59	10.57	0.03
95-192-12	579.78	6.78	6.80	6.76	6.78	0.04	10.57	10.59	10.58	10.58	0.02
95-192-13	626.85	6.82	6.82	6.84	6.83	0.02	10.59	10.60	10.59	10.59	0.01
95-192-14	673.28	6.79	6.79	6.77	6.78	0.02	10.55	10.58	10.55	10.56	0.03
95-192-15	724.04	6.78	6.70	6.86	6.78	0.16	10.55	10.54	10.54	10.54	0.01
95-192-16	772.00	6.84	6.81	6.88	6.84	0.07	10.60	10.60	10.62	10.61	0.02
95-192-17	821.65	6.74	6.75	6.73	6.74	0.02	10.58	10.57	10.56	10.57	0.02
95-192-18	874.74	6.79	6.82	6.76	6.79	0.06	10.58	10.58	10.60	10.59	0.02
95-192-19	924.52	6.82	6.84	6.86	6.84	0.04	10.56	10.55	10.56	10.56	0.01
95-192-20	974.92	6.76	6.76	6.78	6.77	0.02	10.55	10.54	10.54	10.54	0.01
95-192-21	1015.86	6.84	6.85	6.86	6.85	0.02	10.59	10.60	10.59	10.59	0.01
STOP											



15 mg/L Clay Solution												
Sample Number	Cumulative Volume Filtered (mL)	Na (mg/L)					Cl (mg/L)					
		1	2	3	Avg	Two Std Deviation	1	2	3	Avg	Two Std Deviation	
95-188-1	0	6.06	6.06	6.10	6.07	0.05	9.34	9.40	9.30	9.35	0.10	
95-188-2	53.34	6.07	6.09	6.09	6.08	0.02	9.35	9.37	9.35	9.36	0.02	
95-188-3	112.59	6.08	6.10	6.10	6.09	0.02	9.35	9.37	9.37	9.36	0.02	
95-188-4	167.38	6.06	6.04	6.05	6.05	0.02	9.31	9.30	9.32	9.31	0.02	
95-188-5	220.21	6.05	6.05	6.06	6.05	0.01	9.34	9.33	9.34	9.34	0.01	
95-188-6	269.93	6.06	6.04	6.06	6.05	0.02	9.35	9.35	9.38	9.36	0.03	
95-188-7	318.2	6.05	6.06	6.03	6.05	0.03	9.33	9.32	9.33	9.33	0.01	
95-188-8	367.68	6.07	6.08	6.07	6.07	0.01	9.34	9.34	9.35	9.34	0.01	
95-188-9	419.93	6.06	6.10	6.04	6.07	0.06	9.36	9.35	9.36	9.36	0.01	
95-188-10	468.1	6.05	6.05	6.07	6.06	0.02	9.34	9.35	9.34	9.34	0.01	
95-188-11	516.5	6.05	6.03	6.04	6.04	0.02	9.33	9.33	9.34	9.33	0.01	
95-188-12	563.49	6.07	6.07	6.06	6.07	0.01	9.36	9.35	9.36	9.36	0.01	
95-188-13	613.15	6.06	6.10	6.05	6.07	0.05	9.33	9.37	9.33	9.34	0.05	
95-188-14	663.23	6.05	6.03	6.02	6.03	0.03	9.34	9.35	9.35	9.35	0.01	
95-188-15	712.64	6.03	6.02	6.03	6.03	0.01	9.34	9.34	9.30	9.33	0.05	
95-188-16	761.39	6.05	6.06	6.04	6.05	0.02	9.34	9.35	9.35	9.35	0.01	
95-188-17	810.99	6.04	6.03	6.04	6.04	0.01	9.34	9.32	9.34	9.33	0.02	
95-188-18	859.12	6.06	6.08	6.08	6.07	0.02	9.33	9.32	9.32	9.32	0.01	
95-188-19	906.56	6.09	6.08	6.10	6.09	0.02	9.36	9.35	9.36	9.36	0.01	
95-188-20	952.21	6.07	6.06	6.08	6.07	0.02	9.34	9.37	9.33	9.35	0.04	
95-188-21	992.98	6.06	6.09	6.06	6.07	0.03	9.34	9.33	9.33	9.33	0.01	
95-188-22	1024.19	6.06	6.04	6.10	6.07	0.06	9.35	9.33	9.35	9.34	0.02	
STOP												

25 mg/L Clay Solution												
Sample Number	Cumulative Volume Filtered (mL)	Na (mg/L)					Cl (mg/L)					
		1	2	3	Avg	Two Std Deviation	1	2	3	Avg	Two Std Deviation	
95-180-1	0.00	6.09	6.12	6.15	6.12	0.06	9.39	9.45	9.46	9.43	0.08	
95-180-2	51.02	5.99	6.00	6.02	6.00	0.03	9.24	9.30	9.20	9.25	0.10	
95-180-3	105.37	6.02	6.04	6.05	6.04	0.03	9.25	9.25	9.35	9.28	0.12	
95-180-4	157.01	5.75	5.80	5.82	5.79	0.07	8.85	8.90	8.85	8.87	0.06	
95-180-5	208.82	5.55	5.54	5.57	5.55	0.03	8.57	8.63	8.60	8.60	0.06	
95-180-6	266.01	5.57	5.58	5.60	5.58	0.03	8.56	8.61	8.42	8.53	0.20	
95-180-7	313.88	5.54	5.56	5.58	5.56	0.04	8.53	8.50	8.50	8.51	0.03	
95-180-8	369.31	5.56	5.60	5.58	5.58	0.04	8.59	8.60	8.61	8.60	0.02	
95-180-9	416.34	5.55	5.57	5.60	5.57	0.05	8.56	8.59	8.54	8.56	0.05	
95-180-10	461.76	5.56	5.60	5.59	5.58	0.04	8.54	8.54	8.57	8.55	0.03	
95-180-11	508.92	5.56	5.58	5.60	5.58	0.04	8.54	8.53	8.47	8.51	0.08	
95-180-12	552.86	5.55	5.54	5.53	5.54	0.02	8.53	8.52	8.64	8.56	0.13	
95-180-13	598.14	5.54	5.50	5.54	5.53	0.05	8.53	8.57	8.53	8.54	0.05	
95-180-14	644.79	5.56	5.58	5.50	5.55	0.08	8.55	8.57	8.57	8.56	0.02	
95-180-15	683.02	5.55	5.59	5.50	5.55	0.09	8.56	8.60	8.58	8.58	0.04	
95-180-16	727.25	5.56	5.54	5.59	5.56	0.05	8.54	8.57	8.54	8.55	0.03	
95-180-17	771.04	5.54	5.56	5.50	5.53	0.06	8.60	8.35	8.67	8.54	0.34	
95-180-18	816.63	5.55	5.50	5.57	5.54	0.07	8.56	8.69	8.50	8.58	0.19	
95-180-19	861.53	5.56	5.58	5.54	5.56	0.04	8.54	8.54	8.57	8.55	0.03	
95-180-20	910.13	5.55	5.50	5.59	5.55	0.09	8.55	8.56	8.57	8.56	0.02	
95-180-21	953.98	5.56	5.60	5.57	5.58	0.04	8.56	8.57	8.48	8.54	0.10	
95-180-22	1015.72	5.56	5.56	5.52	5.55	0.05	8.55	8.59	8.67	8.60	0.12	
95-180-23	1041.99	5.55	5.50	5.58	5.54	0.08	8.55	8.59	8.50	8.55	0.09	
STOP												

50 mg/L Clay Solution												
Sample Number	Cumulative Volume Filtered (mL)	Na (mg/L)					Cl (mg/L)					
		1	2	3	Avg	Two Std Deviation	1	2	3	Avg	Two Std Deviation	
95-174-1	0	6.18	6.20	6.21	6.20	0.03	9.54	9.58	9.60	9.57	0.06	
95-174-2	62.43	6.11	6.17	6.10	6.13	0.08	9.57	9.61	9.57	9.58	0.05	
95-174-3	108.27	6.19	6.24	6.19	6.21	0.06	9.55	9.49	9.50	9.51	0.06	
95-174-4	158.97	5.76	5.80	5.79	5.78	0.04	8.87	8.90	9.08	8.95	0.23	
95-174-5	203.17	5.37	5.41	5.40	5.39	0.04	8.28	8.30	8.42	8.33	0.15	
95-174-6	247.38	5.36	5.37	5.38	5.37	0.02	8.27	8.31	8.28	8.29	0.04	
95-174-7	291.55	5.37	5.37	5.31	5.35	0.07	8.28	8.34	8.27	8.30	0.08	
95-174-8	339.33	5.36	5.40	5.41	5.39	0.05	8.27	8.39	8.27	8.31	0.14	
95-174-9	392.35	5.35	5.36	5.37	5.36	0.02	8.26	8.29	8.23	8.26	0.06	
95-174-10	441.07	5.37	5.43	5.38	5.39	0.06	8.28	8.32	8.30	8.30	0.04	
95-174-11	488.5	5.36	5.46	5.39	5.40	0.10	8.27	8.24	8.29	8.27	0.05	
95-174-12	534.34	5.37	5.40	5.38	5.38	0.03	8.27	8.34	8.24	8.28	0.10	
95-174-13	581.68	5.36	5.43	5.31	5.37	0.12	8.25	8.31	8.27	8.28	0.06	
95-174-14	635.66	5.35	5.32	5.39	5.35	0.07	8.24	8.27	8.30	8.27	0.06	
95-174-15	682.77	5.35	5.34	5.37	5.35	0.03	8.24	8.23	8.27	8.25	0.04	
95-174-16	727.77	5.39	5.42	5.40	5.40	0.03	8.26	8.24	8.31	8.27	0.07	
95-174-17	780.04	5.36	5.47	5.32	5.38	0.16	8.23	8.34	8.21	8.26	0.14	
95-174-18	818.74	5.36	5.33	5.41	5.37	0.08	8.25	8.27	8.26	8.26	0.02	
95-174-19	863.83	5.35	5.38	5.39	5.37	0.04	8.24	8.27	8.34	8.28	0.10	
95-174-20	904.81	5.37	5.56	5.30	5.41	0.27	8.26	8.34	8.20	8.27	0.14	
95-174-21	940.77	5.36	5.38	5.32	5.35	0.06	8.26	8.29	8.31	8.29	0.05	
95-174-22	985.83	5.35	5.49	5.30	5.38	0.20	8.24	8.21	8.31	8.25	0.10	
95-174-23	1033.35	5.37	5.40	5.42	5.40	0.05	8.24	8.35	8.27	8.29	0.11	
STOP												
Weighted Filtr. Conc. (mg/L)					5.46	0.07				8.42	0.09	
95-174-D Dialysis Conc. (mg/L)					6.25	0.17				9.52	0.23	
95-174-C Centr. Conc. (mg/L)					6.15	0.15				9.36	0.17	

Sample Number	Cumulative Volume Filtered (mL)	75 mg/L Clay Solution									
		Na (mg/L)					Cl (mg/L)				
		1	2	3	Avg	Two Std Deviation	1	2	3	Avg	Two Std Deviation
95-166-1	0.00	6.47	6.54	6.49	6.50	0.07	10.02	9.97	9.85	9.95	0.17
95-166-2	37.03	6.53	6.48	6.59	6.53	0.11	10.10	10.00	10.03	10.04	0.10
95-166-3	68.91	6.43	6.51	6.43	6.46	0.09	10.10	9.99	9.95	10.01	0.16
95-166-4	109.07	6.25	6.27	6.30	6.27	0.05	9.80	9.76	9.82	9.79	0.06
95-166-5	145.40	5.39	5.37	5.42	5.39	0.05	8.30	8.21	8.20	8.24	0.11
95-166-6	189.86	4.98	4.70	5.01	4.90	0.34	7.55	7.58	7.60	7.58	0.05
95-166-7	229.35	4.99	5.12	4.78	4.96	0.34	7.61	7.57	7.61	7.60	0.05
95-166-8	269.00	5.00	4.95	5.10	5.02	0.15	7.58	7.60	7.60	7.59	0.02
95-166-9	311.68	4.91	4.92	4.91	4.91	0.01	7.48	7.47	7.51	7.49	0.04
95-166-10	354.48	4.97	5.08	4.96	5.00	0.13	7.61	7.56	7.61	7.59	0.06
95-166-11	406.81	5.01	5.10	4.96	5.02	0.14	7.58	7.60	7.59	7.59	0.02
95-166-12	447.99	4.99	4.94	5.10	5.01	0.16	7.54	7.59	7.62	7.58	0.08
95-166-13	489.51	4.95	4.98	4.98	4.97	0.03	7.52	7.54	7.50	7.52	0.04
95-166-14	531.09	4.98	4.99	5.00	4.99	0.02	7.59	7.57	7.54	7.57	0.05
95-166-15	564.00	4.97	4.97	4.96	4.97	0.01	7.60	7.57	7.61	7.59	0.04
95-166-16	603.44	4.99	5.02	4.97	4.99	0.05	7.60	7.56	7.51	7.56	0.09
95-166-17	659.28	5.00	4.99	4.96	4.98	0.04	7.48	7.61	7.61	7.57	0.15
95-166-18	701.01	5.00	5.01	5.10	5.04	0.11	7.54	7.59	7.61	7.58	0.07
95-166-19	741.39	5.01	5.00	5.00	5.00	0.01	7.62	7.60	7.60	7.61	0.02
95-166-20	794.53	5.02	5.04	4.98	5.01	0.06	7.59	7.62	7.61	7.61	0.03
95-166-21	837.22	5.00	5.02	5.01	5.01	0.02	7.58	7.60	7.62	7.60	0.04
95-166-22	877.55	4.98	4.98	5.00	4.99	0.02	7.60	7.57	7.54	7.57	0.06
95-166-23	920.30	4.99	4.98	5.10	5.02	0.13	7.57	7.58	7.61	7.59	0.04
95-166-24	974.41	4.99	4.97	5.03	5.00	0.06	7.58	7.60	7.60	7.59	0.02
95-166-25	1011.81	5.00	5.10	4.98	5.03	0.13	7.61	7.59	7.62	7.61	0.03
95-166-26	1036.11	5.01	4.95	5.10	5.02	0.15	7.70	7.60	7.61	7.64	0.11
STOP											

Sample Number	Cumulative Volume Filtered (mL)	100 mg/L Clay Solution									
		Na (mg/L)					Cl (mg/L)				
		1	2	3	Avg	Two Std Deviation	1	2	3	Avg	Two Std Deviation
95-162-1	0.00	6.06	6.12	6.08	6.09	0.06	9.33	9.47	9.40	9.40	0.14
95-162-2	60.15	6.01	6.00	6.05	6.02	0.05	9.27	9.32	9.27	9.29	0.06
95-162-3	101.22	4.90	5.00	5.02	4.97	0.13	7.57	7.49	7.64	7.57	0.15
95-162-4	152.88	4.07	4.09	4.08	4.08	0.02	6.28	6.30	6.27	6.28	0.03
95-162-5	189.62	4.06	4.10	4.12	4.09	0.06	6.27	6.27	6.31	6.28	0.05
95-162-6	226.63	4.06	4.09	4.05	4.07	0.04	6.28	6.33	6.27	6.29	0.06
95-162-7	262.22	4.08	4.09	4.10	4.09	0.02	6.29	6.24	6.37	6.30	0.13
95-162-8	296.90	4.10	4.13	4.09	4.11	0.04	6.34	6.35	6.41	6.37	0.08
95-162-9	336.90	4.11	4.05	4.12	4.09	0.08	6.33	6.37	6.40	6.37	0.07
95-162-10	371.67	4.11	4.09	4.13	4.11	0.04	6.32	6.30	6.41	6.34	0.12
95-162-11	411.68	4.09	4.13	4.10	4.11	0.04	6.31	6.19	6.30	6.27	0.13
95-162-12	451.23	4.10	4.09	4.09	4.09	0.01	6.33	6.37	6.30	6.33	0.07
95-162-13	493.72	4.12	4.10	4.30	4.17	0.22	6.34	6.37	6.34	6.35	0.03
95-162-14	537.16	4.12	4.10	4.23	4.15	0.14	6.35	6.40	6.37	6.37	0.05
95-162-15	578.91	4.27	4.35	4.28	4.30	0.09	6.42	6.50	6.38	6.43	0.12
95-162-16	624.98	4.25	4.26	4.32	4.28	0.08	6.40	6.40	6.49	6.43	0.10
95-162-17	666.57	4.24	4.25	4.30	4.26	0.06	6.41	6.49	6.40	6.43	0.10
95-162-18	713.19	4.27	4.25	4.26	4.26	0.02	6.40	6.43	6.41	6.41	0.03
95-162-19	762.04	4.23	4.20	4.28	4.24	0.08	6.39	6.40	6.43	6.41	0.04
95-162-20	806.88	4.22	4.23	4.20	4.22	0.03	6.38	6.49	6.42	6.43	0.11
95-162-21	850.81	4.26	4.35	4.29	4.30	0.09	6.39	6.40	6.43	6.41	0.04
95-162-22	898.67	4.23	4.20	4.25	4.23	0.05	6.37	6.37	6.31	6.35	0.07
95-162-23	944.99	4.23	4.32	4.30	4.28	0.09	6.30	6.31	6.35	6.32	0.05
95-162-24	993.29	4.22	4.23	4.37	4.27	0.17	6.32	6.37	6.30	6.33	0.07
95-162-25	1042.14	4.23	4.30	4.35	4.29	0.12	6.34	6.43	6.37	6.38	0.09
95-162-26	1068.37	4.31	4.35	4.50	4.39	0.20	6.42	6.50	6.45	6.46	0.08
STOP											

Sample No.	Cumulative Volume Filtered (mL)	102.45 mg/L Clay Solution					Two Std Deviation
		Al (µg/L)					
		1	2	3	Average		
95-210-1A	0.00	0.39	0.46	0.36	0.40	0.10	
95-210-1	65.50	1.10	1.24	1.00	1.11	0.24	
95-210-2	126.02	1.01	1.09	0.90	1.00	0.19	
95-210-3	187.84	1.17	1.04	1.19	1.13	0.16	
95-210-4	247.29	0.65	0.69	0.60	0.65	0.09	
95-210-5	308.53	1.04	1.03	1.03	1.03	0.01	
95-210-6	373.46	0.58	0.64	0.56	0.59	0.08	
95-210-7	434.79	0.90	1.02	0.80	0.91	0.22	
95-210-8	495.56	0.51	0.68	0.42	0.54	0.26	
95-210-9	554.67	0.57	0.59	0.58	0.58	0.02	
95-210-10	617.28	0.48	0.48	0.43	0.46	0.06	
95-210-11	675.74	1.14	1.06	1.20	1.13	0.14	
95-210-12	737.22	0.46	0.49	0.52	0.49	0.06	
95-210-13	797.30	0.51	0.57	0.49	0.52	0.08	
95-210-14	854.36	0.45	0.41	0.43	0.43	0.04	
95-210-15	906.81	0.40	0.43	0.47	0.43	0.07	
95-210-16	940.67	0.34	0.28	0.46	0.36	0.18	

Sample No.	Cumulative Volume Filtered (mL)	281.45 mg/L Clay Solution											
		Al (µg/L)						Na (mg/L)					
		1	2	3	Average	Two Std Deviation	1	2	3	Average	Two Std Deviation		
95-214-1	0.00	5.12	5.23	5.01	5.12	0.22	29.23	29.26	29.26	29.25	0.03		
95-214-2	61.48	1.52	1.48	1.53	1.51	0.05	29.33	29.34	29.32	29.33	0.02		
95-214-3	121.83	1.10	1.1	1.50	1.23	0.46	29.33	29.34	29.32	29.33	0.02		
95-214-4	182.49	0.96	0.92	0.91	0.93	0.05	29.27	29.30	29.28	29.28	0.03		
95-214-5	241.73	1.10	1.07	1.19	1.12	0.12	29.45	29.50	29.42	29.46	0.08		
95-214-6	301.90	0.88	0.95	0.80	0.88	0.15	29.58	29.60	29.56	29.58	0.04		
95-214-7	361.41	0.72	0.8	0.61	0.71	0.19	29.58	29.60	29.60	29.59	0.02		
95-214-8	421.19	0.67	0.61	0.73	0.67	0.12	29.58	29.59	29.58	29.58	0.01		
95-214-9	481.72	0.63	0.73	0.59	0.65	0.14	29.56	29.60	29.58	29.58	0.04		
95-214-10	541.33	0.62	0.64	0.62	0.63	0.02	29.55	29.58	29.60	29.58	0.05		
95-214-11	599.74	0.54	0.57	0.52	0.54	0.05	29.57	29.58	29.62	29.59	0.05		
95-214-12	658.45	0.67	0.75	0.61	0.68	0.14	29.53	29.55	29.56	29.55	0.03		
95-214-13	718.18	0.62	0.51	0.79	0.64	0.28	29.61	29.60	29.60	29.60	0.01		
95-214-14	777.66	0.64	0.69	0.64	0.66	0.06	29.58	29.60	29.56	29.58	0.04		
95-214-15	837.88	0.47	0.49	0.52	0.49	0.05	29.55	29.56	29.58	29.56	0.03		
95-214-16	897.29	0.51	0.48	0.56	0.52	0.08	29.52	29.50	29.52	29.51	0.02		
95-214-17	955.56	0.49	0.52	0.40	0.47	0.12	29.54	29.56	29.56	29.55	0.02		
95-214-18	1003.57	0.52	0.67	0.76	0.65	0.24	29.51	29.52	29.50	29.51	0.02		

Sample No.	Cumulative Volume Filtered (mL)	281.45 mg/L Clay Solution									
		K (mg/L)			Mg (mg/L)						
		1	2	3	Average	Two Std Deviation	1	2	3	Average	Two Std Deviation
95-214-1	0.00	4.42	4.44	4.48	4.45	0.06	8.70	8.72	8.68	8.70	0.04
95-214-2	61.48	4.38	4.38	4.40	4.39	0.02	8.68	8.70	8.68	8.69	0.02
95-214-3	121.83	4.38	4.38	4.40	4.39	0.02	8.70	8.70	8.76	8.72	0.07
95-214-4	182.49	4.40	4.38	4.40	4.39	0.02	8.73	8.74	8.78	8.75	0.05
95-214-5	241.73	4.41	4.40	4.44	4.42	0.04	8.72	8.74	8.76	8.74	0.04
95-214-6	301.90	4.43	4.44	4.46	4.44	0.03	8.70	8.70	8.74	8.71	0.05
95-214-7	361.41	4.40	4.42	4.46	4.43	0.06	8.73	8.74	8.74	8.74	0.01
95-214-8	421.19	4.43	4.42	4.46	4.44	0.04	8.70	8.70	8.72	8.71	0.02
95-214-9	481.72	4.43	4.42	4.44	4.43	0.02	8.71	8.72	8.74	8.72	0.03
95-214-10	541.33	4.39	4.40	4.44	4.41	0.05	8.74	8.78	8.74	8.75	0.05
95-214-11	599.74	4.38	4.40	4.44	4.41	0.06	8.72	8.74	8.74	8.73	0.02
95-214-12	658.45	4.44	4.44	4.46	4.45	0.02	8.71	8.72	8.72	8.72	0.01
95-214-13	718.18	4.45	4.46	4.48	4.46	0.03	8.74	8.78	8.76	8.76	0.04
95-214-14	777.66	4.47	4.48	4.50	4.48	0.03	8.73	8.76	8.74	8.74	0.03
95-214-15	837.88	4.39	4.40	4.44	4.41	0.05	8.72	8.74	8.72	8.73	0.02
95-214-16	897.29	4.38	4.40	4.42	4.40	0.04	8.70	8.76	8.76	8.74	0.07
95-214-17	955.56	4.37	4.40	4.42	4.40	0.05	8.73	8.74	8.74	8.74	0.01
95-214-18	1003.57	4.41	4.40	4.42	4.41	0.02	8.72	8.74	8.74	8.73	0.02



281.45 mg/L Clay Solution									
Sample No.	Cumulative Volume Filtered (mL)	Ca (mg/L)				Alkalinity (mg/L as CaCO3)			
		1	2	3	Average	Two Std Deviation	1	Two Std Deviation	
95-214-1	0.00	25.90	26.00	26.02	25.97	0.13	125.46	1.51	
95-214-2	61.48	25.74	25.76	25.82	25.77	0.08	124.76	1.50	
95-214-3	121.83	25.88	25.86	25.86	25.87	0.02	125.35	1.50	
95-214-4	182.49	25.88	25.92	25.90	25.90	0.04	125.37	1.50	
95-214-5	241.73	25.91	25.94	25.90	25.92	0.04	124.37	1.49	
95-214-6	301.90	25.68	25.80	25.86	25.78	0.18	123.76	1.49	
95-214-7	361.41	25.76	25.80	25.82	25.79	0.06	123.87	1.49	
95-214-8	421.19	25.79	25.80	25.82	25.80	0.03	124.57	1.49	
95-214-9	481.72	25.78	25.82	25.84	25.81	0.06	124.37	1.49	
95-214-10	541.33	25.67	25.76	25.80	25.74	0.13	125.87	1.51	
95-214-11	599.74	25.59	25.58	25.60	25.59	0.02	125.63	1.51	
95-214-12	658.45	25.68	25.70	25.72	25.70	0.04	125.67	1.51	
95-214-13	718.18	25.67	25.70	25.72	25.70	0.05	124.69	1.50	
95-214-14	777.66	25.67	25.72	25.74	25.71	0.07	125.03	1.50	
95-214-15	837.88	25.68	25.70	25.72	25.70	0.04	125.64	1.51	
95-214-16	897.29	25.68	25.70	25.72	25.70	0.04	124.47	1.49	
95-214-17	955.56	25.88	25.80	25.86	25.85	0.08	124.58	1.49	
95-214-18	1003.57	25.75	25.82	25.84	25.80	0.09	124.87	1.50	

Sample No.	Cumulative Volume Filtered (mL)	281.45 mg/L Clay Solution									
		Cl (mg/L)					F (mg/L)				
		1	2	3	Average	Two Std Deviation	1	2	3	Average	Two Std Deviation
95-214-1	0.00	22.35	22.44	22.42	22.40	0.09	5.20	5.28	5.18	5.22	0.11
95-214-2	61.48	21.58	21.82	21.68	21.69	0.24	5.23	5.30	5.20	5.24	0.10
95-214-3	121.83	22.43	22.42	22.50	22.45	0.09	5.20	5.28	5.18	5.22	0.11
95-214-4	182.49	22.44	22.46	22.50	22.47	0.06	5.21	5.28	5.18	5.22	0.10
95-214-5	241.73	22.46	22.48	22.50	22.48	0.04	5.24	5.30	5.20	5.25	0.10
95-214-6	301.90	22.44	22.46	22.52	22.47	0.08	5.22	5.28	5.18	5.23	0.10
95-214-7	361.41	22.35	22.46	22.48	22.43	0.14	5.22	5.28	5.18	5.23	0.10
95-214-8	421.19	22.42	22.40	22.50	22.44	0.11	5.19	5.25	5.16	5.20	0.09
95-214-9	481.72	22.44	22.40	22.50	22.45	0.10	5.17	5.22	5.14	5.18	0.08
95-214-10	541.33	22.33	22.40	22.48	22.40	0.15	5.17	5.22	5.14	5.18	0.08
95-214-11	599.74	22.06	22.22	22.46	22.25	0.40	5.13	5.19	5.10	5.14	0.09
95-214-12	658.45	22.35	22.44	22.38	22.39	0.09	5.14	5.20	5.12	5.15	0.08
95-214-13	718.18	22.35	22.38	22.40	22.38	0.05	5.17	5.23	5.14	5.18	0.09
95-214-14	777.66	22.37	22.40	22.38	22.38	0.03	5.17	5.23	5.14	5.18	0.09
95-214-15	837.88	22.36	22.40	22.38	22.38	0.04	5.17	5.23	5.14	5.18	0.09
95-214-16	897.29	22.27	22.34	22.36	22.32	0.09	5.20	5.27	5.16	5.21	0.11
95-214-17	955.56	22.21	22.28	22.40	22.30	0.19	5.20	5.27	5.18	5.22	0.09
95-214-18	1003.57	22.30	22.30	22.34	22.31	0.04	5.18	5.24	5.16	5.19	0.08

Sample No.	Cumulative Volume Filtered (mL)	281.45 mg/L Clay Solution									
		NO <sub>3</sub> (mg/L)			SO <sub>4</sub> (mg/L)						
		1	2	3	Average	Two Std Deviation	1	2	3	Average	Two Std Deviation
95-214-1	0.00	0.77	0.76	0.75	0.76	0.02	18.74	18.93	18.55	18.74	0.38
95-214-2	61.48	0.75	0.74	0.73	0.74	0.02	18.73	18.92	18.54	18.73	0.38
95-214-3	121.83	0.75	0.74	0.73	0.74	0.02	18.65	18.84	18.46	18.65	0.38
95-214-4	182.49	0.76	0.75	0.74	0.75	0.02	18.73	18.92	18.54	18.73	0.38
95-214-5	241.73	0.75	0.74	0.73	0.74	0.02	18.70	18.89	18.90	18.83	0.23
95-214-6	301.90	0.75	0.74	0.73	0.74	0.02	18.73	18.92	18.54	18.73	0.38
95-214-7	361.41	0.74	0.73	0.72	0.73	0.02	18.72	18.92	18.56	18.73	0.36
95-214-8	421.19	0.76	0.75	0.74	0.75	0.02	18.73	18.92	18.54	18.73	0.38
95-214-9	481.72	0.75	0.74	0.73	0.74	0.02	18.70	18.90	18.52	18.71	0.38
95-214-10	541.33	0.75	0.74	0.73	0.74	0.02	18.73	18.92	18.54	18.73	0.38
95-214-11	599.74	0.75	0.74	0.73	0.74	0.02	18.70	18.90	18.52	18.71	0.38
95-214-12	658.45	0.74	0.73	0.72	0.73	0.02	18.71	18.90	18.52	18.71	0.38
95-214-13	718.18	0.73	0.72	0.71	0.72	0.02	18.77	18.96	18.58	18.77	0.38
95-214-14	777.66	0.74	0.73	0.72	0.73	0.02	18.72	18.92	18.54	18.73	0.38
95-214-15	837.88	0.73	0.72	0.71	0.72	0.02	18.73	18.92	18.54	18.73	0.38
95-214-16	897.29	0.72	0.71	0.70	0.71	0.02	18.70	18.90	18.52	18.71	0.38
95-214-17	955.56	0.72	0.71	0.70	0.71	0.02	18.72	18.90	18.52	18.71	0.38
95-214-18	1003.57	0.74	0.73	0.72	0.73	0.02	18.72	18.90	18.52	18.71	0.38

Sample No.	Cumulative Volume Filtered (mL)	424.72 mg/L Clay Solution									
		Al ( $\mu\text{g/L}$ )					Na (mg/L)				
		1	2	3	Average	Two Std Deviation	1	2	3	Average	Two Std Deviation
95-212-1	0.00	1.03	1.10	0.89	1.01	0.21	29.85	30.12	29.87	29.95	0.15
95-212-2	58.96	3.69	3.75	3.67	3.70	0.08	28.75	28.96	28.74	28.82	0.12
95-212-3	119.48	1.93	1.80	1.98	1.90	0.19	28.64	28.64	28.67	28.65	0.02
95-212-4	178.07	1.16	1.04	1.26	1.15	0.22	28.34	28.25	28.32	28.30	0.05
95-212-5	235.91	1.03	1.06	1.07	1.05	0.04	29.25	29.23	29.37	29.28	0.08
95-212-6	294.52	0.73	0.77	0.72	0.74	0.05	29.80	29.92	29.87	29.86	0.06
95-212-7	354.13	2.14	2.24	2.06	2.15	0.18	29.79	29.67	29.79	29.75	0.07
95-212-8	414.46	0.55	0.57	0.59	0.57	0.04	29.78	29.73	29.82	29.78	0.05
95-212-9	474.84	0.51	0.53	0.48	0.51	0.05	29.68	29.67	29.67	29.67	0.01
95-212-10	535.85	1.11	1.10	1.16	1.12	0.06	29.73	29.76	29.72	29.74	0.02
95-212-11	595.31	0.94	0.92	0.94	0.93	0.02	29.83	29.68	29.84	29.78	0.09
95-212-12	655.23	0.41	0.40	0.37	0.39	0.04	29.83	29.92	29.82	29.86	0.06
95-212-13	705.05	0.90	0.97	0.85	0.91	0.12	29.85	29.87	29.87	29.86	0.01
95-212-14	763.36	0.37	0.43	0.49	0.43	0.12	29.84	29.81	29.87	29.84	0.03
95-212-15	822.07	0.47	0.47	0.59	0.51	0.14	29.84	29.86	29.81	29.84	0.03
95-212-16	882.06	0.26	0.24	0.21	0.24	0.05	29.83	29.86	29.86	29.85	0.02
95-212-17	938.25	0.47	0.40	0.49	0.45	0.09	29.81	29.80	29.74	29.78	0.04
95-212-18	989.69	0.34	0.37	0.48	0.40	0.15	29.82	29.79	29.78	29.80	0.02
95-212-19	1015.65	3.34	3.40	3.24	3.33	0.16	29.82	29.82	29.90	29.85	0.05

Sample No.	Cumulative Volume Filtered (mL)	424.72 mg/L Clay Solution											
		K (mg/L)						Mg (mg/L)					
		1	2	3	Average	Two Std Deviation	1	2	3	Average	Two Std Deviation		
95-212-1	0.00	4.37	4.41	4.42	4.40	0.05	8.62	8.75	8.57	8.65	0.19		
95-212-2	58.96	4.02	4.01	4.06	4.03	0.05	8.63	8.67	8.63	8.64	0.05		
95-212-3	119.48	4.37	4.40	4.31	4.36	0.09	8.35	8.30	8.42	8.36	0.12		
95-212-4	178.07	4.36	4.39	4.31	4.35	0.08	8.00	8.01	8.09	8.03	0.10		
95-212-5	235.91	4.35	4.35	4.37	4.36	0.02	7.78	7.79	7.67	7.75	0.13		
95-212-6	294.52	4.38	4.38	4.32	4.36	0.07	7.78	7.82	7.82	7.81	0.05		
95-212-7	354.13	4.37	4.37	4.31	4.35	0.07	7.82	7.82	7.78	7.81	0.05		
95-212-8	414.46	4.36	4.39	4.33	4.36	0.06	7.76	7.82	7.76	7.78	0.07		
95-212-9	474.84	4.37	4.37	4.32	4.35	0.06	8.00	8.09	7.97	8.02	0.12		
95-212-10	535.85	4.35	4.32	4.40	4.36	0.08	8.16	8.21	8.16	8.18	0.06		
95-212-11	595.31	4.38	4.41	4.32	4.37	0.09	8.17	8.18	8.09	8.15	0.10		
95-212-12	655.23	4.37	4.39	4.37	4.38	0.02	8.24	8.18	8.24	8.22	0.07		
95-212-13	705.05	4.39	4.43	4.31	4.38	0.12	8.32	8.32	8.35	8.33	0.03		
95-212-14	763.36	4.38	4.35	4.40	4.38	0.05	8.35	8.24	8.35	8.31	0.13		
95-212-15	822.07	4.38	4.28	4.38	4.35	0.12	8.35	8.35	8.35	8.35	0.00		
95-212-16	882.06	4.37	4.37	4.40	4.38	0.03	8.34	8.25	8.34	8.31	0.10		
95-212-17	938.25	4.35	4.43	4.35	4.38	0.09	8.47	8.37	8.34	8.39	0.14		
95-212-18	989.69	4.37	4.31	4.39	4.36	0.08	8.47	8.47	8.48	8.47	0.01		
95-212-19	1015.65	4.38	4.38	4.42	4.39	0.05	8.46	8.45	8.48	8.46	0.03		

Sample No.	Cumulative Volume Filtered (mL)	424.72 mg/L Clay Solution									
		Ca (mg/L)					Alkalinity (mg/L as CaCO <sub>3</sub> )				
		1	2	3	Average	Two Std Deviation	1	Average	Two Std Deviation		
95-212-1	0.00	25.73	25.89	25.62	25.75	0.27	125.59	125.59	1.88		
95-212-2	58.96	24.37	24.52	24.46	24.45	0.15	125.35	125.35	1.88		
95-212-3	119.48	23.86	23.57	23.79	23.74	0.30	124.92	124.92	1.87		
95-212-4	178.07	23.51	23.57	23.69	23.59	0.18	122.00	122.00	1.83		
95-212-5	235.91	25.24	25.36	25.21	25.27	0.16	121.95	121.95	1.83		
95-212-6	294.52	25.66	25.75	25.42	25.61	0.34	120.64	120.64	1.81		
95-212-7	354.13	25.70	25.73	25.70	25.71	0.03	122.63	122.63	1.84		
95-212-8	414.46	25.73	25.72	25.71	25.72	0.02	120.57	120.57	1.81		
95-212-9	474.84	25.72	25.70	25.70	25.71	0.02	120.85	120.85	1.81		
95-212-10	535.85	25.72	25.73	25.70	25.72	0.03	121.56	121.56	1.82		
95-212-11	595.31	25.72	25.70	25.71	25.71	0.02	122.05	122.05	1.83		
95-212-12	655.23	25.72	25.76	25.71	25.73	0.05	122.18	122.18	1.83		
95-212-13	705.05	25.70	25.72	25.70	25.71	0.02	122.32	122.32	1.83		
95-212-14	763.36	25.73	25.71	25.76	25.73	0.05	122.22	122.22	1.83		
95-212-15	822.07	25.74	25.75	25.77	25.75	0.03	123.05	123.05	1.85		
95-212-16	882.06	25.72	25.73	25.76	25.74	0.04	123.02	123.02	1.85		
95-212-17	938.25	25.70	25.64	25.90	25.75	0.27	123.76	123.76	1.86		
95-212-18	989.69	25.66	25.91	25.57	25.71	0.35	124.23	124.23	1.86		
95-212-19	1015.65	25.70	25.87	25.76	25.78	0.17	124.54	124.54	1.87		

Sample No.	Cumulative Volume Filtered (mL)	424.72 mg/L Clay Solution									
		Cl (mg/L)					F (mg/L)				
		1	2	3	Average	Two Std Deviation	1	2	3	Average	Two Std Deviation
95-212-1	0.00	21.23	21.40	21.26	21.30	0.18	5.19	5.22	5.22	5.21	0.03
95-212-2	58.96	21.04	21.02	21.02	21.03	0.02	5.18	5.20	5.18	5.19	0.02
95-212-3	119.48	19.34	19.34	19.30	19.33	0.05	5.17	5.18	5.20	5.18	0.03
95-212-4	178.07	19.28	19.25	19.28	19.27	0.03	5.16	5.15	5.11	5.14	0.05
95-212-5	235.91	20.54	20.59	20.50	20.54	0.09	5.15	5.15	5.18	5.16	0.03
95-212-6	294.52	20.43	20.45	20.50	20.46	0.07	5.18	5.14	5.18	5.17	0.05
95-212-7	354.13	20.78	20.80	20.76	20.78	0.04	5.20	5.22	5.19	5.20	0.03
95-212-8	414.46	21.02	21.02	21.00	21.01	0.02	5.20	5.20	5.22	5.21	0.02
95-212-9	474.84	20.68	20.60	20.68	20.65	0.09	5.18	5.18	5.20	5.19	0.02
95-212-10	535.85	20.88	20.87	21.00	20.92	0.14	5.17	5.18	5.20	5.18	0.03
95-212-11	595.31	21.06	21.08	21.06	21.07	0.02	5.19	5.20	5.18	5.19	0.02
95-212-12	655.23	21.21	21.20	21.20	21.20	0.01	5.19	5.20	5.20	5.20	0.01
95-212-13	705.05	21.16	21.18	21.16	21.17	0.02	5.17	5.22	5.18	5.19	0.05
95-212-14	763.36	21.21	21.20	21.21	21.21	0.01	5.18	5.19	5.18	5.18	0.01
95-212-15	822.07	21.22	21.20	21.23	21.22	0.03	5.19	5.18	5.19	5.19	0.01
95-212-16	882.06	21.21	21.16	21.23	21.20	0.07	5.17	5.16	5.17	5.17	0.01
95-212-17	938.25	21.23	21.20	21.22	21.22	0.03	5.18	5.18	5.20	5.19	0.02
95-212-18	989.69	21.20	21.22	21.23	21.22	0.03	5.16	5.17	5.16	5.16	0.01
95-212-19	1015.65	21.20	21.20	21.23	21.21	0.03	5.17	5.18	5.16	5.17	0.02

Rio Grande Sample - 4,100 mg/L Suspended Solids

Sample No.	Cumulative Volume Filtered (mL)	Na (mg/L)					K (mg/L)				
		1	2	3	Average	2 Std Deviation	1	2	3	Average	2 Std Deviation
95-202-1	57.82	98.88	99.00	98.83	98.90	0.17	6.50	6.52	6.50	6.51	0.02
95-202-2	115.64	99.59	99.67	99.51	99.59	0.16	6.62	6.62	6.60	6.61	0.02
95-202-3	173.21	95.68	96.02	95.62	95.77	0.43	6.40	6.42	6.44	6.42	0.04
95-202-4	202.81	94.89	94.80	95.02	94.90	0.22	6.40	6.40	6.42	6.41	0.02
95-202-5	250.70	94.36	94.40	94.36	94.37	0.05	6.39	6.40	6.40	6.40	0.01
95-202-6	291.15	94.66	94.60	94.72	94.66	0.12	6.39	6.40	6.40	6.40	0.01
95-202-7	327.91	94.58	94.62	94.60	94.60	0.04	6.39	6.38	6.40	6.39	0.02
95-202-8	372.86	94.26	94.30	94.24	94.27	0.06	6.39	6.38	6.40	6.39	0.02
95-202-9	423.31	94.69	94.66	94.65	94.67	0.04	6.39	6.40	6.40	6.40	0.01
95-202-10	483.63	94.58	94.60	94.56	94.58	0.04	6.38	6.38	6.42	6.39	0.05
95-202-11	543.95	94.59	94.62	94.60	94.60	0.03	6.38	6.40	6.40	6.39	0.02
95-202-12	591.11	94.66	94.62	94.66	94.65	0.05	6.39	6.38	6.40	6.39	0.02
95-202-13	643.48	94.58	94.58	94.60	94.59	0.02	6.38	6.40	6.40	6.39	0.02
95-202-14	694.16	94.59	94.62	94.60	94.60	0.03	6.37	6.40	6.38	6.38	0.03
95-202-15	828.24	94.58	94.60	94.58	94.59	0.02	6.37	6.40	6.38	6.38	0.03
95-202-16	871.35	94.69	94.80	94.69	94.73	0.13	6.39	6.40	6.40	6.40	0.01
95-202-17	910.77	94.66	94.68	94.70	94.68	0.04	6.38	6.38	6.38	6.38	0.00
95-202-18	957.09	94.59	94.62	94.60	94.60	0.03	6.38	6.40	6.40	6.39	0.02
95-202-19	996.36	94.25	94.25	94.20	94.23	0.06	6.39	6.40	6.38	6.39	0.02
95-202-20	1091.81	94.26	94.30	94.26	94.27	0.05	6.39	6.40	6.40	6.40	0.01
95-202-21	1130.62	94.59	94.60	94.60	94.60	0.01	6.38	6.38	6.40	6.39	0.02
95-202-22	1185.09	94.88	94.86	94.88	94.87	0.02	6.37	6.40	6.38	6.38	0.03



Rio Grande Sample - 4,100 mg/L Suspended Solids

Sample No.	Cumulative Volume Filtered (mL)	Mg (mg/L)						Ca (mg/L)					
		1	2	3	Average	2 Std Deviation	1	2	3	Average	2 Std Deviation		
95-202-1	57.82	13.99	14.00	14.00	14.00	0.01	87.87	88.00	87.90	87.92	0.14		
95-202-2	115.64	13.99	13.98	14.00	13.99	0.02	89.87	89.90	89.80	89.86	0.10		
95-202-3	173.21	13.57	13.60	13.60	13.59	0.03	88.24	88.32	88.32	88.29	0.09		
95-202-4	202.81	13.33	13.33	13.35	13.34	0.02	84.23	84.20	84.22	84.22	0.03		
95-202-5	250.70	13.32	13.30	13.32	13.31	0.02	84.23	84.22	84.22	84.22	0.01		
95-202-6	291.15	13.26	13.30	13.26	13.27	0.05	84.52	84.52	84.50	84.51	0.02		
95-202-7	327.91	13.25	13.26	13.26	13.26	0.01	84.35	84.36	84.32	84.34	0.04		
95-202-8	372.86	13.32	13.30	13.30	13.31	0.02	84.44	84.44	84.46	84.45	0.02		
95-202-9	423.31	13.24	13.26	13.26	13.25	0.02	84.43	84.44	84.46	84.44	0.03		
95-202-10	483.63	13.32	13.30	13.30	13.31	0.02	84.39	84.40	84.40	84.40	0.01		
95-202-11	543.95	13.24	13.24	13.26	13.25	0.02	84.41	84.40	84.40	84.40	0.01		
95-202-12	591.11	13.32	13.30	13.32	13.31	0.02	84.43	84.44	84.44	84.44	0.01		
95-202-13	643.48	13.33	13.34	13.34	13.34	0.01	84.45	84.46	84.44	84.45	0.02		
95-202-14	694.16	13.34	13.36	13.34	13.35	0.02	84.43	84.46	84.44	84.44	0.03		
95-202-15	828.24	13.35	13.36	13.36	13.36	0.01	84.45	84.46	84.44	84.45	0.02		
95-202-16	871.35	13.33	13.34	13.34	13.34	0.01	84.46	84.46	84.46	84.46	0.00		
95-202-17	910.77	13.34	13.34	13.34	13.34	0.00	84.44	84.46	84.44	84.45	0.02		
95-202-18	957.09	13.31	13.30	13.30	13.30	0.01	84.46	84.44	84.44	84.45	0.02		
95-202-19	996.36	13.33	13.34	13.34	13.34	0.01	84.43	84.46	84.46	84.45	0.03		
95-202-20	1091.81	13.33	13.34	13.36	13.34	0.03	84.44	84.46	84.44	84.45	0.02		
95-202-21	1130.62	13.34	13.34	13.36	13.35	0.02	84.43	84.44	84.44	84.44	0.01		
95-202-22	1185.09	13.34	13.34	13.36	13.35	0.02	84.44	84.46	84.46	84.45	0.02		

Rio Grande Sample - 4,100 mg/L Suspended Solids

Sample No.	Cumulative Volume Filtered (mL)	Cl (mg/L)			F (mg/L)						
		1	2	3	Average	2 Std Deviation	1	2	3	Average	2 Std Deviation
95-202-1	57.82	24.65	24.78	25.02	24.82	0.38	1.48	1.56	1.56	1.53	0.09
95-202-2	115.64	25.35	25.28	25.68	25.44	0.43	1.49	1.52	1.58	1.53	0.09
95-202-3	173.21	23.35	23.47	23.47	23.43	0.14	1.28	1.30	1.32	1.30	0.04
95-202-4	202.81	22.46	22.44	22.45	22.45	0.02	1.02	1.02	1.00	1.01	0.02
95-202-5	250.70	22.46	22.44	22.46	22.45	0.02	1.02	1.02	1.04	1.03	0.02
95-202-6	291.15	22.47	22.46	22.44	22.46	0.03	1.03	1.02	1.04	1.03	0.02
95-202-7	327.91	22.45	22.46	22.44	22.45	0.02	1.02	1.04	1.02	1.03	0.02
95-202-8	372.86	22.47	22.46	22.48	22.47	0.02	1.03	1.04	1.04	1.04	0.01
95-202-9	423.31	22.46	22.44	22.40	22.43	0.06	1.03	1.02	1.04	1.03	0.02
95-202-10	483.63	22.44	22.42	22.40	22.42	0.04	1.03	1.02	1.02	1.02	0.01
95-202-11	543.95	22.49	22.46	22.42	22.46	0.07	1.04	1.02	1.04	1.03	0.02
95-202-12	591.11	22.48	22.50	22.50	22.49	0.02	1.03	1.02	1.04	1.03	0.02
95-202-13	643.48	22.44	22.46	22.42	22.44	0.04	1.03	1.02	1.04	1.03	0.02
95-202-14	694.16	22.44	22.46	22.42	22.44	0.04	1.02	1.04	1.04	1.03	0.02
95-202-15	828.24	22.45	22.46	22.46	22.46	0.01	1.03	1.04	1.04	1.04	0.01
95-202-16	871.35	22.46	22.46	22.42	22.45	0.05	1.03	1.04	1.04	1.04	0.01
95-202-17	910.77	22.45	22.44	22.46	22.45	0.02	1.03	1.04	1.04	1.04	0.01
95-202-18	957.09	22.45	22.44	22.46	22.45	0.02	1.03	1.02	1.02	1.02	0.01
95-202-19	996.36	22.44	22.46	22.40	22.43	0.06	1.04	1.02	1.04	1.03	0.02
95-202-20	1091.81	22.46	22.44	22.46	22.45	0.02	1.04	1.02	1.04	1.03	0.02
95-202-21	1130.62	22.45	22.46	22.46	22.46	0.01	1.03	1.04	1.02	1.03	0.02
95-202-22	1185.09	22.45	22.46	22.46	22.46	0.01	1.03	1.04	1.02	1.03	0.02

Rio Grande Sample - 4,100 mg/L Suspended Solids						
Sample No.	Cumulative Volume Filtered (mL)	SO <sub>4</sub> (mg/L)				2 Std Deviation
		1	2	3	Average	
95-202-1	57.82	82.46	82.50	82.54	82.50	0.08
95-202-2	115.64	83.43	83.52	83.48	83.48	0.09
95-202-3	173.21	80.13	80.12	80.20	80.15	0.09
95-202-4	202.81	78.68	78.82	78.64	78.71	0.19
95-202-5	250.70	78.65	78.70	78.68	78.68	0.05
95-202-6	291.15	78.65	78.72	78.68	78.68	0.07
95-202-7	327.91	78.66	78.68	78.68	78.67	0.02
95-202-8	372.86	78.62	78.70	78.60	78.64	0.11
95-202-9	423.31	78.59	78.62	78.60	78.60	0.03
95-202-10	483.63	78.60	78.62	78.62	78.61	0.02
95-202-11	543.95	79.00	78.98	78.90	78.96	0.11
95-202-12	591.11	78.99	78.98	79.00	78.99	0.02
95-202-13	643.48	78.97	78.98	79.00	78.98	0.03
95-202-14	694.16	78.69	78.72	78.72	78.71	0.03
95-202-15	828.24	78.99	79.00	79.00	79.00	0.01
95-202-16	871.35	78.97	79.02	79.00	79.00	0.05
95-202-17	910.77	78.97	79.00	79.00	78.99	0.03
95-202-18	957.09	78.66	78.72	78.80	78.73	0.14
95-202-19	996.36	78.69	78.72	78.70	78.70	0.03
95-202-20	1091.81	78.70	78.72	78.70	78.71	0.02
95-202-21	1130.62	78.87	78.88	78.88	78.88	0.01
95-202-22	1185.09	78.89	78.88	78.92	78.90	0.04

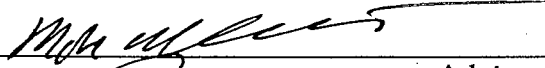
Rio Puerco Sample - 32,100 mg/L Suspended Solids														
Sample No.	Cumulative Volume Filtered (mL)	Na (mg/L)			K (mg/L)			2 Std Deviation	1	2	3	Average	2 Std Deviation	
		1	2	3	Average	2 Std Deviation	1							
95-208-1	28.23	123.76	123.54	124.72	124.01	1.25	5.25	5.30	5.30	5.28	0.06			
95-208-2	50.52	126.67	126.58	126.68	126.64	0.11	5.32	5.34	5.32	5.33	0.02			
95-208-3	74.07	121.04	121.40	121.20	121.21	0.36	5.16	5.18	5.18	5.17	0.02			
95-208-4	108.01	121.04	121.36	121.24	121.21	0.32	5.16	5.16	5.20	5.17	0.05			
95-208-5	135.46	121.04	121.34	121.26	121.21	0.31	5.15	5.16	5.16	5.16	0.01			
95-208-6	166.94	121.04	121.36	121.24	121.21	0.32	5.15	5.16	5.18	5.16	0.03			
95-208-7	199.52	121.04	121.36	121.26	121.22	0.33	5.16	5.18	5.18	5.17	0.02			
95-208-8	228.47	121.07	121.38	121.26	121.24	0.31	5.16	5.15	5.16	5.16	0.01			
95-208-9	276.28	121.13	121.42	121.28	121.28	0.29	5.15	5.18	5.16	5.16	0.03			
95-208-10	321.35	121.09	121.40	121.38	121.29	0.35	5.16	5.18	5.16	5.17	0.02			
95-208-11	363.28	121.06	121.40	121.42	121.29	0.40	5.15	5.16	5.18	5.16	0.03			
95-208-12	416.65	121.07	121.42	121.40	121.30	0.39	5.15	5.18	5.18	5.17	0.03			
95-208-13	473.87	121.08	121.42	121.40	121.30	0.38	5.16	5.16	5.18	5.17	0.02			

Rio Puerco Sample - 32,100 mg/L Suspended Solids												
Sample No.	Cumulative Volume Filtered (mL)	Mg (mg/L)						Ca (mg/L)				
		1	2	3	Average	2 Std Deviation	1	2	3	Average	2 Std Deviation	
95-208-1	28.23	19.59	19.40	19.62	19.54	0.24	58.35	58.92	58.32	58.53	0.68	
95-208-2	50.52	19.24	19.34	19.30	19.29	0.10	57.25	57.82	57.32	57.46	0.62	
95-208-3	74.07	18.51	18.46	18.48	18.48	0.05	55.70	55.68	55.42	55.60	0.31	
95-208-4	108.01	18.52	18.50	18.52	18.51	0.02	55.69	55.80	55.62	55.70	0.18	
95-208-5	135.46	18.53	18.50	18.56	18.53	0.06	55.72	55.42	55.70	55.61	0.34	
95-208-6	166.94	18.57	18.60	18.62	18.60	0.05	55.69	55.42	55.70	55.60	0.32	
95-208-7	199.52	18.53	18.56	18.50	18.53	0.06	55.67	55.44	55.70	55.60	0.28	
95-208-8	228.47	18.49	18.48	18.50	18.49	0.02	55.68	55.64	55.72	55.68	0.08	
95-208-9	276.28	18.48	18.50	18.52	18.50	0.04	55.68	55.62	55.72	55.67	0.10	
95-208-10	321.35	18.52	18.50	18.52	18.51	0.02	55.64	55.62	55.70	55.65	0.08	
95-208-11	363.28	18.54	18.56	18.54	18.55	0.02	55.68	55.62	55.70	55.67	0.08	
95-208-12	416.65	18.50	18.52	18.52	18.51	0.02	55.68	55.68	55.70	55.69	0.02	
95-208-13	473.87	18.53	18.56	18.50	18.53	0.06	55.69	55.62	55.72	55.68	0.10	

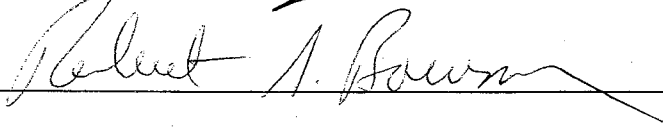
Rio Puerco Sample - 32,100 mg/L Suspended Solids												
Sample No.	Cumulative Volume Filtered (mL)	Cl (mg/L)						F (mg/L)				
		1	2	3	Average	2 Std Deviation	1	2	3	Average	2 Std Deviation	
95-208-1	28.23	18.57	18.27	18.62	18.49	0.38	2.68	2.64	2.60	2.64	0.08	
95-208-2	50.52	15.47	15.52	15.60	15.53	0.13	2.55	2.56	2.58	2.56	0.03	
95-208-3	74.07	14.46	14.42	14.42	14.43	0.05	2.44	2.40	2.42	2.42	0.04	
95-208-4	108.01	14.44	14.40	14.42	14.42	0.04	2.44	2.42	2.42	2.43	0.02	
95-208-5	135.46	14.43	14.38	14.40	14.40	0.05	2.44	2.44	2.40	2.43	0.05	
95-208-6	166.94	14.30	14.30	14.36	14.32	0.07	2.44	2.44	2.40	2.43	0.05	
95-208-7	199.52	14.31	14.32	14.36	14.33	0.05	2.45	2.44	2.46	2.45	0.02	
95-208-8	228.47	14.32	14.30	14.36	14.33	0.06	2.45	2.46	2.46	2.46	0.01	
95-208-9	276.28	14.33	14.30	14.32	14.32	0.03	2.44	2.46	2.48	2.46	0.04	
95-208-10	321.35	14.33	14.32	14.30	14.32	0.03	2.45	2.46	2.42	2.44	0.04	
95-208-11	363.28	14.35	14.32	14.32	14.33	0.03	2.45	2.46	2.42	2.44	0.04	
95-208-12	416.65	14.34	14.32	14.40	14.35	0.08	2.45	2.46	2.44	2.45	0.02	
95-208-13	473.87	14.32	14.30	14.14	14.25	0.20	2.44	2.40	2.44	2.43	0.05	

Rio Puerco Sample - 32,100 mg/L Suspended Solids							
Sample No.	Cumulative Volume Filtered (mL)	SO <sub>4</sub> (mg/L)					2 Std Deviation
		1	2	3	Average		
95-208-1	28.23	299.90	298.02	300.12	299.35	2.31	
95-208-2	50.52	295.66	296.18	296.92	296.25	1.27	
95-208-3	74.07	290.44	290.42	291.12	290.66	0.80	
95-208-4	108.01	290.79	290.72	290.98	290.83	0.27	
95-208-5	135.46	290.16	290.28	290.24	290.23	0.12	
95-208-6	166.94	291.01	291.12	291.17	291.10	0.16	
95-208-7	199.52	290.16	290.98	290.20	290.45	0.92	
95-208-8	228.47	290.24	290.35	290.39	290.33	0.16	
95-208-9	276.28	290.18	290.68	290.72	290.53	0.60	
95-208-10	321.35	290.17	290.25	290.74	290.39	0.62	
95-208-11	363.28	290.18	290.22	290.68	290.36	0.56	
95-208-12	416.65	290.22	290.28	290.70	290.40	0.52	
95-208-13	473.87	290.14	290.26	290.58	290.33	0.45	

This thesis is accepted on behalf of the  
Faculty of the Institute by the following committee:

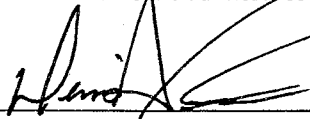
  
\_\_\_\_\_  
Advisor

  
\_\_\_\_\_

  
\_\_\_\_\_

\_\_\_\_\_  
Date

I release this document to the New Mexico Institute of Mining and Technology.

  
\_\_\_\_\_  
Student's Signature

9/11/02  
\_\_\_\_\_  
Date